Space Elevator

Dynamics Reference Manual

Done by David Lang
in behalf of
Institute for Scientific Research, Inc.
In response to a Funding Contract from NASA, MSFC

12 April 2006

TABLE OF CONTENTS

INTRODUCTION

This manual is a preliminary work aimed at providing a source of convenient dynamics-related information for those involved with all aspects of space elevator (SE) development and design. For some, this manual may serve as a primer of SE dynamics, for all, it is a source of specific constants, attributes and SE behaviors. This manual is a work in progress as much remains to be addressed as work proceeds on the project. Each section of the manual addresses a special aspect of information pertaining to the SE.

The dynamics attributes have been mostly derived from the time-domain simulation called GTOSS (Generalized Tethered Object Simulation). An outline of GTOSS is included (in Appendices A through D, etc) to allow the user to assess the pertinence of this simulation in providing such results for each aspect of SE dynamics. Related materials s re-organized and derived from these studies by the author appear in the papers listed among the references.

***General Note to ISR**: Some items below could possibly be included for future efforts*

a. Thermal response
b. Climber attitude dynamics
c. Ocean wave effects on longitudinal dynamics
d. Sun-Moon tidal effects
e. Aerodynamic pull-down response
f. Breakage debris-footprints
g. General pull-down response

1.0 GENERAL DATA, PARAMETERS, FORMULAS

1.1 USEFUL NUMERICAL CONSTANTS

This section addresses physical constants typically used in SE design calculations; these are broken down into physical constants, and broadly dynamics-related attributes.

1.1.1 General Physical Constants

Below are physical constants frequently used in SE calculations. These data are presented in metric and English units.

Nom. Ribbon Length	= **100,000 km = 10^7 m** = 328,083,985 = 3.28083985x10^8 ft
Nom. Ballast Mass	= **634,279.7 kg** = 43,462 slugs = 1,398,348.5 lbm
Earth Rotation rate	= 7.292115 x10^{-5} rad/sec
Earth Rotation rate "squared"	= 5.3174943 x10^{-9} rad/sec^2
"SE Book" Earth Radius (Re)	= **6378.00 km = 6,378,000 m** = 20,925,197 = 2.0925197 x10^7 ft
Nom. Total Ribbon Mass	= **865,077 kg** = 1,907,170 = 1.907170x10^6 lbm = 59,276.8 = 5.92768 x10^4 slugs
Ribbon Modulus of Elasticity	= **1.2996 x10^{11} N/m^2** (Pascals) = 188,500,00 = 1.885 x10^8 psi
Gravity Accel at Ballast radius	= **0.03522 m/sec^2** = 0.11556 ft/sec^2 = 0.0036 g's
Centrip. Accel at Ballast radius	= **0.5656 m/sec^2** = 1.8558 ft/sec^2
Gravity Force on nom ballast	= **22,357 N** = 5,026 lbf
Centrif. Force on nom ballast	= **358,775 N** = 80,656 lbf
Net force to "swing" nom ballast	= **336,419 N** = 75,630 lbf

"R_{earth}/Ribbon Len" ratio = 0.06378

$\sqrt{Re/R_L}$ = 0.25255

Accel of Grav at GEO approx = **0.3048 m/sec^2**
= 1.0 ft/sec^2

Some related Parameter values as they appear in GTOSS

Accel Grav @earth surface = **9.798222 m/sec^2**
= 32.1464 ft/sec^2

Earth Revolution Period = 86,164.1 sec

Nom. Radius vector to Ballast = **106,377.96 km**
= **10.637796 x10^7 m**
= 349,009,071 = 3.4900971x10^8 ft

Nom. Earth Radius (Re) = **6378.16 km = 6,378,160.1 m**
= 20,925,722 = 2.0925722 x10^7 ft

1.1.2 Ribbon Attribute Constants

All deductions are based on the following assumptions/ribbon properties:

With the exception of the total operational ribbon *elongation* (a value determined via GTOSS), these deductions are based on classical linear string theory and basic physics relationships, and thus only reflect ball-park values and should be applied with temperance.

Young's Modulus (E) = **1,000 GPa** (= 10^{12} N/m^2 = 1.45x10^{12} psi)
Elastic (load bearing) Cross sect. at Ground = **3 mm^2** (= 3.00x10^{-6} m^2 = .00465 in^2)
Elastic (load bearing) Cross sect. at GEO = **7.68 mm^2** (= 7.68x10^{-6} m^2 = .0119 in^2)

Stretched length of tapered Ribbon = **100,000 km** (3.2808x10^8 ft)
Un-Stretched length of tapered Ribbon = **95,292 km** (= 3.1264x10^8 ft)
Total Elongation of tapered Ribbon = **4,708 km** (= 15,446,000 ft = 2,925 miles)

Note: this corresponds to an average strain of 4.9% (data from GTOSS simulation)

Ribbon (CNT) intrinsic density = **1.3 g/cm^3** (1.3x10^3 kg/m^3 =2.52 slug/ft^3 = 81.1 lbm/ft^3)

Ribbon lineal-density (@Ground) = **0.0387 g/cm** (3.87 kg/km = 2.60 lbm/1000ft)

Ribbon lineal-density (@GEO) = **0.0997 g/cm** (9.97 kg/km = 6.70 lbm/1000ft)

The term "Lift-off mass", refers to the total mass of the Crawler + Useful cargo. These calculations do not make a distinction between what portion of Lift-off mass is useful, and what is purely "crawler mechanism related". In particular, for practical operations, Lift-off mass may have to be notably less than the static ribbon tension of 20 tons (or 40,000 lbs); See items 3 thru 8 below.

1.1.3 Elevator Dynamical Attribute Values

Based on the above data, we can make the following deductions:

1.1.3.1 Stress wave propagation speed

Transmission Speed of Stress disturbance (longitudinal ribbon wave)

= **27,700 m/s**
= **27.7 km/s**
= 91,000 ft/sec
= 62,000 mph

This parameter depends only upon the material's modulus and intrinsic density; the above values would be very approximate due to the composite nature of the ribbon, and are based on CNT intrinsic properties alone.

Point of Interest: this is the fastest that mechanical information can be transmitted within the CNT ribbon material; for instance, if the ribbon were cut at the ground, it would take on the order of 1 hour for the Ballast mass to get the message, that is, for the zero stress condition at the anchor to propagate up to the ballast. GTOSS has verified this end-to-end transmission time (transmission time is a function of the "number of nodes" and "integration interval" for discrete simulation, approaching the theoretical value as both progress towards "finer" values).

1.1.3.2 Transverse wave propagation speed

Speed of propagation of Transverse ribbon waves

= **6766 m/s**
= **6.77 km/s**
= 22,200 ft/s
= 15,136 mph

This parameter depends upon the tension and lineal-density of the ribbon material.

Point of Interest: If you throw an instantaneous "transverse kink" in the ribbon at the ground, it will take on the order of **45 sec** to reach LEO regions (ie. 300 km altitude), about **1.5 hrs** to reach **GEO**, and about **4 hrs** to reach the **ballast mass** (making a round trip excursion of a transverse wave reflected off the ballast mass be 8 hrs).

Point of Interest: Comparing propagation speeds of Longitudinal versus Transverse ribbon waves, it is seen that the **lowest string-mode frequency** is about **1/4** that of the **lowest longitudinal-mode frequency**.

Point of Interest: Avoiding LEO debris may be practical via SE base-motion. If a re-positioning of the order of a 100-200 meters is sufficient, then this might be attainable via a sliding mechanism on the base station as opposed to moving the anchor platform itself, thus providing quick response. This, combined with the short time to LEO would allow very quick response to a debris detection event. Thus ocean-based stations, and/or over-the-horizon radar debris detection may be a viable scheme.

Point of Interest: Avoiding near GEO debris will require some planning; however, objects in the GEO regime are moving much slower, and spend far more time visible above the radar horizon thus it is less likely to sneak up on the SE as is possible un-charted LEO objects.

1.1.3.3 Effective end-to-end spring rate

Effective End-to-End spring rate (K_{eff}) at the Anchor

= **.039 N/m** (1 N => 26 m)
= **39 N/km**
= .0027 lb/ft (1 lb => 370 ft)

This is based on operational Tension/Total Elongation (from GTOSS data), and also

using classical strain-modulus relationships (with average ribbon attributes at Ground and GEO), yielding about the same result. Notes examine implications of K_{eff} .

Point of Interest: Based on a classical uniform string calculation, the value of K_{eff} is bounded below by a calculation corresponding to a "uniform ribbon" based on the elastic attributes at the anchor (yielding a K_{eff} = .030 N/m); the upper bound corresponds to elastic attributes at GEO (yielding a K_{eff} =.047 N/m).

Point of Interest: The above calculation of static K_{eff}, does not mean that such a spring rate would necessarily be realized under significantly Transient conditions, since the classical end-to-end spring rate is based on the entire length of a string instantaneously elongating to participate in resisting applied load. This is because it would take an hour for a strain gradient induced by load (at the earth) to distribute itself along the entire length of the ribbon, thus time become a factor. However, if the system transients were left to damp-out, then the final static elongation would be consistent with this type calculation of K_{eff}.

Point of Interest: Consider an SE with an attached payload whose weight is just equal to the static tension (ie. an essentially neutrally buoyant elevator); now imagine that you could step onto the payload, adding your weight to it, and further suppose that you and the payload were free to translate downward freely (say, over a deep pit in the ground); your added weight would cause the payload to ultimately sink down about 17,000 meters (ie. 55,000 ft or about 10 miles).

1.1.3.4 Climber bobbing period

Liftoff Mass Bobbing Period

Period = 1/Frequency = **1.04 hrs**

This parameter has been simplistically calculated based on a simple 2 DOF dual-mass spring system (assuming the spring is massless) and a lift-off mass of 16,490 kg (18 tons = 36,360 lb_m).

Point of Interest: If one had, say, an **18** ton Liftoff mass attached to a **20** ton-tensioned SE ribbon, and then cut the restraining link between the payload and ground, then a yo-yo bobbing-type oscillation would ensue, with the payload bounding upwards towards the ballast for about 1/2 hr, then bounding back downward, this whole process taking a little over an hour for a classical spring-mass system. Related SE phenomenon could actually take somewhat longer because as the liftoff mass rises, gravity decreases and centripetal acceleration increases, both effects attributing to a greater altitude (amplitude) being realized than predicted by a simple spring mass system.

Point of Interest: Simulations of this using GTOSS indeed exhibits these tendencies (with the above characteristic frequency appearing). In this case, the resultant response was not constrained, resulting in elevator and lift-off mass both moving away from the earth. Thus, other complex non-linear behaviors manifest themselves, such as: motion of ballast and lift-off masses as whole away from and through the earth's inverse square gravity field, excitation of longitudinal modes due to a sharp change in tension as the anchor was severed, finite times of longitudinal wave transmission/and strain-relaxation, etc.

1.1.3.5 Climber bobbing amplitude

Liftoff Mass Bobbing-Mode Amplitude

= **822,000 m**
= 822 km
= 510 miles

This amplitude depends upon the relationship of the static tension to the Lift-off mass. The calculation uses the same data as in 1.1.3.4 above, except, simplistically assumes a single mass-spring system (ie. the ballast mass is assumed "fixed", otherwise the motion is unbounded).

Point of Interest: While this oscillation amplitude would likely never be realized in practice, rather it is included to promote an understanding of the compliant nature of the climber-ribbon system.

1.1.3.6 Climber acceleration potential

Payload Bobbing-Mode Immediate Acceleration Potential

= **1.08 m/sec^2**
= 0.11 g

Point of Interest: This value is arbitrarily based on the free release of an 18 ton Lift-off mass on a ribbon tensioned at 20 tons (the acceleration thus being the ratio of 2 tons/18 tons). Given the low spring rate of the ribbon, a free-release represents the maximum practical acceleration attainable at liftoff.

1.1.3.7 Transverse string mode periods

Classical 1st and 2nd String-Mode Transverse Periods (approx)

1st mode period = **7.5** hrs
2nd mode period = **3.8** hrs

1.1.3.8 Pendulus libration periods

Pendulus In-Plane Period (approx)

= **5.65** days
= 135.6 hrs

Pendulus Out-of-Plane Period (approx)

= **0.98** days
= 23.95 hrs

1.1.3.9 Coriolis effects

Coriolis Acceleration:

The following table quantifies the Coriolis acceleration associated with certain rates of traversal of the elevator Ribbon, and provides typical related force associated with a Climber mass of **16,490 kg (18 tons = 36,360 lbm)**.

Traverse **Rate** (m/s)	Traverse **Rate** (km/hr)	Coriolis **Acc** (m/s^2)	Effec. **Force** (N)	Effec. **Force** (lbf)
50	180	.0073	134	30
100	360	.0146	328	60
200	720	.0292	656	120

Point of Interest: Consider the classical "Clothes-Line" effect (force resolution) in which the tension in a line is employed to equilibrate a normal load by way of deflecting the "clothes-line" (a tangent of small angle effect). If a line is under 178,000 N (40,000 lbf) of tension, then a 0.04 deg deflection would equilibrate a normal force of 267 N (60 lbf); this corresponds to a reverse effective Coriolis force of a 100 m/s traversal rate.

For the earth's rotation rate, the Coriolis relationship used is:

$$\boldsymbol{A}_{cor} = 1.46\boldsymbol{x}10^{-4}\,\dot{\boldsymbol{R}} \ (\mathrm{m/s^2})$$

1.1.3.10 Ribbon tangential velocity

Tangential Velocity at GEO and Ballast Altitudes:

@ GEO V_T = **2,580 m/s**
= 8,460 ft/s

@ Ballast V_T = **7292 m/s**
= 23, 900 ft/s

Point of Interest: This is tangential velocity relative to the anchor point. Note also that V_T at the Ballast is of the order of the low earth orbit speed.

1.2 ATTRIBUTES OF "CONSTANT STRESS" SE DESIGN

The classic problem of SE design is to achieve the most efficient use of ribbon material; thus, ideally, no section of ribbon is ever under or over-utilized, meaning that nominally, each point on the ribbon experiences the same level of stress, that level being the nominal operating stress with an assumed factor or safety of 2 for example. Typically values of operating stress for the ribbon have been quoted in the 50-60 giga-Pascal range. Thus material.

Point of Interest: Common Scotch tape if it were made of material capable of sustaining 60 GPa stress, could suspend two Cadillac automobiles (11,000 lbs).

The intrinsic technical problem that has historically confronted the SE is been the fact that it must suspend not only the weight of a payload, but more significantly, the weight of itself. Every ribbon particle below GEO altitude creates net force down, and above GEO, a net force upward. GEO then becomes the point at which an SE ribbon would experience the greatest force, and thus have the greatest cross-sectional area; thus proceeding in either direction from GEO, an maximally efficient ribbon would taper ever smaller. The relationship governing the ribbon's cross sectional area as a function of altitude to achieve this efficiency (uniform stress) is well known, and involves both the material density and strength in exponential form. This leads to the exponentially tapered ribbon design, with maximum width at GEO, tapering to lesser widths at both the ground and the ballast mass. Such design takes into account both inverse square earth gravity as well as linearly altitude-dependent centrifugal force.

It is this resulting dual tapered ribbon profile that is used within GTOSS to generate the dynamic responses summarized in this handbook. More details on the GTOSS simulation of the tapered ribbon are found in Appendix D

Thus, if one designs the ribbon taper properly to produce uniform material efficiency, and then simulates the SE in an environment properly representing planetary and dynamic effects, then, the resulting stress profile (ie. stress as a function of altitude along the ribbon) should so manifest uniformity. This was done with GTOSS, and the result is shown in the plot below:

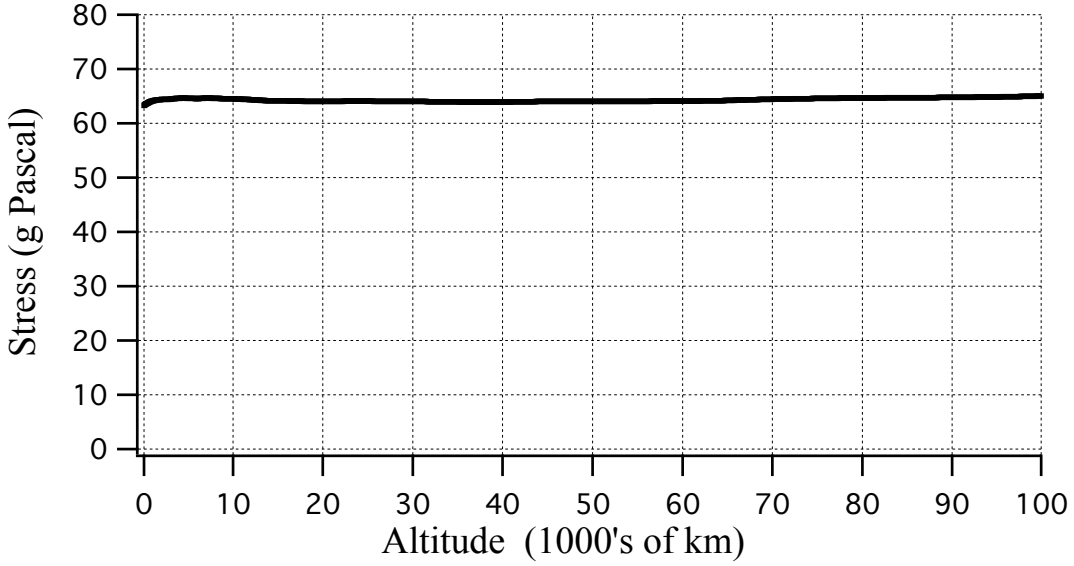

1.2.1 Tapered Ribbon Properties Plots

This uniform stress plot (above) results from the interplay of the ribbon's design profile for density, exponentially tapered elastic cross sectional area, and modulus that was used within GTOSS (shown in the figures below). The slight droop in the stress curve near the earth can be attributed to approximation errors associated with curve-fitting the ribbon profile's taper gradient near the earth.

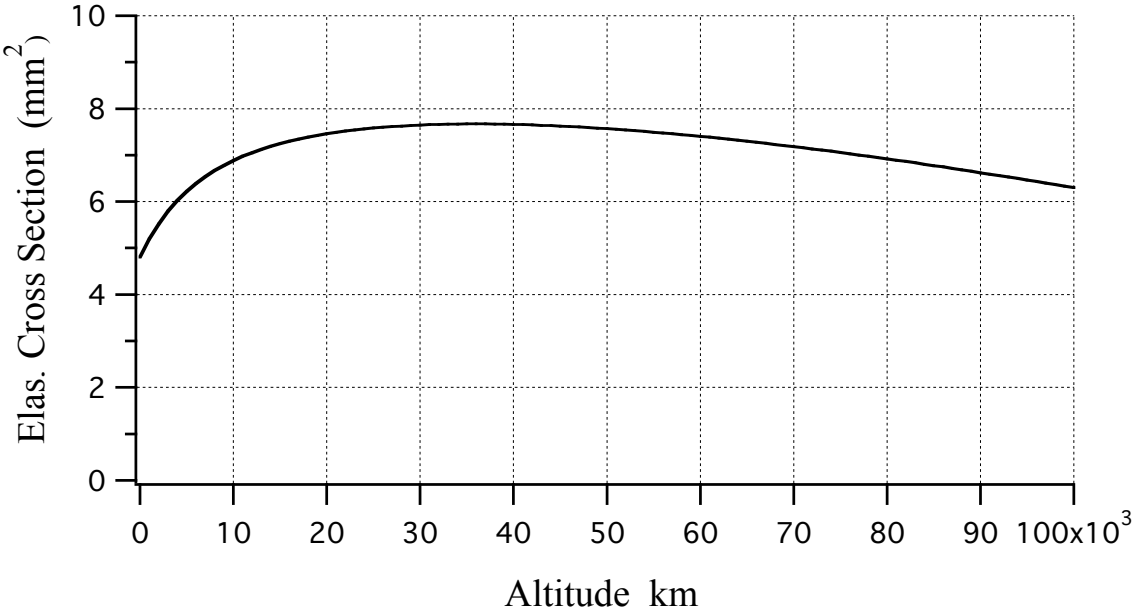

Based on the elastic cross sectional area profile and a nominal value of ribbon material's bulk density of 1.3 gm/cm^3, the lineal density profile shown below was derived for use in GTOSS.

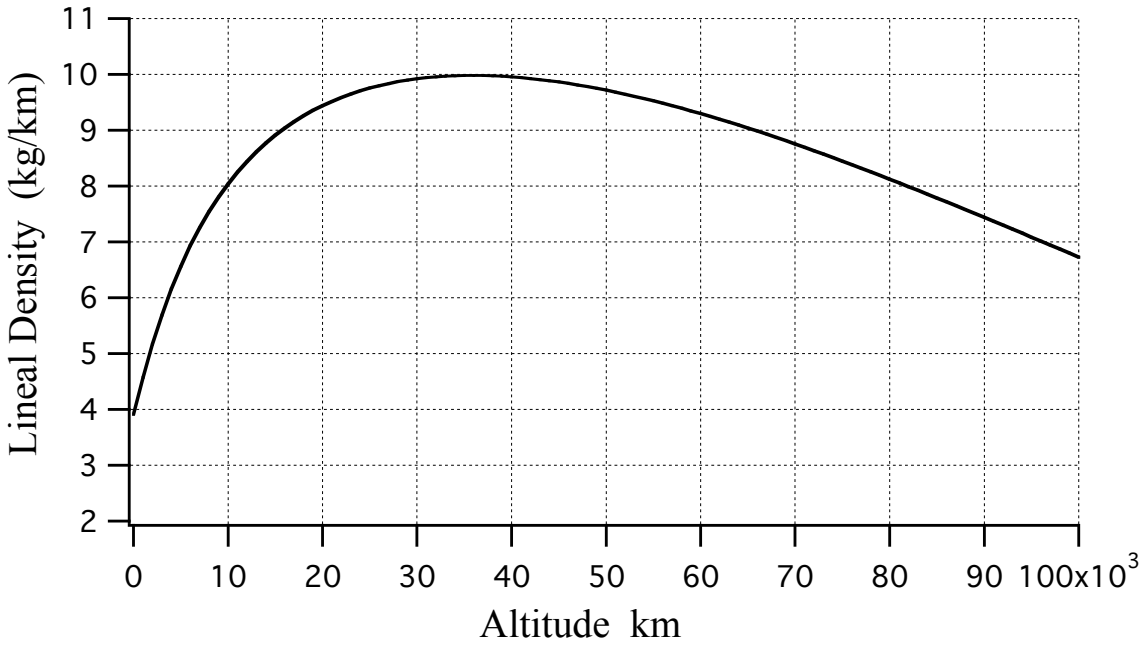
Lineal Density (kg/km)
11
10
9
8
7
6
5
4
3
2
0
10
20
30
40
50
60
70
80
90
100x10^3
Altitude km

1.2.2 Ribbon Taper Tabulated Properties

All data below is consistent with that provided by Dr. Bradley Edwards, even though the data is presented below at different levels of resolution.

1.2.2.1 High resolution tabular data

High resolution Tabular data: Earth's Surface to GEO altitude ("Radius" is the distance from the center of the earth to a point on the ribbon).

Radius (m)	**Tension** (N/m^2)	**Elastic Area** (m^2)	**Ribbon mass** (kg)
6378000	1.95E+05	3.01E-06	0
7378000	2.29E+05	3.52E-06	3908.9
8378000	2.58E+05	3.97E-06	8484.7
9378000	2.85E+05	4.38E-06	13652.1
10378000	3.08E+05	4.73E-06	19342.6
11378000	3.28E+05	5.05E-06	25496.1
12378000	3.46E+05	5.33E-06	32059.9
13378000	3.63E+05	5.58E-06	38988.6
14378000	3.77E+05	5.80E-06	46242.6
15378000	3.90E+05	6.00E-06	53787.6
16378000	4.02E+05	6.18E-06	61593.4
17378000	4.13E+05	6.35E-06	69633.9
18378000	4.22E+05	6.49E-06	77885.7
19378000	4.31E+05	6.63E-06	86328.3
20378000	4.39E+05	6.75E-06	94943.3
21378000	4.46E+05	6.86E-06	103714.4
22378000	4.52E+05	6.95E-06	112626.9
23378000	4.58E+05	7.04E-06	121667.3
24378000	4.63E+05	7.12E-06	130823.8
25378000	4.68E+05	7.20E-06	140085.3
26378000	4.72E+05	7.26E-06	149441.9
27378000	4.76E+05	7.32E-06	158884.3
28378000	4.79E+05	7.38E-06	168404.1
29378000	4.83E+05	7.42E-06	177993.5
30378000	4.85E+05	7.47E-06	187645.2
31378000	4.88E+05	7.51E-06	197352.6
32378000	4.90E+05	7.54E-06	207109.5
33378000	4.92E+05	7.57E-06	216909.9
34378000	4.94E+05	7.59E-06	226748.4
35378000	4.95E+05	7.62E-06	236619.9
36378000	4.96E+05	7.63E-06	246519.6
37378000	4.97E+05	7.65E-06	256442.9
38378000	4.98E+05	7.66E-06	266385.5
39378000	4.98E+05	7.67E-06	276343.4
40378000	4.99E+05	7.67E-06	286312.7

High Resolution Tabular data: GEO altitude to nominal Ballast altitude.

Radius (m)	**Tension** (N/m^2)	**Elastic Area** (m^2)	**Ribbon mass** (kg)
41378000	4.99E+05	7.68E-06	296289.8
42378000	4.99E+05	7.68E-06	306271.1
43378000	4.99E+05	7.68E-06	316253.4
44378000	4.99E+05	7.67E-06	326233.5
45378000	4.98E+05	7.67E-06	336208.5
46378000	4.98E+05	7.66E-06	346175.3
47378000	4.97E+05	7.65E-06	356131.3
48378000	4.96E+05	7.64E-06	366073.9
49378000	4.95E+05	7.62E-06	376000.4
50378000	4.94E+05	7.61E-06	385908.5
51378000	4.93E+05	7.59E-06	395795.8
52378000	4.92E+05	7.57E-06	405660.1
53378000	4.91E+05	7.55E-06	415499.2
54378000	4.89E+05	7.53E-06	425311.1
55378000	4.88E+05	7.50E-06	435093.7
56378000	4.86E+05	7.48E-06	444845.1
57378000	4.84E+05	7.45E-06	454563.5
58378000	4.82E+05	7.42E-06	464247.2
59378000	4.80E+05	7.39E-06	473894.2
60378000	4.78E+05	7.36E-06	483503.1
61378000	4.76E+05	7.33E-06	493072.2
62378000	4.74E+05	7.30E-06	502599.9
63378000	4.72E+05	7.26E-06	512084.8
64378000	4.70E+05	7.23E-06	521525.3
65378000	4.67E+05	7.19E-06	530920.3
66378000	4.65E+05	7.15E-06	540268.2
67378000	4.63E+05	7.12E-06	549567.8
68378000	4.60E+05	7.08E-06	558817.8
69378000	4.57E+05	7.04E-06	568017.1
70378000	4.55E+05	7.00E-06	577164.5
71378000	4.52E+05	6.95E-06	586258.8
72378000	4.49E+05	6.91E-06	595299.1
73378000	4.46E+05	6.87E-06	604284.2
74378000	4.44E+05	6.82E-06	613213.1
75378000	4.41E+05	6.78E-06	622085.0
76378000	4.38E+05	6.73E-06	630898.8
77378000	4.35E+05	6.69E-06	639653.8
78378000	4.32E+05	6.64E-06	648348.9
79378000	4.29E+05	6.59E-06	656983.5
80378000	4.26E+05	6.55E-06	665556.7
81378000	4.22E+05	6.50E-06	674067.9
82378000	4.19E+05	6.45E-06	682516.2
83378000	4.16E+05	6.40E-06	690900.9
84378000	4.13E+05	6.35E-06	699221.6
85378000	4.10E+05	6.30E-06	707477.4

High Resolution Tabular data: GEO altitude to Nominal Ballast altitude (continued)

Radius (m)	**Tension** (N/m^2)	**Elastic Area** (m^2)	**Ribbon mass** (kg)
86378000	4.06E+05	6.25E-06	715667.8
87378000	4.03E+05	6.20E-06	723792.3
88378000	4.00E+05	6.15E-06	731850.4
89378000	3.96E+05	6.10E-06	739841.4
90378000	3.93E+05	6.04E-06	747765.0
91378000	3.89E+05	5.99E-06	755620.7
92378000	3.86E+05	5.94E-06	763408.0
93378000	3.82E+05	5.88E-06	771126.6
94378000	3.79E+05	5.83E-06	778776.2
95378000	3.76E+05	5.78E-06	786356.2
96378000	3.72E+05	5.72E-06	793866.5
97378000	3.68E+05	5.67E-06	801306.7
98378000	3.65E+05	5.61E-06	808676.6
99378000	3.61E+05	5.56E-06	815976.0

High Resolution Tabular data: Nominal Ballast altitude to Beyond.

Radius (m)	**Tension** (N/m^2)	**Elastic Area** (m^2)	**Ribbon mass** (kg)
100378000	3.58E+05	5.51E-06	823204.5
101378000	3.54E+05	5.45E-06	830310.5
102378000	3.51E+05	5.40E-06	837448.4
103378000	3.47E+05	5.34E-06	844463.4
104378000	3.44E+05	5.29E-06	851406.9
105378000	3.40E+05	5.23E-06	858278.9
106378000	3.36E+05	5.18E-06	865079.2
107378000	3.33E+05	5.12E-06	871807.8
108378000	3.29E+05	5.07E-06	878464.6
109378000	3.26E+05	5.01E-06	885049.6
110378000	3.22E+05	4.95E-06	891562.8
111378000	3.18E+05	4.90E-06	898004.2
112378000	3.15E+05	4.84E-06	904373.8
113378000	3.11E+05	4.79E-06	910671.6
114378000	3.08E+05	4.73E-06	916897.8
115378000	3.04E+05	4.68E-06	923052.5
116378000	3.01E+05	4.62E-06	929135.6
117378000	2.97E+05	4.57E-06	935147.4
118378000	2.93E+05	4.52E-06	941088.0
119378000	2.90E+05	4.46E-06	946957.6
120378000	2.86E+05	4.41E-06	952756.2
121378000	2.83E+05	4.35E-06	958484.1

High Resolution Tabular data: Nominal Ballast altitude to Beyond (continued)

Radius (m)	**Tension** (N/m^2)	**Elastic Area** (m^2)	**Ribbon mass** (kg)
122378000	2.79E+05	4.30E-06	964141.6
123378000	2.76E+05	4.24E-06	969728.7
124378000	2.72E+05	4.19E-06	975245.8
125378000	2.69E+05	4.14E-06	980693.0
126378000	2.65E+05	4.08E-06	986070.7
127378000	2.62E+05	4.03E-06	991379.2
128378000	2.59E+05	3.98E-06	996618.6
129378000	2.55E+05	3.92E-06	1001789.3
130378000	2.52E+05	3.87E-06	1006891.6
131378000	2.48E+05	3.82E-06	1011925.9
132378000	2.45E+05	3.77E-06	1016892.4
133378000	2.42E+05	3.72E-06	1021791.6
134378000	2.38E+05	3.67E-06	1026623.8
135378000	2.35E+05	3.61E-06	1031389.3
136378000	2.32E+05	3.56E-06	1036088.5
137378000	2.28E+05	3.51E-06	1040721.8
138378000	2.25E+05	3.46E-06	1045289.7
139378000	2.22E+05	3.41E-06	1049792.5
140378000	2.19E+05	3.36E-06	1054230.7
141378000	2.16E+05	3.32E-06	1058604.7
142378000	2.12E+05	3.27E-06	1062914.9
143378000	2.09E+05	3.22E-06	1067161.7
144378000	2.06E+05	3.17E-06	1071345.7
145378000	2.03E+05	3.12E-06	1075467.3
146378000	2.00E+05	3.08E-06	1079526.9
147378000	1.97E+05	3.03E-06	1083525.1
148378000	1.94E+05	2.98E-06	1087462.3
149378000	1.91E+05	2.94E-06	1091339.1
150378000	1.88E+05	2.89E-06	1095155.8

1.2.2.2 Low resolution tabular data

This data was derived from GTOSS table input, and represents a minimum-data optimal fit of the ribbon taper (assuming a quadratic interpolation for intermediate points). The format of this data is characterized by Region definitions; thus a Region is defined by the Region-Length (as opposed to radius from earth center), and there is then a bounding value of a parameter at each end of the Region. Note that the sum of the Region lengths nominally would total to the ballast altitude.

Low resolution Tabular data:

Earth's surface to nominal Ballast altitude by Regions

Note: this represents an optimal approximation to the ribbon length-varying parameters, assuming quadratic interpolation is used evaluate properties intermediate to the region boundaries.

Lineal Density (kg/km)	**Cross Section** (mm^2)	**Region Δ Length** ΔL (km)
3.9089	3.010	<= value at Earth
		3048
5.6550	4.3825	
		3048
6.8902	5.3298	
		3048
7.8054	5.9981	
		4572
8.7057	6.7012	
		4572
9.2712	7.1393	
		3048
9.5242	7.3331	
		6096
9.8442	7.5666	
		6096
9.9707	7.6659	
		6096
9.9558	7.6659	
		6096
9.8368	7.5666	
		9144
9.5242	7.3331	
		9144
9.0778	6.9957	
		15240
8.1849	6.2656	
		12192
7.3366	5.6398	
		8656.32
6.7265	5.1689	<= value at Ballast

1.3 NOMINAL TENSION AND STRESS STATES

The graphs below illustrate the tension and stress profiles associated static positioning of a 18,000 kg climber at various altitudes. From this, similar tension profiles for an object at other altitudes become readily apparent.

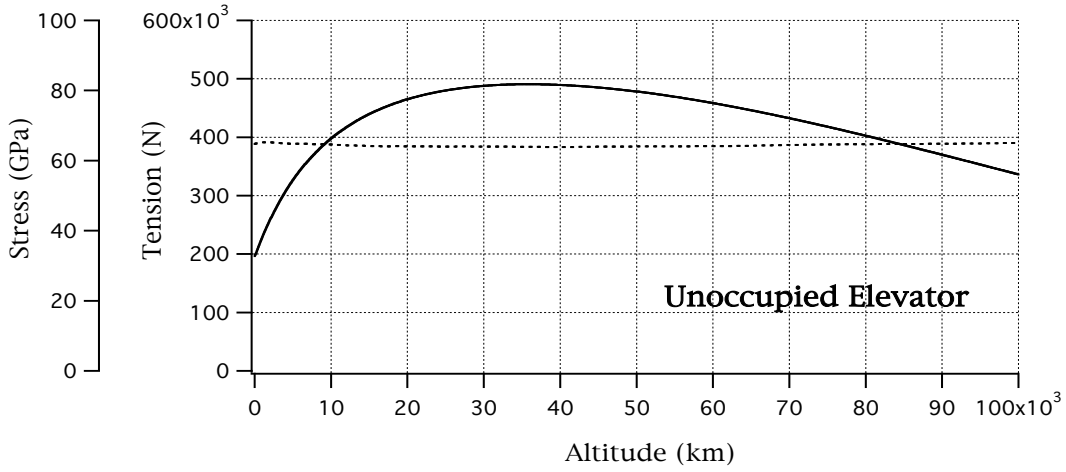

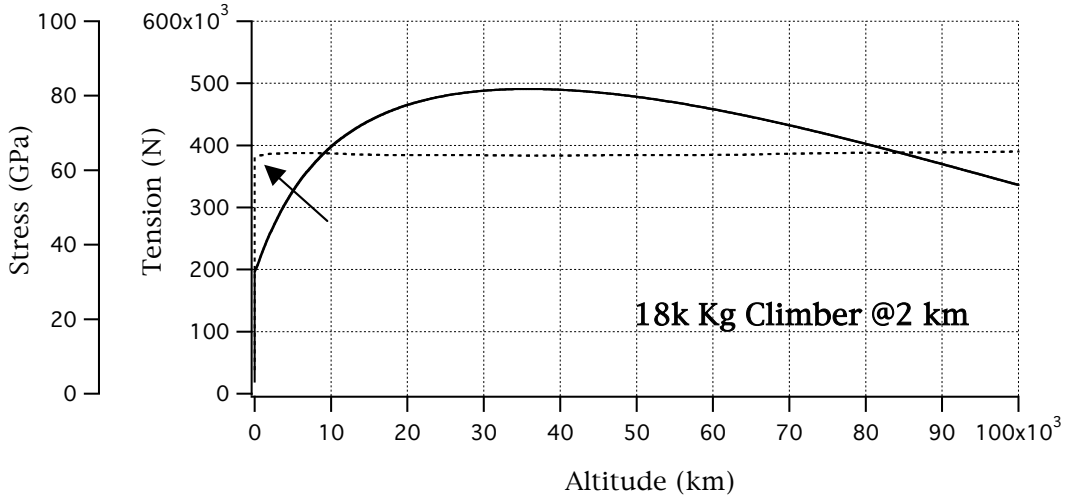

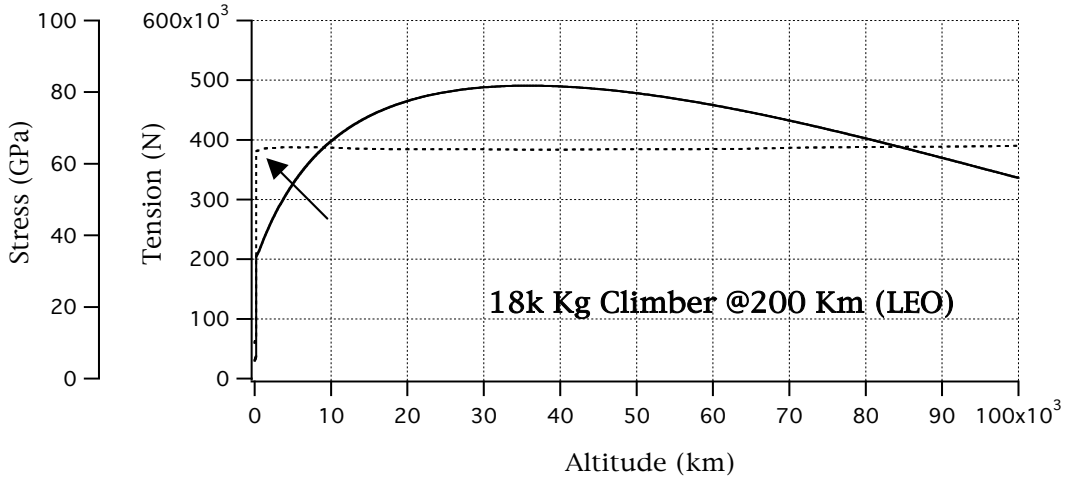

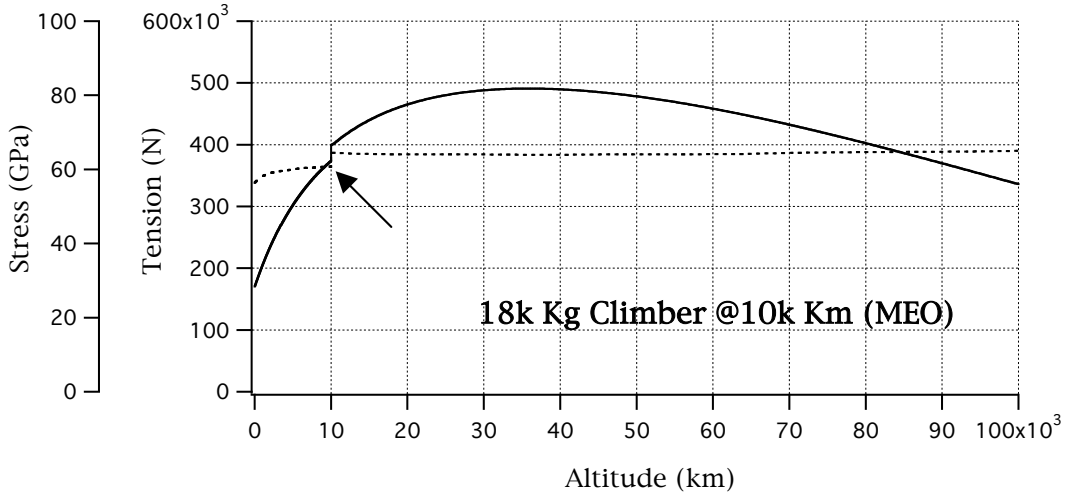
Stress (GPa)
Tension (N)
Altitude (km)
18k Kg Climber @10k Km (MEO)

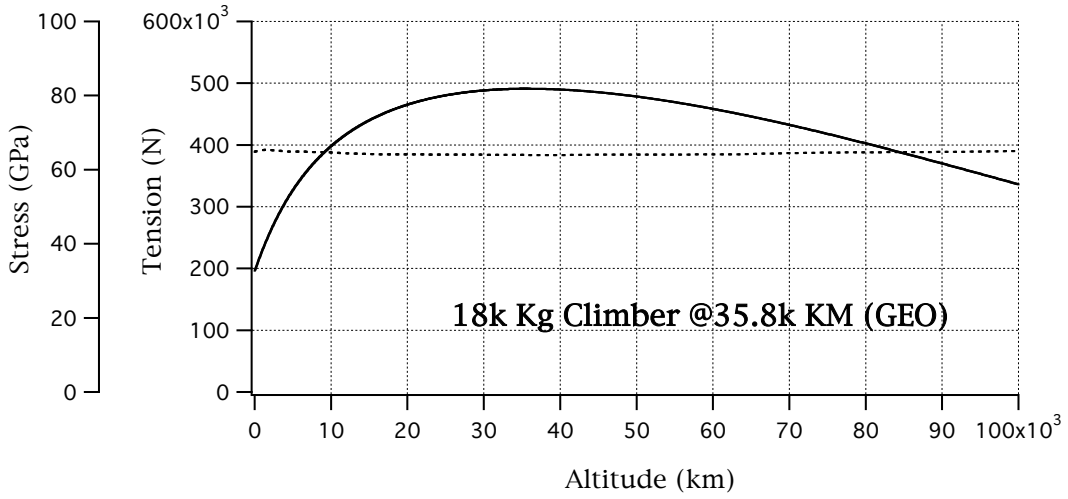
Stress (GPa)
Tension (N)
Altitude (km)
18k Kg Climber @35.8k KM (GEO)

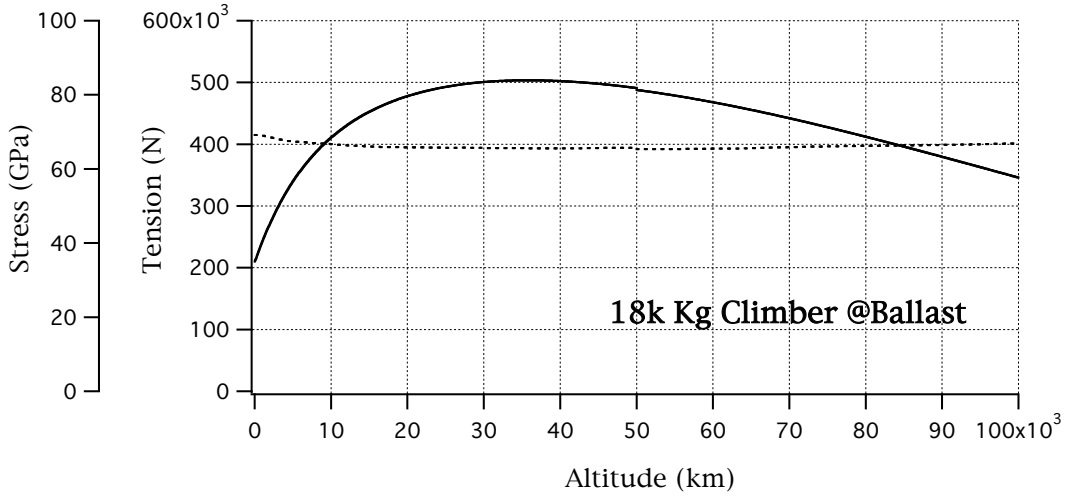
Stress (GPa)
Tension (N)
Altitude (km)
18k Kg Climber @Ballast

The two graphs below provide a low altitude magnified composite view of tension and stress profiles for all the above cases.

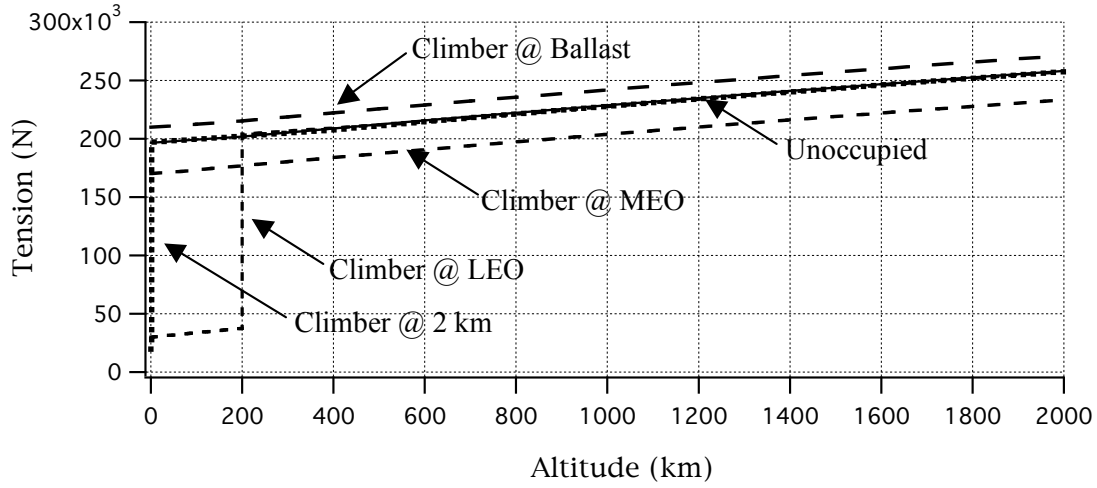

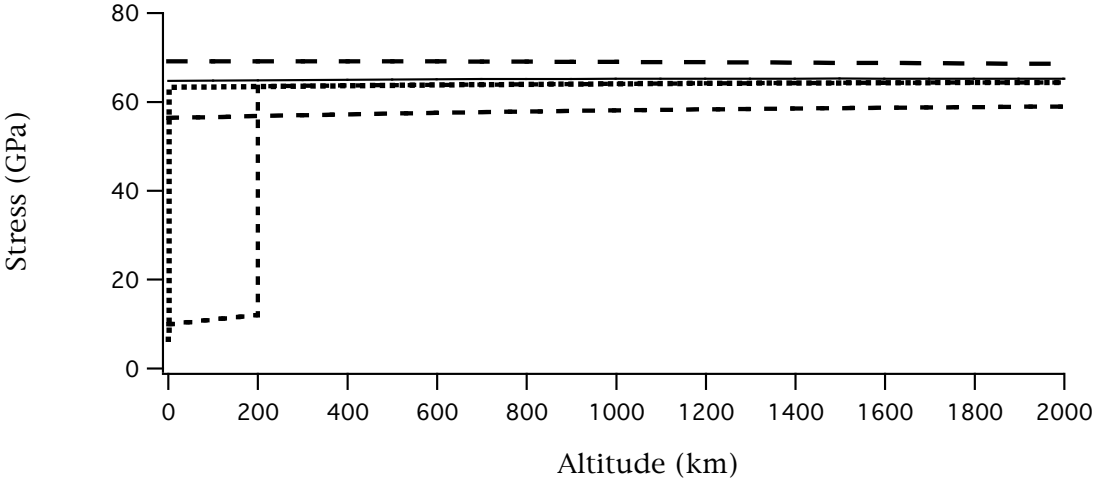

1.4 GRAVITY-WELL SIMULATION CONVERGENCE

To properly simulate a space elevator configuration using a discrete nodal approach, one must pay attention to the spatial-convergence of the simulation as it pertains to the "gravity well" (ie. inverse-square planetary gravity model). The graph below depicts (for the Earth) the tension at the anchor point as a function of the number of "uniformly-spaced" nodes used to simulate the elevator ribbon.

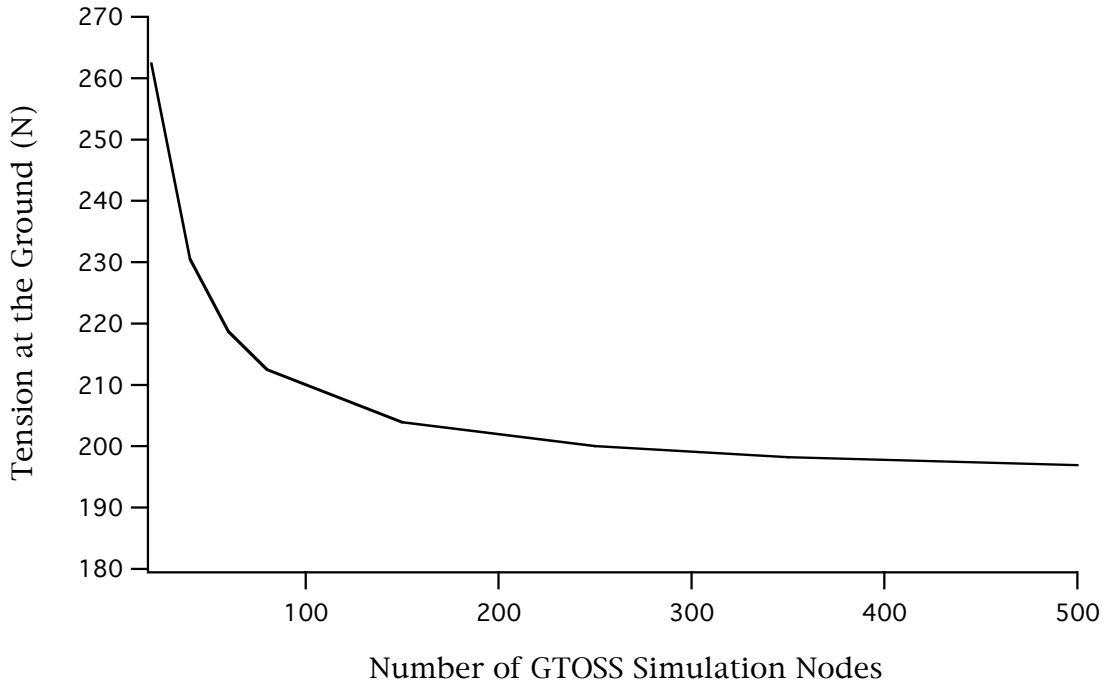

It can be seen that for node-counts greater than 200, the earth's gravity-well is being fairly well acknowledged. For lesser node counts, simulation results may still be acceptable, depending upon the degree to which total-available anchor tension must be fully realized.

Note also, that *non-uniform* distributions of lesser node-counts (for instance 100 nodes from ground to 10,000 km, then 50 nodes between there and ballast, etc) may suffice to fully acknowledge the gravity well.

1.5 USEFUL FORMULAS FOR TETHER DYNAMICS

1.5.1 Definition of Symbols

σ = Stress

ε = Strain

T = Tension

L = Length

E = Young's modulus

d = Elastic diameter

A = Elastic cross sectional area

ρ = Volumetric mass density

ρ_L = Lineal mass density (= $\frac{\rho}{A}$)

β = Material intrinsic damping factor (sec)

δ = End-to-End tether elongation

K_{eff} = Effective end-to-end spring constant

$K_{D_{eff}}$ = Effective end-to-end damping constant

1.5.2 From Classical Small Amplitude String Theory

Transverse: Natural Frequencies f^T_n Wave Propagation Speed S^T

$$f^T_n = \frac{n}{2L}\sqrt{\frac{T}{\rho_L}} = \frac{n}{2L} S^T$$

$$S^T = \sqrt{\frac{T}{\rho_L}}$$

Longitudinal: Natural Frequencies f^L_n Stress Propagation Speed S^L

$$f^L_n = \frac{n}{2L}\sqrt{\frac{AE}{\rho_L}} = \frac{n}{2L} S^L$$

$$S^L = \sqrt{\frac{E}{\rho}} = \sqrt{\frac{AE}{\rho_L}}$$

1.5.3 Plumb-Bob (Yo-Yo) Oscillations

Plumb Bob (Longitudinal) Frequency (2 masses and a spring):

$$f_n^{YoYo} = \frac{1}{2\pi}\sqrt{\frac{K_{eff}\,(M_1 + M_2)}{M_1\,M_2}}$$

1.5.4 Elastic Diameter -vs- End-to-End Spring Rate

Relationship of Equivalent Elastic Diameter to the tether Effective End-to-End Spring-Rate Constant:

$$d = \sqrt{\frac{4\,L\,K_{eff}}{\pi\,E}}$$

$$K_{eff} = \frac{A\,E}{L}$$

1.5.5 Damping Relationships

Definition of **Equivalent End-to-End Damping Constant** $K_{D_{eff}}$: $T_{D_{exp}} = K_{D_{eff}} \frac{d\delta}{dt}$

Where: $T_{D_{exp}}$ is the tension experienced at attach points *due to damping alone*.

Definition of **Material Intrinsic Damping Factor** β: $\sigma = E(\varepsilon + \beta \frac{d\varepsilon}{dt})$

Relationship between Equivalent End-to-End Damping constant and the conventional Spring-Rate constant.

$$K_{D_{eff}} = \beta\, K_{eff}$$

1.5.6 Segment -vs- Overall Effective-Attributes Relations

Relationship between Equivalent End-to-End constants, and an N segment discrete (bead modeled) tether:

$K_{seg} = N K_{eff}$ Where: K_{seg} = Seg-equivalent to the End-to-end spring constant

$K_{Dseg} = N K_{Deff}$ Where: K_{Dseg} = Seg-equivalent to the End-to-end damping constant

1.5.7 Stretched Uniform Spring with Intermediate Mass

This addresses the effect upon oscillation frequency of positioning a concentrated mass, **M**, at an intermediate distance **x** from one end, along a stretched uniform spring of length **L** and an End-to-End Effective spring rate of $\mathbf{K_E}$. The applicability of this simplified model is to approximate Longitudinal Bobbing-Frequencies of a climber mass at any point on the elevator ribbon from ground to ballast.

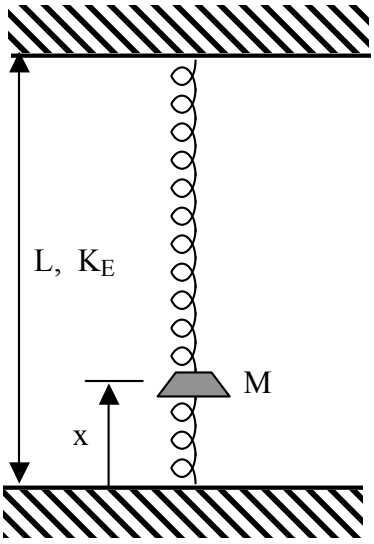

The circular frequency ω is:

$$\omega = \omega_E \sqrt{\frac{1}{\lambda(1-\lambda)}} \qquad \text{with: } f = \frac{\omega}{2\pi} \qquad \text{and Period, } T = \frac{1}{f}$$

$$\text{where: } \lambda = \frac{x}{L} \quad \text{and,} \quad \omega_E = \sqrt{\frac{K_E}{M}}$$

Note that ω_E is simply the circular frequency of mass M, under the action of a single spring with spring constant K_E (which is the lowest effective spring rate associated with the ribbon). The frequency ω_E would be that of the climber positioned near the anchor (or ballast), while *assuming* the (short) ribbon between the climber and anchor (or ballast) does not exist; ω_E would be the *lowest* longitudinal Bobbing frequency associated with the Climber and the elevator-ribbon-system; the longitudinal Bobbing frequency of the ballast being the lowest). Note that the frequency ω_E is NOT close to values of ω corresponding to *small values of* λ, as these frequencies could be quite high (due to the high spring rate of the short ribbon segment between the climber and either end). Values of ω corresponding to small values of λ may only manifest in piecewise fashion due to potential discontinuous non-linear slack-taut motion that may ensue with an actively bobbing climber near either end of the ribbon.

Below is shown a typical plot of Longitudinal Bobbing Period corresponding to values of λ spanning climber positions from the ground to the ballast for the nominal elevator configuration addressed in this handbook.

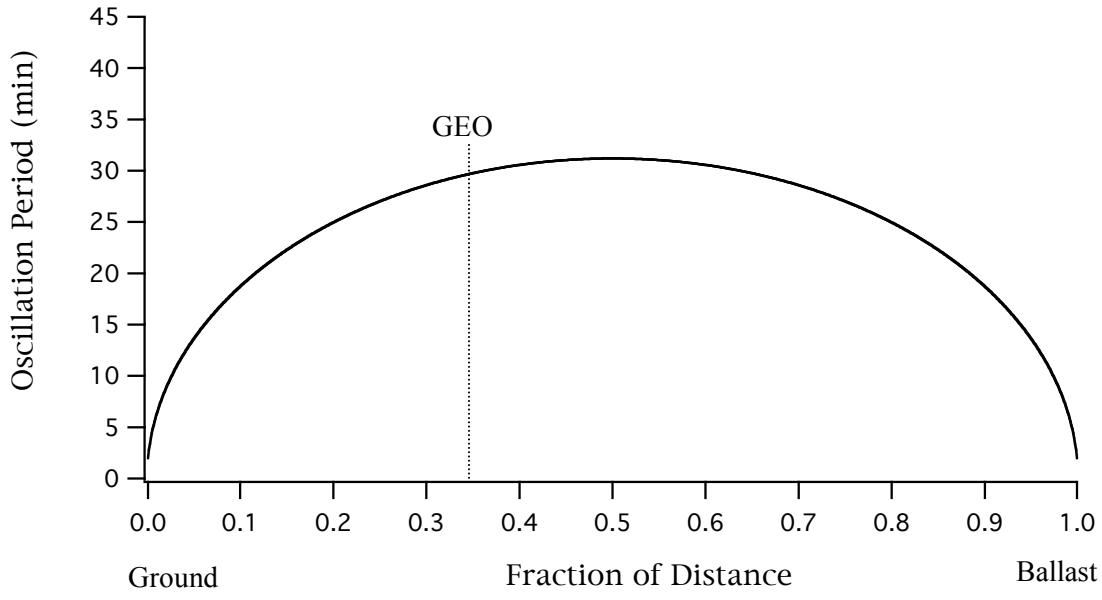

2.0 GENERAL DYNAMICS

2.1 LIBRATION DYNAMICS

The space elevator has two natural modes of oscillation whereby the ribbon, while essentially maintaining a straight line, pendulum's back and forth both in the plane of earth rotation, and normal to the plane of rotation. These are termed "in-plane libration" (east/west motion relative to the vertical), and "out-of-plane libration" (north/south motion relative to the vertical).

For small linear oscillations, the frequencies of these two are:

In-Plane (East-West) Libration: 135.6 hrs = 5.65 days (= 488 Ksec)

Out-of-Plane (North-South) Libration: 23.95 hrs = 0.98 days (= 86.2 Ksec)

Note the difference between in and out-of-plane frequencies; this is characteristic of large scale tether dynamics in free earth orbit, and is even more exaggerated in the case of the space elevator. A heuristic way to look at this difference between in and out-of-plane behavior for the space elevator relates to the fact that in-plane libration involves motion *in the direction of the point of constraint* (ribbon anchor), while out-of-plane libration involves motion *normal to the motion of the anchor*. In the case of in-plane motion for example, a velocity perturbation causing libration deflection eastward also experiences the anchor point progressing eastward under it, thus slowing overall eastward migration of the ribbon, producing a longer time period to reach a given libration angle. Such an intuitive explanation mayor may not be accurate, but what is accurate are the governing equations of motion, in which this effect manifests itself precisely in the equations as certain relative-motion coupling terms, for which an intuitive explanation, while possibly satisfying, is not required to produce the effect.

2.1.1 In-Plane Libration

For a perfectly stable elevator, the ballast has a velocity relative to the earth anchor point of 7292 m/s in-plane (= 23,900 ft/sec = 16,300 mph), and *zero velocity* out-of-plane. All the graphs of libration response below were produced by introducing various "speed perturbations" to the ballast; in the case of in-plane perturbations, these ranged up to about 10% over-speed (relative to the nominal stable in-plane relative velocity).

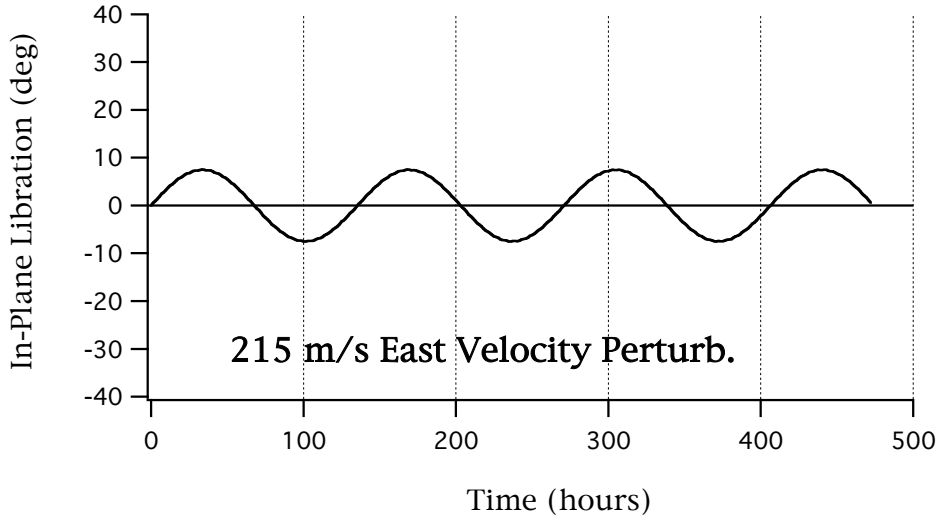

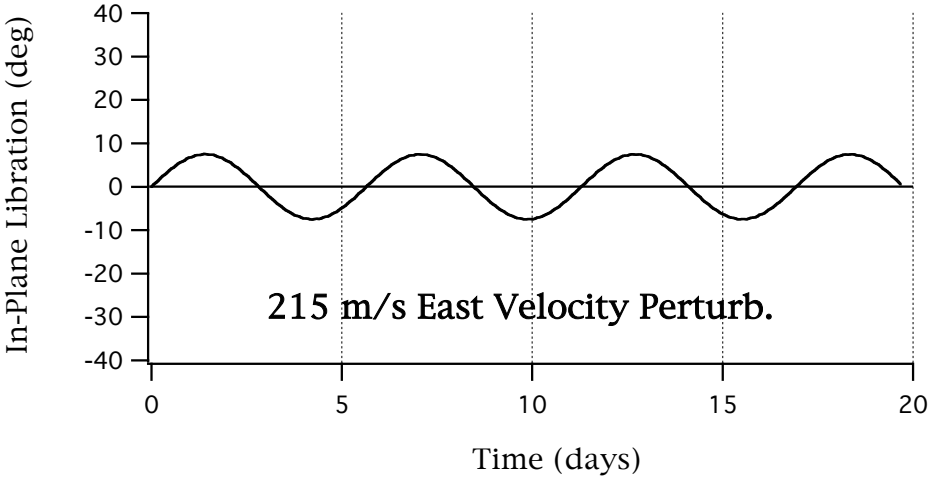

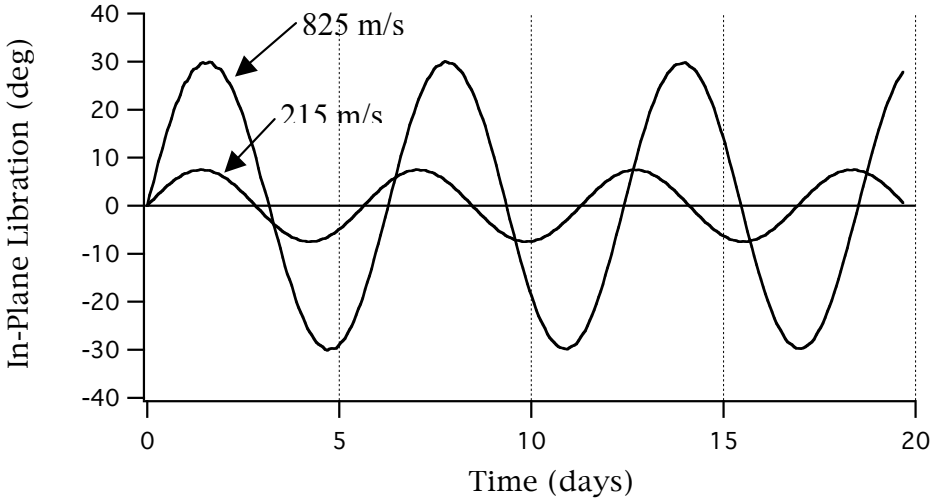

The graph above shows how both amplitude and period increase as in-plane libration perturbation increases.

Below is shown the peak amplitude and period of in-plane libration as a function of perturbation velocity.

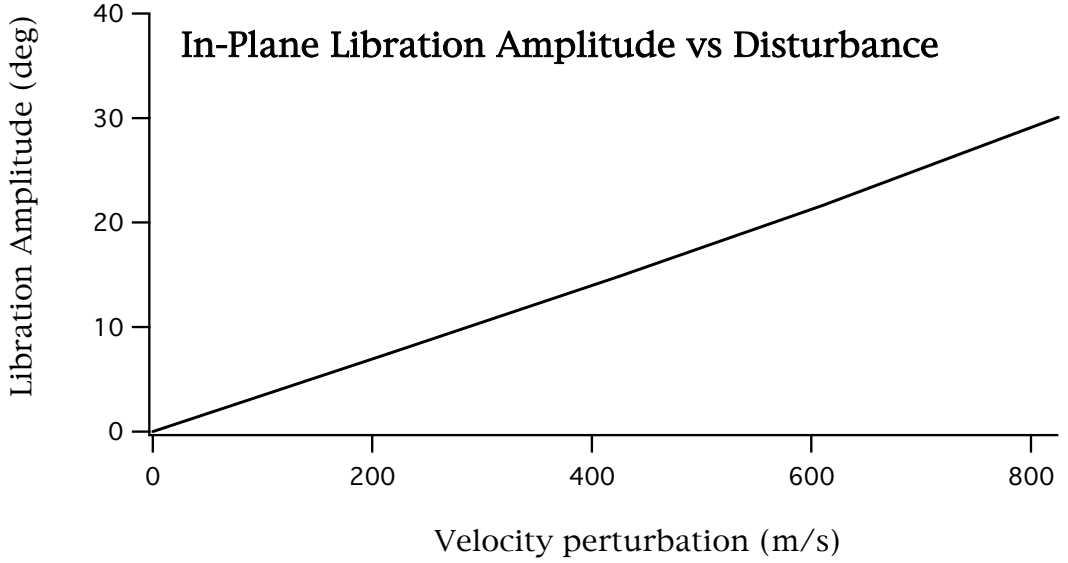

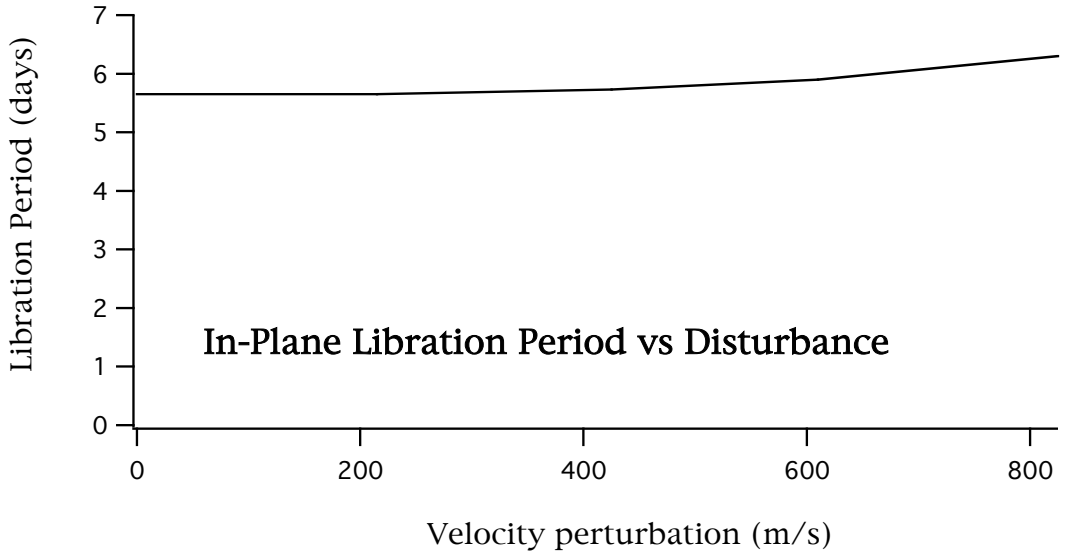

2.1.2 Out-of-Plane Libration

For a perfectly stable elevator, the ballast has an out-of-plane velocity relative to the earth anchor point of *zero*. All the graphs of out-of-plane libration response below were produced by introducing various "speed perturbations" to the ballast; in the case of out-of-plane perturbations, these ranged up to almost 5000 m/s.

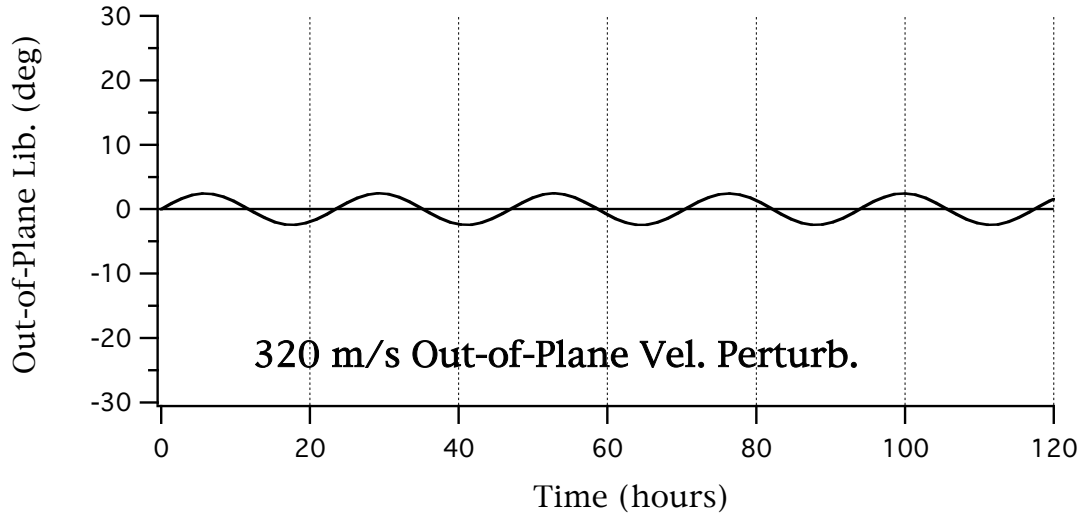
Out-of-Plane Lib. (deg)
30
20
10
0
-10
-20
-30
320 m/s Out-of-Plane Vel. Perturb.
0
20
40
60
80
100
120
Time (hours)

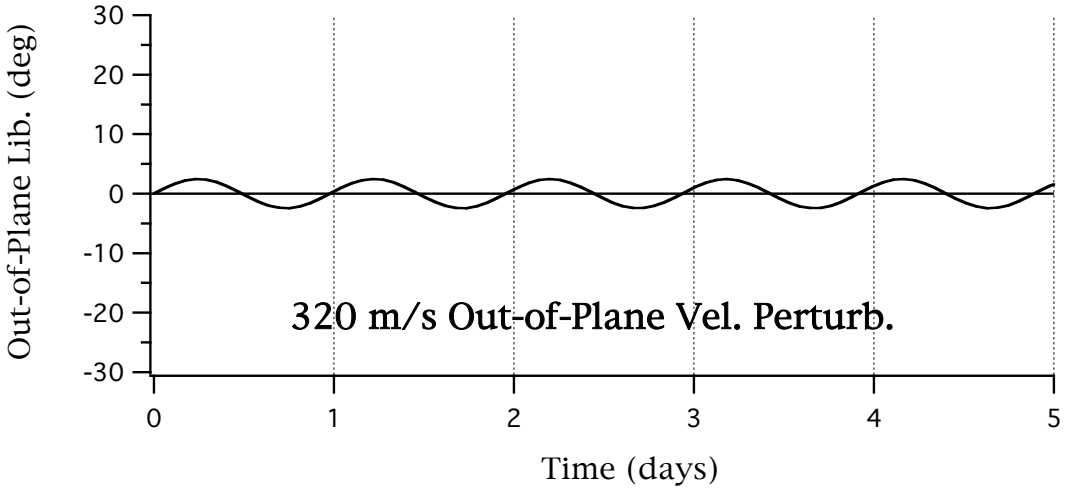
Out-of-Plane Lib. (deg)
30
20
10
0
-10
-20
-30
320 m/s Out-of-Plane Vel. Perturb.
0
1
2
3
4
5
Time (days)

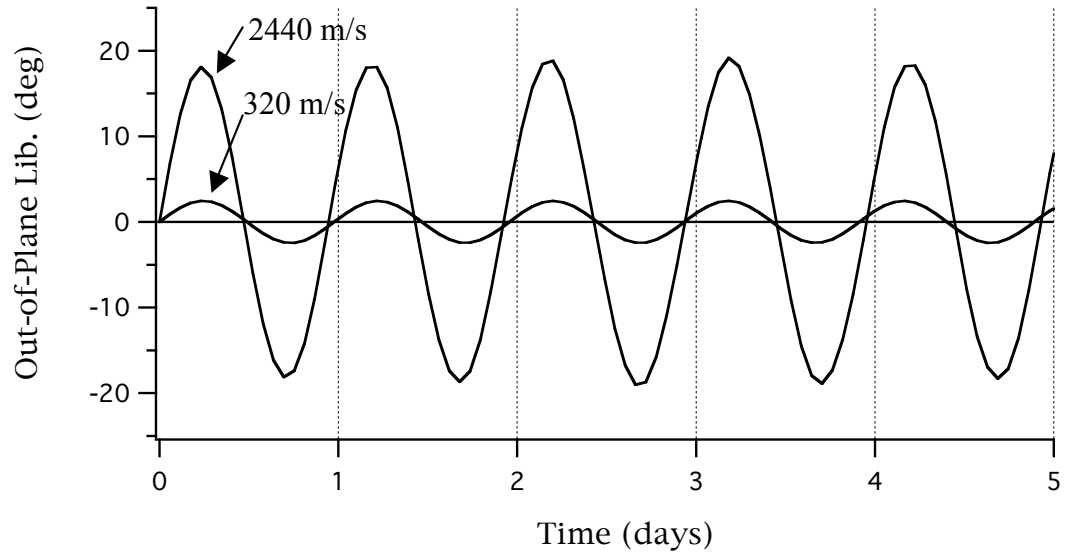
Out-of-Plane Lib. (deg)
2440 m/s
320 m/s
20
10
0
-10
-20
0
1
2
3
4
5
Time (days)

The graph above shows that unlike in-plane libration, out-of-plane libration period is very insensitive to libration amplitude.

The graph below shows how out-of-plane libration amplitude varies as a function of velocity perturbation.

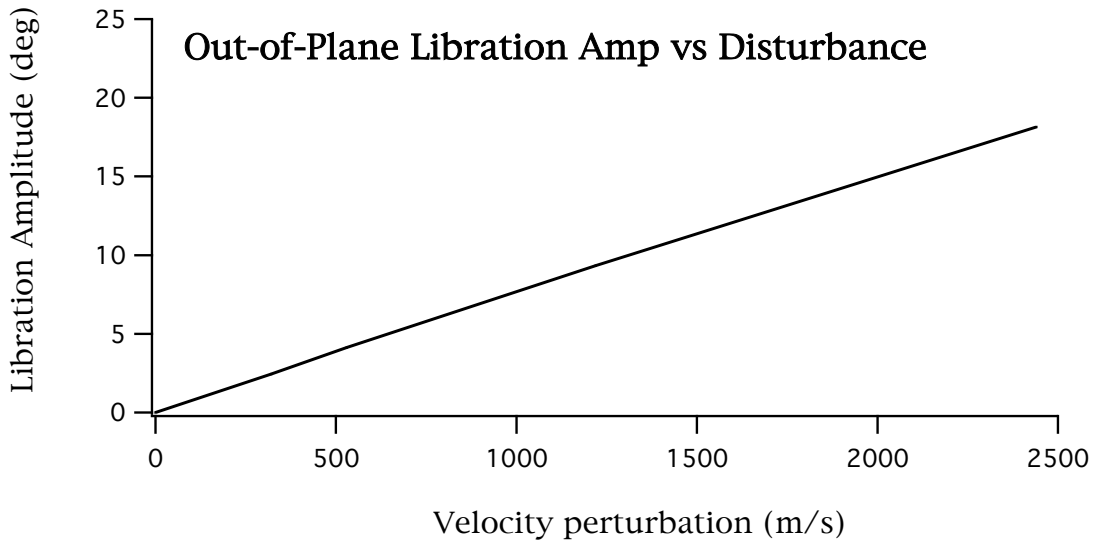

2.1.3 Libration Coupling

> Point of Interest: Coupling of out-of-plane libration into in-plane libration can occur due to the effects of Coriolis acceleration and in/out of plane velocity resolution. At low amplitudes this is very mild; at large amplitudes it can be significant.

The graphs below illustrate coupling of out-of-plane libration into in-plane libration for two different levels of out-of-plane libration.

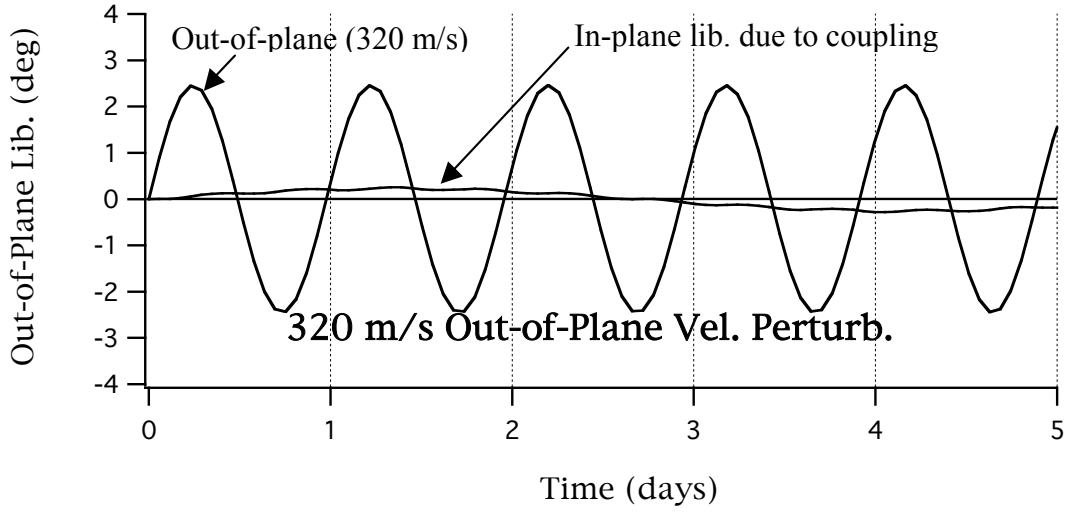

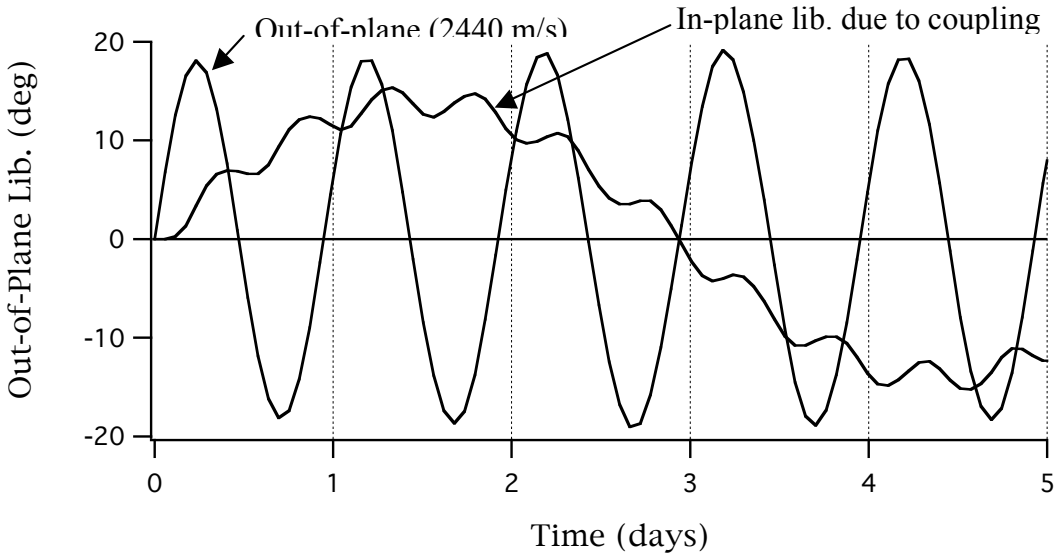
Out-of-plane (2440 m/s)
In-plane lib. due to coupling
Out-of-Plane Lib. (deg)
20
10
0
-10
-20
0
1
2
3
4
5
Time (days)

2.2 LONGITUDINAL DYNAMICS

This section provides information about the various types of dynamics responses characteristic of the longitudinal axis of a space elevator

2.2.1 Longitudinal Bobbing Mass Response

Longitudinal bobbing response of the space elevator manifests different attributes at different altitudes. Longitudinal bobbing was initiated by imparting a 10 m/s positive altitude rate to an otherwise stable elevator configuration. The overview presented here starts with an unoccupied elevator with just a Ballast mass to which an altitude rate is imparted; all other cases have a climber attached in a stable configuration prior to being given a positive altitude rate, thus these results also are equivalent to the sudden arrest of a climber traveling upward at 10 m/s. The results below present disturbances at varying locations of interest along the ribbon.

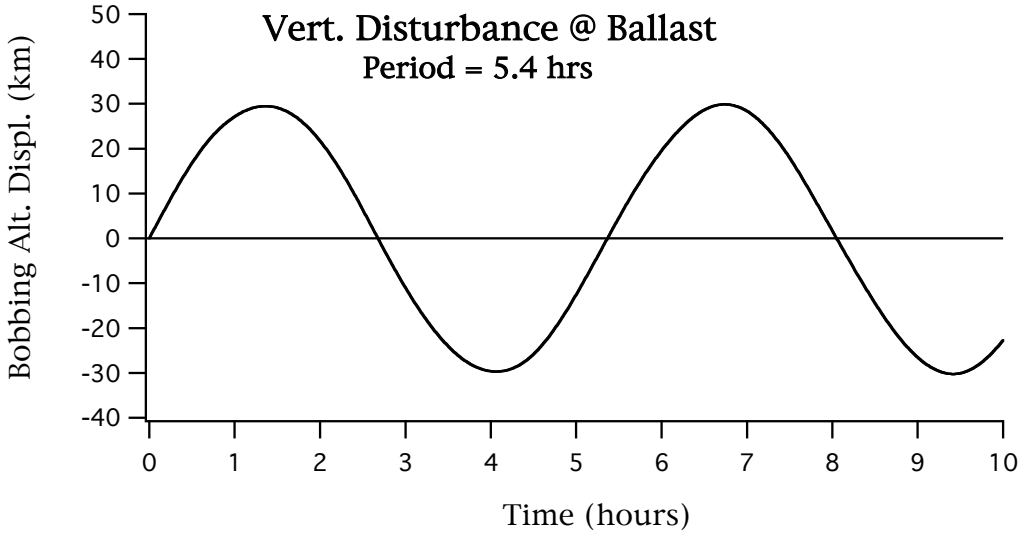

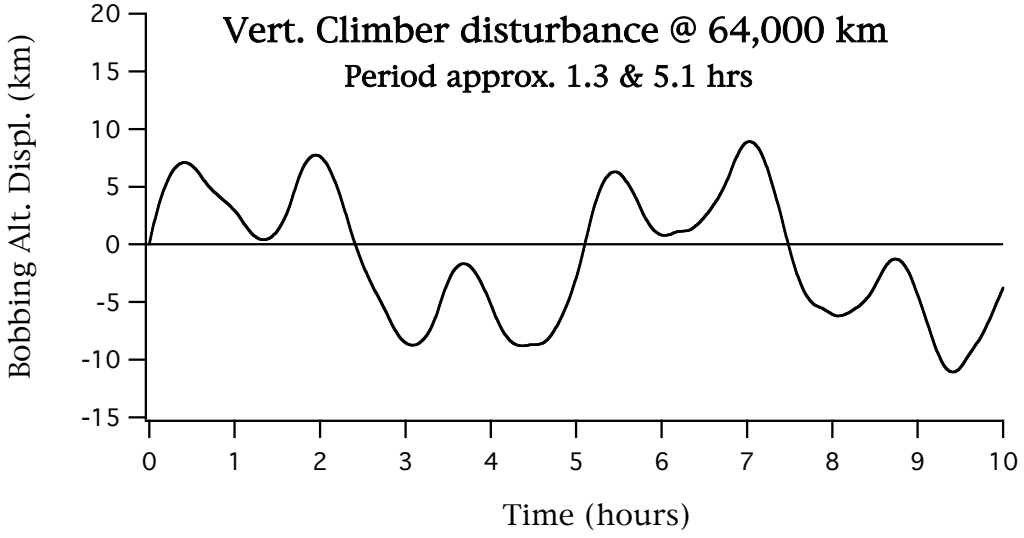

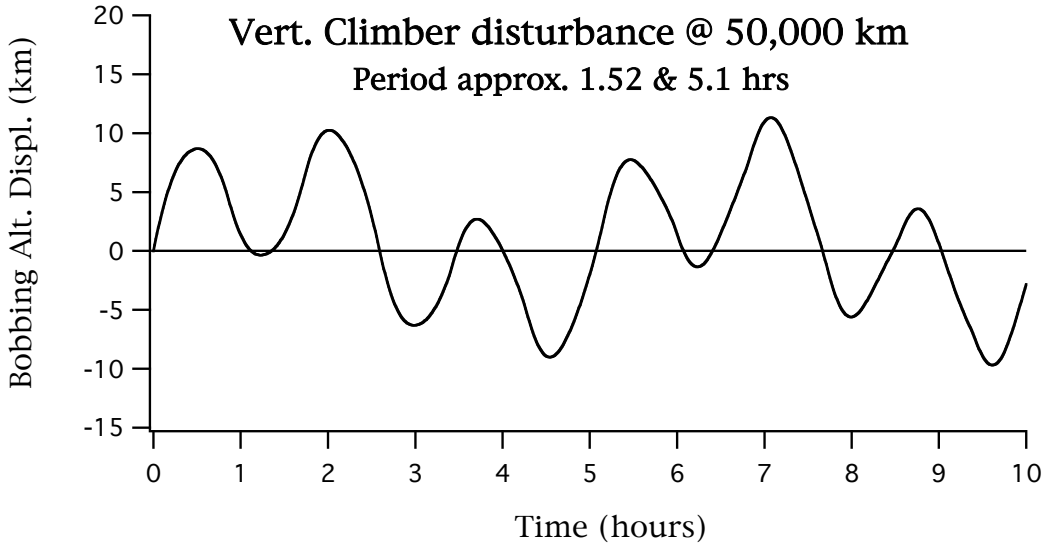
Vert. Climber disturbance @ 50,000 km
Period approx. 1.52 & 5.1 hrs
Bobbing Alt. Displ. (km)
20
15
10
5
0
-5
-10
-15
0
1
2
3
4
5
6
7
8
9
10
Time (hours)

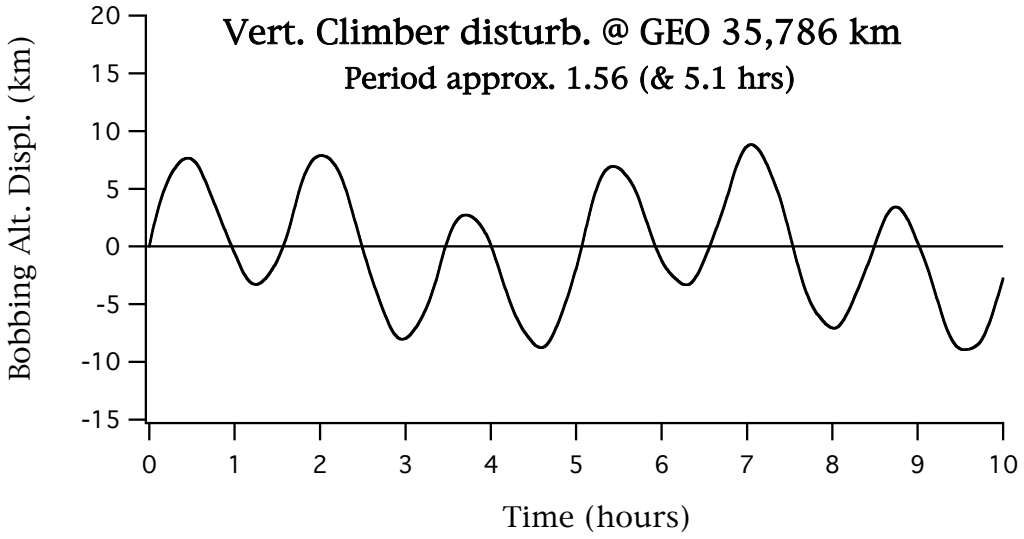
Vert. Climber disturb. @ GEO 35,786 km
Period approx. 1.56 (& 5.1 hrs)
Bobbing Alt. Displ. (km)
20
15
10
5
0
-5
-10
-15
0
1
2
3
4
5
6
7
8
9
10
Time (hours)

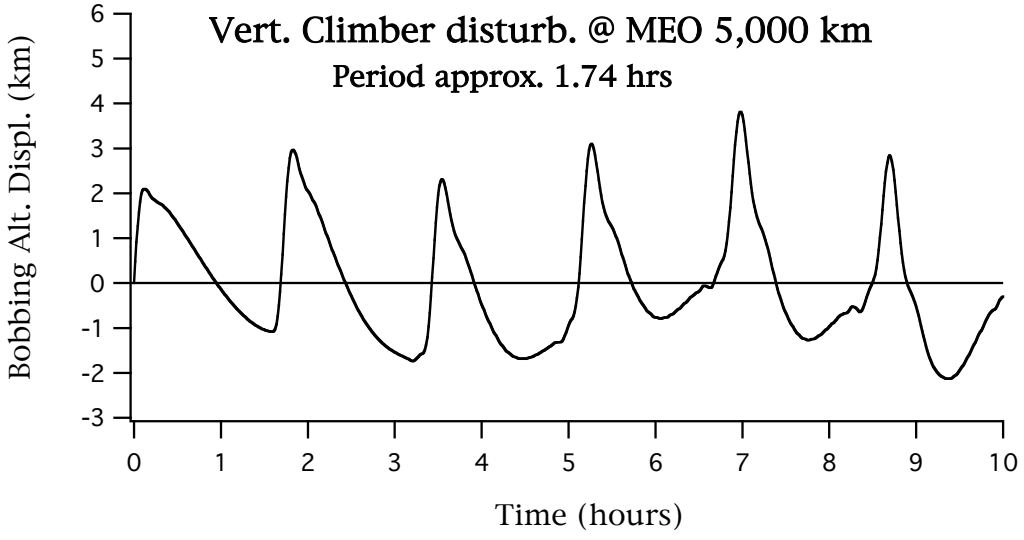
Vert. Climber disturb. @ MEO 5,000 km
Period approx. 1.74 hrs
Bobbing Alt. Displ. (km)
6
5
4
3
2
1
0
-1
-2
-3
0
1
2
3
4
5
6
7
8
9
10
Time (hours)

The response at MEO (above) is starting to manifest the effects of the growing differences in the effective spring rates of the ribbon above and below the climber as the distance between the climber and ground diminishes.

Point of Interest: Only the case of the unoccupied elevator, with the ballast given a longitudinal disturbance, produces what is essentially simple harmonic spring mass response; all other manifestations of longitudinal response are of more a complex vibratory motion. This can be attributed to the fact that the climber might be simplistically thought of a mass attached to two springs of different spring rates (the upper and lower ribbons), each of which is under a different pre-load (due to the presence of the climber itself in the gravity field); and this combined with the significant mass/elasticity of the ribbon itself.

The longitudinal bobbing shown below for the case of a climber at LEO (200 km) appears to present two extremely diverse frequency components, one of 3.25 minute period, and the other, almost 2 hours. The high frequency is due to the interaction of the climber with the high spring rate of the relatively short ribbon section (200 km) interposed between the ground and the climber (this compared to the almost 100,000 km long spring between the ballast). This interaction is shown to be larger damped out by 15 minutes. However, the stress perturbation signature experienced by the ribbon was broadcast in both directions along the ribbon. That headed towards the ground reappears in such a short time (round trip to ground and back being about 7 sec) that it is essentially being seen as a part of the initial response; that headed towards the climber however, has a 1.58 hour round trip facing it. Thus, well over an hour later reappears at the climber to again perturb it. The ensuing re-appearances of this rogue-disturbance become increasing complex by interaction with its own reflections, the climber mass, and the mass of the ribbon itself.

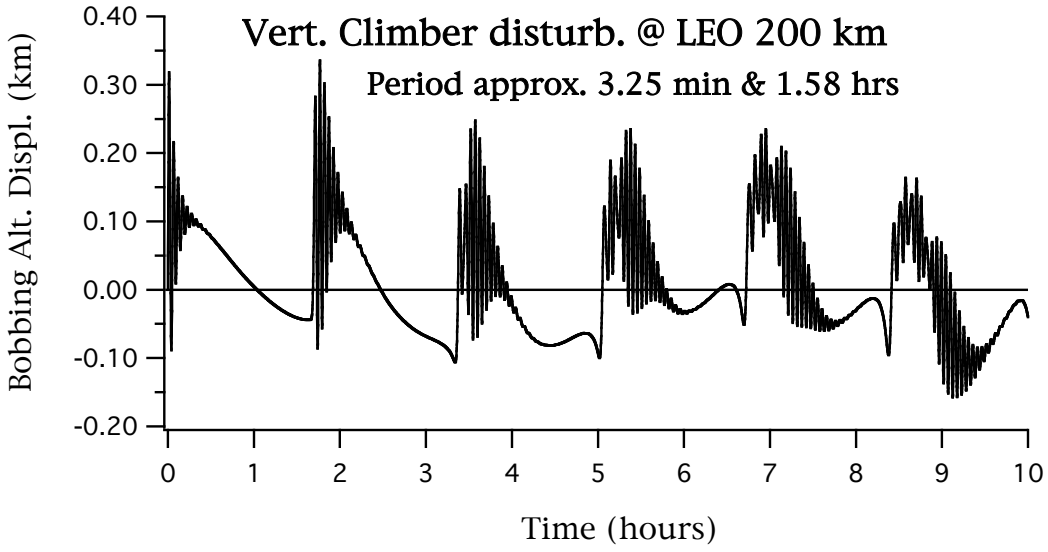

The two graphs below depict these characteristic wave responses in finer detail.

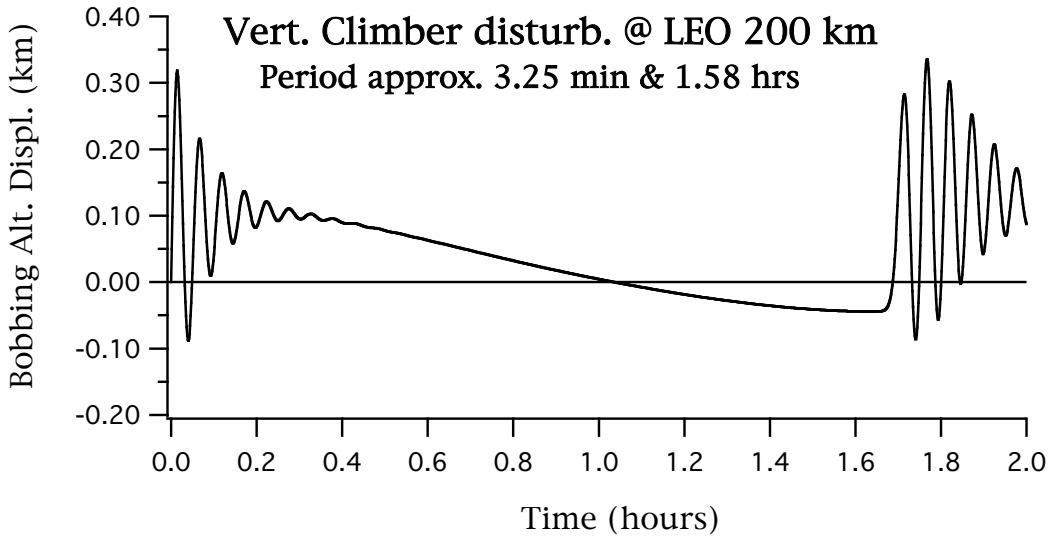

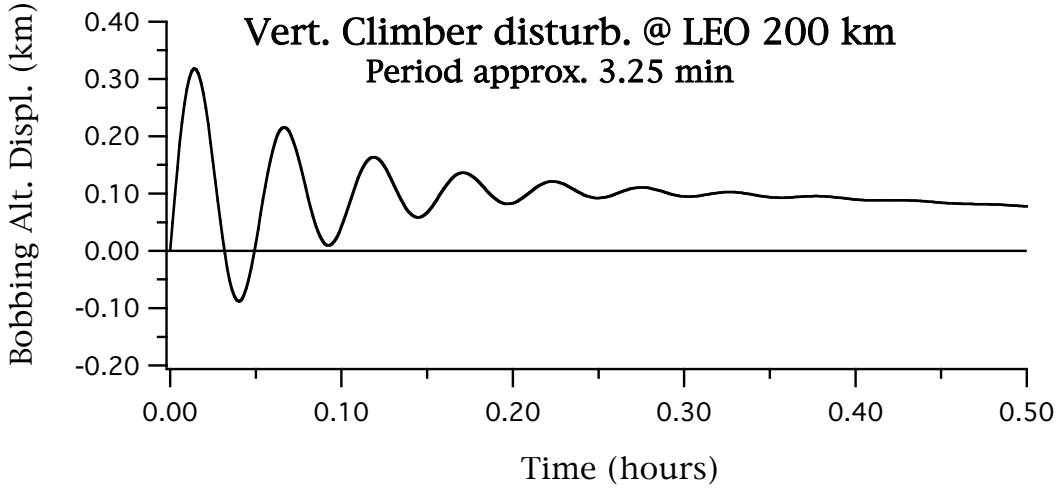

Point of Interest: The longitudinal response shown for the case of the climber at LEO and MEO would be essentially duplicated if the climber were to be suddenly arrested within 200 km of the ballast mass. Such complexity of motion is already beginning to manifest itself in the case (above) of the longitudinal disturbance at 64,000 km.

2.2.2 Longitudinal Stress Response

The case (above) of climber longitudinal bobbing at LEO altitude presented a situation where the propagation and reflection of stress waves along the ribbon was both of sufficiently short and long duration (compared to the original disturbance), that there was both a *coalescence* and a *disassociation* of the reflections with the original disturbance. Two phenomena manifest themselves in longitudinal dynamics, (a). propagation of transient stress disturbances, and, (b) coherent propagations that manifest themselves as longitudinal natural elastic (ie. normal) modes of the ribbon mass-elasticity continuum. As distinguished from random stress disturbance propagation, longitudinal natural modes are characterized by all the particles of the ribbon moving at the same frequency (ie. in phase, but not necessarily in the same direction).

> Point of Interest: the term "Longitudinal Distortion" refers to the amount that a ribbon particle is displaced axially from the position it would occupy were the ribbon in a quiescent state under no external forces. So, by necessity, a perfectly stable elevator would exhibit a **non-zero** longitudinal distortion, this being required to equilibrate the ribbon particles via internal ribbon stress against the external gravity-centripetal field.

Shown below is the Longitudinal Distortion inherent in a stable, unoccupied elevator ribbon. This is a longitudinally un-symmetrical distribution, unlike the distortion distributions of classical natural longitudinal modes. Note that in order to invoke strong natural "longitudinal modal responses", initial peak displacements for the modal initialization must significantly over-shadow this initial strain state; thus, for the natural mode initializations shown later, the peak amplitudes are 100,000 m (compared to 8,000 m for the stable elevator configuration shown below).

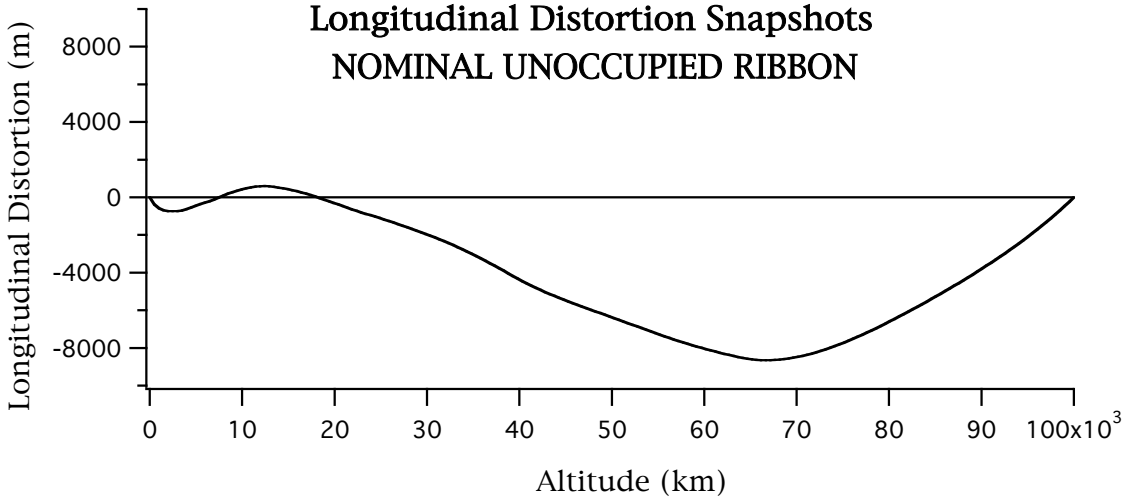

2.2.2.1 Longitudinal natural modes

Examples of response for the first two natural modes are shown below. Note that these modes do not exhibit pristine behavior due to the fact that longitudinal initialization is attempted in the form of sinusoidal shapes applied against the longitudinal distortion extant in the elevator ribbon due to its stabilized state in the presence of the combined gravity-centripetal field. Such anomalies manifest themselves in the form of "modal displacement shapes" and time histories of stress-related parameters (like tension) that do not exhibit pristine sinusoidal shapes. Nodal points (that classically exhibit null response) will correspondingly be ill defined.

Below are results for ribbon response given an initial state corresponding to the first longitudinal natural mode.

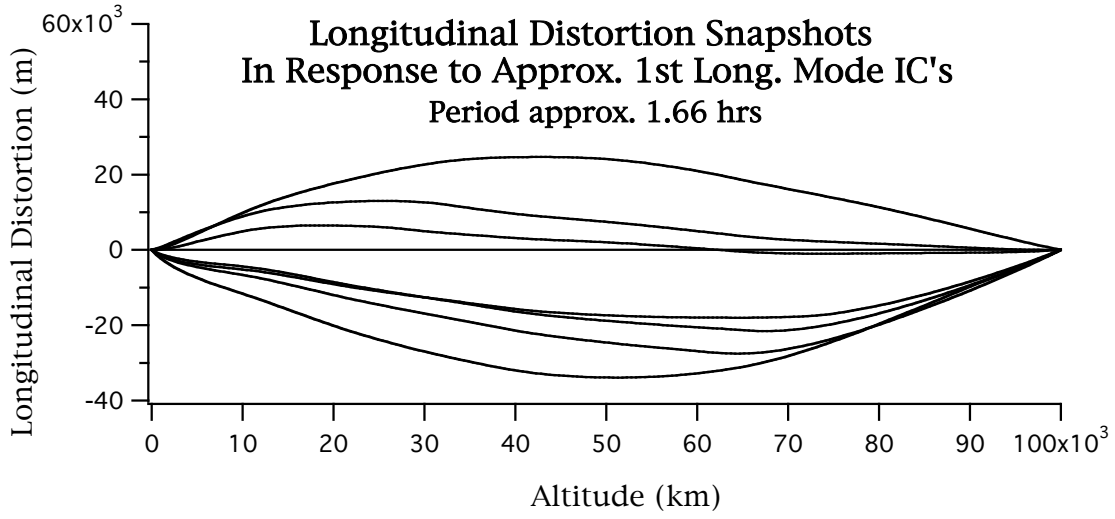

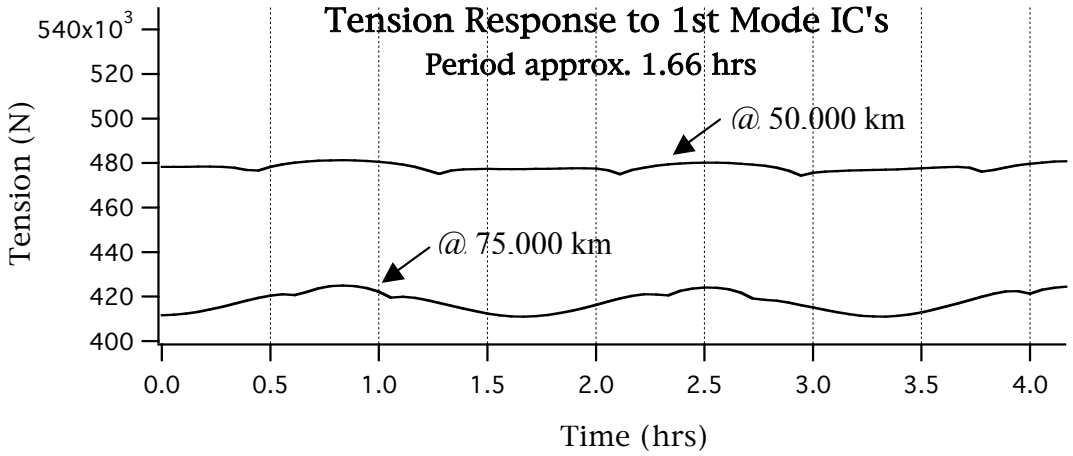

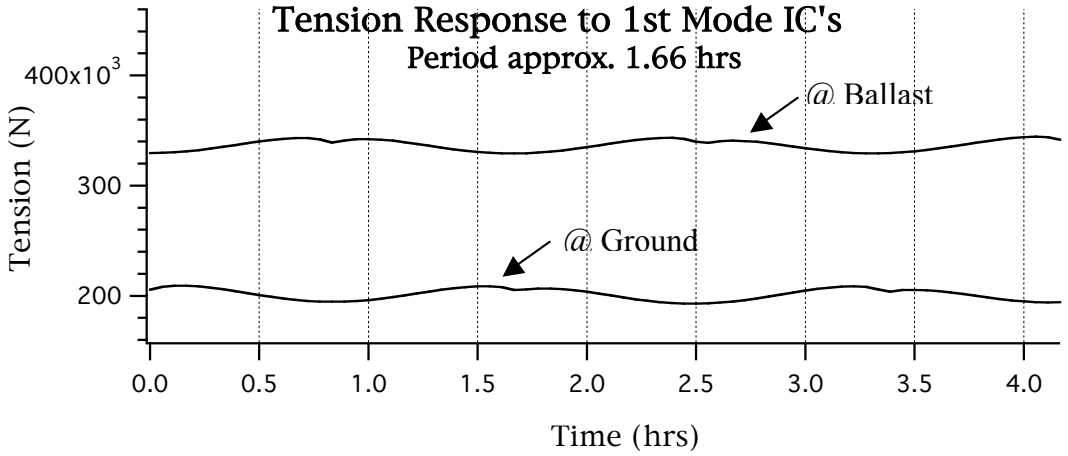

Below are results for ribbon response given an initial state corresponding to the first longitudinal natural mode.

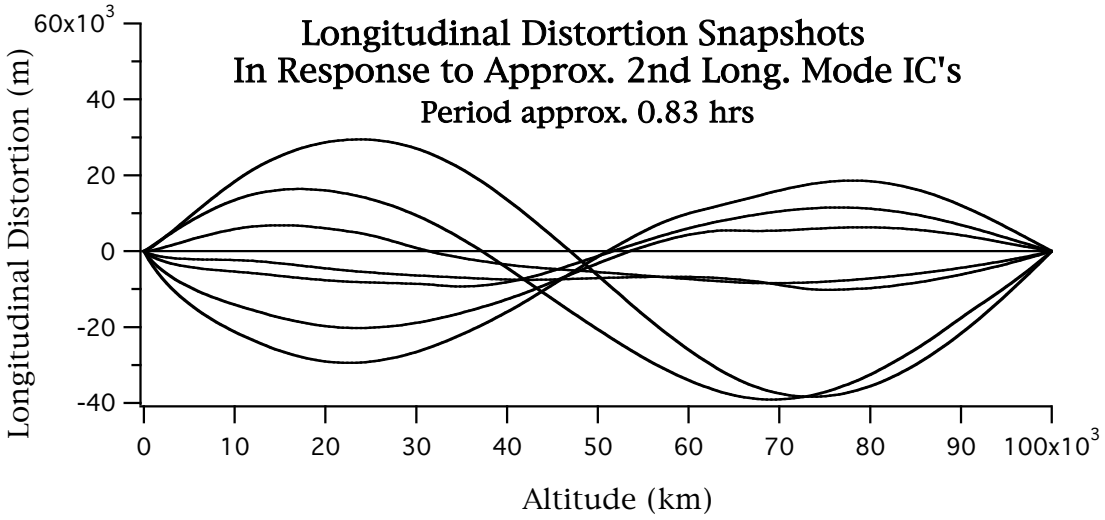

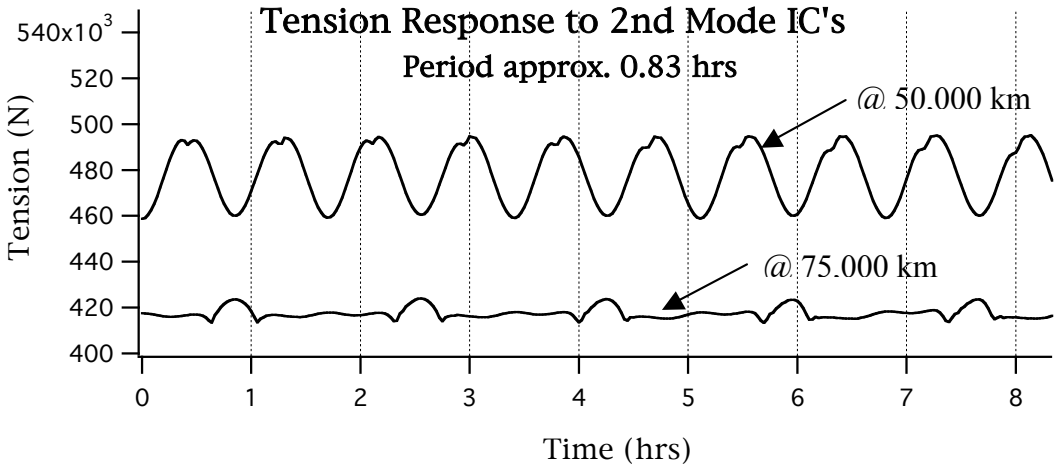

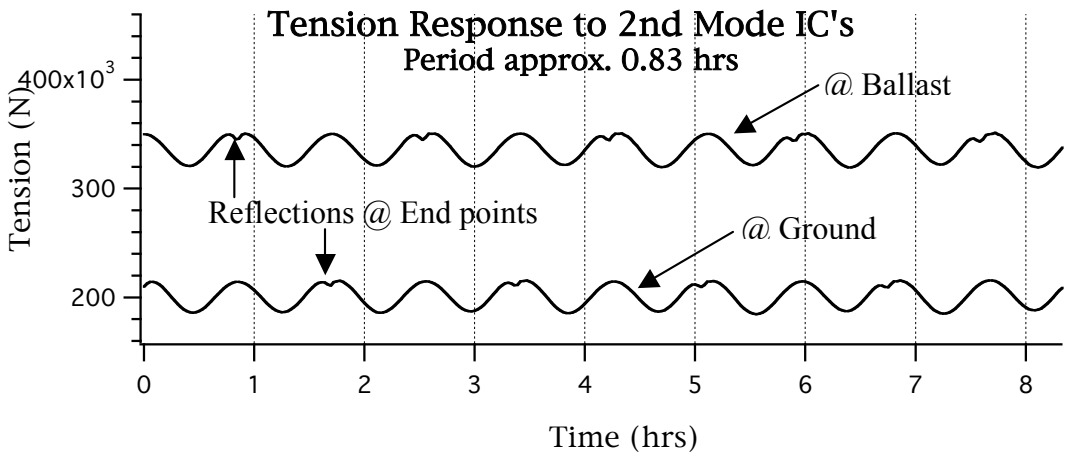

Point of Interest: In the above graph, notice the stress disturbance that appears (at the tension peaks) and alternates between for the ballast and the anchor. This was introduced due to a "Classical longitudinal 2nd mode initial condition" being superimposed onto the initial asymmetric strain distribution of the stabilized ribbon. The disturbance, effectively originating near the ground, is seen to impact and reflect off the ballast in a little less than an hour (the one-way transit time for a ribbon stress wave disturbance), then impact the anchor point about an hour later, thereafter, alternating back and forth from top to bottom. Notice also that this same disturbance is manifesting itself at the mid-point (previous graph) on a more or less hourly basis; this is because the mid point is about a 25 min transit time from either end, and catches the disturbance coming and going).

2.2.2.2 Stress wave propagation

Stress wave propagation is a phenomena related to only two ribbon material properties; modulus of elasticity, and density. It can be thought of as the "speed of sound" for the medium. A steel rod if hit on one end will transmit that impact (which could actually be audible) along the length of the rod at the inherent speed of stress wave propagation. This speed, corresponding to solids, is significantly different from that of air (usually an order of magnitude greater). The graph just above (last graph in the previous section) exhibits this phenomenon.

Stress disturbance can be associated with any phenomenon that creates a strain (stress) gradient. Longitudinal natural modes correspond to a form of stress wave propagation, although in that case it is *coherent;* conventionally, stress wave propagation refers to disturbances of a non-coherent nature. For the further demonstration of stress propagation in the space elevator ribbon, this section will employ the introduction of a stress gradient by way of releasing a portion of slack into the domain of the ribbon.

Specifically, 90 km of slack ribbon are introduced into the ribbon at the anchor; this creates a large low tension disturbance that then propagates up the ribbon towards the ballast. The release profile in time is shown below.

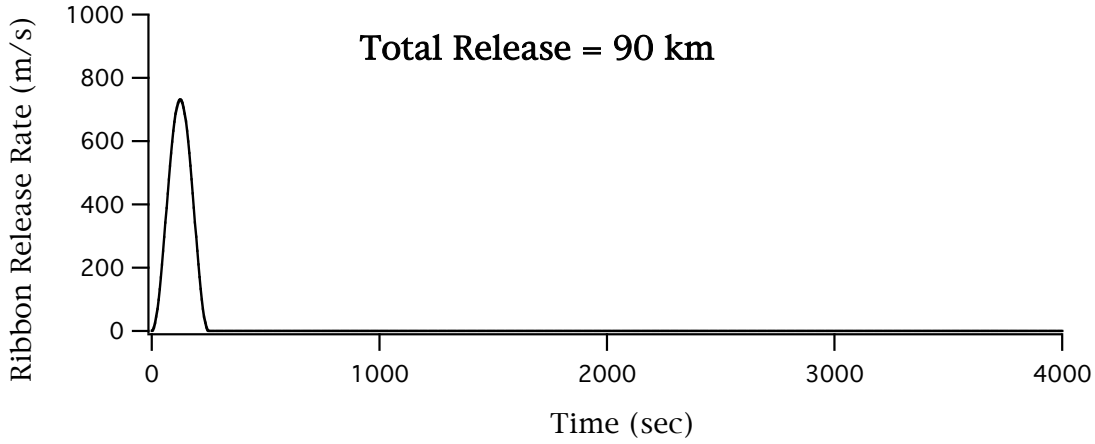

Below is the a series of snapshots of the resulting tension response as it progresses up the ribbon. The snapshot at 3,000 sec shows the stress wave poised to impact the ballast.

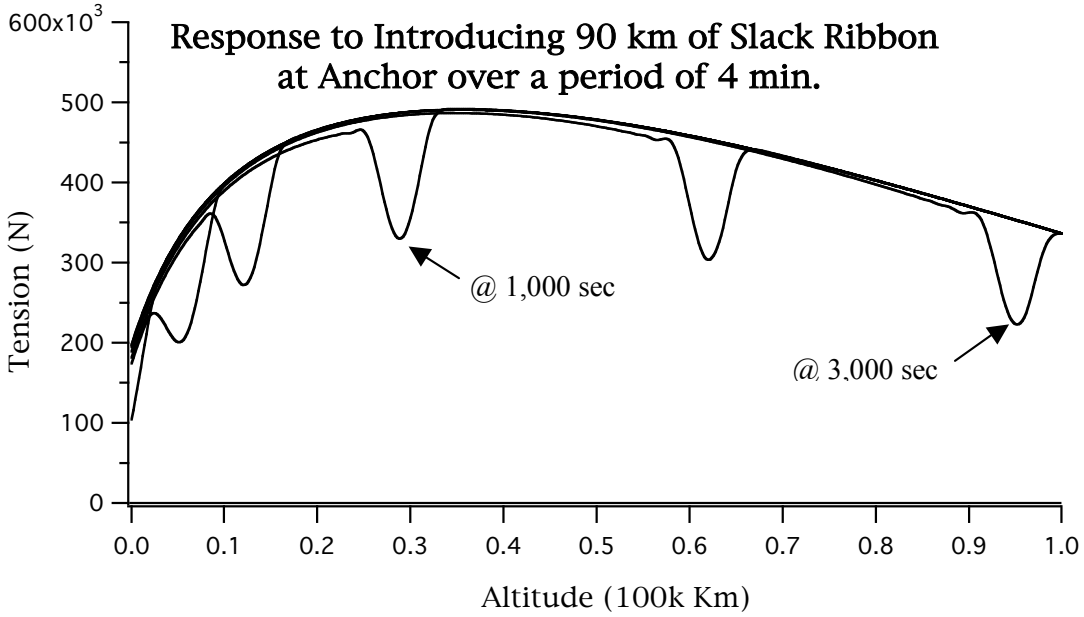

The graph below shows the time history of tension at various altitudes along the ribbon, starting at 2 km, then progressing up through 20k, 40k, 60k, 80k, 99k kilometers. Note that the tension disturbances are uniformly distributed in time (due to the uniform sample distances along the ribbon and the constant transmission speed). The stress wave shown at the 99k km position is poised to reflect off of the ballast, a fact that indeed manifest itself in the tension history at the 80k km point, for which is shown two disturbances, symmetrical-in-time about the reflection time (first disturbance at about 2600 sec, then the reflected disturbance coming back across the 80k km point at about 3800 sec).

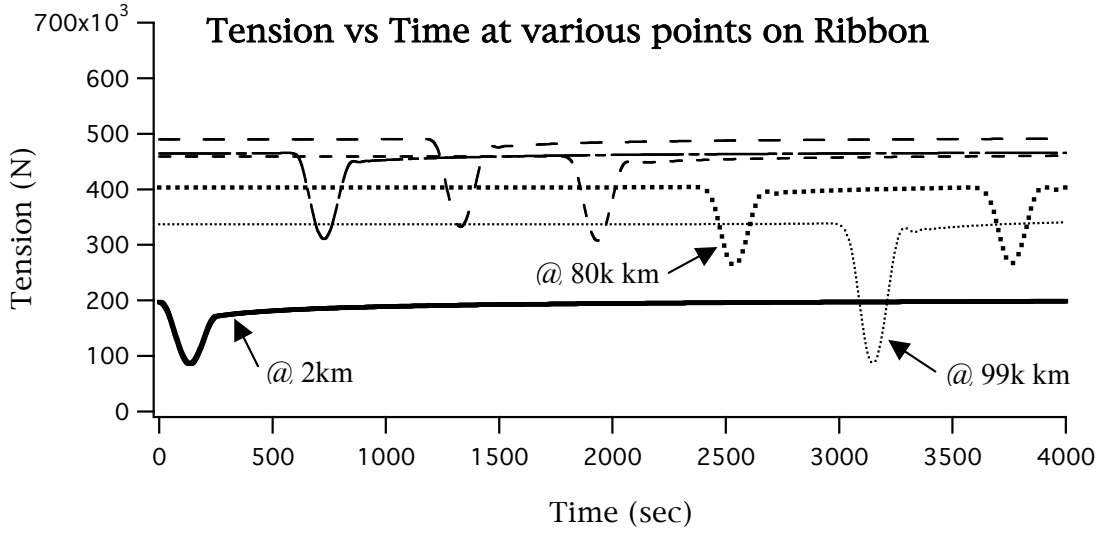

The graphs below show the tension wave reflecting off of the Ballast, then the Anchor.

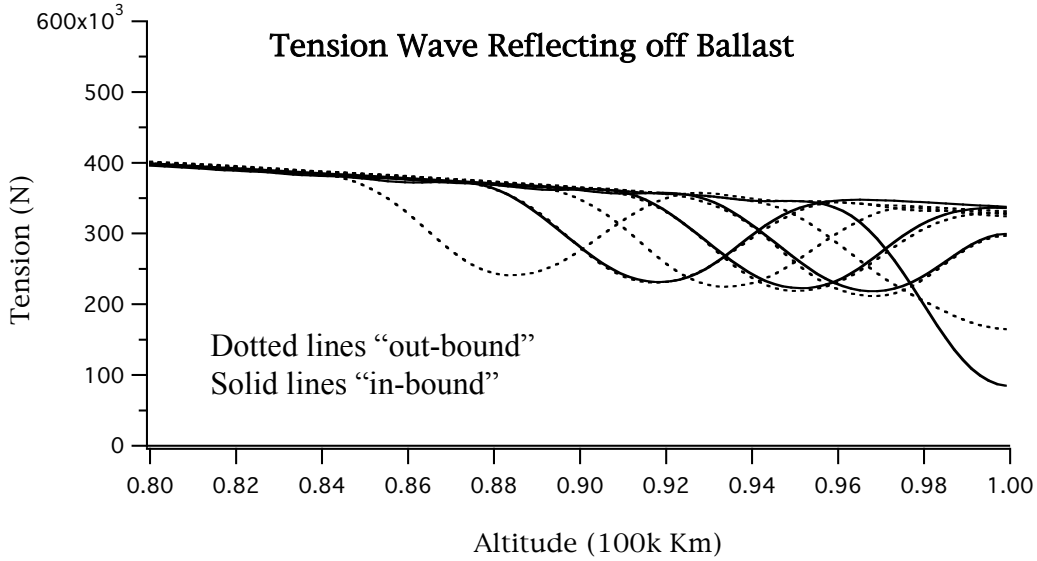

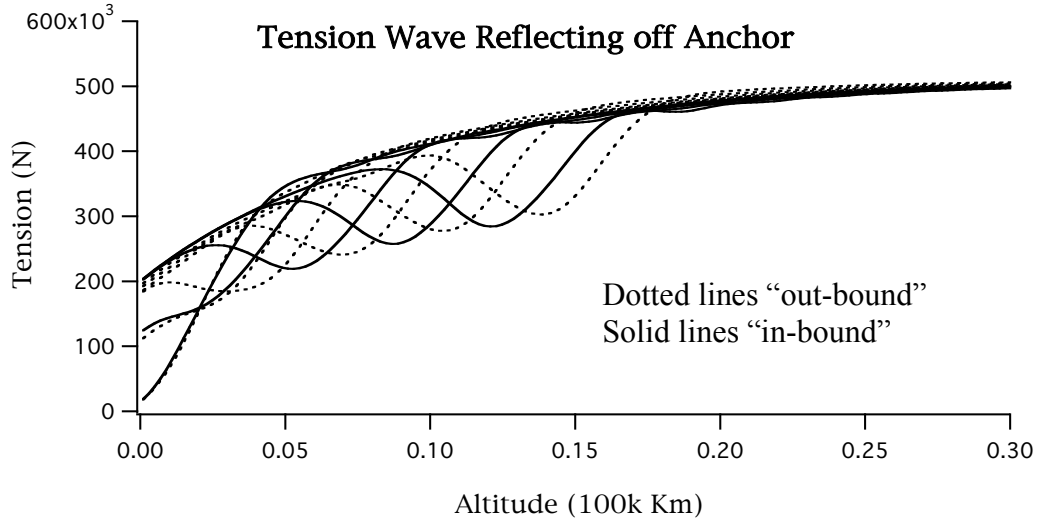

2.3 TRANSVERSE WAVE DYNAMICS

Classical solutions for the one-dimensional string equation require an assumption of uniform and constant string tension along with a constant lineal mass density. Under these conditions, closed form solutions yield the familiar sinusoids for natural (normal) modes of vibration. It would appear that the space elevator ribbon would significantly violate such assumptions since its tension and mass density vary considerably over length. However, the constant-stress space elevator ribbon design, by virtue of its criteria to produce uniform stress distribution under (unoccupied) non-linear gravity and centripetal loading, fortuitously creates approximate lineal properties distribution, which, when combined with ribbon tension variation, can render the coefficient of the one-dimensional classical string equation nearly constant, thus meeting requirements for the classical closed-form solutions in response to initial conditions. Thus the unoccupied ribbon enjoys an approximation the same classical normal modes of vibration as a simple string. Such is born out in the GTOSS simulation of the ribbon in which all these non-linear properties and other effects are combined. Of course if the elevator is occupied by a climber, or subject to disturbances, then resulting modes of vibration may not follow those predicted by classical string equation solutions and response may manifest non-linear attributes that may not be replicable under classical linear analyses.

2.3.1 In-Plane String Modes

This section shows response to initializing the ribbon with 1st and 2nd natural mode conditions corresponding to a string fixed at both ends. This is not exactly the conditions presented by the space elevator since the ballast is free to move in libration. Thus the resulting motion will deviate somewhat from classical string response.

The graph below is a series of in-plane deflection snapshots taken at various times during the 12 hours of simulated time. These are deflections relative to a frame between the anchor and ballast, thus gross pendulus ribbon libration will not be evident.

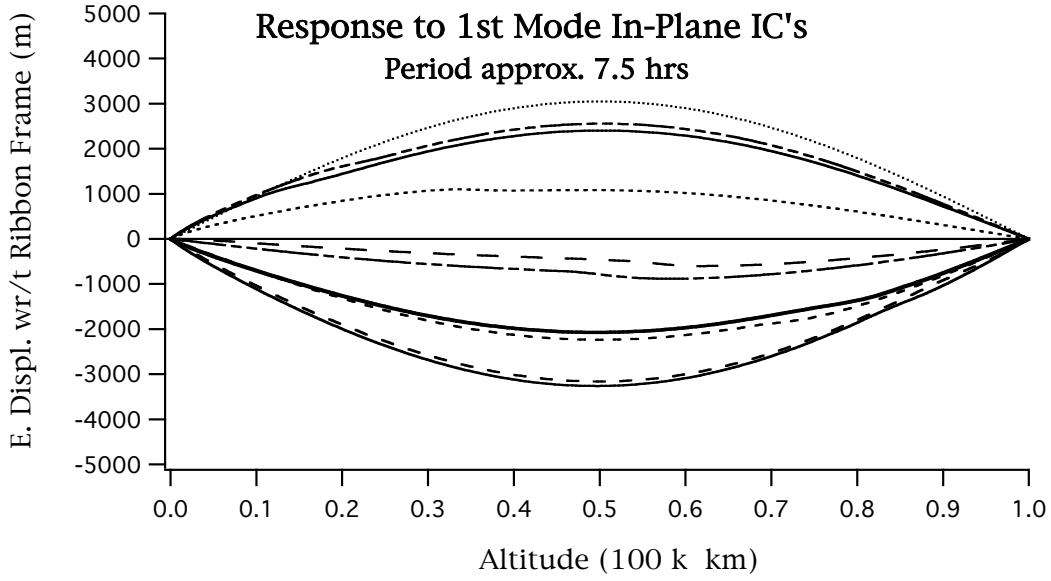

The graph below shows time histories of response (corresponding to the graph above) at the quarter-, and mid-point of the ribbon.

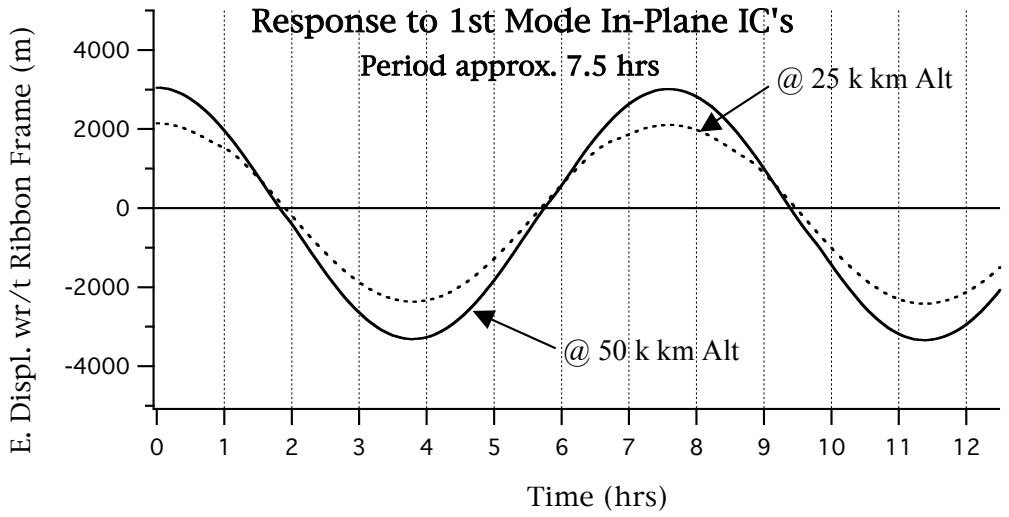

The graph below presents deflection snapshots (similar to above), except these are for the 2nd string mode. Note that initializing the ribbon to a classical 2nd natural mode does not yield as clean a modal response as did the 1st natural mode. The "fine dotted" line is the initial deflection shape; resulting motion exhibits distortion. It might be concluded that the higher the mode number, the more the response will deviate from classical modal response.

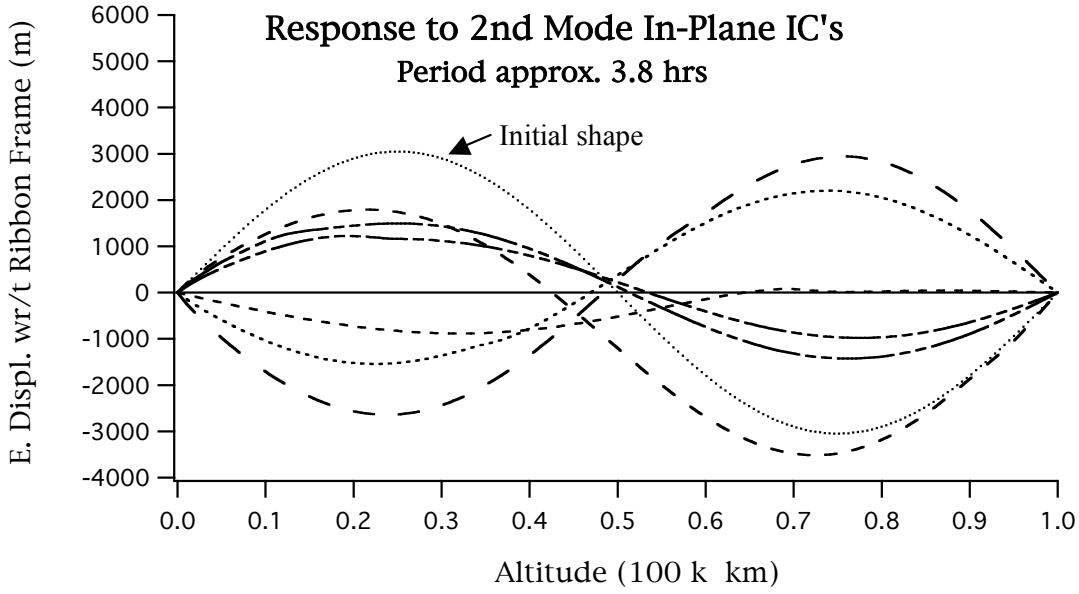

The graph below shows response time histories at the ribbon quarter- and mid-point. This illustrates another view of how resulting response deviates from classical modal response.

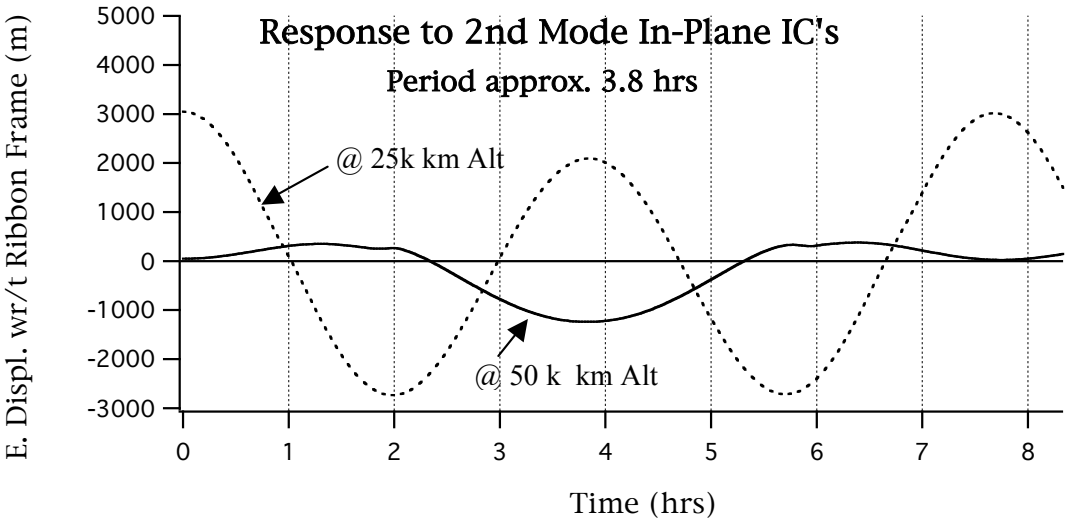

2.3.2 Out-of-Plane String Modes

The results below are identical to those of Section 2.3.1, except pertain to Out-of-Plane natural modes. The deflections in these graphs are relative to a vertical passing through the anchor point, thus they can characterize any gross ballast libration component in the response. The libration evident below has resulted from the fact that the modal initial conditions do not the actual *fixed-free* boundary-conditions of the ribbon, but rather correspond to classical *fixed-fixed* boundary conditions.

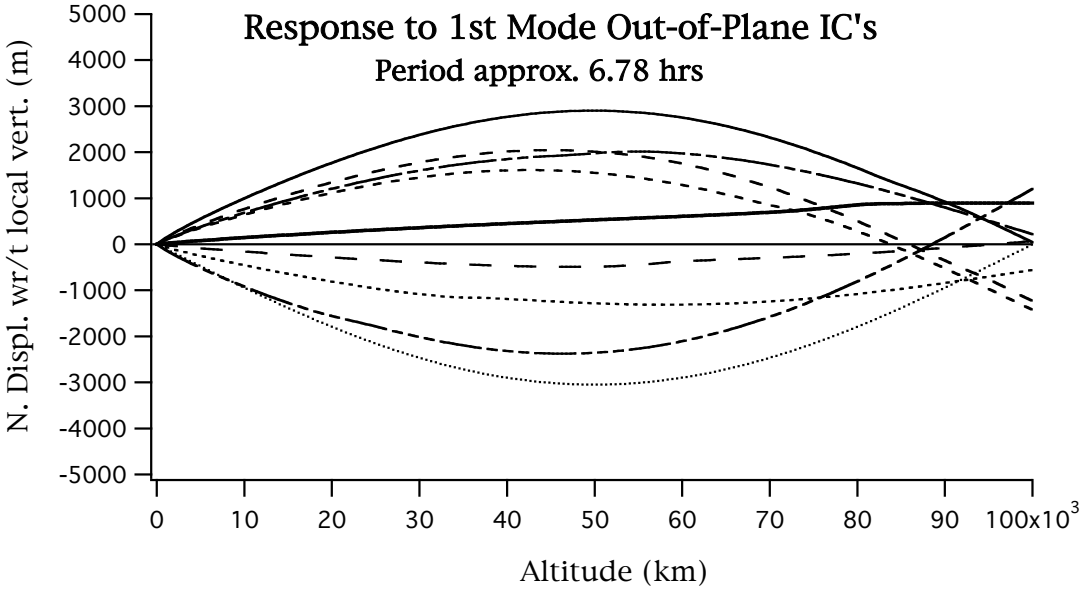

Note in the graphs below that a component of out-of-plane libration has also been induced due to un-balanced out-of-plane modal initial conditions.

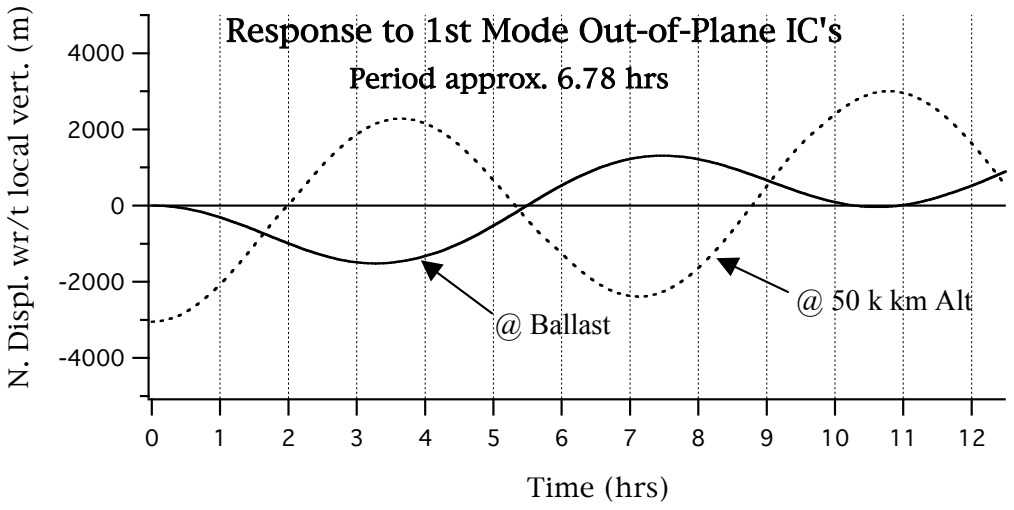

Below are 2nd mode Out-of-Plane response graphs similar to above.

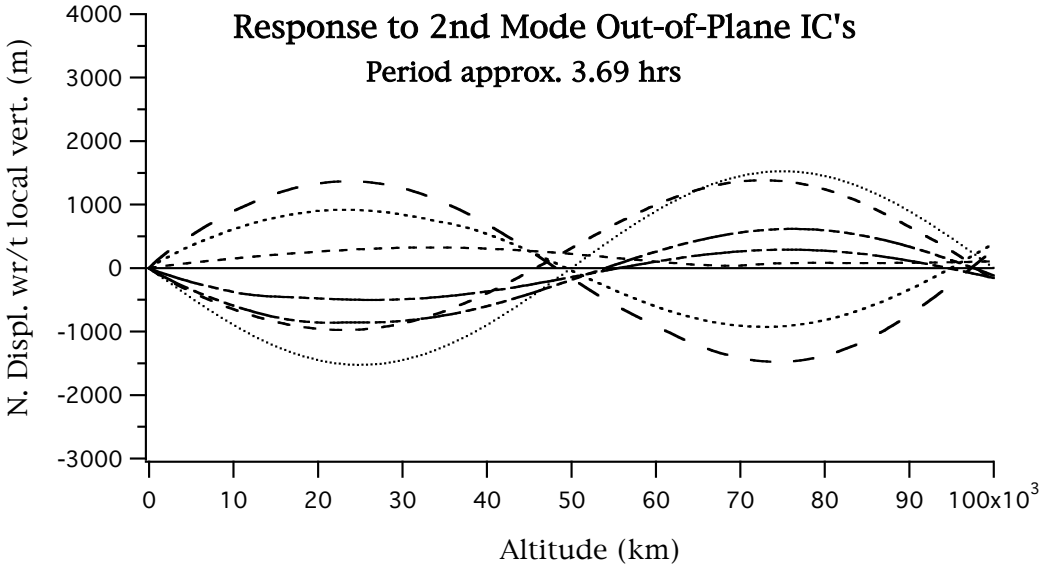

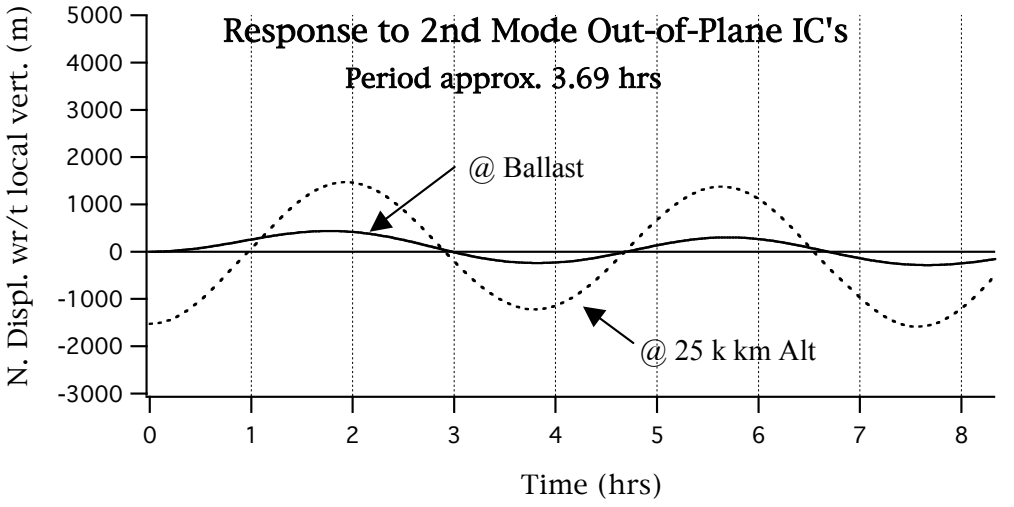

2.3.3 Combined In and Out-of-Plane Deflections

Theoretically, no coupling occurs between normal modes of vibration. Since the constitution of the elevator deviates somewhat from the classical conditions, it is possible that interactions might take place between planes of vibration. This section explores such possible interaction if both in- and out- of-plane modes are excited. In the examples below, the 1st string mode (only) was excited in both planes simultaneously.

The two graphs below show snapshots at various times of the deflection shapes relative to the line between the anchor and the ballast (referred to as the Ribbon frame).

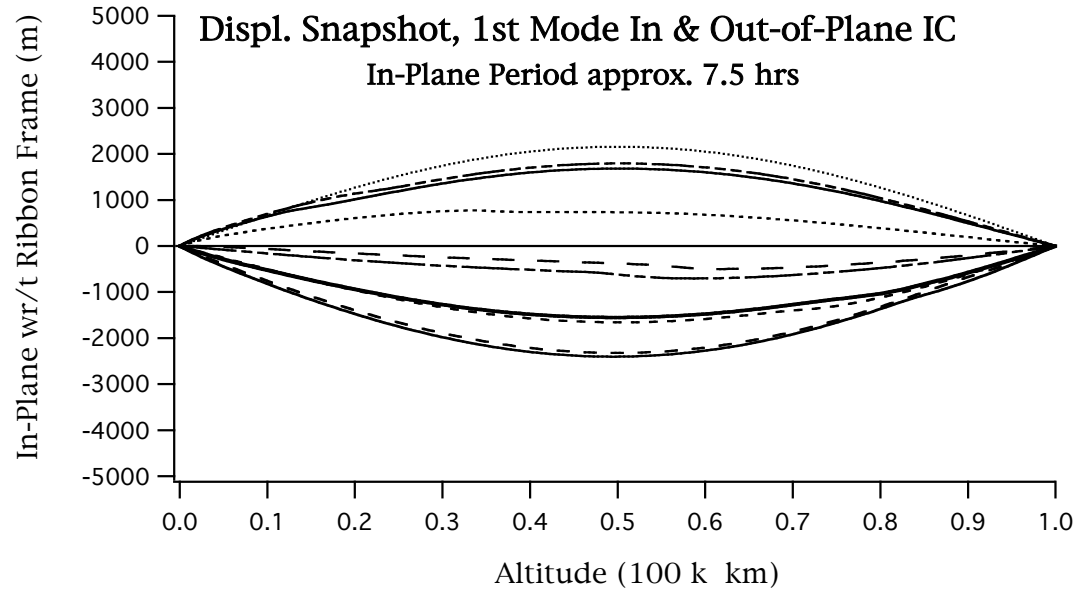

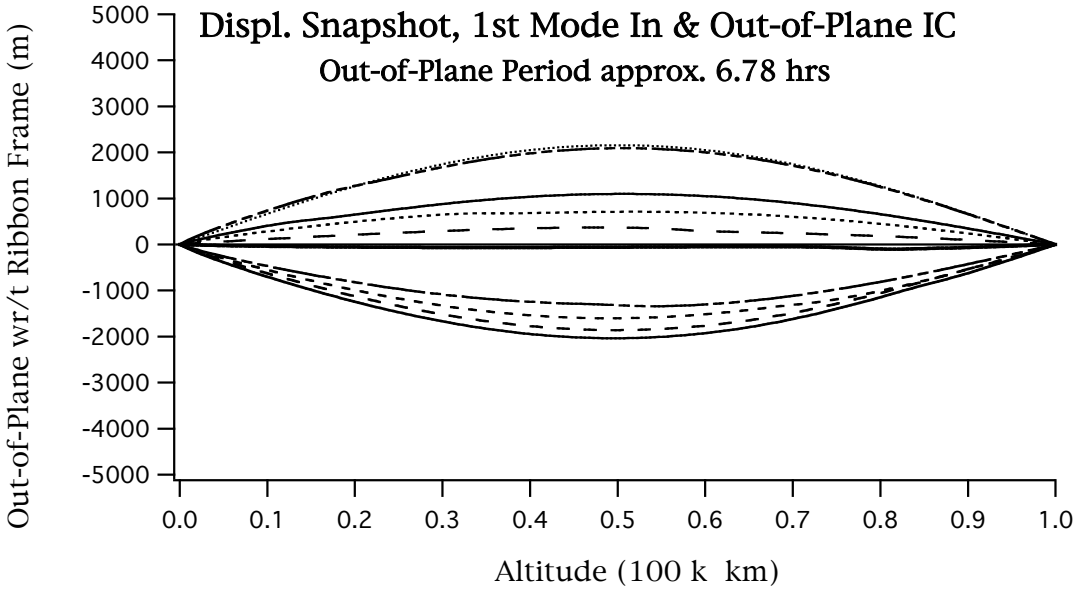

The two graphs indicate that only insignificant coupling (at best) is occurring. Below, is the time history of the mid-point of the ribbon. These are displacements relative to the line between the anchor and the ballast. The dotted line is the "in-plane" response. Again nothing indicates significant coupling between these modes. Note the difference in the natural frequencies of the two modes and, also the fact that the in-plane response is showing small component of in-plane pendulus libration coupling; this libration is an artifact of the simulation (imperfect) initialization rather than having been precipitated by the 1st string mode activity.

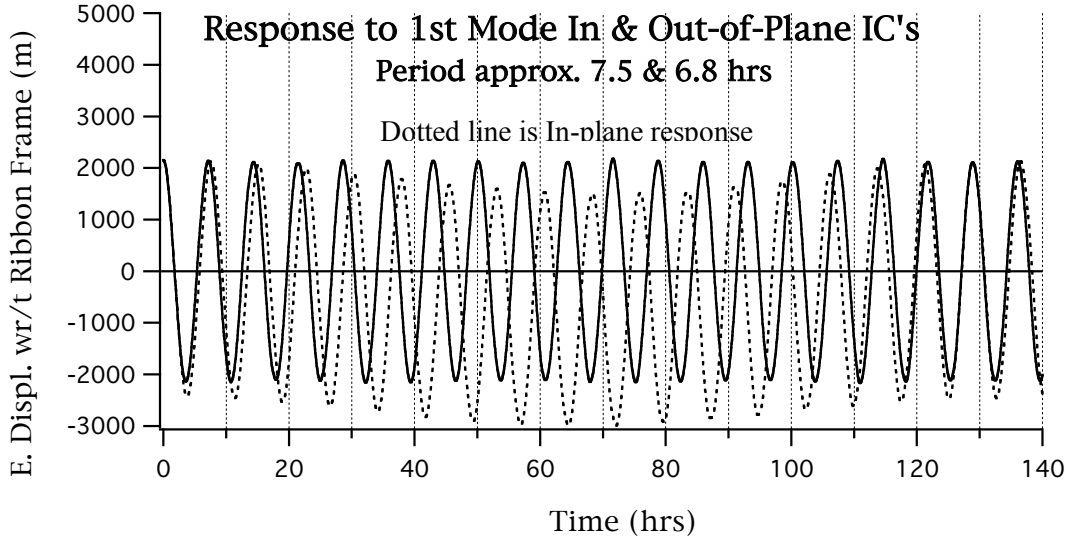

2.3.4 Transverse Wave Propagation

Transverse wave propagation is shown for the elevator ribbon. The wave is In-Plane, and is created as an initial condition at the ground consisting of a transverse deflection in the shape of a stationary 3000 m displacement half-sine wave extending over 5% of the ribbon length. It propagates the length of the ribbon, reflects off the ballast, returns to the anchor, at which it again reflects back upwards towards the ballast. The graph below shows many snapshots of the waves states as it progresses back and forth along the length.

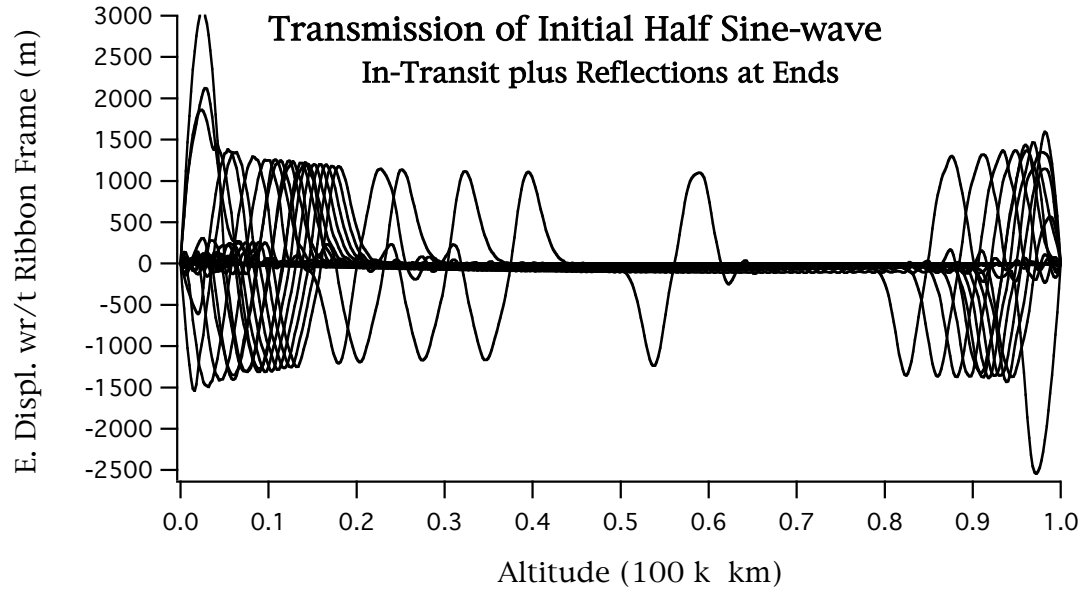

Below shows the initial wave leaving the ground and starting the trip towards the ballast.

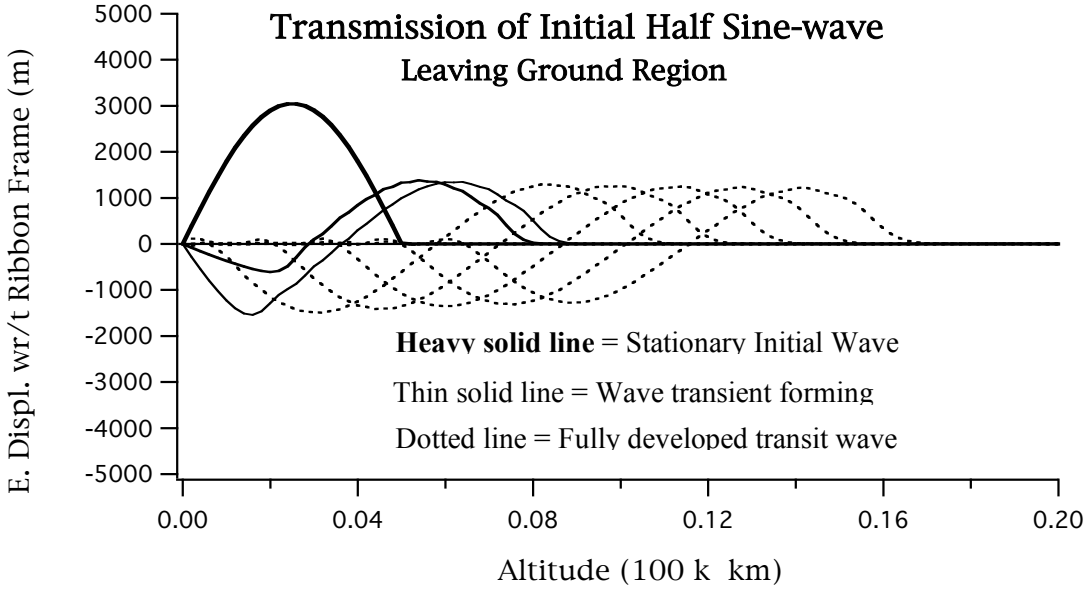

The graph below shows the wave arriving at, then reflecting from the ballast end. Note that the wave has suffered some shape distortion due to the realities of the actual ribbon properties deviating from that which would predicate a classical (ie. un-distorted) wave propagation.

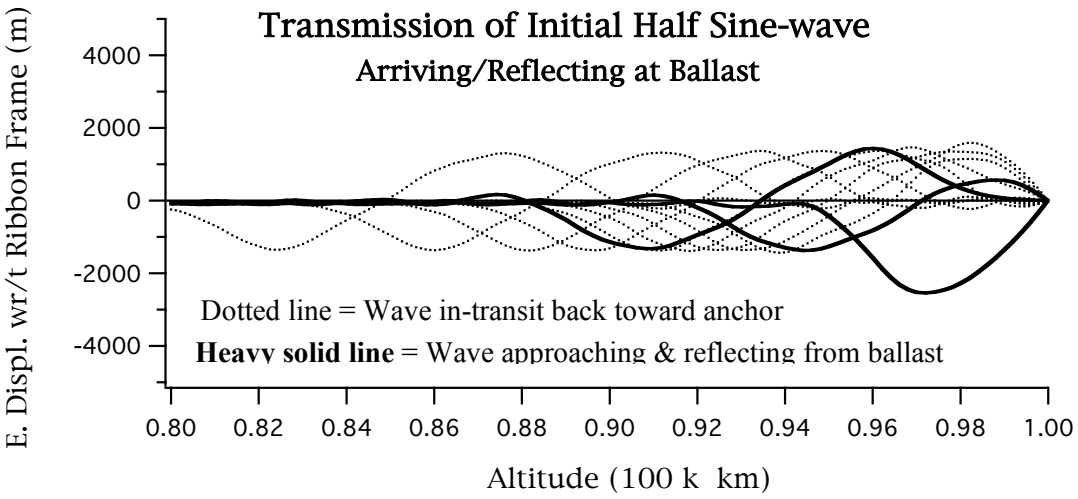

The graph below shows a displacement time-history at an altitude of 30,000 km. The initial pulse (at about 3/4 hours) represents the wave's first appearance at that altitude after it leave the ground. The wave must then make a trip from that point of 70,000 km, to reach and reflect off the ballast; it then makes the same trip back down before reappearing at 30,000 km altitude (the second pulse at about 7 hours). The same scenario ensue except this time it is the ground (only 30,000 k km away), that it travels to, reflects then again makes its appearance at 30,000 k km.

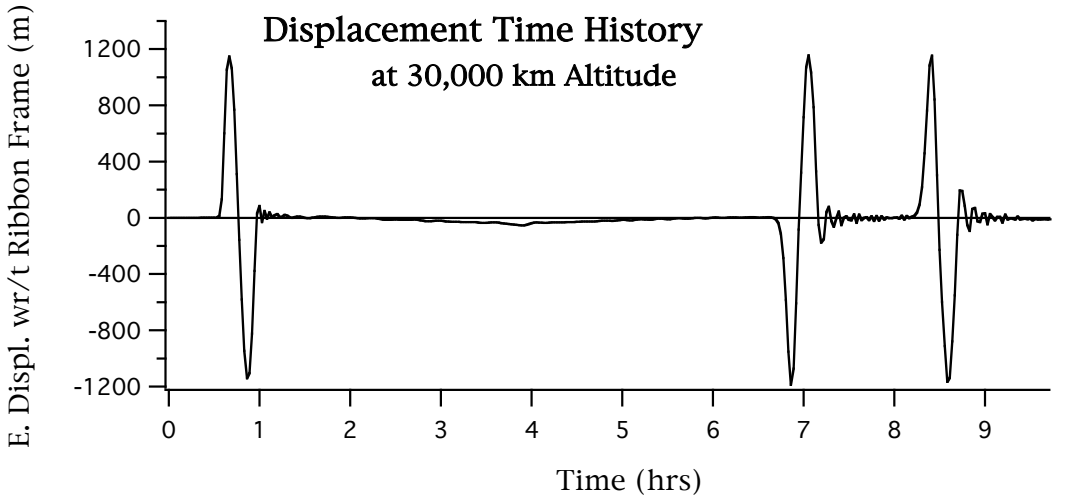

Notice also that the wave shape progressively deteriorates in time due to actual ribbon properties, reflections (and to some degree the numerical simulation process producing these results).

2.4 GRAVITY-WELL SIMULATION CONVERGENCE

To properly simulate a space elevator configuration using a discrete nodal approach, one must pay attention to the spatial-convergence of the simulation as it pertains to the "gravity well" (ie. inverse-square planetary gravity model). The graph below depicts (for the Earth) the tension at the anchor point as a function of the number of "uniformly-spaced" nodes used to simulate the elevator ribbon.

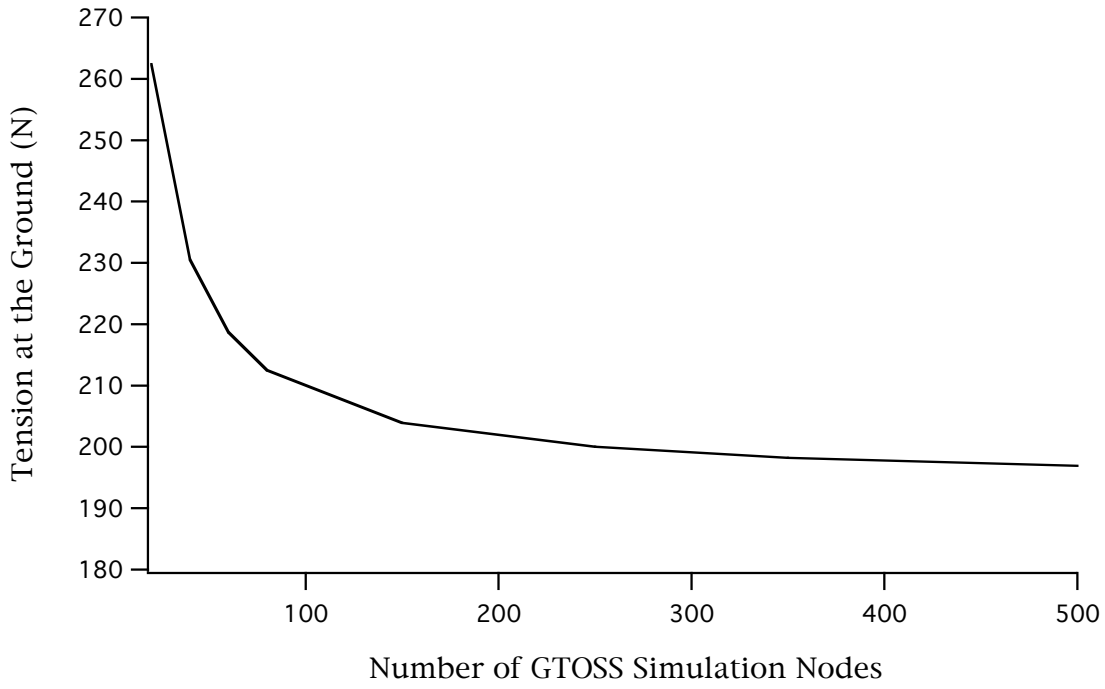

It can be seen that for node-counts greater than 200, the earth's gravity-well is being fairly well acknowledged. For lesser node counts, simulation results may still be acceptable, depending upon the degree to which total-available anchor tension must be fully realized.

Note also, that *non-uniform* distributions of lesser node-counts (for instance 100 nodes from ground to 10,000 km, then 50 nodes between there and ballast, etc) may suffice to fully acknowledge the gravity well.

3.0 DEBRIS AVOIDANCE

3.1 DEBRIS ENVIRONMENT

- *Tracked debris histograms vs altitude bins*
- *Statistical characterization of untracked (small) debris*
- *Characterization of ribbon damage vs type of debris*

3.2 DEBRIS-AVOIDANCE TIMING ENVELOPES/RESPONSE

- *Characterize "tracked-debris lead times"*
- *Characterize "wave transmission time" -vs- debris altitude*
- *Characterize "transverse wave clearance" -vs- altitude*

3.3 SEA PLATFORM PERFORMANCE DATA

- *Plot of minimum time to transverse displacement (no arrest)*
- *Plot of minimum time to "arrested" transverse displacement*
- *Timing considerations for wave cancellation*

3.4 TRANSVERSE WAVES WITH CLIMBER ON RIBBON

- *Plot of transverse wave reflection off of Climber @ LEO*
- *Plot of transverse wave reflections off of Climber @ MEO*
- *Plot of transverse wave reflections off of Climber @ GEO*
- *Plot of transverse wave through-put with Climber @ Launch*
- *Plot of transverse wave through-put with Climber @ LEO*
- *Plot of transverse wave through-put with Climber @ MEO*
- *Plot of transverse wave through-put with Climber @ GEO*

3.5 TRANSVERSE WAVE DAMPING USING BASE MOTION

- *Strobe plots of wave cancellation*
- *Timing data for wave cancellation*

4.0 AERODYNAMIC RESPONSE

This section does not attempt to establish design criteria or limits based on aerodynamic response; rather the intention here is to familiarize the user with inherent mechanisms underlying aerodynamic response, and identify the attributes of response that may be critical in SE design. Much in SE aerodynamic response runs counter to initial intuitive assessments.

Air loads on the SE and the resulting dynamic response were evaluated using the GTOSS subsonic aerodynamic regime capability. More information about the GTOSS air loads model can be found in Appendix B.

4.1 ATMOSPHERIC CHARACTERIZATION

The area of the Pacific ocean, considered to be optimal for location for the space elevator, seems to have little quantified data for the wind environment "at altitude" above sea level; thus it was concluded that at present, "probability of occurrence" type of synthesized wind-altitude envelops would likely not be meaningful. Thus this handbook attempts to address the general attributes of SE aerodynamic response to a simplified wind environment for use in overall preliminary assessment of real wind effects as described below.

Thus, for purposes of preliminary assessment, a constant *wind-versus-altitude* profile was adopted as a reference. The wind level was allowed to buildup linearly with time, starting from no-wind and progressing to full-wind in a period of *two hours*. This was followed by a period of constant wind at peak level (typically two hours). Following this constant wind period, the wind level decreased linearly with time to zero over a period of *two more hours*. The figure below, depicts this for the case of a Category 0 Typhoon, termed a "tropical disturbance".

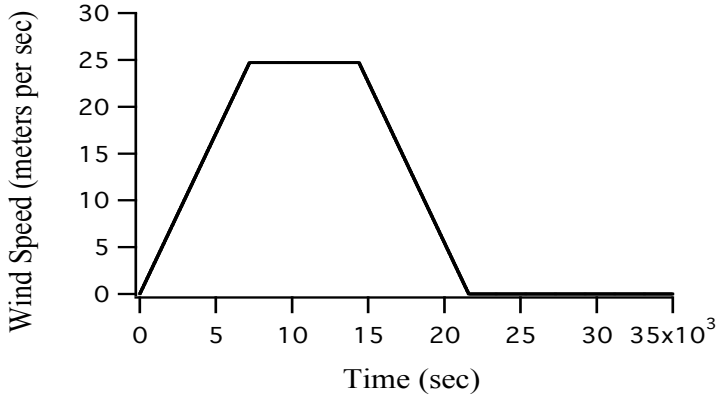

Thus, all wind scenarios started with zero wind, and for those cases of 2 hour peak-wind duration, returned back to zero wind by 21,600 sec (about 6 hrs lapsed time), with runs terminated after 10 hours (35,000 sec) of simulated time. For simplicity of results correlation, all winds blew from West to East, with no northerly component.

This wind categories used were:

(a). Category 0 (average of 25 m/s = 55 mph = 81 ft/s)
(b). Category 1 (average of 33 m/s = 74 mph = 107 ft/s)
(c). Category 2 (average of 40 m/s = 90 mph = 132 ft/s)
(d). Category 3 (average of 54 m/s = 120 mph = 176 ft/s)

Important notes concerning snapshot plots depicting aerodynamic response:

• Many of the figures in this handbook depict a series of *snapshots* of the data, taken at discrete times (frequently a series of more or less uniform time intervals of about 2000 sec).

• For snapshots taken during the initial 2 hour *build up of wind*, data is depicted by the *thinnest solid lines*.

• For snapshots taken during the duration of *peak wind* (2 or 4 hours), data is depicted by *thicker solid lines*.

• For snapshots taken during the 2 hour duration of *diminishing wind*, data is depicted with *long dashes*.

• For snapshots taken after the wind has *diminished again to zero*, data is depicted with *finer dashes*.

4.2 OVERVIEW OF AERODYNAMIC RESPONSE

SE aerodynamic response is characterized by some rather startling and unintuitive attributes. These are:

1. Absence of critical over-stress resulting from ribbon deflection.
2. Apparent ease with which wind load translates ribbon horizontally.
3. Existence of a critical load level, ushering in *non-linear* response to load.
4. Potential for near-horizontal ribbon departure angles.
5. Sensitivity to wind duration (for winds greater than critical level).
6. Accentuation of all load responses when the elevator is occupied by a climber.

The above synopses are further addressed below:

***1. Absence of critical over-stress resulting from ribbon deflection*:** The absence of over-stress under aerodynamic loading is attributable to the following.

• The overall ribbon has an extremely low effective end-to-end spring rate at earth on the order of .04 N/m. This mean that relative to the scale of local atmospheric disturbance,

the ribbon can tolerate a significant amount of elongation without significant rise in tension.

• A ribbon departure of even 200 km downrange, while appearing significant from an anchor-station viewpoint, and presenting a bizarre ribbon departure of near horizontal, in fact represents a minimal increase in overall strain for a 100,000 km long ribbon. Distributed over the length of the ribbon, this corresponds to an increase in strain of about 0.2 % strain, thus insignificant stress increases (note, the SE ribbon nominally operates at about 4%-5% average strain).

• The fact that stress wave propagation time is very short (approximately 1 hour to travel the full 100,000 km length of the ribbon) compared to the time it takes a strong wind to build up, effectively defuses the possibility of localized stress at the source of the disturbance by quickly propagating stress gradients upward along the entire length of the ribbon, distributing strain.

The SE ribbon's low effective spring rate can be intuitively grasped by imagining a length of ribbon that is, say, 1 km long; among others; one measure of this length's elasticity is the effective end-to-end spring rate (see tether formulas in section 1.4). Now, suppose two such lengths of ribbon were connected end-to-end ("springs in series"); this new, 2 km long piece would exhibit a spring rate of 1/2 the value of either length individually. In general, if N of these spring lengths, each of spring rate K, are connected in series, the resultant end-to-end spring rate of the composite spring is K/N; thus, the longer the spring (of a given material), the lower the (overall) spring rate. Thus, it becomes evident that the SE ribbon could exhibit an extremely low spring rate. Note that the spring rate is independent of the amount of tension in a spring; that is, the incremental change in tension resulting from an incremental change in length does not depend upon the spring's preload.

***2. Apparent ease with which wind load translates ribbon horizontally*:** The propensity for the wind to blow the ribbon downrange can be attributed to the aerodynamic model and the ribbon geometry as it yields to the relative wind. In order for the ribbon to sustain horizontal displacement, it is necessary for the vertical and horizontal components of air load to equilibrate respectively the appropriate percentage of vertical and horizontal components of ribbon tension. The aerodynamic source for this equilibration arises over a region of essentially uniform curvature as the ribbon departs the horizontal and proceeds upward to vertical. The aerodynamics model used in this study predicts that if the relative wind has any component normal to the ribbon, then a pressure against the ribbon results, and a force normal to a tangent to the ribbon results. The vector integral of this force distribution provides the required horizontal and vertical force components.

***3. Existence of a critical load level, ushering in non-linear response to load*:** As aerodynamic load increases, both vertical as well as horizontal components of air load are created on the ribbon due to the characteristic curvature induced in the ribbon by horizontal deflection under air load. For quasi-steady response, net *vertical* and *horizontal* load must be zero. As curvature (deflection) occurs, both horizontal and

vertical components of air load build against the equilibrating tension components. Note that as curvature builds, the tension in the ribbon is essentially unaffected (from item 1 above). At some point, *assuming air load does not increase beyond a certain level*, due to the geometry of curvature, the horizontal tension component equilibrates the horizontal air load and horizontal deflection stops increasing. As seen from results, when the critical air load level is reached, then the nature of the aerodynamic response changes drastically from a displacement-sensitive equilibrium restoring process to an unconstrained deflection process in which non-linear effects will dictate if and/or when horizontal deflection will become limited. This point is reached when almost simultaneously both the total horizontal and vertical components of air load becoming equivalent to the tension. At this point, the air load essentially replaces the anchor as the source of vertical equilibrium force, and the horizontal component of tension becomes no longer capable of constraining horizontal deflection.

***4. Potential for near-horizontal ribbon departure angles*:** After the critical air load is reached, then the ultimate amount of horizontal deflection becomes unlimited (in a linear sense), and the resulting extreme curvatures of the ribbon will produce departure angles from the anchor of near (if not actually) horizontal as the ribbon progresses down-range in response to air loads.

***5. Sensitivity to wind duration (for winds greater than critical level)*:** After the critical air load is reached, then the ultimate amount of horizontal deflection becomes a *time-dependent phenomenon*, depending upon duration of wind above the critical level. This in a sense then dictates that the maximum down-range deflection becomes somewhat dependent upon the geographical extent of the wind field; this being because deflection will simply increase until the wind subside, either due to temporal or geographical extent of the wind field.

6. Accentuation of all load responses when the elevator is occupied by a climber: The above explanations of the extent to which the ribbon can be blown horizontal by the wind alludes to the criticality of that condition in which the wind overpowers the *balance* between the only restoring mechanism at the ribbon's disposal, namely its tension, and the air loads. Now, any elevator configuration that includes a climber on the ribbon below GEO will reduce the tension in the atmosphere. The lower the climber, the greater is this reduction. The lower the tension in the ribbon, the more easily the wind can overpower the balance between tension and air load. Thus is all cases of a climber on the ribbon, certain aspects of aerodynamic response can be exacerbated; this effect is progressive until the climber is fairly low in the atmosphere; at low altitudes, as the section of ribbon between the climber and anchor point becomes ever shorter, the effect of lowering tension between climber and ground starts to transform the elevator effectively into the unoccupied elevator case. Imagine a case in which the climber is a 50 m altitude; here, it is clear that if one were to stand back and observe the response, the "big picture" would not differ significantly from the unoccupied case.

Section 4.3 below demonstrates the above.

4.3 DETAILED RESPONSE TO A REFERENCE WIND

The data shown below represent responses to the type of wind profiles described above.

4.3.1 A Typical Aerodynamic Load Distribution Response

The following sets of data correspond to a Category 0 wind and a ribbon width of 10 cm exposed to the lower atmosphere. This case is chosen for in depth description since it exposes many of the unintuitive aspects of SE aerodynamics. In particular the effect of reaching a critical air load level, minimal overstress in the presence of significant horizontal ribbon deflection under air load. Note that the air loads have only "doubled" over the case of the 5 cm ribbon.

Shown below are deflection snapshots over a period of 6 hours. Superimposed on this graph is the maximum deflection for the same wind, but with a ribbon width of 5 cm.

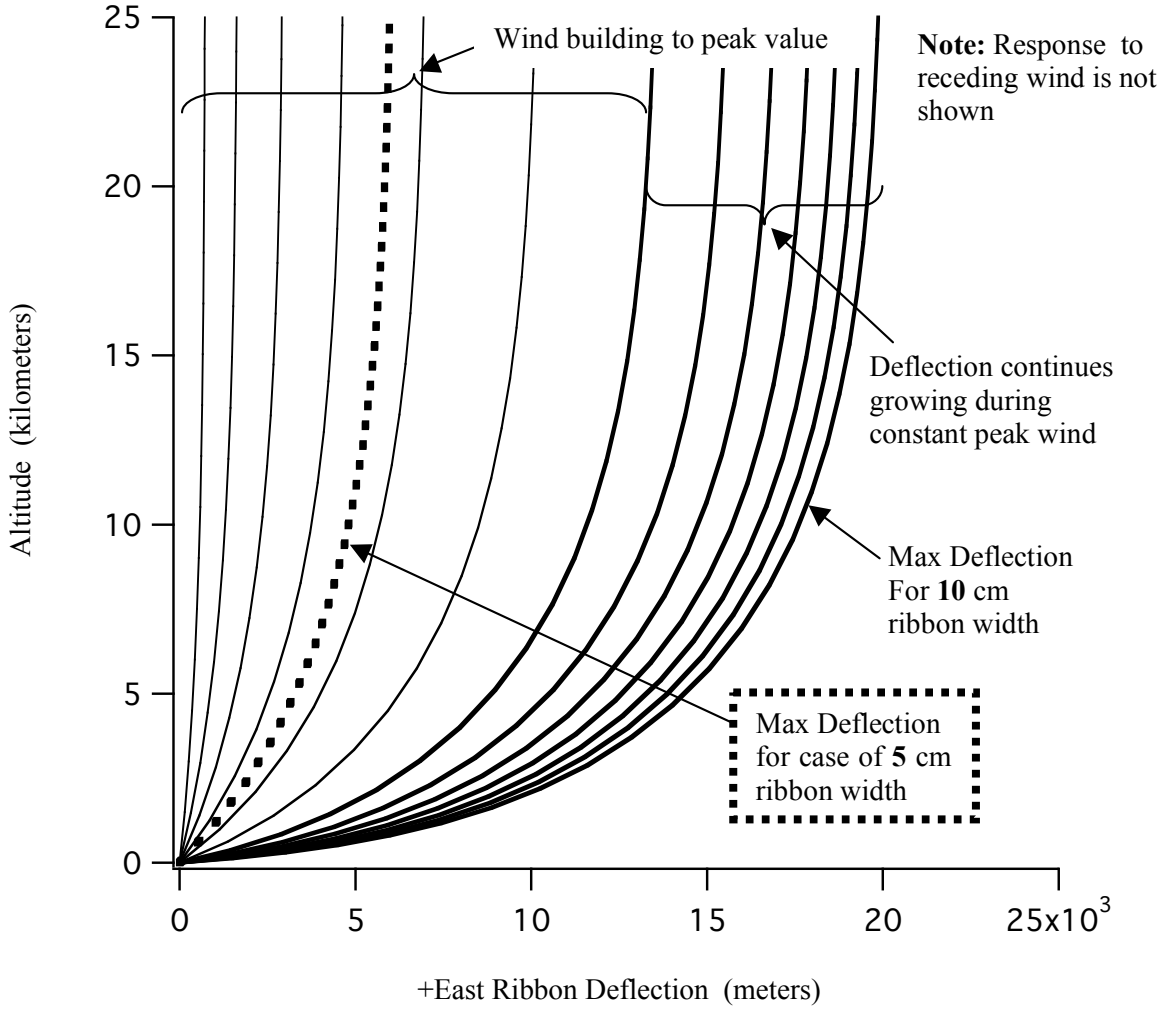

Note the following from the graph above:

• Horizontal and vertical scaling is identical, so true ribbon departure angles are portrayed by these spatial deflections.

• For the 5 cm wide case (heavy dotted line), the maximum deflection was attained simultaneously with peak wind; this max deflection then stayed constant at this value.

• Compare this to the 10 cm case, in which the maximum deflection occurred after peak wind was reached, with peak deflection continually growing for the entire period of constant peak wind.

• This is indicative of the conclusions presented in items 1-5 of section 4.2.

The two graphs below illustrate snapshots of horizontal and vertical air load density taken through the above response.

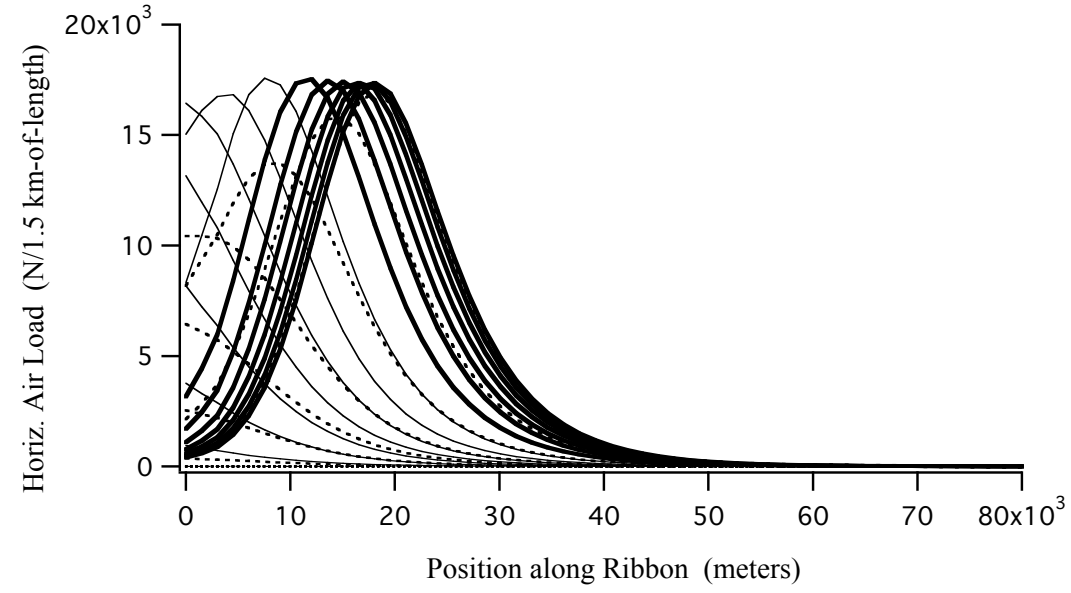

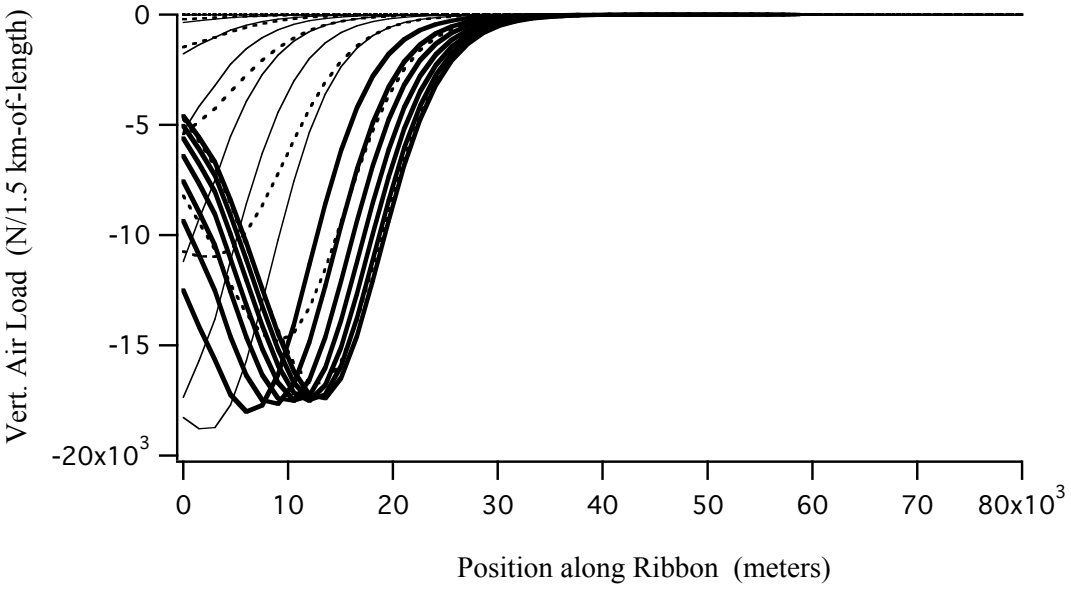

These air loads, plotted against ribbon arc-length, are consistent with the ribbon's becoming increasing horizontal as seen by the migration of peak air load along the ribbon length. This is because as a section of ribbon becomes progressively horizontal, it contributes ever less to horizontal and vertical air load; it is the area of ribbon curvature from horizontal-to-vertical where the air load action is occurring (see the section below for more detailed discussion of aerodynamic response).

This process is accompanied by very little tension change as shown the graph below; this graph is an envelope of tension snapshots along the length of the ribbon at various times covering the duration of the response. The profile is essentially that of the un-occupied, unperturbed elevator.

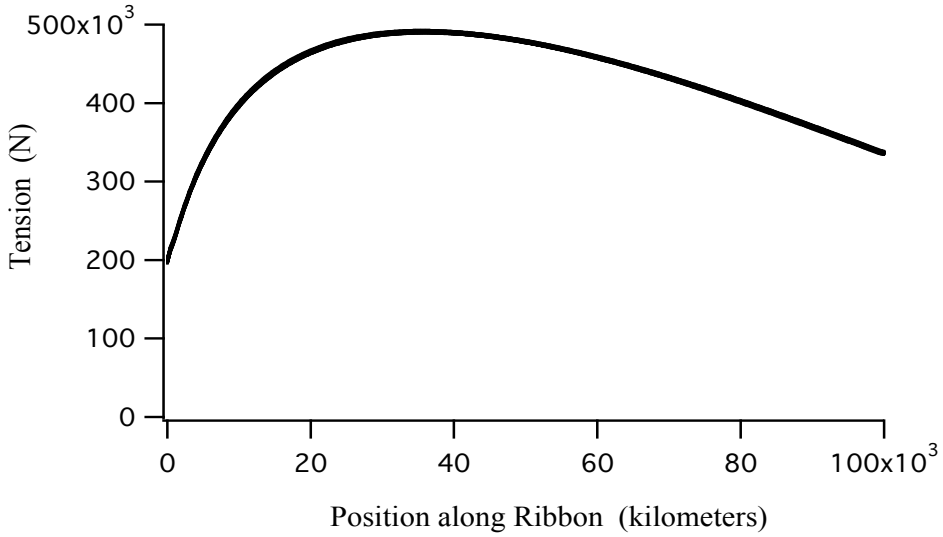

Below, it can be seen that stress has been little affected by the wind response.

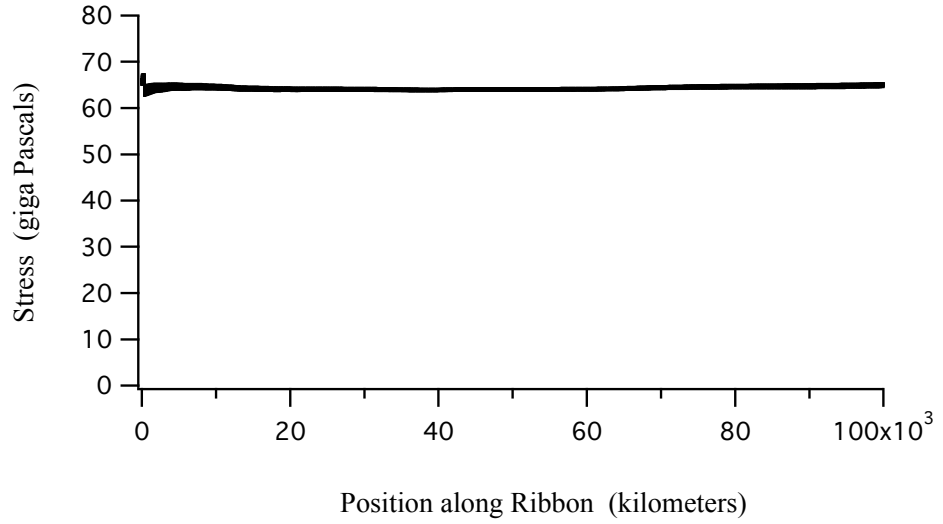

4.3.2 Extreme Aerodynamic Loading

This section addresses the situation where the wind reaches a critical level that essentially transcends the ribbon displacement restoring mechanism, giving the wind almost full control over the ribbon, with almost unlimited ability to displace the ribbon horizontally. A useful analogy for understanding the existence of such a critical load and subsequent unlimited response might be termed the "Rolling Pin Analogy". Consider a rope hanging from the ceiling with a weight attached under gravity as shown below.

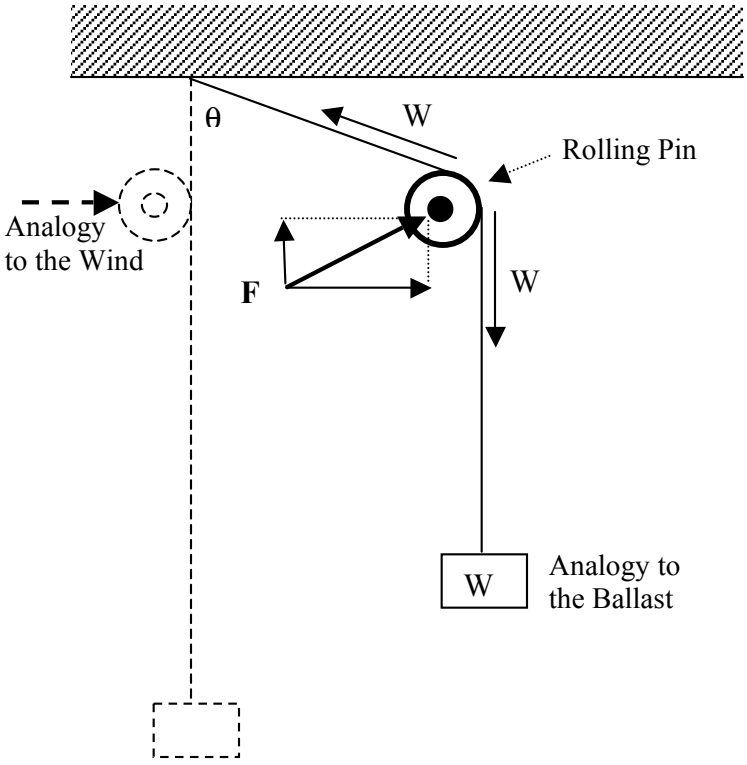

Imagining pushing on the rolling pin to deflect the rope from its initial vertical position. At any subsequent (steady) deflection, the applied force **F** (the rolling pin, or wind, in our analogy) must equilibrate both the vertical and the horizontal components of the weight **W**. Note, all ribbon segments with a *horizontal component of orientation* is subject to generating vertical air load. Note that the weight manifests itself as a tension **W** acting on both sides of the rolling pin since the rolling pin functions as a pulley. It is readily seen that if the horizontal component of **F** exceeds that of **W** (between rolling pin and ceiling), then there is no limit to how far the rolling pin can be moved in the horizontal direction by **F** except for the energy available to the process creating **F**. Likewise, if the vertical component of **F** exceeds W, then there is no limit to how far the weight **W** can be lifted (due to the geometry of horizontal deflection) except for the energy available to the process creating **F**. The application of such an analogy to the elevator ribbon must first establish *uniformity of tension* around the bend of the characteristic curvature of the ribbon under air load (ie. the pulley assumption). This can be established by simulation, and further conceptually corroborated by noting these important facts:

1. Aerodynamic friction manifests virtually zero load tangent to the ribbon curvature (actually zero in the GTOSS aerodynamic model); thus a steady state tension differential cannot be sustained via aerodynamics.

2. The tension disturbance propagation speed of 28 km/sec is so high compared to the rate of onset of air loads due to wind loading, that any tension disturbance gradients will quickly propagate away neutralize any disturbance source and attain gradient-free equilibrium.

3. The low effective spring rate of the ribbon allows it to easily tolerate elongations associated with being displaced downwind by hundreds of kilometers without significant increase in tension.

Now consider a response (shown in section 4.3.3.3) in which the above described critical aerodynamic load has apparently been reached. The resulting horizontal displacement is shown below.

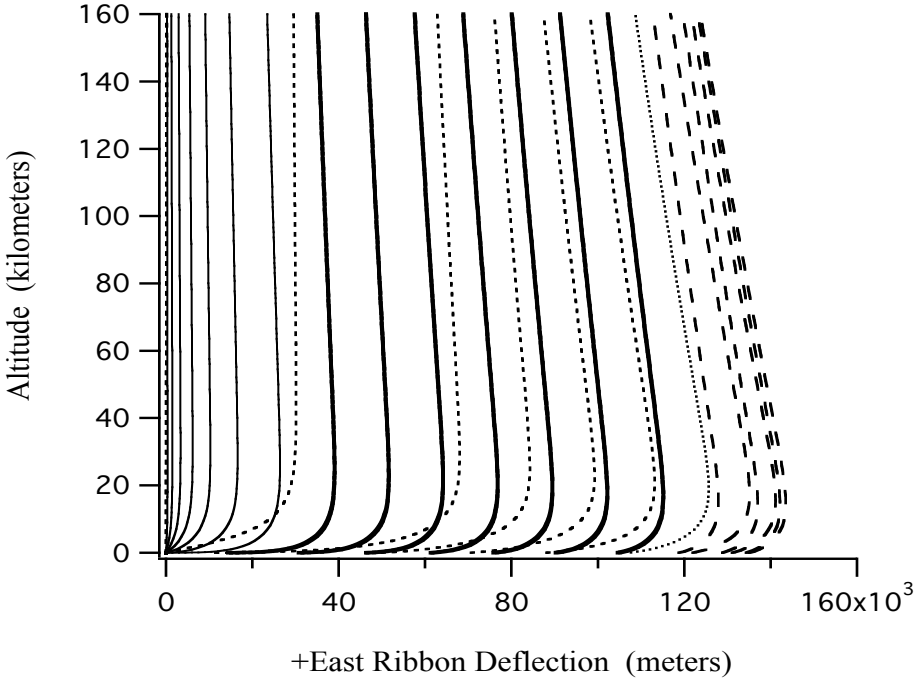

The explanation for such response can be found in examining the air loads on the ribbon and relating that to the rolling pin analogy. In the above ribbon deflection snapshots, notice that the characteristic geometry of the ribbon transition zone from vertical to (more or less) horizontal, uniformly replicates itself from snapshot-to-snapshot, and presents a significant geometrical opportunity for vertical air load to be created. The pressure distribution along the length of the ribbon creates an air load density vector normal to the ribbon's tangent at each point. Integrating this spatial force distribution around this characteristic curvature results in both a horizontal and vertical component of net air load as shown in the diagram below illustrating how air loads distribute themselves along the ribbon.

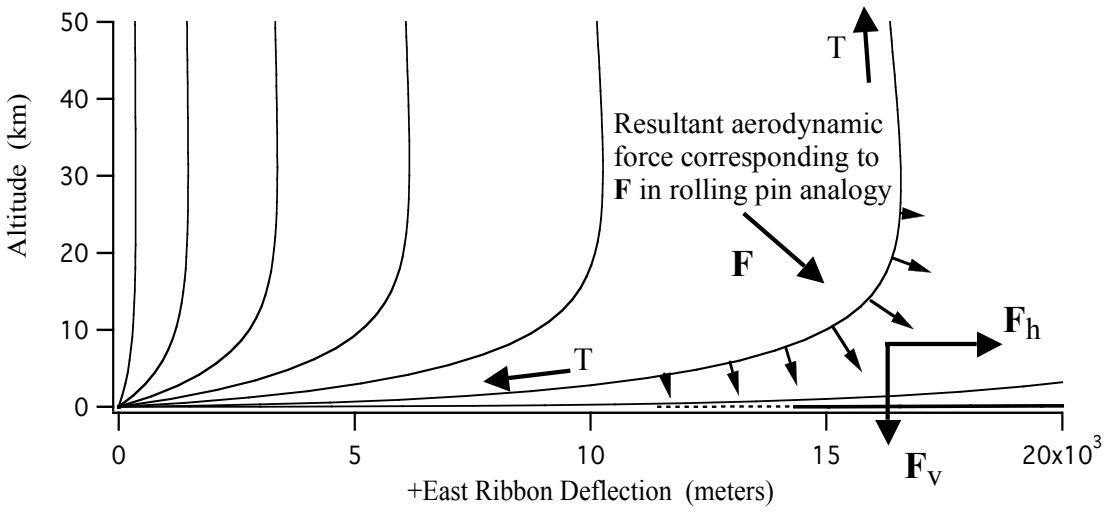

Quantification of the above is provided by the air load density distribution snapshots below corresponding to this particular response (shown in section 4.3.3.3).

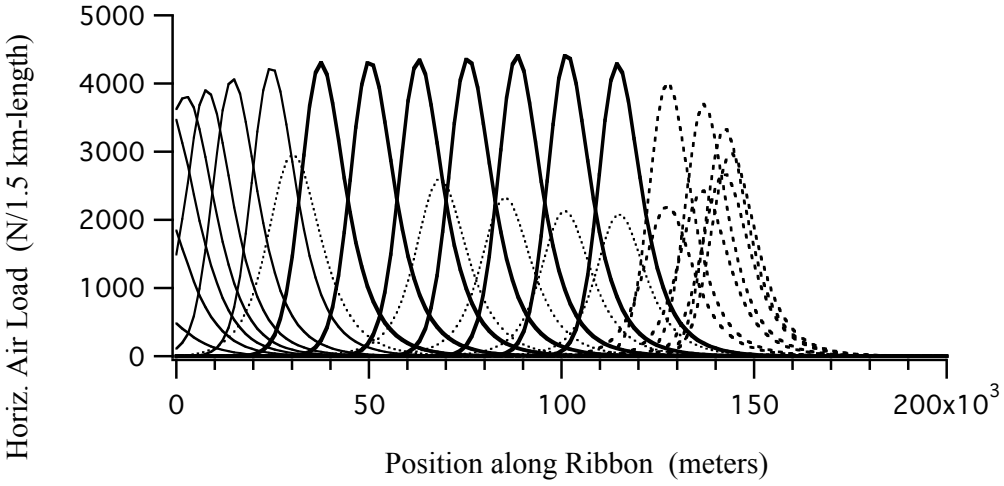

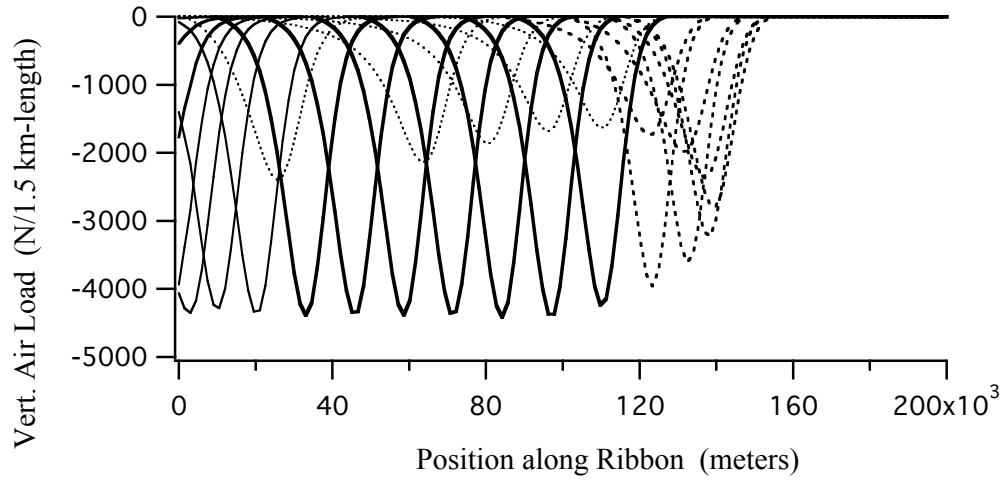

The two graphs above show snapshots of *air load density* versus *length* along the ribbon for the case of the climber at LEO subject to a category 0 wind; at any given point in time, the total vertical or horizontal air load on the ribbon is simply the "area under the curve" for the corresponding snapshot time (with due regard for the units of the ari load density).

It is significant that once the wind velocity attains a critical level, both components of air load density are migrating along the ribbon with their ***magnitudes*** as well as ***ratios*** almost unchanged (the dark solid-line snapshots corresponding to the period of constant peak wind). A progressive flattening phenomenon depends upon the air load being able to equilibrate both the horizontal and vertical components of ribbon tension beneath the climber. Since the ribbon bends from almost horizontal to almost vertical, and since tension is essentially constant over this region, this means that both the horizontal and vertical components of net air load must be nearly equal to the tension. Under these conditions, the ribbon exhibits a compliance to being blown downwind with little apparent resistance; in this case, the "area under the curve" (total horizontal or vertical air load) of the air load snapshots actually become equivalent to the tension in the ribbon.

It appears that once the wind-tension balance reaches a point that the wind can lay the ribbon horizontal, then there may be only insignificant natural restoring mechanism remaining since the energy available to the wind for "performing the work required to displace the ribbon horizontally" is essentially unlimited.

4.3.3 Typical Ribbon Deflection Response Shapes

The graphs in this section further and more dramatically illustrate the observations of section 4.2 above.

4.3.3.1 Deflections for un-occupied elevator

Below is the case of the unoccupied ribbon under a category 3 wind (54 m/s = 120 mph)

The graph below shows snapshots of the entire length of the ribbon, including the time of constant peak-wind and tail-off; comparing **category 3** wind response for an identical configuration (except) under a category 0 wind indicates a factor of 100 greater horizontal response for this category 3 wind. Note the horizontal scaling; while this response is significant, if it were viewed from a real vantage point that encompassed the entire ribbon length, it would appear essentially straight, with horizontal distortion on the order of 1% of its length.

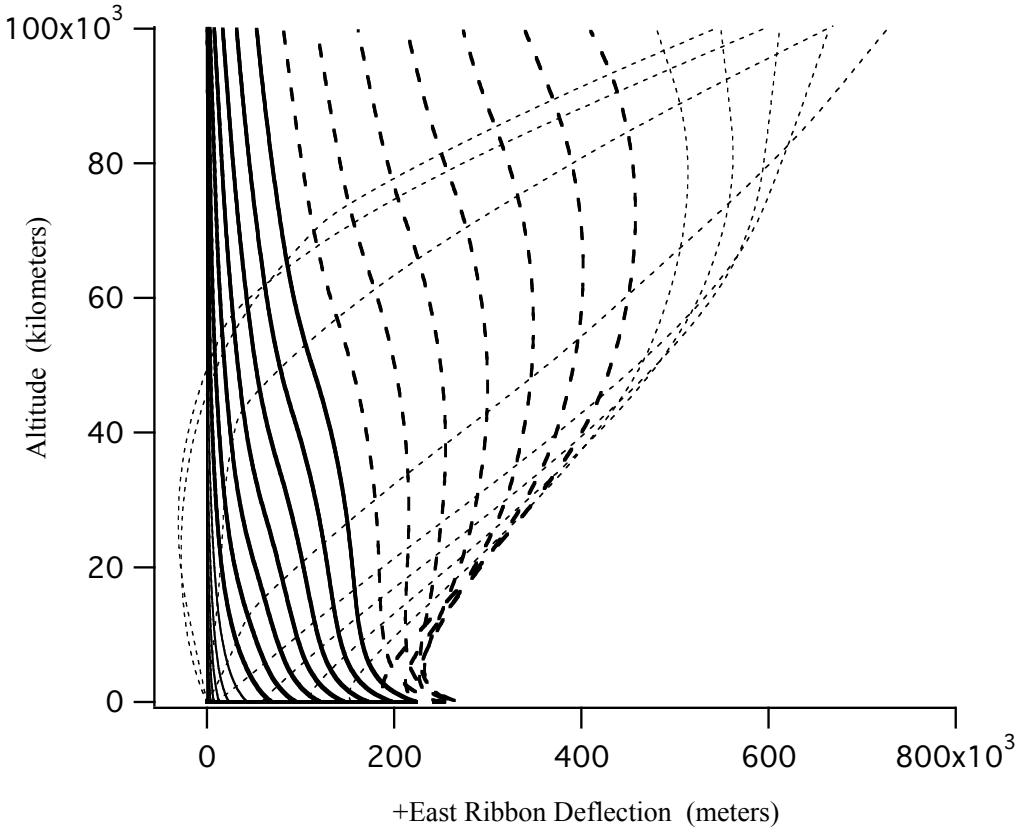

The graph below shows magnified, near-earth, horizontal displacement snapshots with identical vertical and horizontal scaling to depict true geometry and ribbon

departure angles; also shown on this graph is the maximum deflection for the category 0 wind illustrating the overall effects of wind speed on ribbon departure angle.

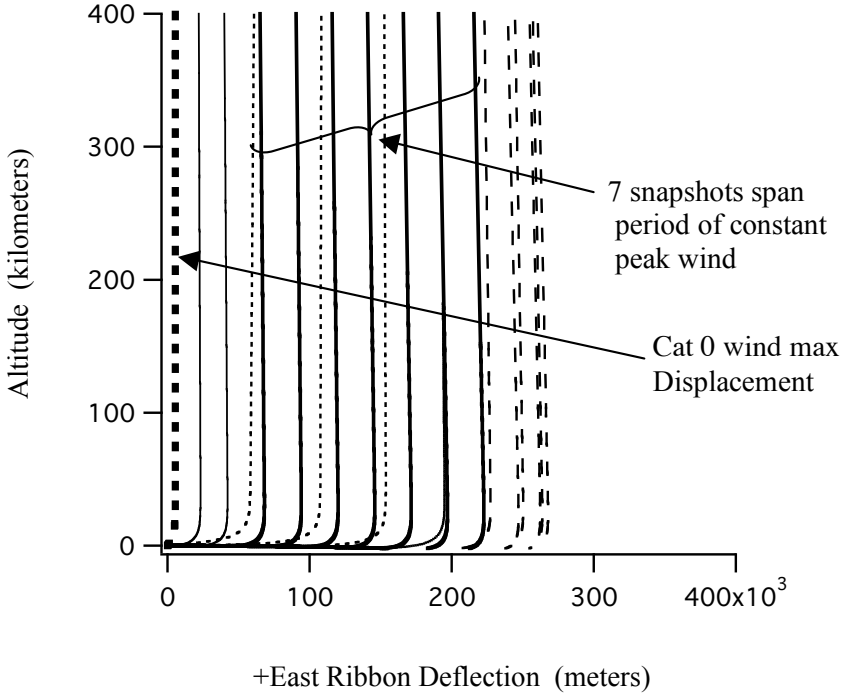

Note the single heavy vertical dashed line nearest the origin (above); this represents the maximum horizontal response for a category 0 wind. It is evident that somewhere between category 0 and 3 wind levels, a threshold was reached for which wind force could overcome any inherent ribbon resistance to horizontal displacement. This supposition is further corroborated by the fact that the *bracketed* snapshots (with heaviest lines near the middle deflections of the graph), encompass exactly the period of constant peak wind, meaning that even with wind not increasing, the horizontal displacement continues to increase.

4.3.3.2 Deflections with climber in low atmosphere

Here, a 20 ton climber is parked in the atmosphere at 9 km, and subjected to the Category 0 wind profile. Note, climber aerodynamics were characterized as a simple drag model with drag coefficient of 1.2 and cross sectional area of 18 m^2, thus only horizontal air load is generated by the climber.

Horizontal ribbon displacement is shown below. Note the one snapshot composed only of dots; this depicts GTOSS finite tether model nodal spacing below and above the climber, and shows a resolution below the climber that is *just adequate* to resolve these aerodynamics; this sparseness was adopted for numerical efficiency. Location of the climber is evidenced by the sharp *bend* at about 9 km along the ribbon. This bend, while not pronounced near the ribbon's initial vertical position, ends up clearly depicted at a *horizontal* distance near 9 km; thus the trajectory of the climber becomes evident.

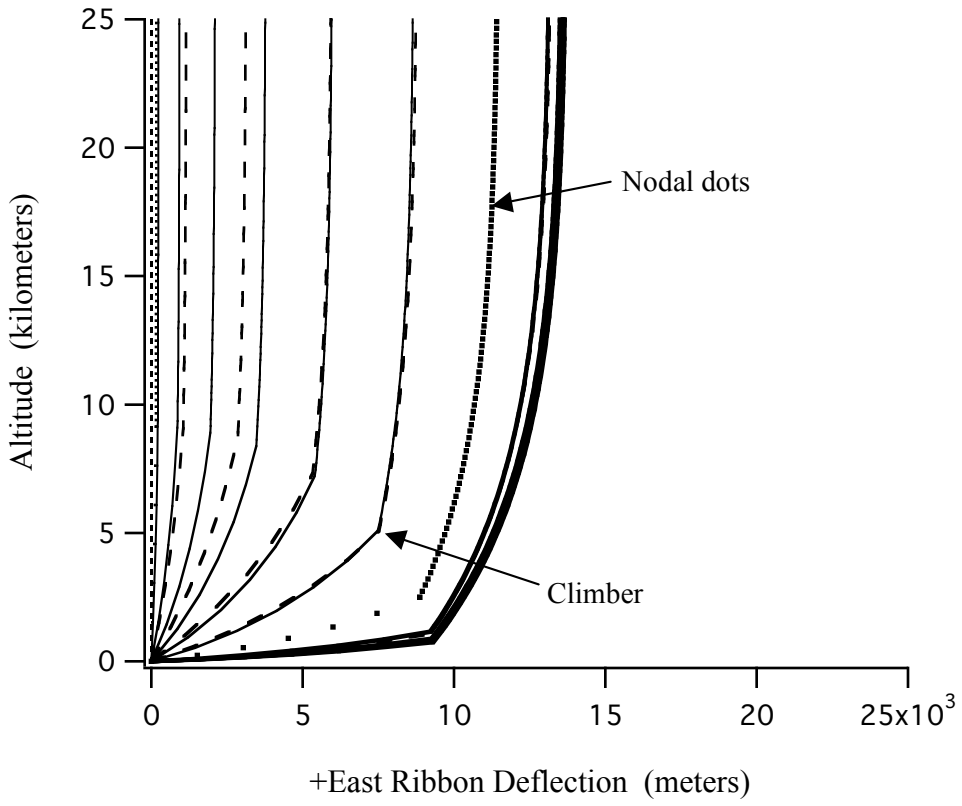

Due to the low tension between the ground and climber, there is little resistance initially to horizontal displacement of the climber; this is exacerbated even further by the additional atmospheric drag on the climber. So the climber and lower ribbon section easily move horizontally pulling the climber even lower; however, once the climber has moved a horizontal distance corresponding to its fixed position on the ribbon (of 9 km), then any additional action by air loads to move the climber horizontally is met by the now nearly horizontal segment of ribbon between the climber and ground. This short segment, with an effective spring rate about 10,000 times greater than the ribbon above, can easily equilibrate any horizontal load with very little additional strain as shown below as a tension time history in the lower ribbon segment. This shows that the tension rises to meet the applied horizontal air load, thus effectively constraining the climber itself (but not the ribbon above) from additional horizontal motion. Once the lower ribbon becomes near horizontal, the situation then mimics the displacement, shape and departure angles of the unoccupied elevator, as witnessed by the fact that in this case, the ribbon above the climber exhibits about 5 km of maximum horizontal displacement *beyond the climber;* this compares closely with the shape and peak displacement of the unoccupied elevator under a category 0 wind. The case of a climber parked in the atmosphere (9 km) more nearly mimics the unoccupied configuration than it does the case with the climber parked at 200 nm (150,000 m).

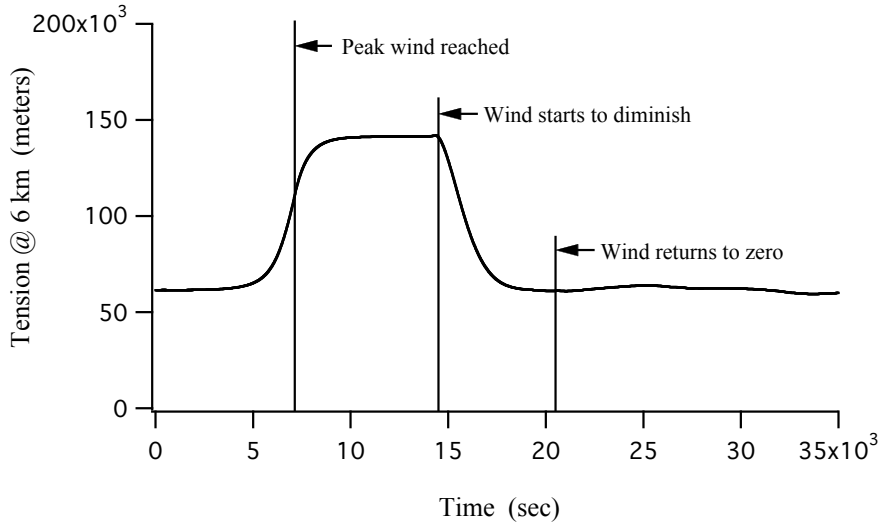

4.3.3.3 Deflections with climber at LEO

Below are snapshots of the ribbon, at 2,000 sec intervals for 10 hours. Subjected to identical winds, a ribbon with a climber at LEO (200 nm) responds vastly different than an unoccupied ribbon. Note different *horizontal scales* between this and the unoccupied ribbon. Maximum atmospheric displacement for an unoccupied ribbon was about 6,000 meters; with a climber at LEO, the maximum displacement is 150,000 meters!

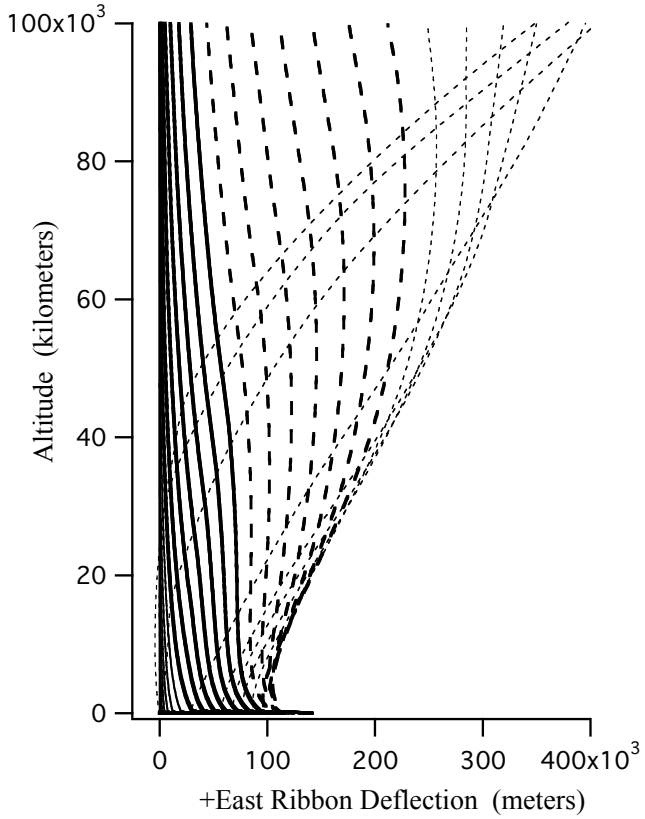

The difference in response can be attributed to the effect of climber mass that serves to modify response in the following two significant ways: (a) by presenting a significant inertia that affects ribbon excursions near the atmosphere, and (b) by creating a significant ribbon tension drop across itself (see graph below), thus presenting to the atmosphere, a ribbon under 4 times less tension than for the unoccupied ribbon. The low tension presents a much more compliant ribbon to the wind than that of the unoccupied ribbon. The tension discontinuity shown below occurs at the climber's position of 370 km altitude (200 nm).

Snapshots below use identical vertical and horizontal axis scaling to depict actual ribbon departure geometry, and indicates a ribbon eventually departing the anchor at near horizontal. One snapshot depicts dots representing GTOSS nodal resolution.

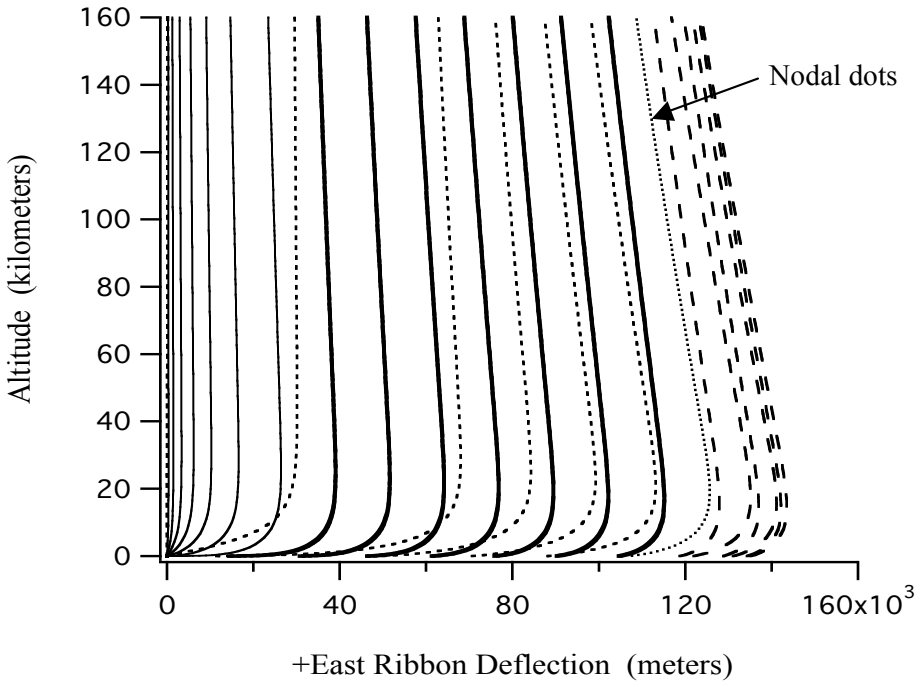

Below is the same as the figure above, except with a much greater vertical scale to show the climber's position. Here, the sharp bend in the ribbon, not seen above due to its scale, clearly depicts the location and effect of the climber. Note also the snapshot, composed of only dots at the nodal points; this shows where the nodal resolution changes at the location of the climber.

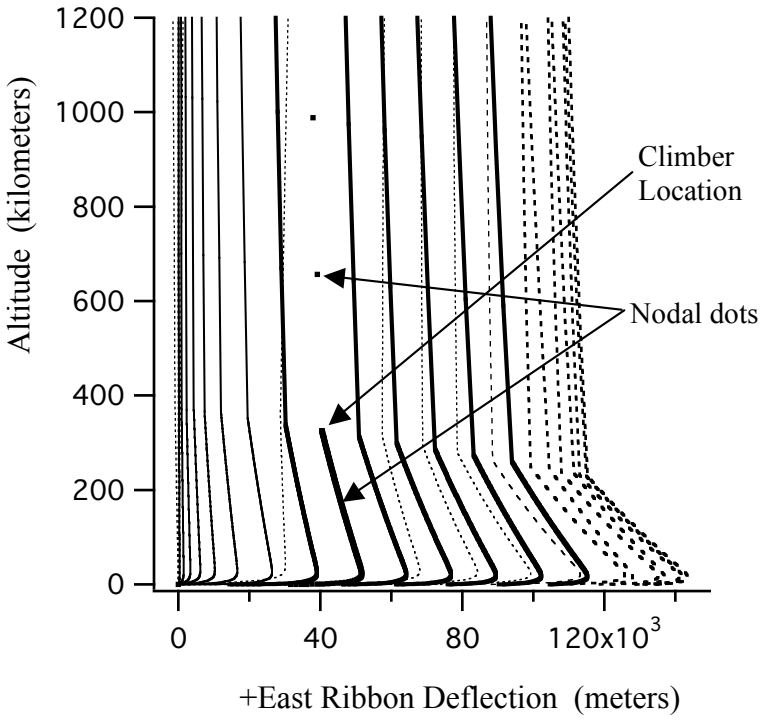

The graph below has magnified but also *identically-scaled* vertical and horizontal axes to provide insight into the deflection mechanism in this case.

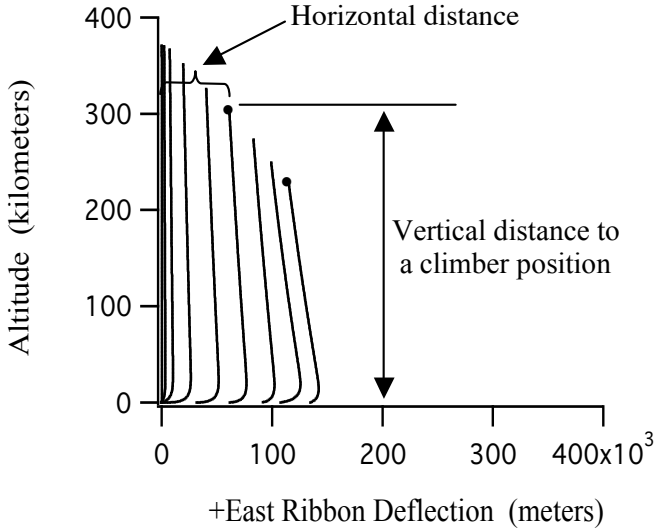

Note, for each snapshot above, the *sum* of the "vertical distance to the climber" plus the "horizontal distance to the anchor" is essentially constant, and equal to the initial vertical altitude of the climber. By the time the simulation has terminated, the climber has been displaced downward by about 140 km, accompanied by no significant tension increases. This is consistent with both the insignificant increase in upper ribbon strain corresponding to this amount of climber displacement, as well as the upper ribbon's low effective end-to-end spring rate. Using an upper ribbon spring rate of 0.04 N/m, this decrease in climber altitude corresponds to a tension increase of 5000 N (out of 200,000 N extant in the ribbon above the climber); the corresponding strain increase in the upper ribbon due to this displacement is only 0.14 percent.

4.4 RIBBON HORIZONTAL DISPLACEMENT

This shows horizontal ribbon displacement response to reference wind variations of:

1. Peak Wind value varying between Category 0 and 3
2. For Category 3 wind, the Duration of Peak Wind, varying between 1 and 4 hours
3. For Category 0 wind, Ribbon Width varying between 5 and 20 cm.

4.4.1 Horizontal Displacement vs Wind Speed (Unoccupied)

Round markers are simulation-run data points; *dotted* lines are interpolation.

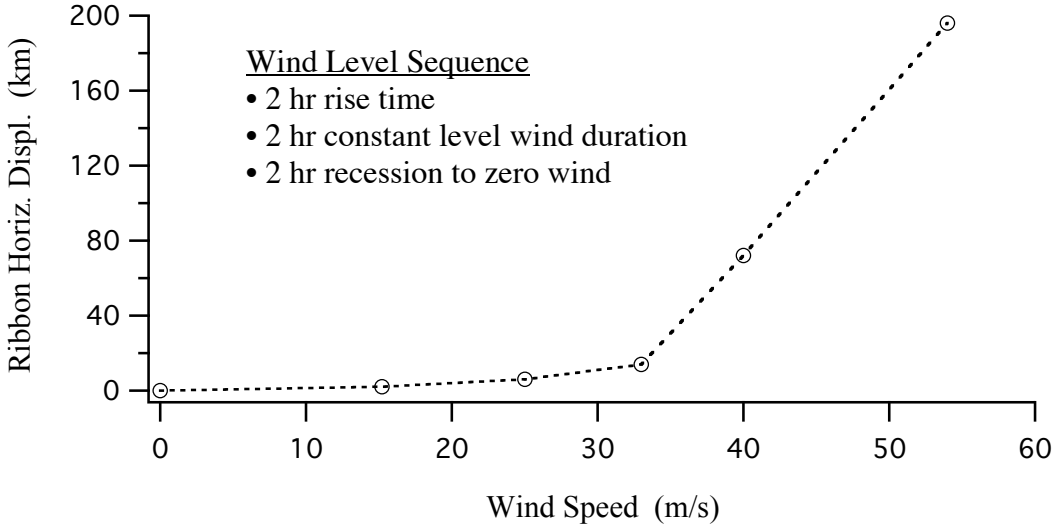

Note the sharp break in the displacement response above; this is indeed the point at which total air load achieves a level capable of equilibrating (virtually simultaneously) both vertical and horizontal components of ribbon tension. At this point, the wind essentially gains control of the ribbon, and limitation to further displacement will either be at the whim of the weather, or, will await second-tier effects (due to extreme displacements) to start manifesting themselves. Shown below is the same graph as above, except with (a)

magnified scale limited to 0-30 m/s wind speed, and (b) the corresponding departure angle is overlaid on the graph.

To aid in the interpretation of this phenomenon, the graph below shows (for lower wind speeds) is the relationship between departure angle and horizontal displacement.

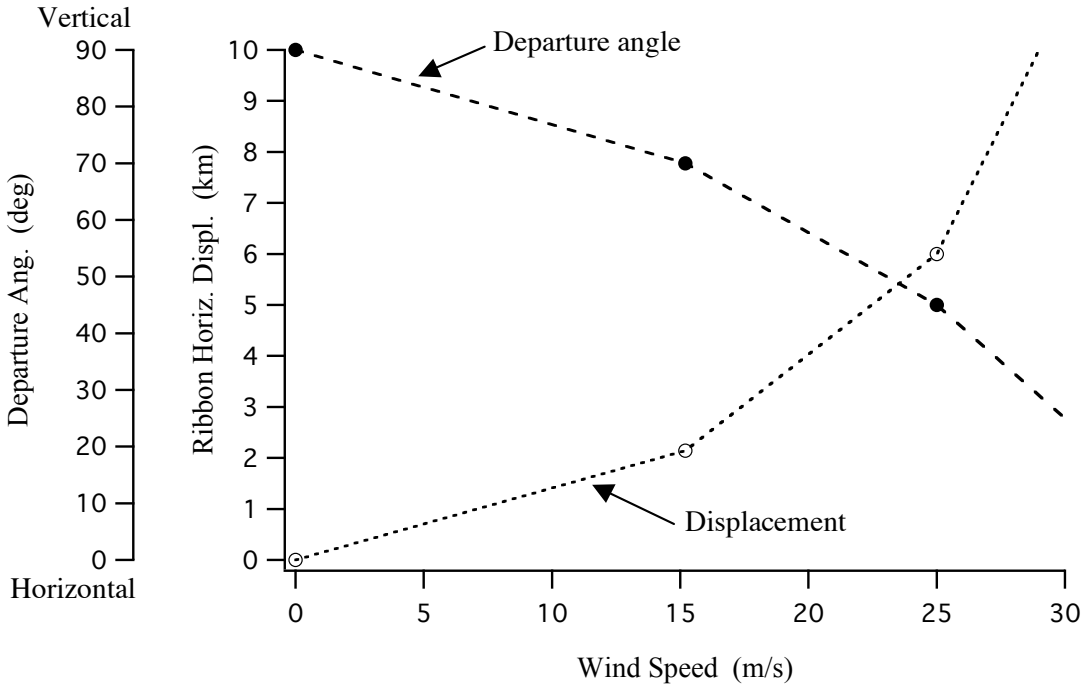

4.4.2 Horizontal Displacement vs Wind Duration (Unoccupied)

Shown below is response to a Category 3 wind level for an unoccupied ribbon. *Round* markers are simulation-run data points; *dotted* lines are interpolation.

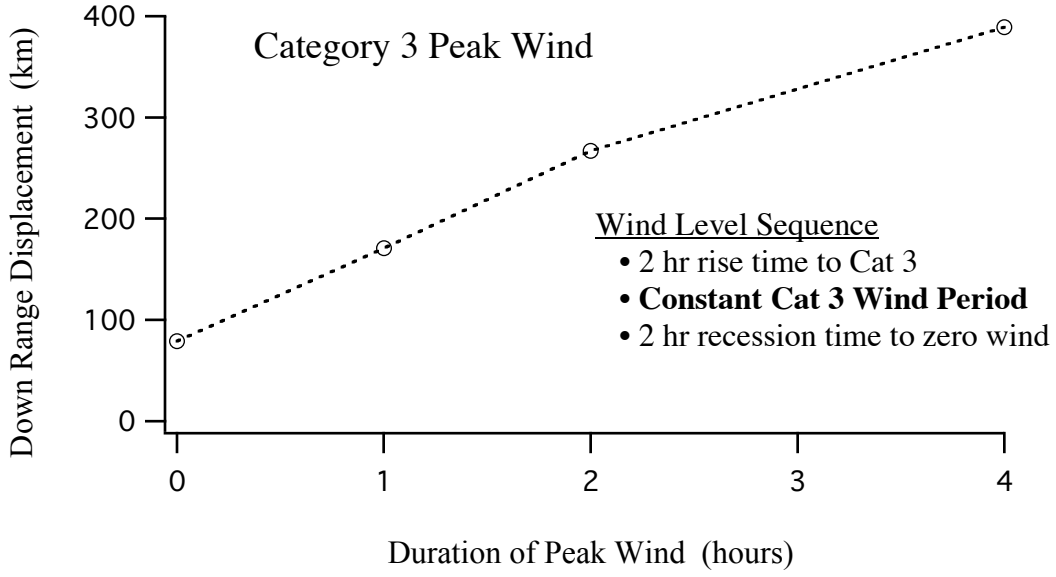

Note: a "duration of zero" here means that as soon as the wind rises to the Category 3 level, it immediately starts to recede with no dwell time at category 3 level. It is apparent that the displacement-duration relationship is essentially linear up until sometime after 2 hours wind duration at which point, secondary effects are starting to come into play to eventually attenuate the progression of downrange displacement. This could be slowly increasing ribbon tension, geometry changes due to downrange distance (such as earth curvature).

4.4.3 Horizontal Displacement vs Ribbon Width (Unoccupied)

The graph below shows the ribbon horizontal displacement sensitivity to ribbon width for an unoccupied elevator ribbon. This data corresponds to a Category 0 peak wind level.

Round markers are simulation-run data points; *dotted* lines are interpolation.

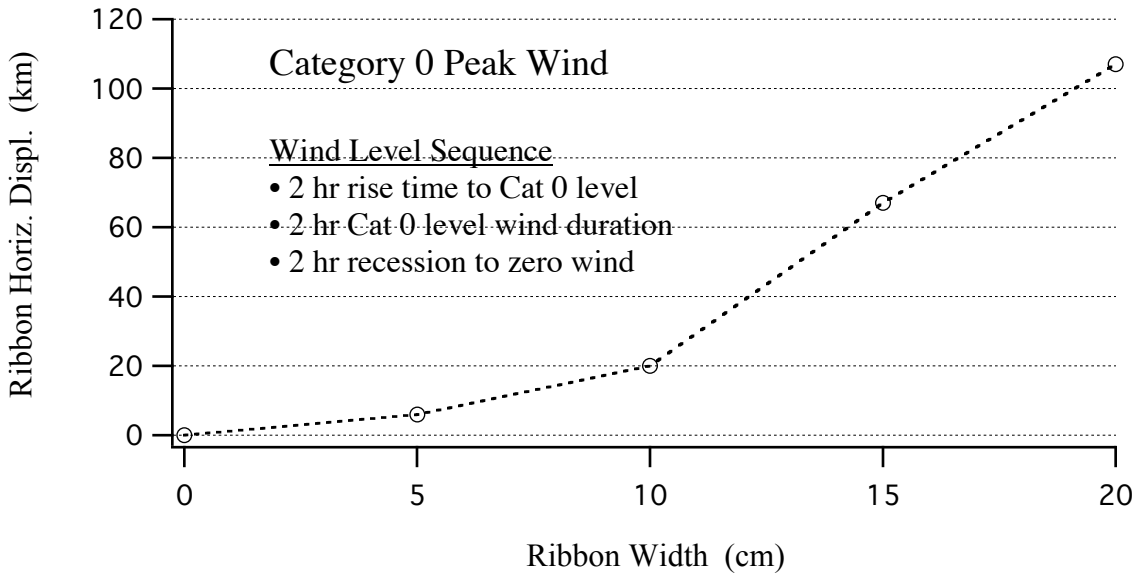

4.4.4 Horizontal Displacement vs Wind Speed (Climber in Atmosphere)

The graphs below correspond to a climber parked at 9 km altitude on a 5 cm SE ribbon subjected to various wind levels. The presence of the climber in the atmosphere exhibits both beneficial as well as detrimental effects.

Beneficial effects pertaining to horizontal displacement:

• The fact that the portion of the ribbon between the climber and the anchor point becomes quickly horizontal under aerodynamic response means that this very stiff horizontal section of ribbon easily equilibrates the horizontal loads that can be developed in the high aerodynamic pressure regions associated with lower altitudes. This effect clearly manifests itself in the

deflection -vs- wind speed graphs below when compared to the unoccupied ribbon (section 4.4.1 above).

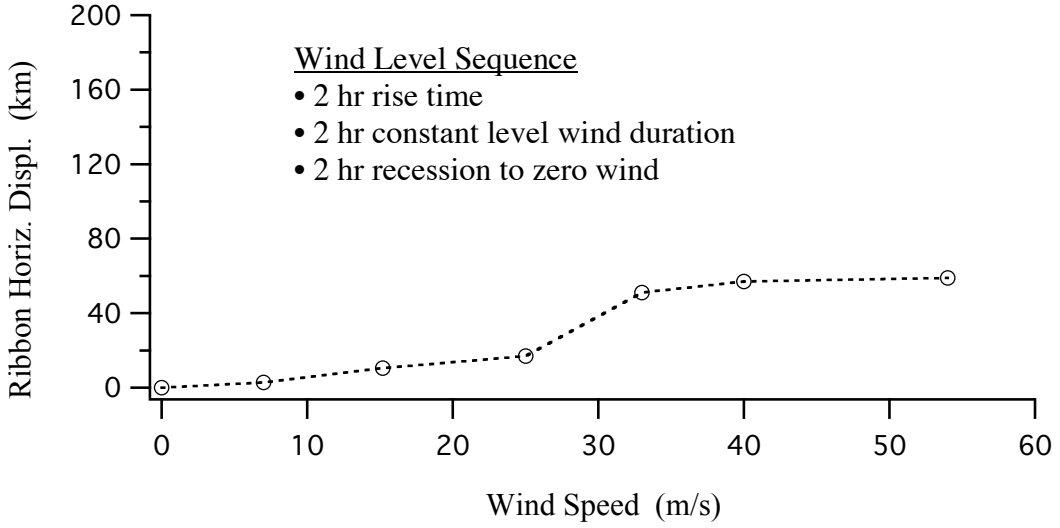

Round markers are simulation-run data points; *dotted* lines are interpolation.

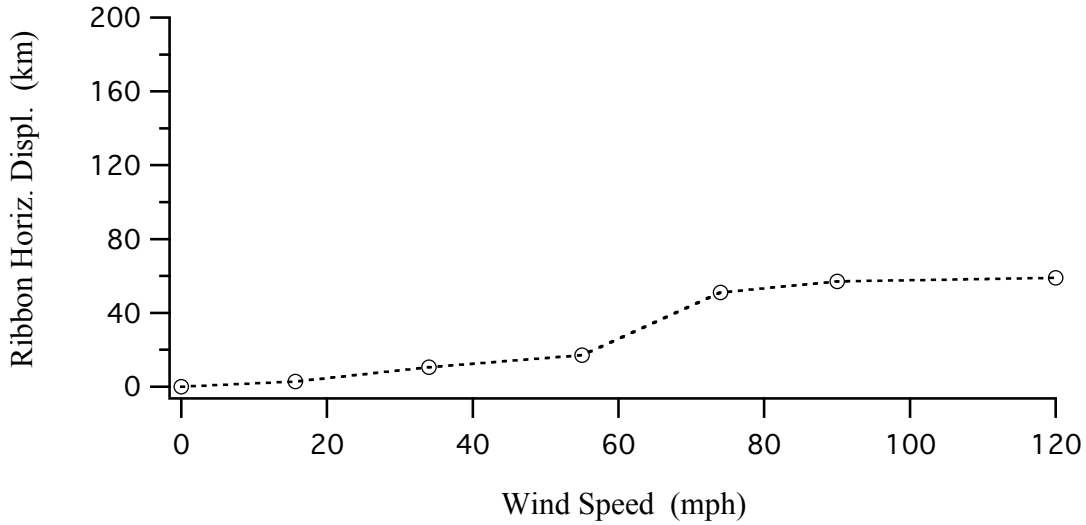

4.4.5 Horizontal Displacement vs Wind Speed (Climber at LEO)

The graphs below correspond to a climber parked at LEO altitude on a 5 cm SE ribbon subjected to various wind levels. The presence of the climber in the atmosphere exhibits detrimental effects regarding horizontal displacement.

Round markers are simulation-run data points; *dotted* lines are interpolation.

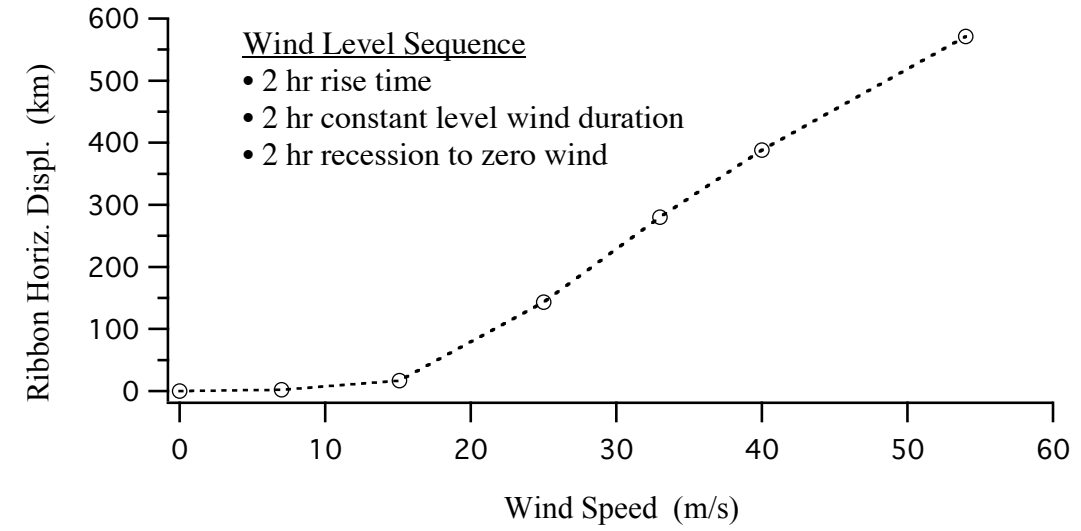

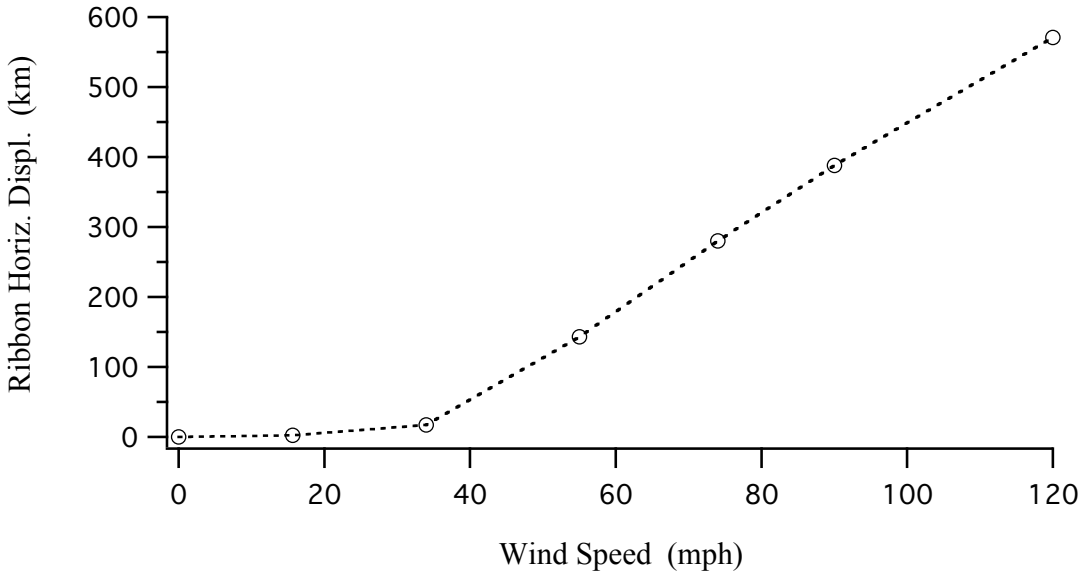

4.5 RIBBON DEPARTURE ANGLES

The departure angle of the ribbon is the angle that the ribbon makes with the "local vertical" reference, thus 90 degrees indicates a ribbon's proceeding straight up, vertically, from the anchor point. While this parameter is not indicative of over stressing, or other structural failure per se for the ribbon, it does have profound implication on anchor station design, and general operations in the presence of wind. These results may well speak for operational constraints of climber launches based on wind predictions for the anchor location. Due to the possibility of low-to-horizontal departure angles, additional design criteria may be levied on the rib on to tolerate sea water contamination. Additionally, practical response to the potential for low departure angles my dictate anchor station design that provides an actual ribbon attach point elevated considerably above sea level.

4.5.1 Departure Angle vs Wind Speed (Unoccupied)

Round markers are simulation-run data points; *dotted* lines are interpolation.

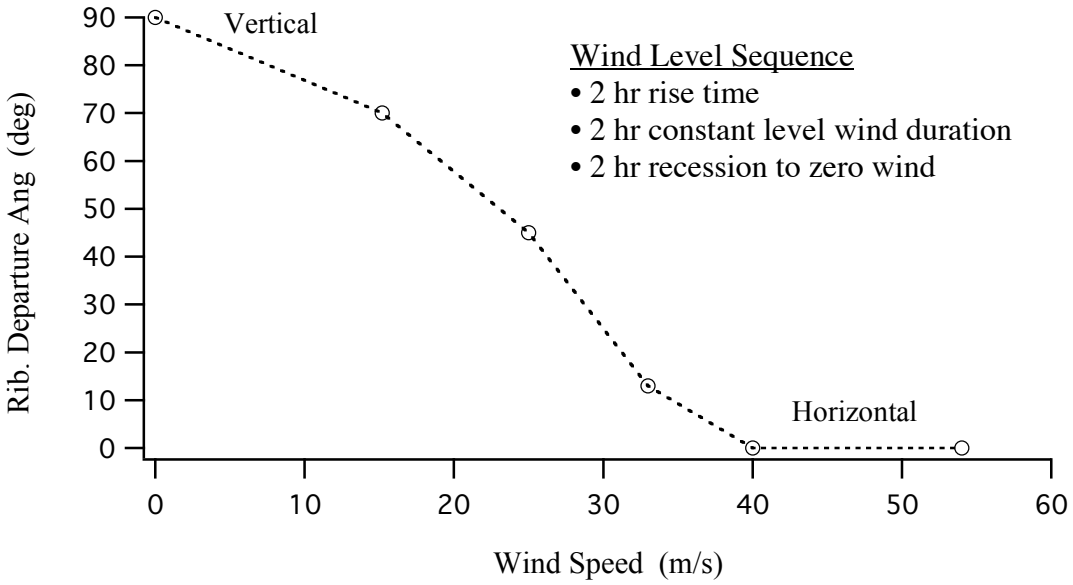

4.5.2 Departure Angle vs Ribbon Width (Unoccupied)

The graph below shows the ribbon departure angle sensitivity to ribbon width for an unoccupied elevator ribbon. This data corresponds to a Category 0 peak wind level.

Round markers are simulation-run data points; *dotted* lines are interpolation.

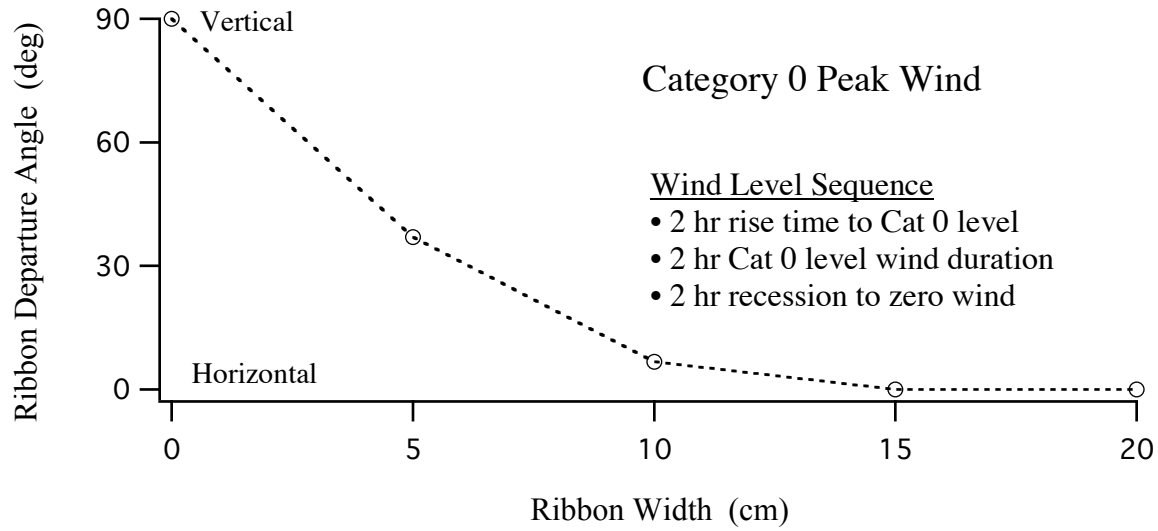

4.5.3 Departure Angle vs Wind Speed (Climber in Atmosphere)

The graphs below correspond to a climber parked at 9 km altitude on a 5 cm SE ribbon subjected to various wind levels. The presence of the climber in the atmosphere exhibits detrimental effects regarding ribbon departure angles.

Detrimental effects pertaining to ribbon departure angle:
• Due to the low tension between the climber and anchor point, and the aerodynamic drag of the climber itself, even winds less than category 0 will virtually lay the climber down creating a horizontal departure angle. This effect clearly manifests itself in the departure angle -vs- wind speed graphs below.

Round markers are simulation-run data points; *dotted* lines are interpolation.

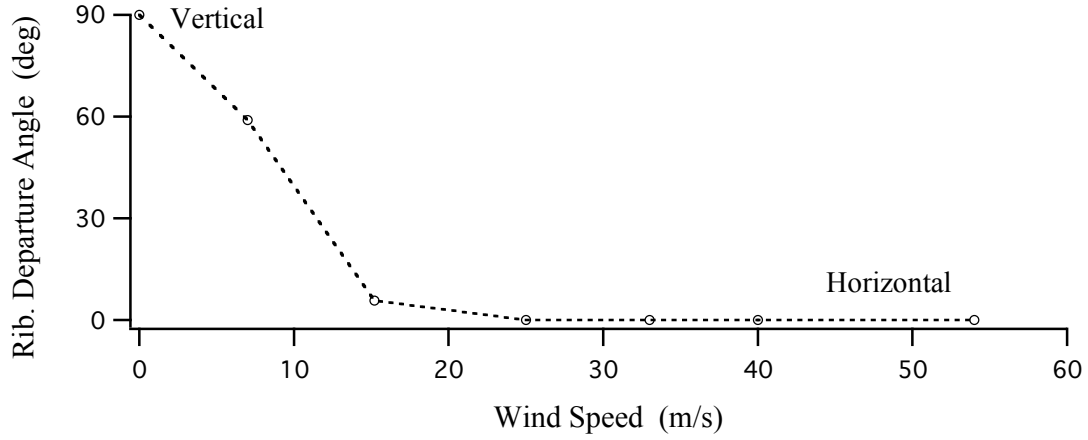

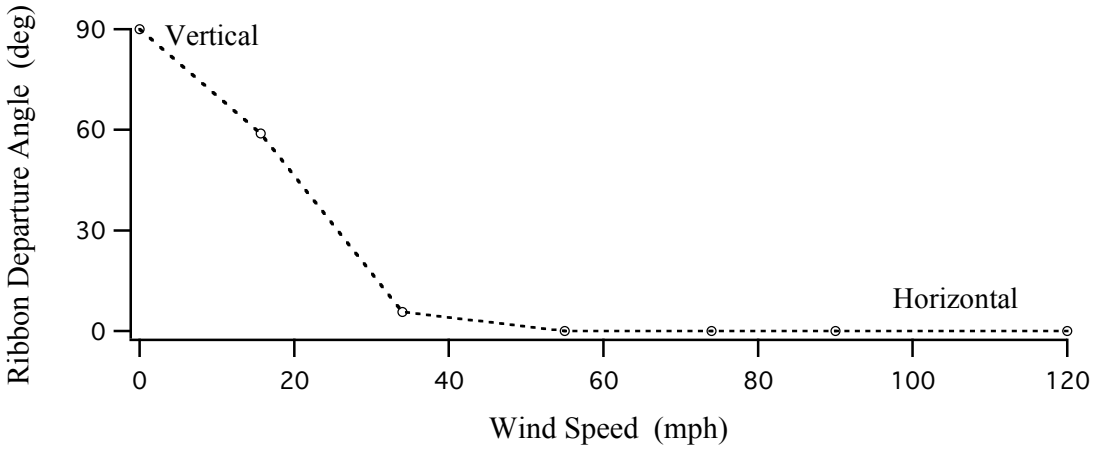

4.5.4 Departure Angle vs Wind Speed (Climber at LEO)

The graphs below correspond to a climber parked at LEO altitude on a 5 cm SE ribbon subjected to various wind levels. The presence of the climber at LEO exhibits detrimental effects regarding ribbon departure angles.

Detrimental effects pertaining to ribbon departure angle:

• Due to the low tension between the climber and anchor point, even winds less than category 0 will virtually lay the ribbon down creating a horizontal departure angle. This effect clearly manifests itself in the departure angle -vs- wind speed graphs below.

Round markers are simulation-run data points; *dotted* lines are interpolation.

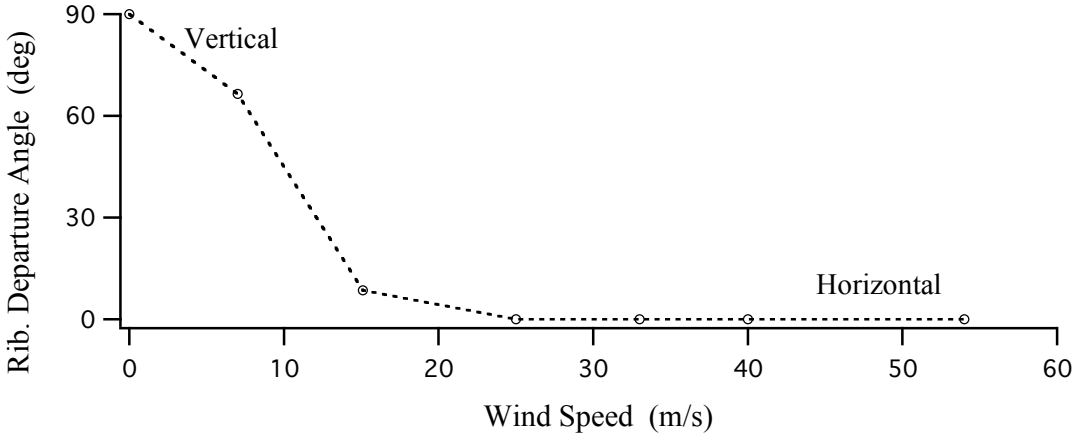

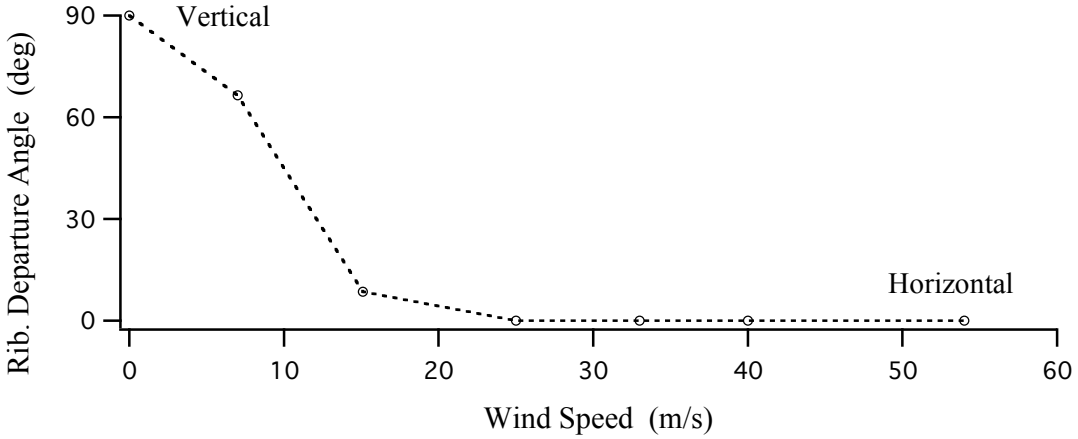

Point of Interest: It is evident that in both cases of a Climber occupying the ribbon (ie. at LEO and within the atmosphere), that the ribbon departure angle quickly goes to horizontal under wind levels of Category 0, and likely at even lesser winds. This speaks for the possibility of elevator launch restrictions when appreciable winds are predicted.

4.6 STRESS RELATED TO WIND RESPONSE

By design, nominal unoccupied SE stress levels are near constant; the question arises whether and how much wind can magnify these stress levels. This section addresses this by showing graphs of stress profile vs ribbon length for various conditions.

4.6.1 Stress Profile vs Wind (Unoccupied)

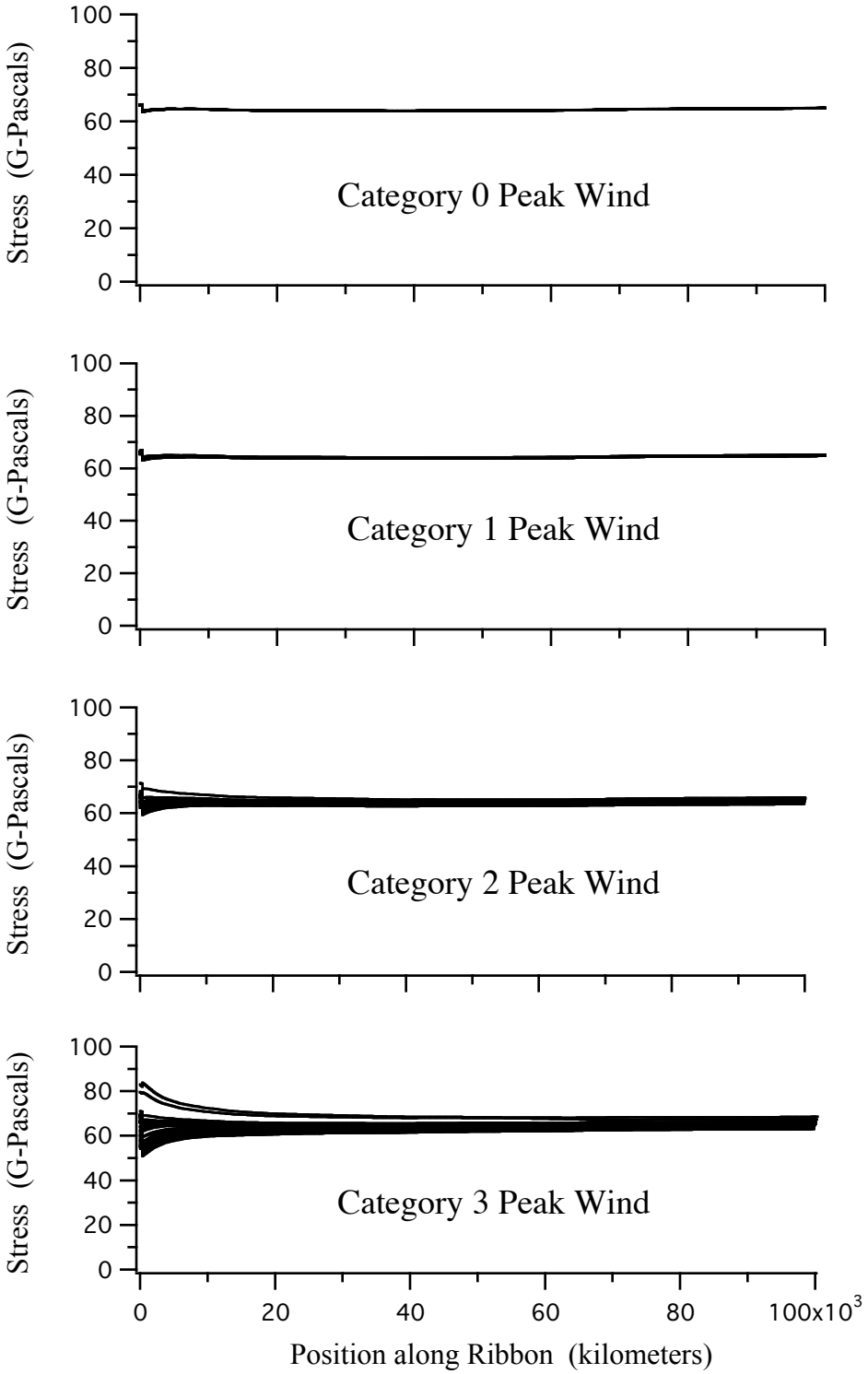

4.6.2 Stress Profile vs Ribbon Width (Cat 0, Unoccupied)

Here, the ribbon width is being varied, all subject to a Category 0 wind level. The wind level follows this scenario:

- 2 hr rise time to Cat 0 level
- 2 hr Cat 0 level wind duration
- 2 hr recession to zero wind

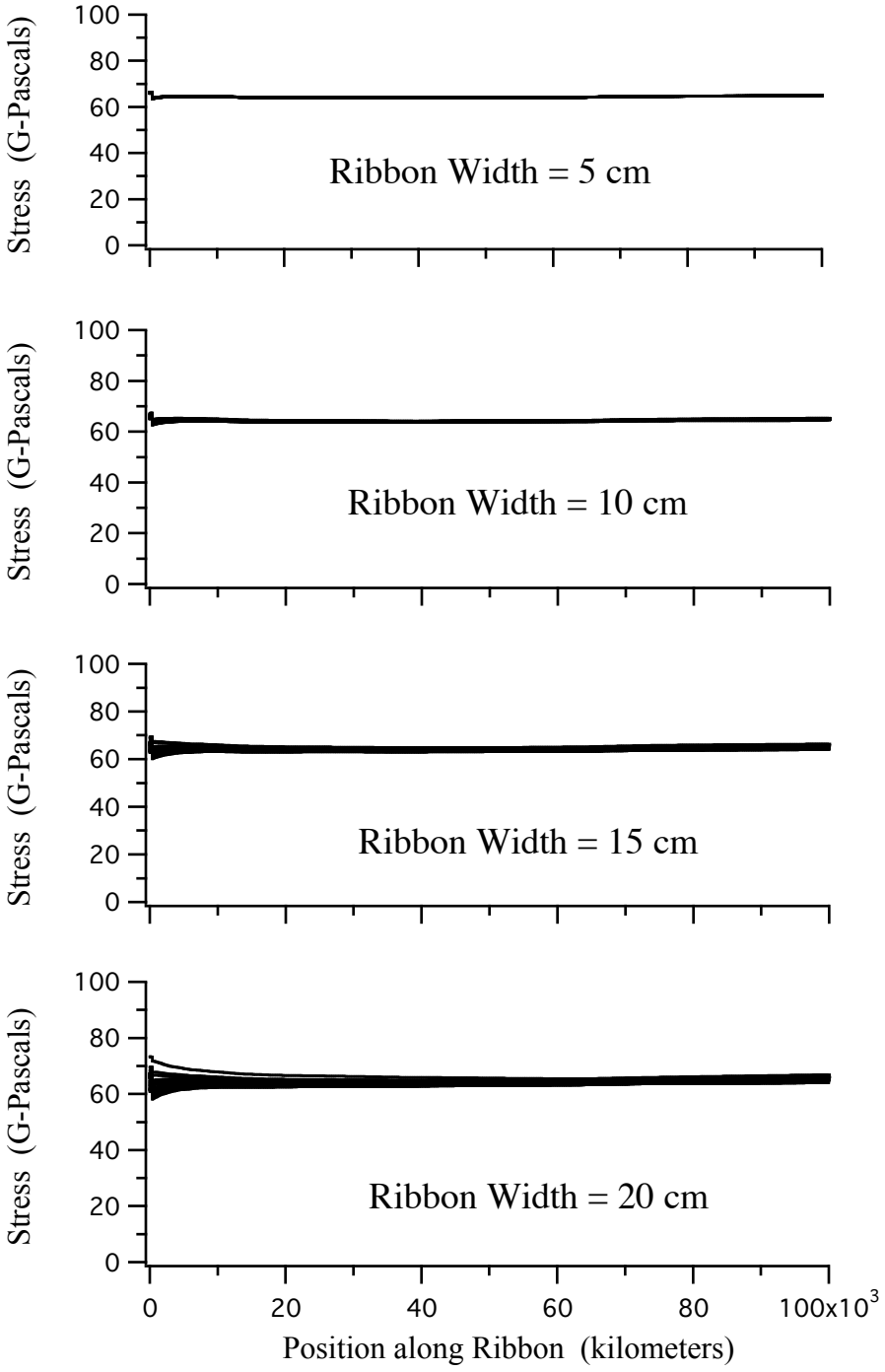

4.6.3 Stress Profile vs Wind (Climber in Atmosphere)

Note the characteristic tension drop across the climber at 9km, that manifests itself as the discontinuity at the 9 km point on the ribbon. The ribbon above the climber is characteristically showing very little stress increase due to aerodynamic displacement, thus the horizontal axis is scaled to show only the first 40 km of ribbon. It is the short section of ribbon below the climber

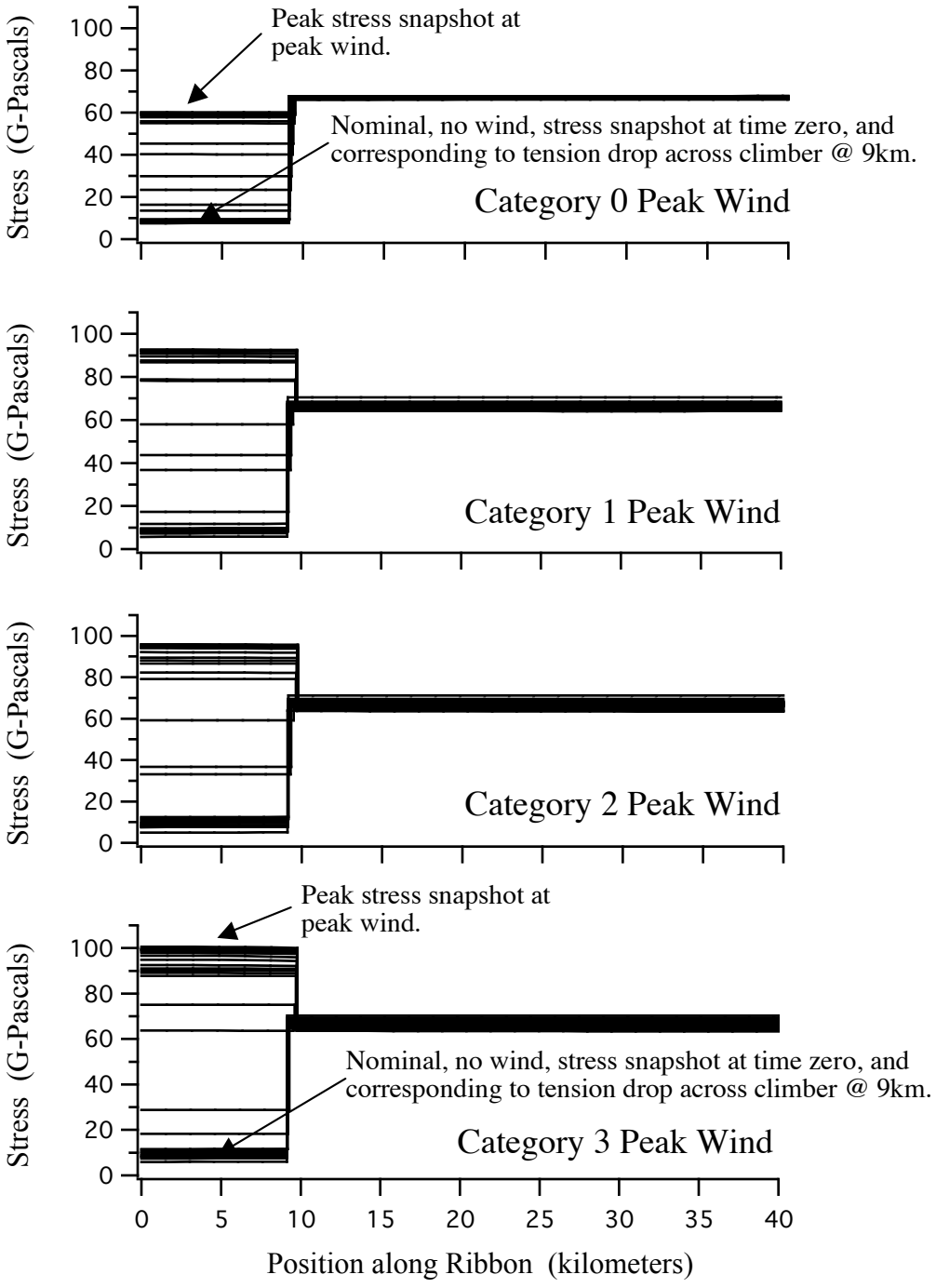

(between climber and anchor) that is showing significant stress response. This can be explained as follows. First note that these graphs consist of a series of snapshots of stress profile along the ribbon at various points in time throughout the entire 6 hours of active wind. All these profiles exhibit identical snapshots during the period that the wind is insignificant, such as initially before it has built to peak values (this is the regime that is manifesting itself as the lowest stress values being experienced in the region between ground and 9 km). As wind level increases with time, the stress snapshots in this region also start to increase. This is because as wind increases, the climber is being laid down ever more horizontal, thus the short ribbon section below the climber is functioning to equilibrate the total horizontal air loads on the ribbon. While normally, the tension in the ribbon below the climber exhibits a lower value than that above, in this case, as the ribbon becomes horizontal, its tension starts to assume the full level required to equilibrate the horizontal component of air load; this component of the process essentially imbues the lower ribbon (originally under reduced stress) with stress levels consistent with an unoccupied elevator under air load. Now, added to this increasing tension is the air load that arises from the fact that the climber *itself* has aerodynamic drag subject to lower altitude high atmospheric density. All this combines to create a condition of *significant* stress increase in the lower ribbon for the case of the climber in the atmosphere.

Note, that the stress above 9 km shows almost no increase due to the extremely low effective spring rate of the ribbon above the climber as described in preceding sections.

4.6.4 Stress Profile vs Wind (Climber at LEO)

This section shows stress level response for an elevator with a climber parked on the ribbon at LEO, or 200 nm (370 km).

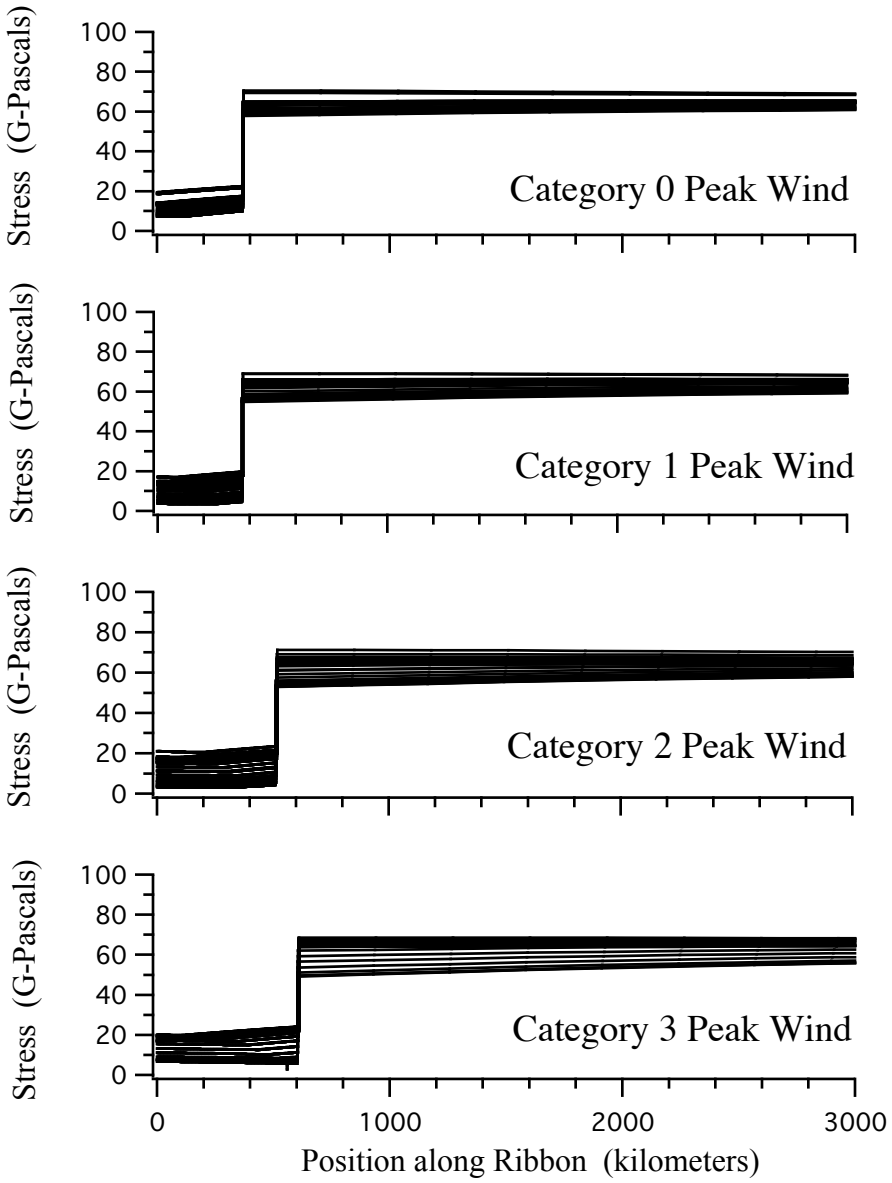

Note that similar tendencies are being exhibited in this case as that for the case of the climber parked in the atmosphere, except, here stress amplification is greatly mitigated over the atmospheric case. The section of ribbon between anchor and climber exhibits a much smaller effective spring rate than that for the atmospheric climber. Note that as peak wind levels increase the ribbon is being stretched (seen in the migration of the climber's position to greater distances from the ground, ie. moving towards the right in the series of snapshot graphs).

Stress profiles over the remainder of the ribbon are typical and show no specific tendency toward increased stress.

Note, results for the Category 3 wind were curtailed due to limitations on run time during analysis, so the response tendencies being logically established as wind peak progressed through category 0, 1, 2, are not fully developed for the category 3 wind.

5.0 CLIMBER DYNAMICS

Construction and operational payload climbers traversing the ribbon, will excite transverse and longitudinal *string mode* responses and elevator libration motion (the simple pendulum-like motion of the elevator about its anchor point). Such responses will reflect all the potentially non-linear effects related to tapered ribbon design, inverse-square gravity field, centrifugal forces, Coriolis effects, atmospheric disturbance, and climber speed modulation.

The section summarizes various typical dynamic response characteristics of the SE due to the action of a climber. The rationale' and details of the simulation of this using GTOSS is presented in Appendix B. The material shown directly below can aid significantly in interpreting various un-intuitive climber response attributes

NEAR-GROUND OPERATIONS

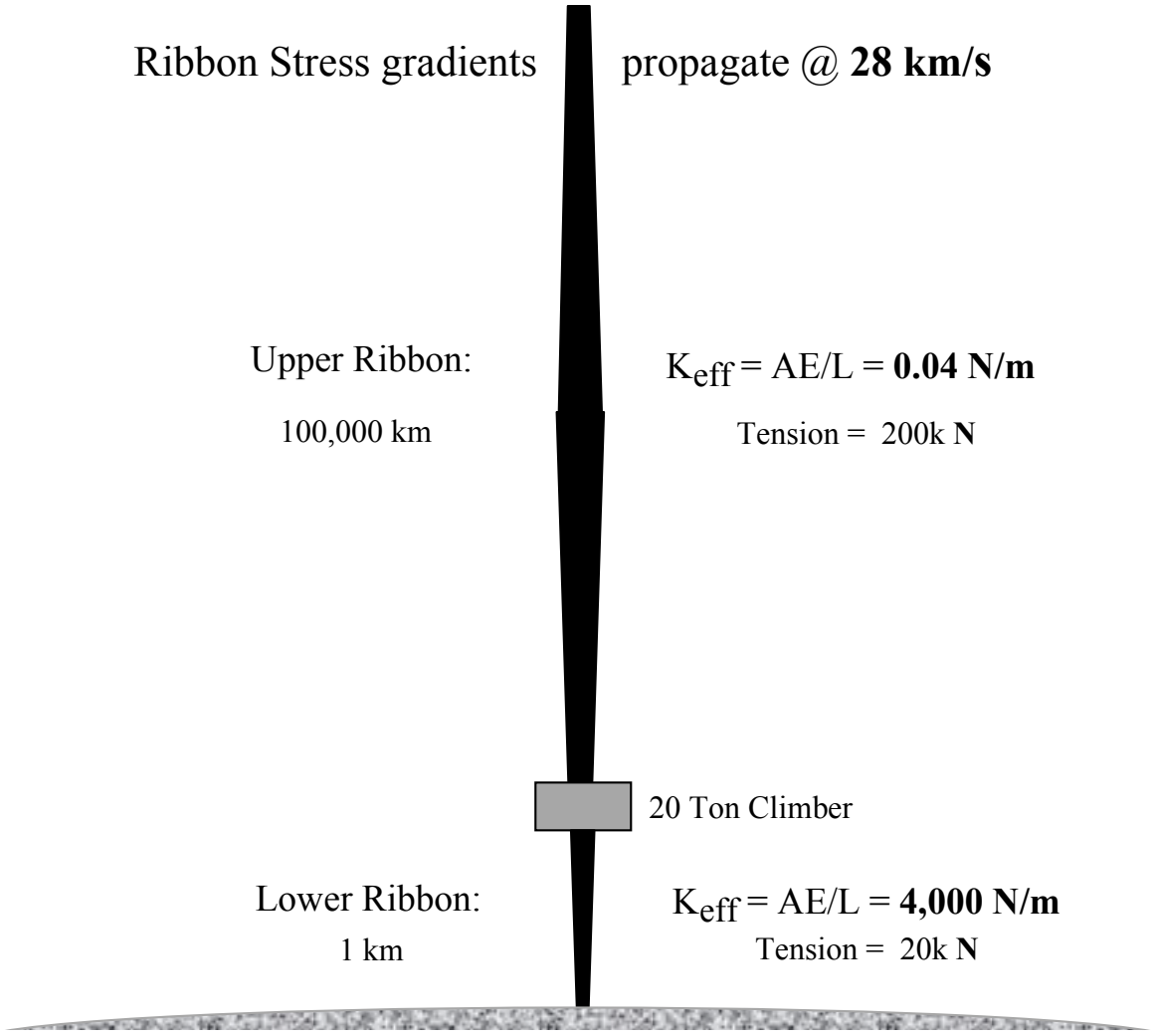

The facts below are based on the diagram above.

5,000,000 m Upper Ribbon elong. ➡ **200,000** N Tens
5 m Lower Ribbon elong. ➡ **20,000** N Tens

1000 m of Upper Ribbon Δ elong. ⇨ **0.001** % Δ Strain
1 m of Lower Ribbon Δ elong. ➡ **0.1** % Δ Strain

1000 m of Upper Ribbon Δ elong. ⇨ **40** N Δ Force
1 m of Lower Ribbon Δ elong. ➡ **4000** N Δ Force

Elevator Ribbon nominally operates at **4** to **5**% strain

5.1 LIBRATION RESPONSE TO CLIMBING

Libration response for 200 & 400 km/hr transit to MEO
Libration response for 200 & 400 km/hr transit to GEO
Libration response for 200 & 400 km/hr transit to Ballast

Minimum-Maximum Libration -vs- transit speed MEO
Minimum-Maximum Libration -vs- transit speed GEO
Minimum-Maximum Libration -vs- transit speed Ballast

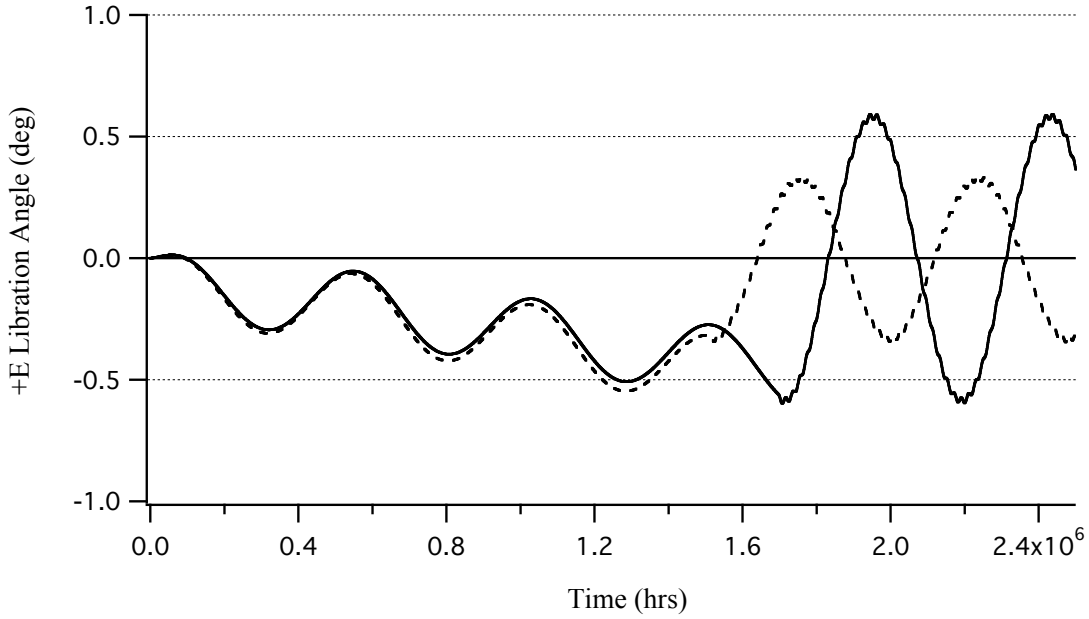

5.2 LONGITUDINAL RESPONSE TO CLIMBER LIFTOFF

Launch-liftoff response plots (Low acceleration)
Launch-liftoff response plots (Hi acceleration)

5.3 LONGITUDINAL RESPONSE TO TRANSIT RESUME

Transit Resume response @ LEO (Low acceleration)
Transit Resume response @ LEO (Hi acceleration)
Transit Resume response @ MEO (Low acceleration)
Transit Resume response @ MEO (Hi acceleration)
Transit Resume response @ GEO (Low acceleration)
Transit Resume response @ GEO (Hi acceleration)

5.4 LONGITUDINAL RESPONSE TO CLIMBING ARREST

Low acceleration arrest response Off Launch Pad
Low acceleration arrest response LEO
Low acceleration arrest response MEO
Low acceleration arrest response GEO
Sudden arrest response Off Launch Pad
Sudden arrest response @ LEO
Sudden arrest response @ MEO
Sudden arrest response @ GEO

5.5 STRESS PROFILES RELATED TO CLIMBER ACTIVITY

Identification of max stress climbing activity
Max Stress profiles

6.0 CONSTRUCTION DEPLOYMENT DYNAMICS

6.1 OVERVIEW

The purpose of this section of the handbook is not to present a solution to the initial construction deployment problem for the space elevator, but rather to expose and discuss the nature of the dynamics issues inherent in this mission, and explore the intrinsic ingredients that might constitute a successful deployment mission design.

There are currently two different approaches identified to deploying the initial elevator ribbon. Both envision the starting point as a space craft containing (either initially or via build-up by multiple courier-missions) all of the: Ribbon, Ballast mass, Ballast-end controller-craft, Anchor-end controller-craft, and required propulsion/systems capability and propellant; from a dynamics standpoint, these two approaches differ primarily in their starting point and maneuvering strategy.

The deployment scenarios are either:

(1) Start with a space-craft at GEO, thus deploying Ribbon downward from there (along with a coordinated *upward* maneuvering of the GEO craft). An overview of proposed mission details of this concept can be further explored in the book "The Space Elevator" by Bradley Edwards and Eric Westling.

or,

(2) Start with a space-craft in LEO, thus deploying the Ribbon and Ballast mass upward, creating a *combined system* with ever longer orbital period, until a configuration is attained whose geometry has grown to include GEO altitude and beyond, and manifests an "orbital period" corresponding to earth rotation rate. Details of this mission design can be explored in the paper entitled "LEO Based Space Elevator Ribbon Deployment" by Ben Shelef, Gizmonics, Inc.

Note: Bear in mind when interpreting results or speculating on dynamic behaviors for a system of the geometrical extent of the space elevator (ie ribbon lengths on the order of multiple earth radii), and moving in the inverse square central force field of the earth, the term "orbit" can loose much of its conventional significance. Previous knowledge of conventional "orbital mechanics", must be used with caution, as it is no longer clear what, if anything, is in "orbit" for the space elevator (even while in "free flight" before attachment to earth), and furthermore, contrary to what might be termed "conventional wisdom", the motion of the center-of-mass of such a system does not in fact execute a classical "Keplerian" particle trajectory, a statement whose truth is based on the easily demonstrable fact that the net force on the center-of-mass of a *system of particles* does not constitute a "central force field" (ie. a force field always directed toward a single point); solutions to a single particle's motion in this "central force field" definition is the basis for the classical Keplerian "orbital classification's" in terms of "total energy". Of course, for much conventional application, the system of particles are relatively closely allied, or clustered together (unlike the space elevator system) and the net force on the center of mass approximates a central force field.

6.2 THE DEPLOYMENT VENUE

The process of deploying a ribbon the physical extension of which is on the order of the space elevator (earth to 100,000 km) is found to be a very delicate control process. Little of the knowledge base derived from actual orbital tether deployment operations has bearing on this procedure due to a host of attributes that make this process unlike any ever attempted by mankind. To understand these technical issues facing deployment, one must have a grasp of the physical factors inherent in this process, in short, the nature of the *deployment venue*.

Consider the following observations:

1. Regardless of whether such a deployment starts at LEO (progressing primarily upward initially), or at GEO (progressing primarily downward initially), the *target configuration* that must ultimately be attained for both is one of a vertical ribbon extending from near ground up to "centrifugally effective altitudes", ie. an altitude at which a net tension in the ribbon is maintained (due to centrifugal force) such that at least a condition of *neutral buoyancy* is achieved. Such a configuration (until actually attached to the earth) is also neutrally stable! Neutral stability results because any perturbation from a "balanced state" tending to move the ribbon (and its attendant end masses) upward, results in net forces that will themselves result in yet more upward motion, to wit: If the ribbon translates upward, every particle of mass becomes attracted less toward the earth by virtue of the inverse square gravity field, thus a net reduction in downward force ensues, *and by the same token*, every particle of the system as it moves away from earth is subject to less "centrifugal effect", *all said effects contributing to the initial perturbation conspiring to move the system away from earth*. Conversely, if the ribbon moves closer to earth, just the opposite of the all the above ensues, the net effect being to progressively pull the system towards earth. Of course, at the "balance point" the system will theoretically remain stationary (until perturbed).

2. Note that the "balance point depends upon the mass distribution of the system. This distribution depends upon the ribbon configuration (ie. density and taper as a function of altitude), as well as how much ribbon has been deployed. Likewise the balance point depends upon how much fuel remains in both the GEO-craft and the Deploy-end-craft at the termination of the deployment.

3. To insure stability of the final system (in preparation for anchor attachment) will require the availability of active-propulsion since there is little the system as a whole can do in terms of additional ribbon deployment to overcome an insipient move away from the balance point. Such imbalances can result from a combination of many factors, ranging from uncertainties in state-recognition (that could obscure detection of an intrinsic state-move away from balance), to, the transport time delays inherent in control effects at one end of the ribbon reaching the other end. Note that the time for tension gradients (stress wave propagation) to traverse the ribbon from earth to GEO are 20 minutes, and almost 1 hour from earth to Ballast.

4. Not only is the final configuration neutrally stable, but in order to *minimize* the need for onboard propulsion fuel, the progression of intermediate states comprising the deployment, must be delicately balanced between the gravitational attraction and the centrifugal effects, a problem that becomes increasing difficult as ribbon extension projects the end objects into the increasingly non-linear *lower* regions of the inverse square gravity field.

5. As the ribbon is extended in altitude, a tangential velocity gradient is required to maintain a vertical position initially free of libration; this amounts to a significant delta-V that must eventually be dealt with, otherwise, the ribbon configuration will have been erected with a possibly undesirable amount of residual libration motion (especially for an infant ribbon). Note that at **GEO** altitude, a point on the ribbon has **2,580 m/s** (8,460 ft/s) tangential velocity relative to the anchor point; at **Ballast** Altitude, a point on the ribbon has **7292 m/s** (23,900 ft/s) tangential velocity relative to the anchor point (note that this latter velocity is on the order of the insertion velocity required for low earth orbit).

6. These tangential velocity gradients manifest themselves as Coriolis acceleration during deployment, an effect which cannot be practically countered for *interior ribbon points*, rather only for the end-mass GEO-craft or Deploy-craft where propulsion can be practically situated. So the possibility for inducing ribbon transverse string mode oscillation also exists.

7. The ribbon must ultimately be maintained *delicately poised* between the conflicting tendencies of centrifugal and gravitational effects with virtually no outside control effectors other than (a) position state of the end-masses, (b) distributed mass within the ribbon, and (c) onboard propulsion.

8. Vast changes (*orders* of magnitude) in ribbon *effective end-to-end spring constant* are experienced over the course of this extremely long-length deployment. While for short ribbons (at deploy initiation), the end-to-end spring-rate and related natural frequencies can be quite high (stiff), near the terminal phase when vertical control at the bottom becomes critical, a ballast-to-earth length (infant) ribbon will exhibit a spring rate on the order of .004 N/m (.0003 lb/ft); for a GEO length ribbon, this will be .012 N/m (.001 lb/ft). Correspondingly, all the natural frequencies of the ribbon system change drastically over this time frame. This happens for all the natural modes of oscillation, including the end-mass bobbing modes, the longitudinal string modes, and the transverse modes. This means that control systems designed to cope with this problem will have to adapt to a vast range of frequencies; this exacerbates the problems of band-pass filtering of sensor data, and subsequent control effectiveness.

9. Small incipient departure from the neutral stability point of the configuration likely cannot be sensed directly via accelerometers since the entire system is “falling” in the gravity field, thus departure will have to be detected via a manifestation of position or velocity dispersions (GPS, while it should be useful near earth, may possibly be less effective for such a role when sensing altitude at GEO).

6.3 DEPLOYMENT STRATEGIES

Given an *unlimited supply of fuel* for the end-craft, this could be accomplished in a fairly straightforward fashion. However, in the grander sense, the economics of lofting fuel and other resources to LEO or GEO, ultimately renders this is a problem for non-linear, multivariate modern control theory and/or artificial neural-network approaches. This is because:

1. The "Plant model" is very non-linear and complex, and
2. There is a potential for (large) fuel budget requirements that reflect conventional bi-propellant propulsion, that while providing sufficient thrust levels, reflect Isp's on the order of only 450 (max) to accomplish the mission via brute force, thus requiring huge amounts of fuel to be transported to GEO (or equivalent), unless control techniques are employed to minimize total impulse (thus a need for optimal control), or,
3. Modest fuel budgets that reflect electro-magnetic propulsion which is typified by Isp's on the order of 1000's, but, very low thrust levels, in which case control will have to be optimal to allow effective usage of such minimal effectors.

In overview, this control problem can be thought of as the management of the following attributes of the combined system:

A. Intelligent identification of the many time-varying elastic frequencies associated with the deployment (meaning the rejection of spurious state indications related to oscillatory components),

B. Utilization of the dynamic balancing of the *total system* (upper/lower craft, and ribbon) as it is growing in length, delicately poised in the combined centrifugal and inverse-square gravity force fields, all to minimize fuel necessary to perform the deployment,

C. Management of the system libration as it traverses the Coriolis acceleration field,

D. Final balancing of the system as it is poised for anchor tie-down, which implies management of touchdown latitude/longitude (as well as on-going lat/long management during the deployment), and fine altitude rate control near touchdown.

The possible useful control effectors for this combined maneuver are then:

- Active 3-axis propulsion on Upper end-body, and
- Active 3-axis propulsion on Lower end-body, and
- The ribbon deployment-scenario (essentially deployment rate -vs- time).

The possible sensors are:

- Amount and Rate of ribbon deployed,
- Ribbon Tension at either (or both) ends of ribbon,
- Position, velocity, and acceleration at either (or both) ends of ribbon.

6.4 RIBBON/DEPLOY-CRAFT SIMULATION CONFIGURATION

This section describes the geometry of the system being studied for the deployment simulations. When parked at GEO, the initial configuration contains all the ribbon to be deployed (100,000 km) as well as the GEO-craft (destined to be the Ballast Mass), and the Deploy-craft that guides and controls the bottom end of the ribbon, destined to be *grappled* at the ground anchor. At separation prior to deployment, the Deploy-craft (while connected to GEO-craft by the ribbon) becomes independent of the GEO craft.

6.4.1 Initial Conditions of Simulation

After defining and verifying the overall system geometry and configuration, all GTOSS ribbon deployment simulation runs were started with the same initial conditions (with the exception of Deploy-craft initial separation rates, that were dependent upon chosen deployment scenarios). Thus, mainly what was varied were control system modes and strategies (and attendant gains, limits, dead bands, etc, within those selected control system scenarios), and the ribbon deployment scenarios. Initial runs to determine basic system tendencies were made with no control system modes invoked, and employed a constant deploy rate throughout.

Since the GTOSS tether model uses a fixed number of nodes, there typically arises a numerical efficiency issue associated with the start of a deployment simulation. This is because the node-count specification for the tether must be sufficient to describe the tether dynamics when the tether is *fully deployed*, which means that when the tether is initially deployed, the node density will be much greater than required. Since, high nodal density results in high inherent natural frequencies, this in turn dictates smaller numerical integration step sizes, thus high CPU load to advance the simulation solution time (initially).

This is usually not an insurmountable problem, but is somewhat exacerbated for the space elevator deployment due to the many orders-of-magnitude change in ribbon length during elevator ribbon deployment. The solution is to start a deployment with an *initial amount of tether* already deployed in conjunction with user-specified integration step-size staging to advance the deployment initially with small step size but, while quickly reducing step size as deployed length increases (note: doubling deployed length usually allows a doubling of step size).

For this reason, this deployment simulation starts with an initial 10 km of ribbon already deployed (between the GEO-craft and Deploy-craft situated directly below). This initially deployed ribbon is such a miniscule proportion of the fully deployed ribbon (plus representing a mission phase easily accomplished by an un-eventful maneuvering of the Deploy-craft, in conjunction with a benign deployment of ribbon), it is safely judged to have no bearing on the outcome of the full deployment (that of which, is indeed a significantly challenging process).

6.4.2 GEO-Craft Configuration

The GEO-craft (TOSS Object 3 in the simulations) initially has a mass of approximately 69 metric tons (69,000 kg, =152,000 lbm, =4700 slugs). This initial mass includes the entire initial ribbon to be deployed (about 40 metric tons). The remaining 29 tons (69 - 40 = 29) represents the fuel, mechanisms, propulsion systems, and reflects a ribbon-to-ballast ratio of about 1.364, a current base-line elevator design point. The difference between 69 tons and 54 tons (54 = 1.364 x 40) represents expendables that will not ultimately end up at ballast altitude. During the course of the deployment, mass will be lost from the GEO-craft both due to ribbon deployment as well as propulsion expendables. The GEO-craft is simulated as 3 DOF point mass.

6.4.2.1 GEO-craft control systems

Control in both the vertical direction as well as the horizontal plane will likely be required for the deployment of the ribbon and ballast mass, hence numerous control modes were developed in the attempt to deploy and stabilize the configuration. Note that these are simplistic control modes, and in no way represent an engineering approach that would be acceptable for *final* vehicle/mission design; rather these modes were provided to examine the nature of the control dynamics problems that will likely be confronted in the system design. The modes implemented in GTOSS to accomplish this examination were:

Vertical Control: Vertical control of (both of) the "end-Craft" for the elevator deploy mission has the following two main tasks to accomplish:

(1). Maintain Altitude -vs- Time profiles that will result in a dynamic balancing of the vertically extending elastic system delicately poised between the gravity-well forces and the centrifugal force field as ribbon grows in length. Failure to accomplish this task will result in either the entire system flying off into a useless "orbit", or "crashing to earth". Furthermore, inefficiency in performing an effective balancing act, while surmountable by copious application of propulsion, can render the entire proposition impractical due to the large values of total impulse that can result; note that such a deployment when transpiring at deployment rates on the order of 200 km/hr can easily take a week of operation (and likely longer to achieve practical control). Constant active propulsive make-up of control-inadequacies for such an undertaking has vast implications on total impulse required.

(2). Damp vertical oscillations that arise due to various aspects of the vertical maneuvering and deployment. For instance, vertical maneuvering required to maintain the vertical balance between the gravity field and centrifugal field during deployment will tend to stimulate vertical modes of oscillation. These modes can be a combination of end-body bobbing modes as well as longitudinal elastic ribbon modes. Another form of vertical response arises due to the continuing accommodation of the ribbon end-to-end effective-stiffness time-gradient to the ever increasing gravitational attraction during deployment; this can induce end-body bobbing response.

The following vertical control modes were added for (all) TOSS Objects to facilitate examination of the vertical control issues for this deployment,

GTOSS Object: Vertical Control Modes:

- Maintain constant vertical thrust
- Maintain constant vertical velocity
- Maintain constant vertical acceleration
- Maintain vertical thrust -vs- time-profile
- Maintain vertical velocity -vs- time-profile
- Maintain centrifugal counter-force altitude to equilibrate tether tension
- Maintain a factor times vertical velocity of another object
- Maintain vertical velocity greater than a specified velocity
- Maintain vertical velocity less than a specified velocity
- Maintain altitude -vs- time-profile
- Maintain vertical greater than a velocity -vs- time-profile
- Maintain vertical velocity within a dead-band of zero
- Maintain altitude-profile of vertical velocity

Horizontal Control: Vertical control of (both of) the "end-Craft" for the elevator deploy mission has the following three main tasks to accomplish:

(1) Limit Total System Libration to within practical design margins (this necessitates horizontal thrusting designed to more or less negate the induced Coriolis acceleration associated with the deployment along a local vertical).

(2) Maintain Earth Longitude/Latitude to within limits to effect a practical rendezvous of the Deploy-craft with the anchor station for initial grappling. This control requirement, while related to the requirement (1) above, goes beyond that requirement since the precision of this final rendezvous far exceeds the requirements associated with general libration response of the elevator system as a whole.

(3) Dampen (or otherwise manage) transverse ribbon response that may be excited by various aspects of the deploy mission (such as horizontal accelerations of the GEO- and Deploy-craft, wind disturbances once into the atmosphere, etc).

The following horizontal control modes were added for (all) TOSS Objects within GTOSS to facilitate examination of the horizontal control issues for this deployment,

GTOSS Object: Horizontal Control Modes:

- Maintain constant Horizontal thrust
- Maintain constant Horizontal velocity
- Maintain constant Horizontal acceleration
- Maintain Horizontal thrust -vs- time-profile
- Maintain Horizontal velocity -vs- time-profile
- Maintain constant earth Latitude/Longitude with Dead Band
- Maintain constant negative Coriolis acceleration
- Maintain constant earth Lat/Long within dead-band + neg. Coriolis acceleration
- Maintain constant earth Lat/Long w/proportional control

Note: The above defined GTOSS control system implementations are in no way to be construed as ideal or optimal for final mission design, nor have they been implemented as such. They are mainly intended to provide a primitive level of stability to assist in demonstrating the possibility of, and exploring problems inherent in, performing such a deployment mission.

6.4.3 Deploy-Craft Configuration

The Deploy-craft, residing at the bottom end of the ribbon, is largely an unknown entity at this point in the space elevator design cycle. Its control agenda is similar to, yet different from that played by the GEO-craft. The Deploy-craft vehicle is primarily a thrusting controller, whose job it is participate in maintaining overall stability and quiescence of the system as it elongates, and finally to effect a precise earth latitude-longitude homing maneuver for terminal rendezvous with the anchor station. Depending on what (other functions) one imagines the role of this vehicle to play, a range of masses could be assigned. For the purpose of this study, a middle-of-the-road value of 1500 kg (100 slugs, =3200 lbm) was used. This vehicle is being simulated as a 3 DOF object in GTOSS.

6.4.3.1 Deploy-craft control systems

Control in both the vertical and horizontal plane will be required for the Deploy-craft. If for nothing else, this will be necessary to effect a graceful terminal rendezvous with the anchor station. All the various control modes implemented in GTOSS to accomplish control tasks associated with the GEO-craft (see section 6.4.2.1 above) were also available for the Deploy-craft.

6.4.4 Ribbon Configuration

The initial space craft configuration parked at GEO contains all the ribbon to be deployed. In a current nominal deployment mission scenario, this ribbon is envisioned to be in the form of two 20 (metric) ton spools of ribbon. These would be deployed simultaneously as one ribbon of 10 cm width. It is assumed that this infantile ribbon would have the identical longitudinal design-taper configuration as the mature elevator configuration (whose taper and other attributes are fully defined in an earlier section of this Dynamics Handbook).

The ribbon properties for the initial deployment mission is thus derived as a "scaled-down" version of the mature ribbon. This is done by noting that the mass of the mature elevator ribbon is 825 tons (1,820,000 lbm, =56,572 slugs), so calculating the mass ratio between the initial 40 ton ribbon and the mature ribbon would provide the ratio between the lineal density (ρ) of the initial ribbon and the mature ribbon. This is:

$$\frac{\rho_i}{\rho_m} = \frac{M_i}{Mm} = \frac{40}{825} = 0.0485$$

Where:

ρ_i is the Initial construction ribbon density

ρ_m is the Mature ribbon density

M_i is the Initial construction ribbon total mass

Mm is the Mature ribbon total mass

So would the elastic area of the two ribbons exhibit this same ratio, thus:

$$\frac{A_i}{Am} = 0.0485$$

Where:

A_i is the Initial construction elastic cross sectional area

Am is the Mature ribbon elastic cross sectional area

D_i is the Initial construction effective elastic diameter

Dm is the Mature ribbon effective elastic diameter

Then, since GTOSS requires an equivalent elastic diameter, note that the ratios of elastic area relates to elastic diameter as per:

$$\frac{D_i}{Dm} = \sqrt{\frac{\rho_i}{\rho m}} = \sqrt{0.0485}$$

This then provides all that is needed define a new tapered ribbon specification for use within GTOSS.

6.4.4.1 Tapered ribbon deployment topology

Within GTOSS, all the ribbon is initially contained within the GEO-craft and is deployed downward with respect to the GEO-craft. This means that the ribbon taper definition within the GTOSS non-uniform tether data protocol must be defined such that the *first* part of the ribbon to emerge upon deployment will be that part destined to be grappled at the anchor station, and the *last* portion of ribbon to be deployed must be that destined for the Ballast altitude. Note that this is true only for the mission in which everything deploys downward with respect to a GEO-craft (for the LEO mission deployment scenario, *exactly the opposite* would be true). The definition of this required ribbon data for the GEO mission will be found in the associated input data files for GTOSS. Below are graphs of the length-varying longitudinal properties of the initial deployment ribbon used in the GTOSS simulations of the initial deployment mission.

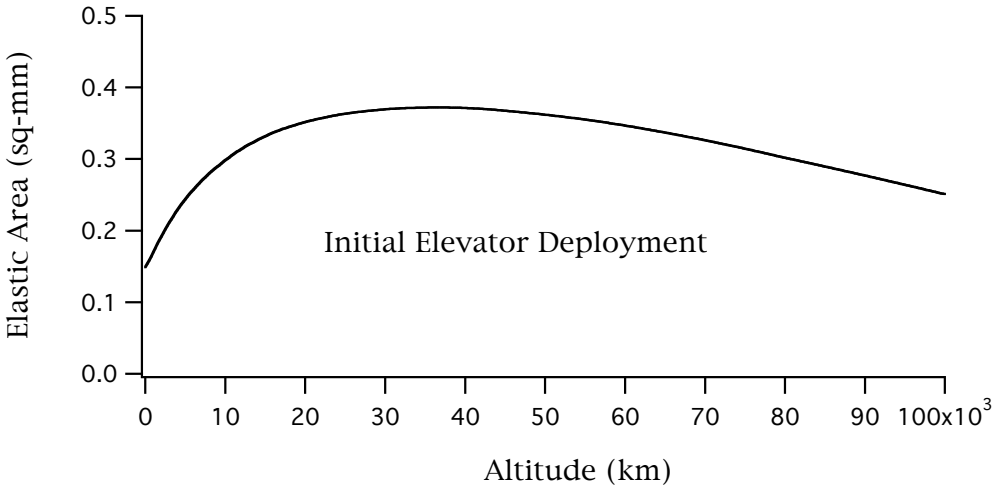

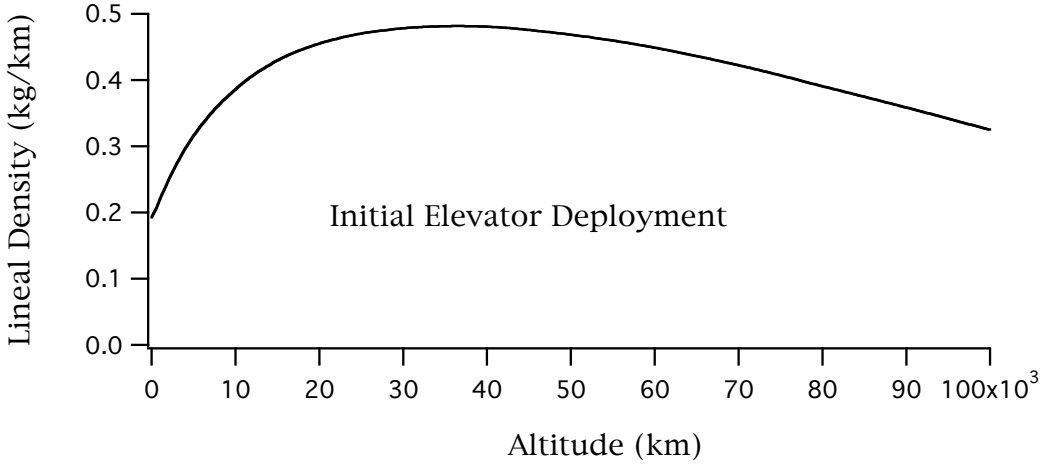

The table below (and continued on next page) represents an optimal approximation to ribbon length-varying parameters for initial deployment ribbon configuration (when quadratic interpolation is used).

Lineal Density (kg/km)	**Cross Section** (mm^2)	**Region Δ Length** ΔL (km)
0.189	0.146	<= value at Earth
		3048
0.273	0.212	
		3048
0.333	0.258	
		3048
0.377	0.290	
		4572
0.421	0.324	
		4572
0.448	0.345	
		3048
0.460	0.355	

		6096
0.476	0.366	
		6096
0.482	0.371	
		6096
0.481	0.371	
		6096
0.477	0.366	
		9144
0.460	0.355	
		9144
0.439	0.338	
		15240
0.355	0.273	
		12192
0.326	0.250	
		8656.32
0.326	0.250	<= value at Ballast

6.4.4.2 Tether/Object topology

The simulation runs employ the planet-fixed Reference Point option within GTOSS. In this scheme:

- the Reference Point (fixed in earth) is **Object 1**
- the Deploy-craft (the space vehicle at the *bottom end* of the ribbon) is **Object 2**
- the GEO-craft (destined to arrive at Ballast altitude) is **Object 3**.

The tether undergoing deployment is TOSS tether number 1; this tether is connected between Objects 2 and 3 with the X-end (deployment/emission end of tether) located at the upper (GEO) object.

Important Note: There is yet **one more tether** being employed in this deployment simulation. This is TOSS tether number 2 that extends between the Deploy-craft and the earth-fixed Reference Point (the anchor station). This tether is a massless tether (thus exerting no inertial loading on the dynamics of the solution) and is initially given a length that is so long as to render its tension zero throughout the full deployment. Its purpose is to effect an eventual grappling of the Deploy-craft at the anchor station, thus allowing for simulation of the tie-down of the elevator ribbon to the anchor point. This is accomplished by specifying a Tension-command scenario for this massless tether, that will be enabled at the time that the deploy-craft is sufficiently near the anchor point. This tension command will immediately define a new deployed length for this tether that will produce the specified tension level needed to secure the ribbon. At this point, continued upward deployment of the GEO-craft could ensue, except now under the conditions of an anchored lower ribbon end.

6.4.4.3 System mass balance

Both the GEO-craft and the Deploy-craft can loose mass during the deployment operation.

The GEO-craft looses mass due to:

- Deployment of the ribbon (ie. up to 40 tons when full deployment has occurred if the GEO-craft arrives at nominal Ballast-altitude),
- Propulsion.

The Deploy-craft looses mass due to:

- propulsion only (since ribbon is exclusively deployed from the GEO-craft).

To enable mass loss effects, GTOSS must be instructed specifically to allow this to occur. Deployment and propulsion mass changes are enabled independently of one another.

To enable mass change due to Deployment, a general TOSS input control flag that specifically enables such mass changes, must be set.

To enable mass loss due to Propulsion, a non-zero value of Isp must be specified (since Isp occurs in the denominator of the mass-flow calculation); failure to specify a non-zero value of Isp while it will inhibit mass loss due to propulsion, will not disable calculation of "total thrusting impulse" that will still be available for post processing examination.

6.5 NATURAL SYSTEM TENDENCIES

This section examines the natural tendencies of a system in which an object is deployed from GEO towards the earth without the benefit of any control intervention. While this is a unique behavior simply reflecting the response of a greatly-extending system of particles embedded in an inverse square central force field, it nevertheless is found to manifest some interesting tendencies that are indicative of what a controller must deal with to successfully deploy an elevator ribbon. This particular simulation run starts with both craft at GEO, and starts the Deploy-craft towards the earth at a speed of 200 km/hr; the tether also deploys at this same rate throughout the simulation. These runs are made using first a massless tether, then a distributed mass tether, to obtain information about the effects of distributed mass on the system dynamics.

Massless Ribbon Simulation

In the massless case, the GEO-craft looses no mass during the deployment (since the deploying ribbon has no mass related to it). Both deployments take about 5 days. With the exception of tension gradients and transients that are attendant to the longitudinal mass distribution and elastic modes inherent in the distributed mass model, in this

simplified, no-control case, the behavioral trends were *similar* between the massless and distributed mass ribbon cases. The massless simulation was done primarily as a *ballpark verification* of the higher fidelity massive-ribbon simulation. It is clear that due to the significance of 40 tons of ribbon mass immersed in the gravity field, that a massive ribbon model is required to thoroughly examine the nature of this deployment problem.

Massive Ribbon Simulation

The results of this uncontrolled deployment is shown below. The initial hours of deployment are essentially tension-free, so the Deploy-craft (hooked on the end of the ribbon) having been given an initial vertical velocity is just behaving as it should (essentially Keplerian orbit moving posigrade wr/t the GEO object), all-the-while the GEO craft essentially sits at GEO (as it should). Now, *as soon as tension manifests itself*, the deploy-craft (smaller mass) starts to librate noticeably (typical tether behavior). The onset of tension (too small to be evident in the tension graph shown farther on in this section) manifests itself in relative range-rate as shown in the graph below

The first graph compares the constant 200 km/hr deploy rate to the range-rate between the GEO-craft and Deploy-craft. The transient appearing at about ½ day into the deployment relates to the initial impact of the Deploy-craft with the ribbon as it's recession rate "catches up" to the amount of ribbon having already been deployed (ie the "slack" is being removed from the system); the ribbon is intentionally deployed at a rate slightly in excess of the initial separation rate of the two vehicles, so as gravity slowly accelerates the Deploy-craft away from the GEO-craft eventually, this slack removal results in a minor impact loading event. Following this impact event, the range rate between the Deploy-craft and GEO-craft become essentially congruent with ribbon deployment until near the end of the deployment, when other effects come into play.

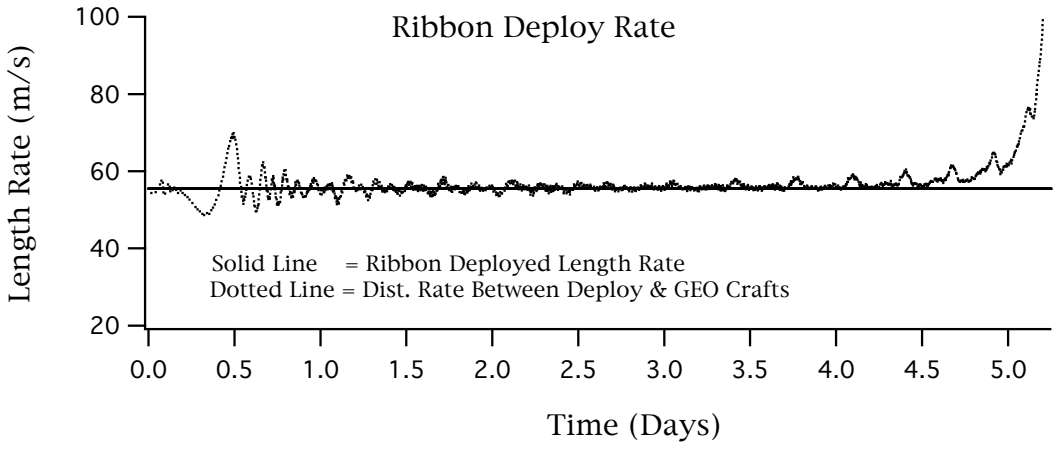

The graph below simply shows the resultant deployed length resulting from the constant deploy rate being commanded.

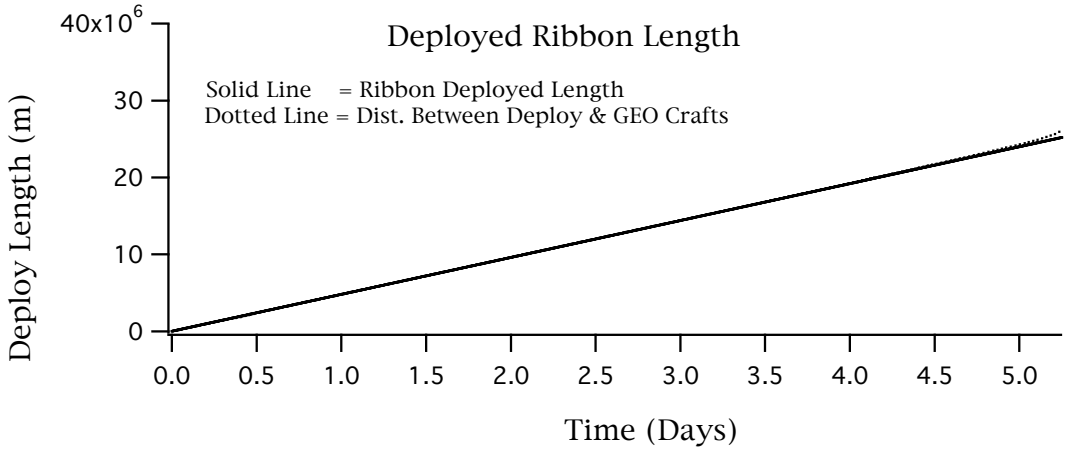

The steady increase in tension at both ends of the ribbon is seen in the graph below. The higher tension at the GEO-craft is responsible for pulling the GEO-craft earthward and the resulting significant posigrade motion of the GEO-craft with respect to its initial geosynchronous state. The sharp tension increase at the Deploy-craft near the end of deployment is due to its diving ever more rapidly into the inverse-square gravity-well.

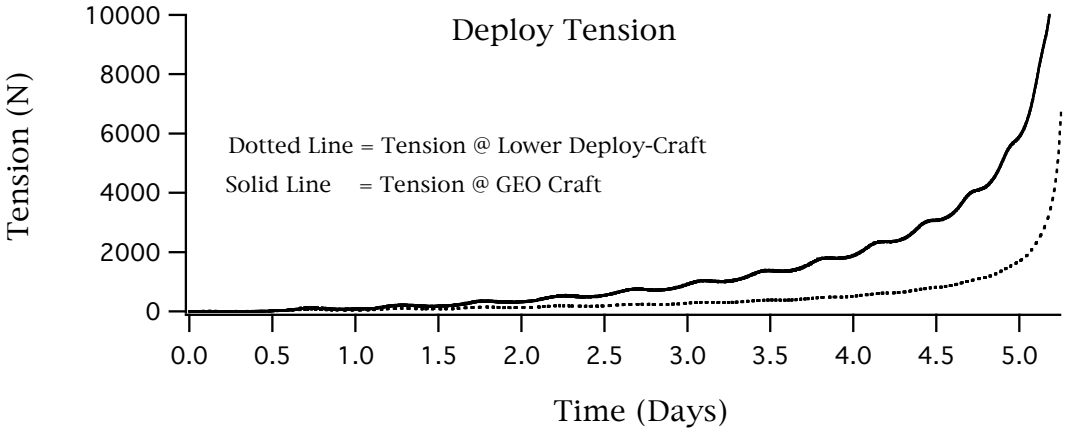

Altitude rates of both end-objects, shown in the two graphs below, expose the sharp increase at 4.5 days of the Deploy-craft's accelerating encounter with gravity, *dragging everything down with it*.

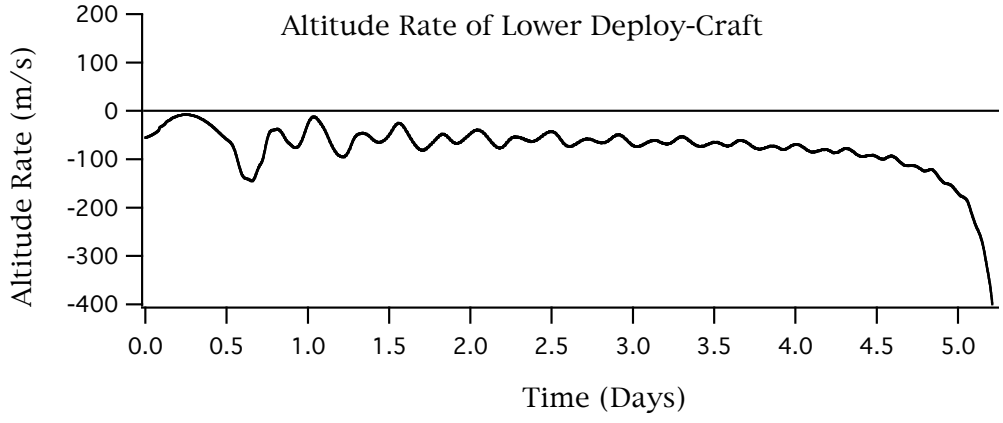

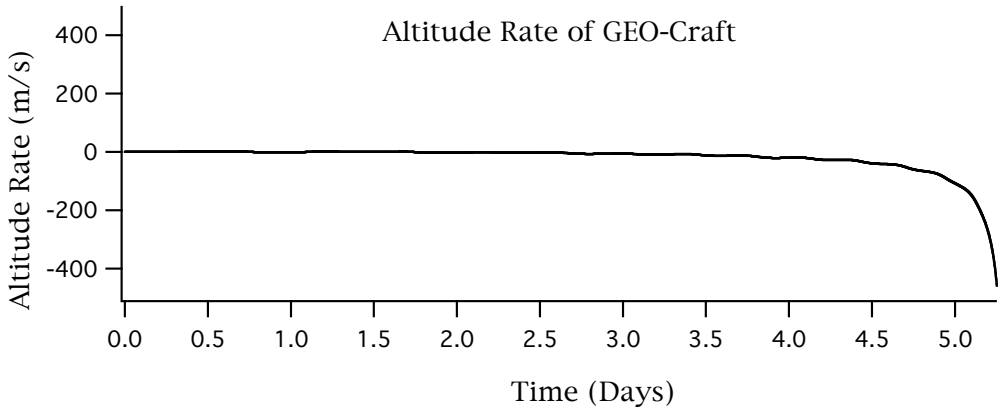

The two graphs below compare the altitude response between the *massless ribbon* and the *distributed mass ribbon* models. In general, it is seen that the GEO-craft and Deploy-craft both loose altitude considerably more and/or faster for the distributed mass case than the massless case. This phenomenon is attributable to different reasons for each object. For the GEO-craft it is because the mass of the ribbon has come into play as it moves into the gravity well. On the other hand, for the Deploy-craft, it is because as the massive ribbon is drawn into the gravity-well *in its own right*, the Deploy-craft is progressively deprived of its *supporting-spring*.

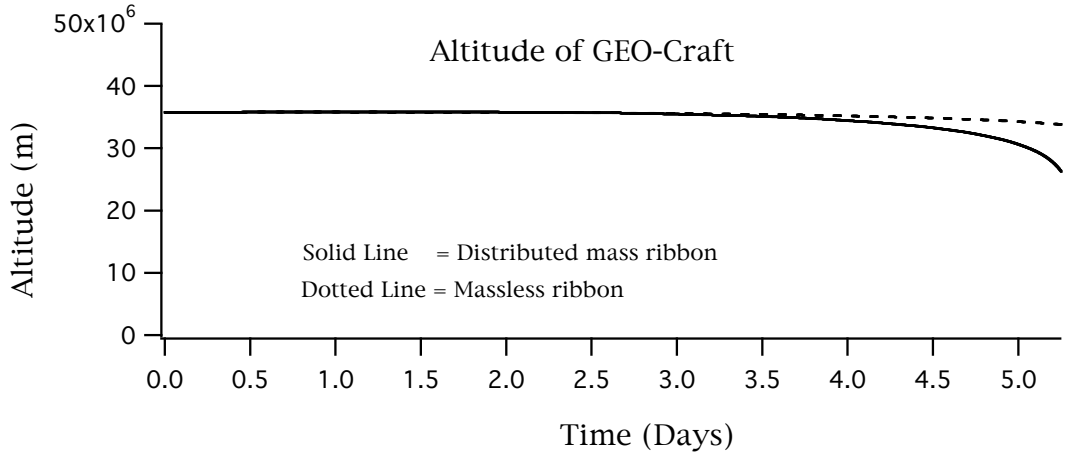

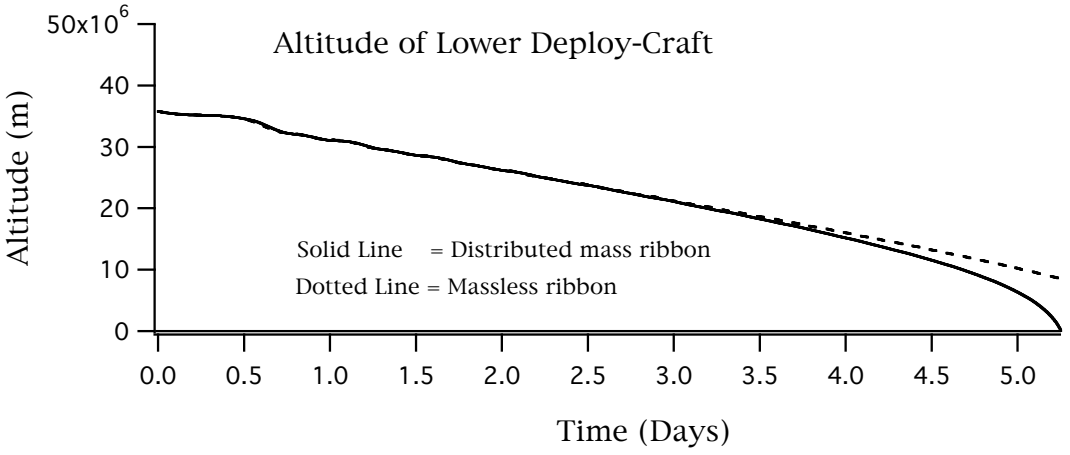

The pronounced increase in gravity on the Deploy-craft at 4.5 days is shown below.

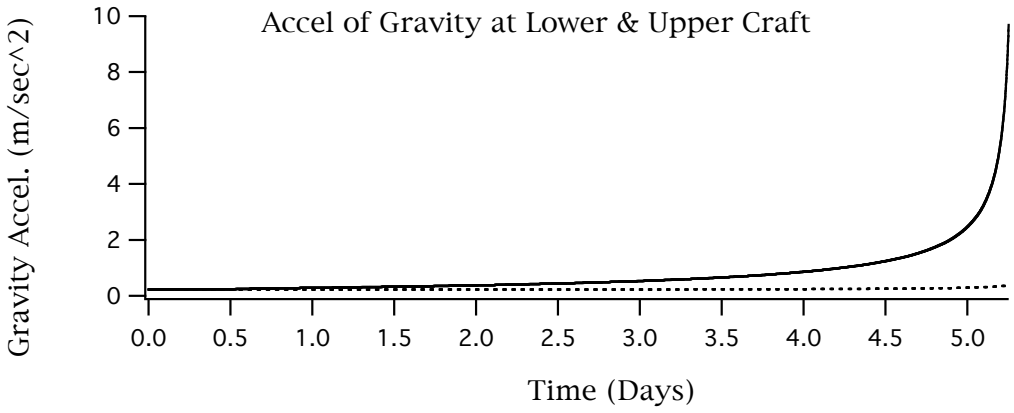

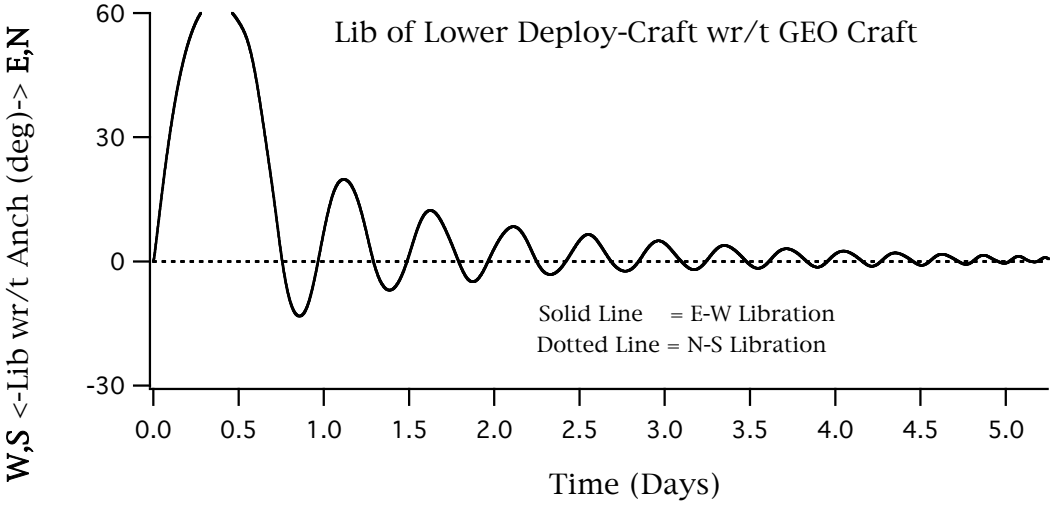

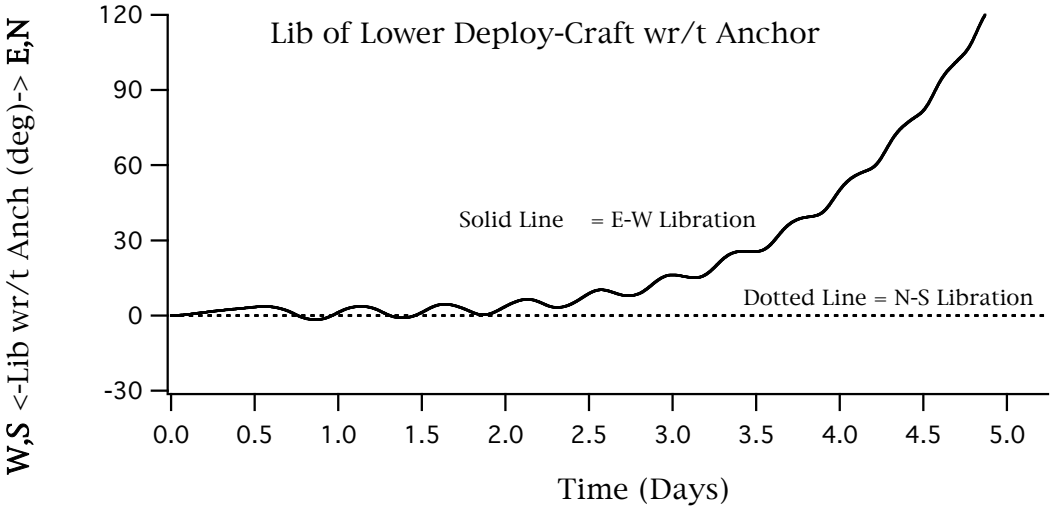

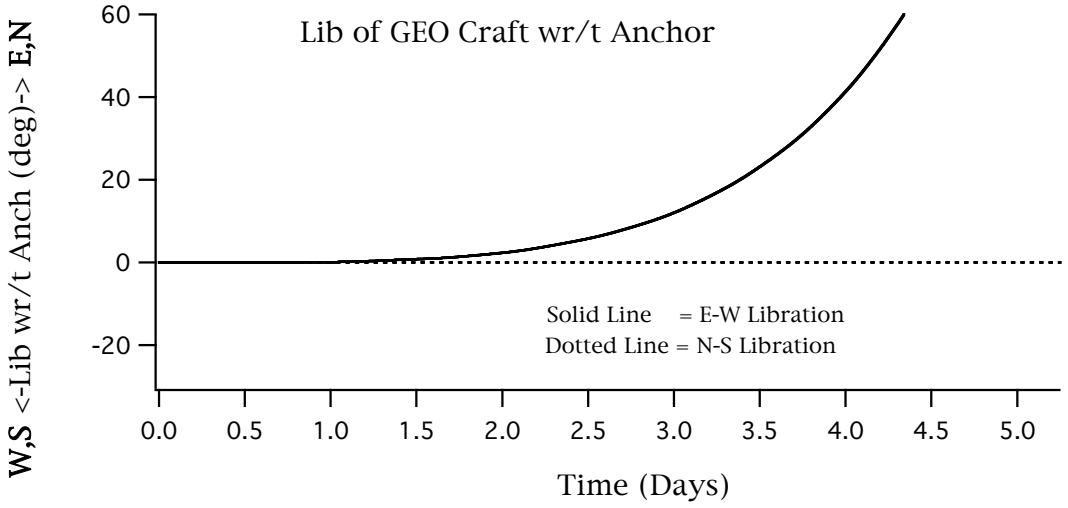
Lib of GEO Craft wr/t Anchor
W,S <-Lib wr/t Anch (deg)-> E,N
60
40
20
0
-20
Solid Line = E-W Libration
Dotted Line = N-S Libration
0.0
0.5
1.0
1.5
2.0
2.5
3.0
3.5
4.0
4.5
5.0
Time (Days)

6.6 UNDER-EQUILIBRATED SYSTEM (FALL-DOWN)

This simulation is the first in this series using the various end-object control modes that were developed in GTOSS to examine this problem (the detail definitions of these control modes can be seen in the addenda to the Dynamics Handbook). The outcome of this particular simulation does not represent a successful deployment mission, but rather illustrates a potential failure mode when the GEO-craft's vertical control mode fails to properly equilibrate the increasing tension as the ribbon plunges into the gravity-well.

Ribbon was deployed with a Type 1 deployment scenario (deploy rate a linear function of time), and simply generated a constant rate of deploy of 200 kh/hr. The GEO object was controlled in the vertical axis by a type 6 control mode (that attempted to equilibrate net tension, via altitude increase); the various control parameters and gains failed to allow this to occur sufficiently to preclude the system from being dragged down to earth. Horizontal axis control was accomplished via a type 9 controller, that simply held (via feedback proportional control) a constant latitude and longitude. Gains for this mode were too high, resulting in noticeable transverse string-mode excitation in the ribbon, especially early in the deployment when tension was low, and any over-thrusting in the horizontal direction could easily excite ribbon displacements.

As the Deploy-craft starts to come under the influence of the increasing "gravity well", the low spring rate of the long length of ribbon, that has been deployed under almost no tension, *presents almost no resistance to stretch*, and (depending upon the mass of the Deploy-craft) it can dip increasingly into the 1/R**2 gravity, rapidly developing a "dive to earth" in the final hours of deployment. This of course is not appropriate mission design, and clearly points out the need to modulate ribbon deployment consistent with raising the altitude of the GEO-craft to equilibrate tension, as well as curtailing deployment rate late in the mission to insure a state of vertical equilibrium exists between gravity and the ribbon elasticity as gravity onset rate becomes great; this of course speaks for a long mission duration.

Ribbon deploy rate is shown below:

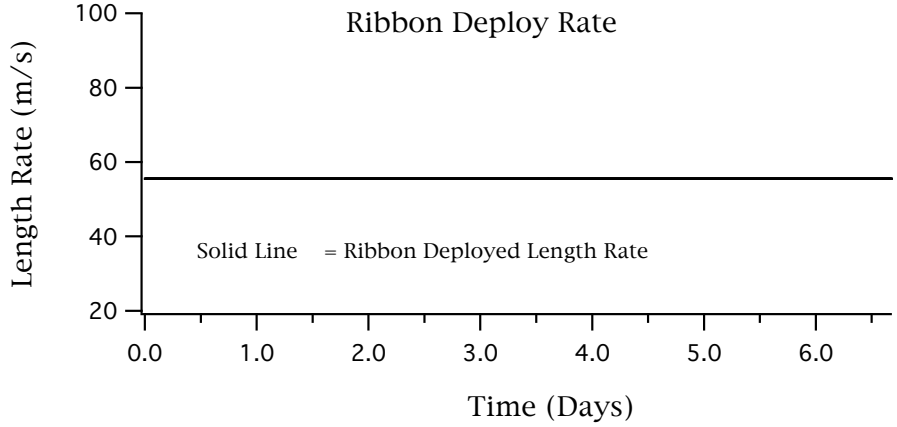

Altitude history of the top/bottom of the ribbon is shown below. The GEO-craft is rising, attempting to equilibrate tension, however, control mode settings are not aggressive enough to effectively counter tension. Also, the effect of the (over deployed) ribbon's low spring rate can be clearly seen in the diving plunge to earth of the Deploy-craft. For effective mission design, the GEO-craft should exhibit a noticeably progressive acceleration of altitude-rate starting about mid-deployment.

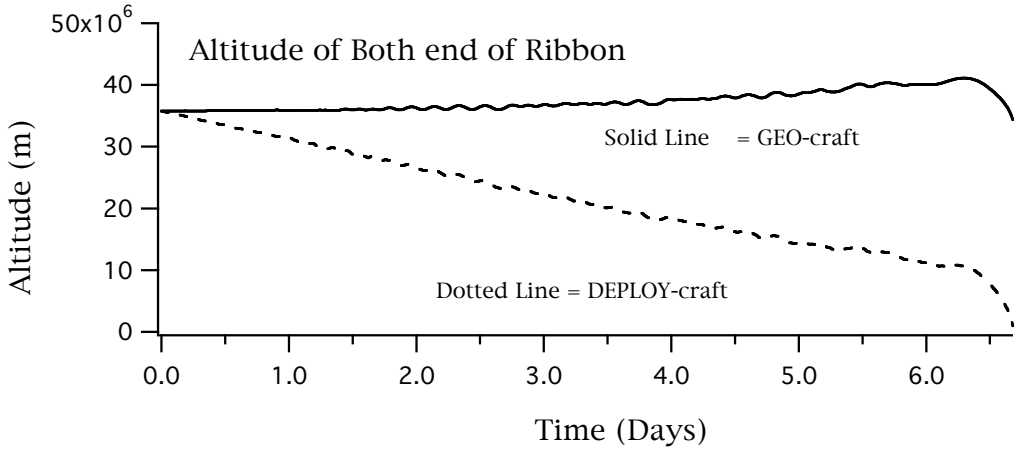

Rapidly increasing gravity at both ends of ribbon is evident below, GEO-craft is dotted.

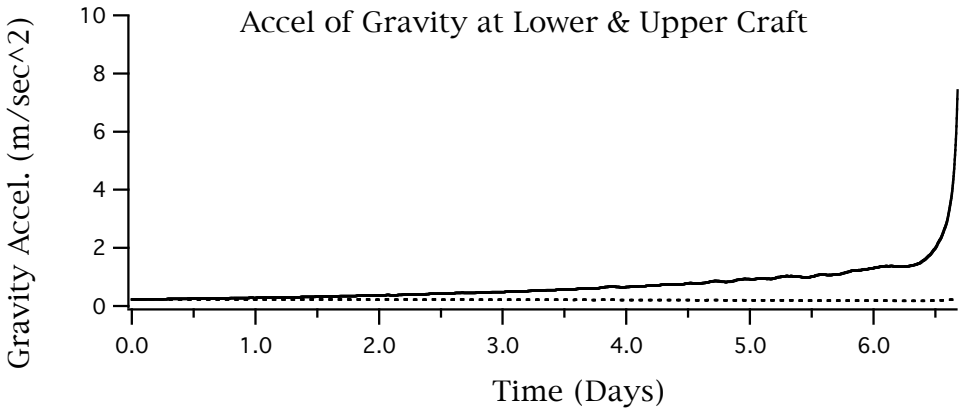

The tension below betrays inappropriate control system settings and gains that are exciting the ribbon and system.

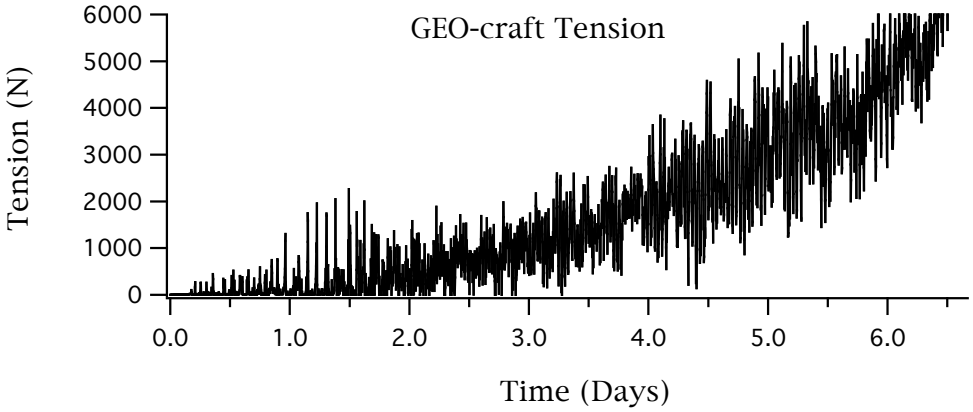

The graphs below shows that the horizontal mode control of the GEO-craft and Deploy-craft were functioning to maintain a semblance of tracking on the specified latitude and longitude of zero. This position of the Deploy-craft is clearly not tight enough to effect an operational rendezvous with the anchor, but the Coriolis effects are seen to be effectively countered (in terms of gross libration of the system).

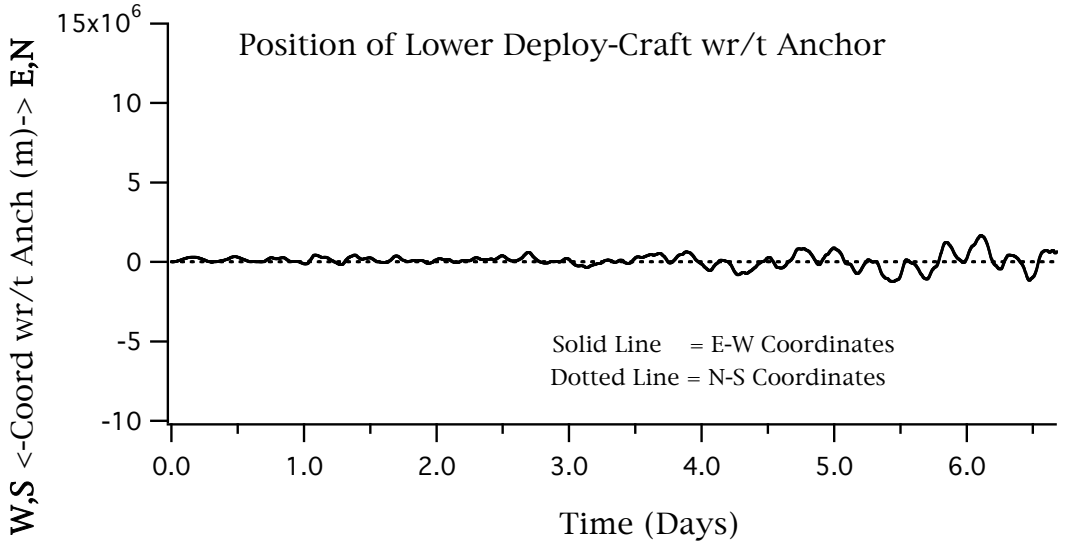

It can be seen below that the elevator as a whole built up libration oscillation as the deployment neared termination.

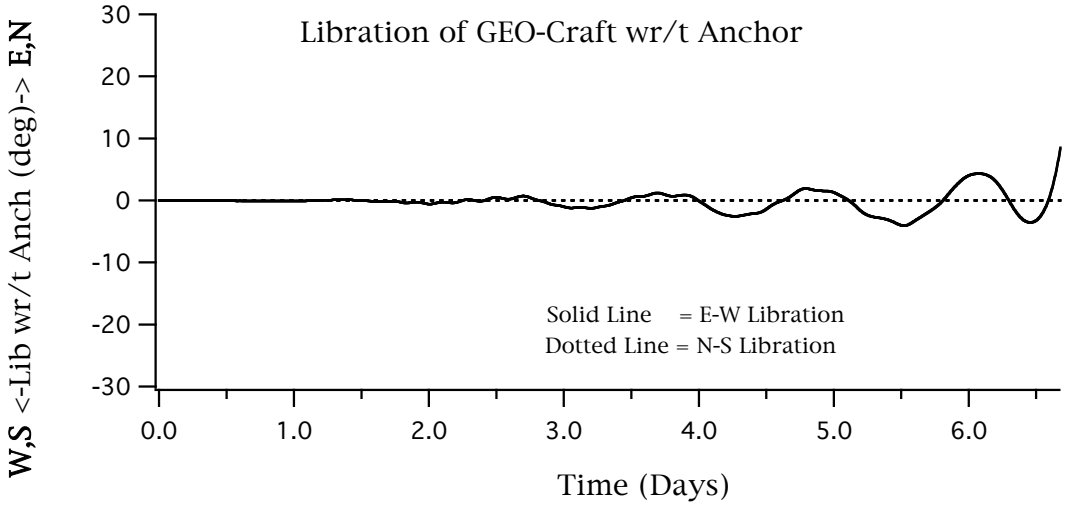

Conclusion:

This case illustrates a semblance of control in the horizontal plane, but is significantly lacking in the vertical axis, in short it is catastrophically failing to equilibrate the system during ribbon extension. The next case will illustrate the extreme in the opposite direction.

6.7 OVER-EQUILIBRATED SYSTEM (FLY-AWAY)

The outcome of this particular simulation does not represent a successful deployment mission, but rather illustrates another potential failure mode when the GEO-craft's vertical control mode becomes over-aggressive in equilibrating the increasing tension as the ribbon plunges into the gravity-well.

Ribbon was deployed with a Type 1 deployment scenario (deploy rate a linear function of time) starting with a rate of 200 kh/hr, but then slowly reducing this rate over time as the ribbon is lowered. The GEO object was controlled in the vertical axis by a type 6 control mode (that attempted to equilibrate net tension, via altitude increase); the various control parameters and gains resulted in an over-equilibration of the system, which subsequently hurtles off to ever higher altitudes. Horizontal axis control was accomplished via a type 9 controller, that simply held (via feedback proportional control) a constant latitude and longitude; gains for this mode were too high, resulting in noticeable transverse string-mode excitation in the ribbon, especially early on when tension was low, and any over-thrusting in the horizontal direction could easily excite ribbon displacements.

As the Deploy-craft starts to come under the influence of the "gravity well", the vertical equilibration algorithm starts a slow vertical/horizontal oscillation mode as a result of interaction of the vertical control with the Coriolis effects due to the ever increasing vertical velocity. It is at the apex of one of these vertical oscillations that the system becomes over-equilibrated to an extent that the thrust effectors can no longer contain the net vertical impetus and the system departs from earth-bound flight.

The graph below shows the ribbon deployment rate, illustrating the tail-off in rate as the altitude reduces (note, this is rate as a function of time however, so any rate-altitude relationship is an implied one, which is an important distinction, since near the end, the altitude of the Deploy-craft starts to actually increase in time, a problem which is more successfully countered in the example simulation of Section 6.9).

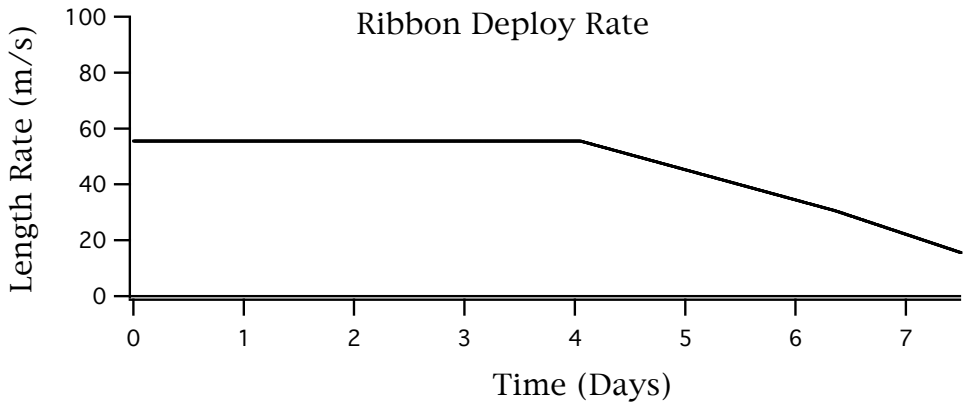

The ultimate failure of this deployment mission is clearly seen in the GEO- and Deploy-craft altitude histories shown below. The GEO-craft is rising, attempting to equilibrate tension, but at about 6 days into the mission, a vertical instability starts manifesting itself, and after a few cycles of this, the system's acceleration field instability overwhelms the control effectors, and the system irretrievably departs controlled flight!

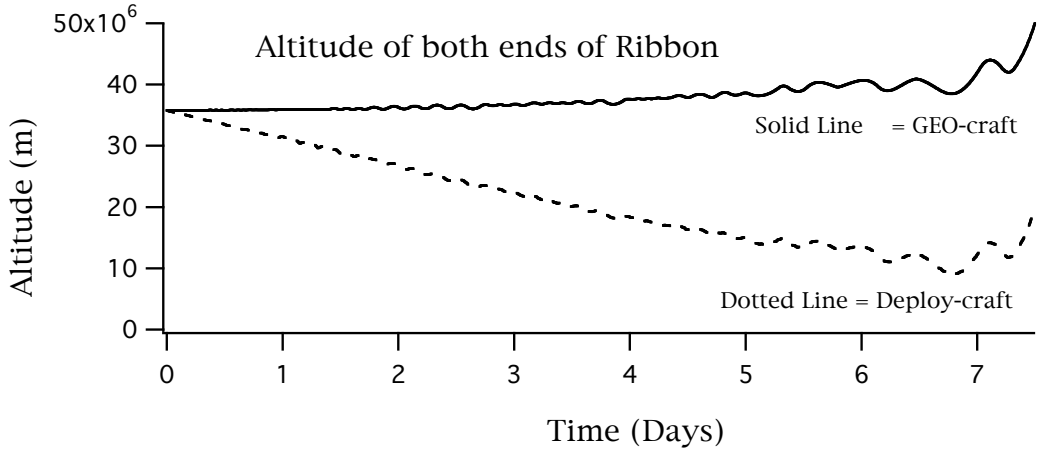

In the graph below, it is seen that the system as a whole has failed to "bite into the gravity well" sufficiently to prevent a centrifugal departure.

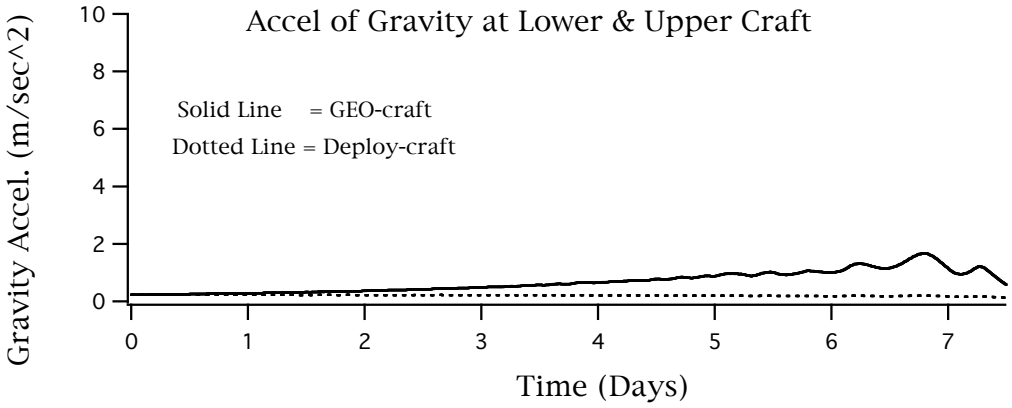

The tension below betrays inappropriate control system settings and gains that are exciting the ribbon and system.

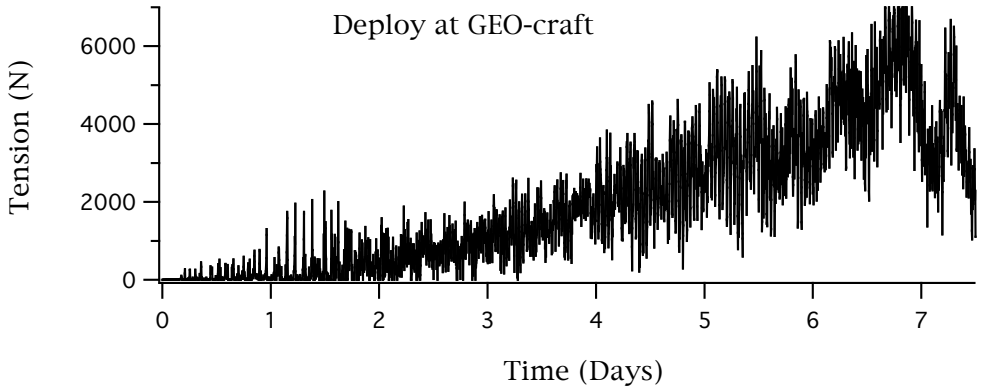

The tension variations seen above are indicative of the need for any elevator ribbon deployment control system design to be able to properly reject "noise" in the tension signal so as to deduce the intrinsic tension level, against which the GEO-craft must fly a compensating equilibrium-altitude maneuver.

The libration of the Deploy-craft relative to the GEO-craft shown below illustrates the potential for minimal control of libration of the Deploy-craft during its deployment; tether deployment tends to be stable (the inverse of tether retrieval, an intrinsic tendency that is a manifestations of the well known "skaters-effect").

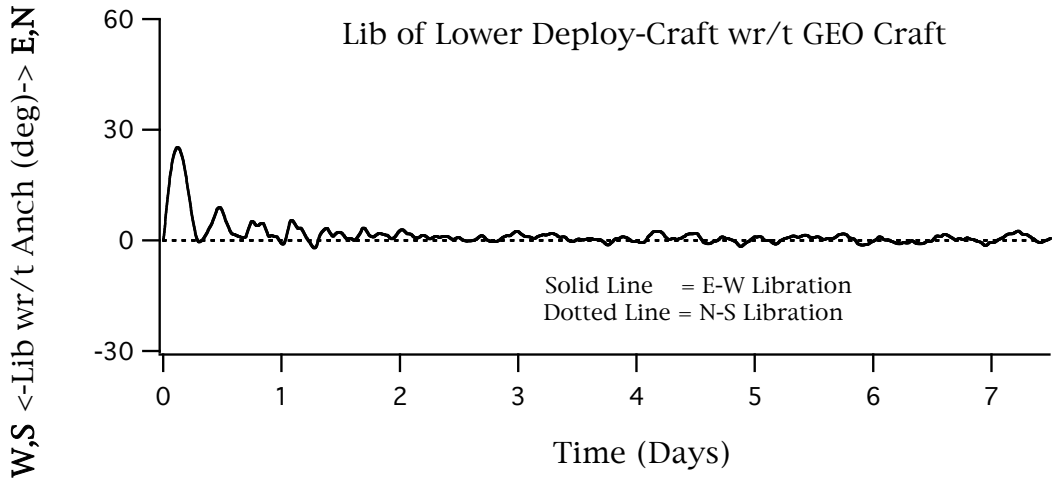

The libration of the GEO-craft relative to the earth anchor point shown below shows that the departure of the system from controlled flight is attended by increasing angular disturbance as well as increasing altitude, and effect consistent with gravity field dynamics.

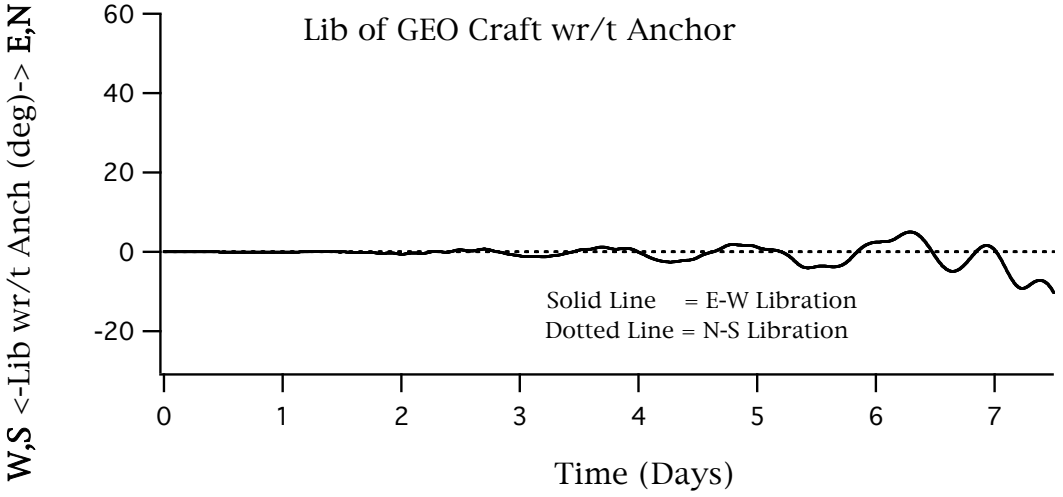

6.8 END-BODY LIBRATION CONTROL EFFECTS

This examination centered on determining the effects of enabling/disabling Horizontal control for the ribbon's end objects (GEO-craft and Deploy-craft). Horizontal control took the form of various types of algorithms for this study, ranging from direct control of earth referenced latitude/longitude coordinates, to simple tangential velocity make-up (to counteract Coriolis effects), and combinations of these with various control logic implementations (dead-band based on-off control, classical proportional control, etc). Note that algorithms controlling longitude, also then *indirectly* serve to control tangential velocity, thus performing a tangential velocity make-up (counter-Coriolos) maneuver.

6.8.1 No Libration Control on Either Upper or Lower Craft

Here, the deployment took place with no Horizontal control being enabled on any of the end-craft; this means no attempt is made to track an earth fixed point, nor, to compensate for Coriolis effects. Below is the deployed ribbon time history (typical of all the following series of Horizontal control runs).

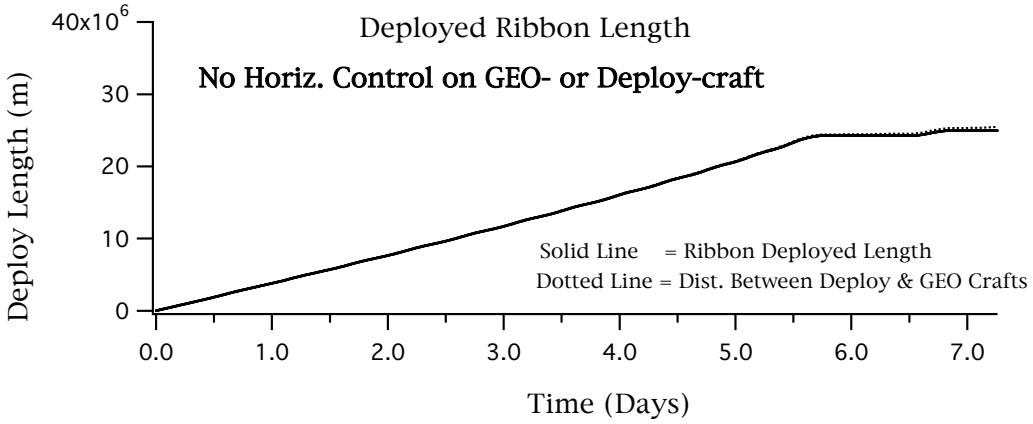

The graph below shows the Libration of the GEO craft as viewed from the anchor station. It is clear that large and impractical angular dispersions are occurring in this case.

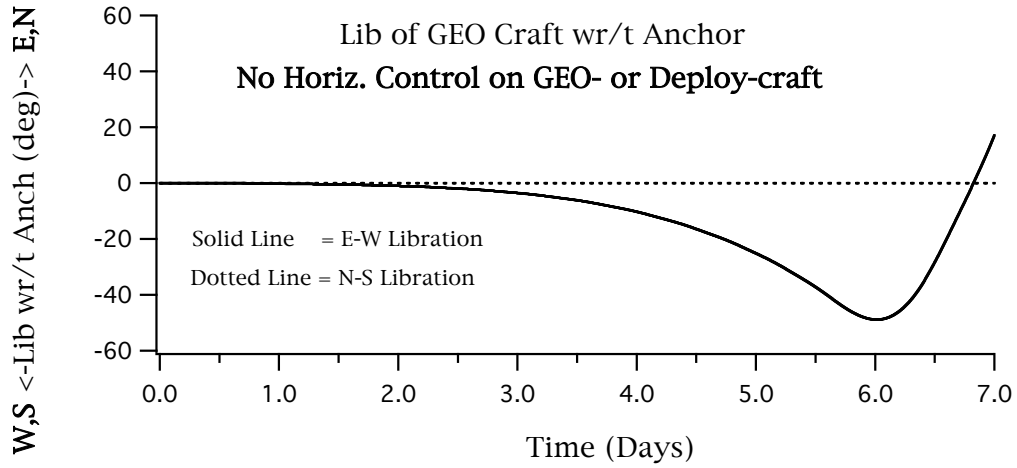

The altitude response of both end-objects are shown below. In this case, the vertical control was not aggressively attempting to raise the altitude of the GEO craft to compensate for the rising tension; had it done so, much greater positive altitude rates would have been realized, that would have exacerbated the GEO-craft libration (shown above), since the Coriolis acceleration is directly proportional to the altitude rate.

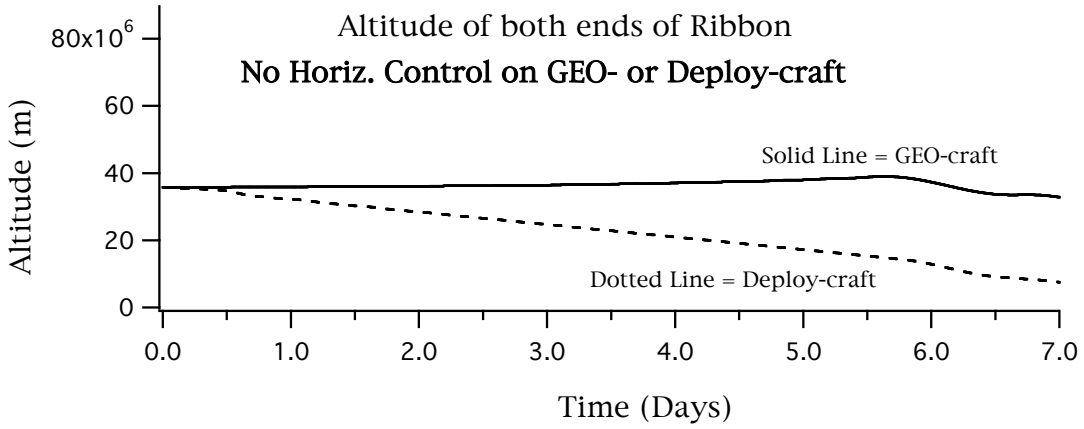

The Libration of the (lower) Deploy-craft relative to the anchor (shown below) is seen to follow the GEO-craft trend fairly closely.

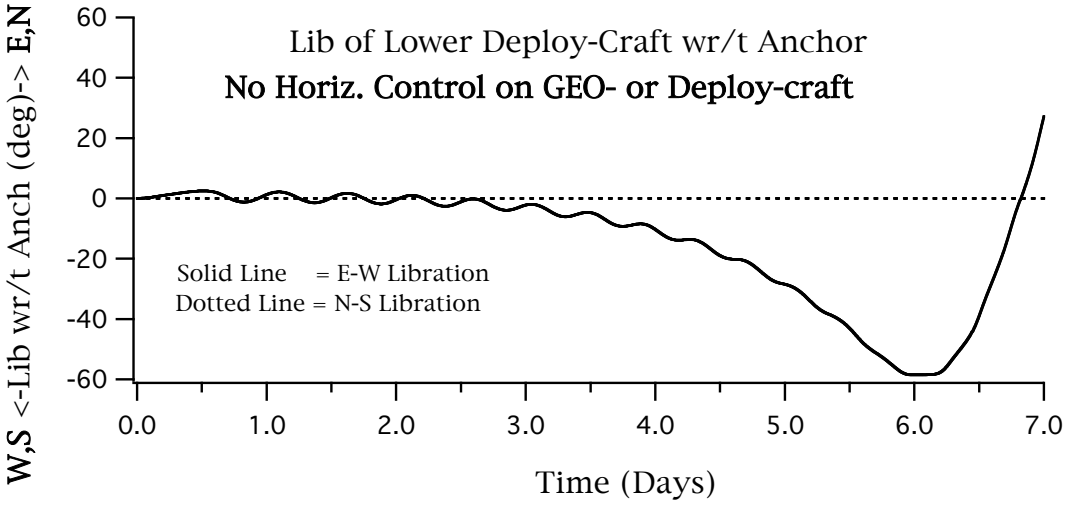

The above correlates well with the Libration of the Deploy-craft relative to the GEO-craft (shown in the following graph below), indicating that the Deploy-craft remains more or less directly below the GEO-craft as it executes major libration excursions. This is highly suggestive that it may be possible to employ minimal, or no, Horizontal control on the Deploy-craft until the final terminal-phase rendezvous with the anchor (so as to enable precise grappling at the ground).

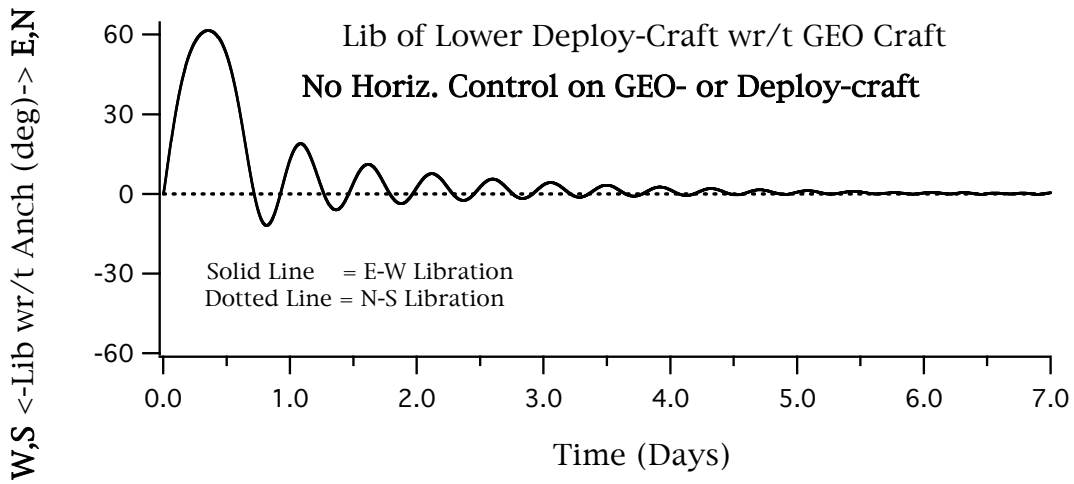

While the graph above indicates that the Deploy-craft is vertically-tracking the GEO-craft during it's uncontrolled deployment, nevertheless, by this same token, the Deploy-craft is realizing large excursions relative to the anchor point (shown in the previous graph above). This also suggests that if the GEO-craft is successfully Horizontally controlled, then the Deploy-craft may simply follow suit.

6.8.2 No Libration Control on Lower Deploy-craft

In the example above, it is clear that deploying with no Horizontal control on either end-object would likely be impractical. In the next two runs, the effects are examined of only one or the other of the end-craft having Horizontal control disabled to determine which is the most critical. In this run, the GEO-craft has Horizontal control enabled via classical proportional feedback control, BUT, the (lower) Deploy-craft, had its Horizontal control disabled. It is seen in the graph below, that Horizontal control on the GEO-craft has arrested its large un-compensated Librations (due to Coriolis effects) very nicely.

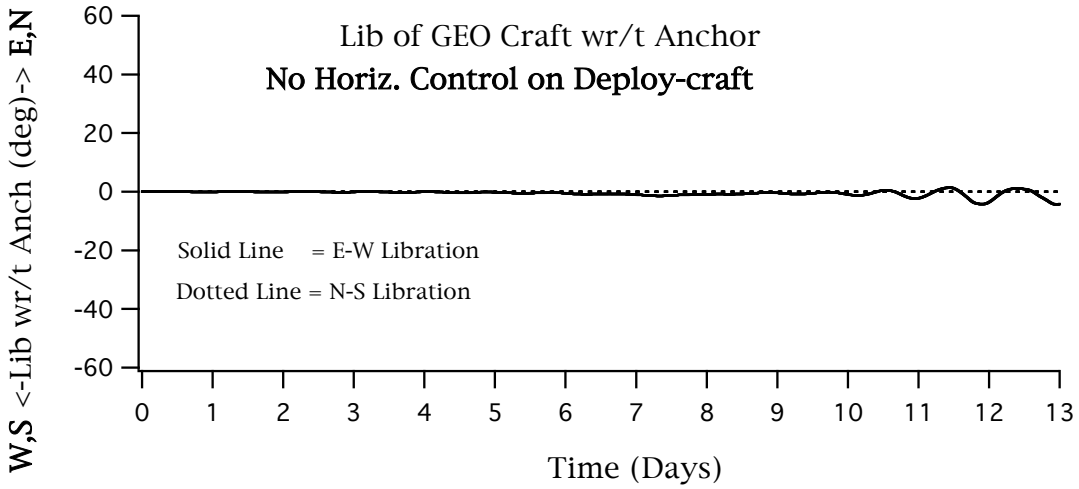

Consistent with the previous suppositions, now that the GEO-craft is stabilized, the Deploy-craft is behaving quite well, and tracking beneath the GEO-craft. The early initial librations of the Deploy-craft relative to the GEO-craft are simply relative-orbital effects due to the manner in which this deployment is initiated; that is, the Deploy-craft is essentially ejected from the GEO-craft as a free-flying object (under virtually no tension initially), and when the ribbon finally becomes taut (tension manifesting itself), the Deploy-craft "pendulums" beneath the GEO-craft. The progressively decreasing libration of the Deploy-craft relative to the GEO-craft is typical of space tether deployment of this type (that exhibits a stabilizing factor due to the increasing the *equivalent moment of inertia* of the tether relative to the GEO-craft; in short, the "skaters effect"). The apparent ever-increasing stability depicted in the graph below also reflects the fact that as distance increases between the GEO- and Deploy-craft, apparent libration also diminishes; just the opposite will be true when the Deploy-craft is viewed from the anchor point.

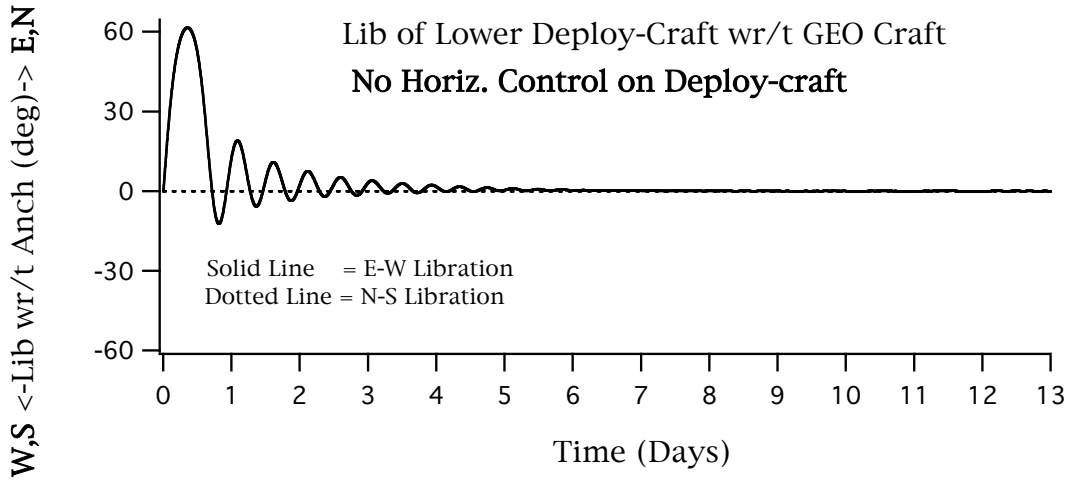

The need for precision terminal phase Horizontal control to facilitate grappling at the anchor is shown below. Even though the Libration (angular dispersion) of the Deploy-craft relative to the GEO-craft was ever decreasing, when viewed from the anchor point, even slight GEO-referenced libration angles equate to significant "miss distances".

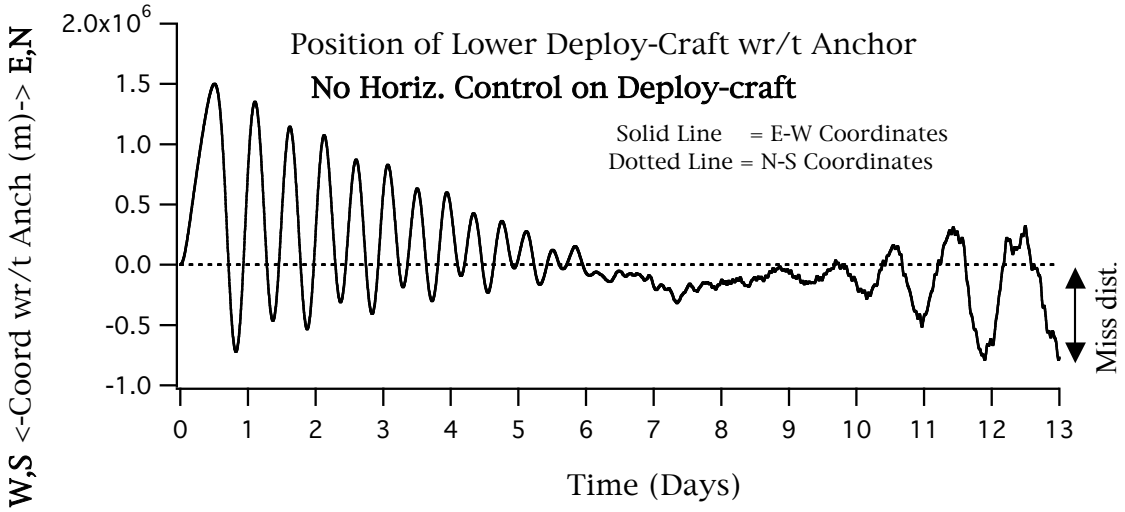

6.8.3 No Libration Control on Upper GEO-craft

From the above examples there is strong suggestion that the primary driver of this deployment as it regards Libration dispersions is likely the GEO-craft; this is probably because it eventually experiences much greater altitude rates than the Deploy-craft. The example above indicated strongly that only very little Horizontal control maybe required for the Deploy-craft.

Even as the Deploy-craft is starting to attenuate its altitude rate as it nears earth, nevertheless the gravity-well is picking up intensity as an inverse square function, thus the GEO-craft must be increasing its altitude-rates to ever greater values to compensate for the rising tension. Failure to do so will result in it's getting pulled down; the only means to counter this is through either dynamic equilibrium (that entails large altitude rates) or thrust (impractically expensive due to the long deployment time frames with the corresponding implied total impulse).

The example below confirms that the GEO-craft will need Libration control to effect a successful deployment of the ribbon to the anchor. Note that this example falls to earth in fairly short time, thus the large values of Libration that were accrued in the previous (and much longer duration simulation) due to the greater altitude rates involved are not demonstrated in this example, but would have been had the system not crashed to earth prematurely.

The first graphs shows the altitude of the end-craft for this case, indicating the resulting pull-down.

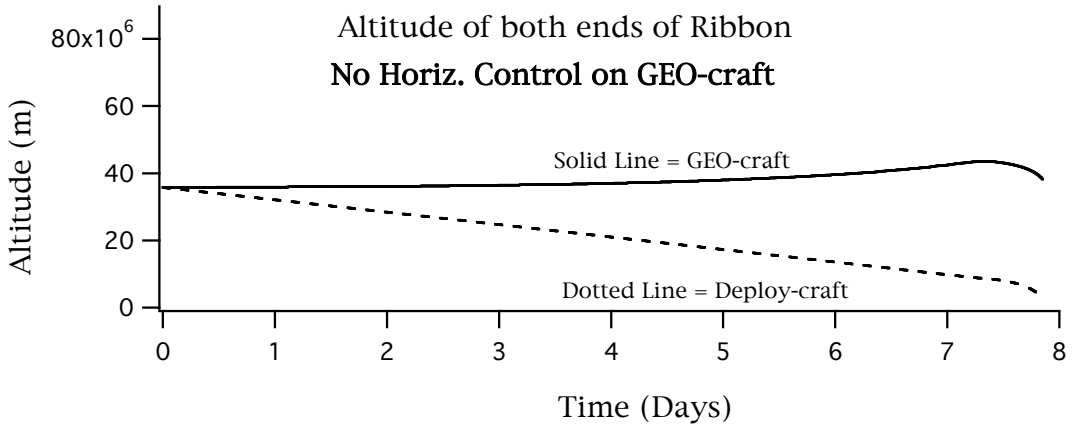

Libration of the GEO-craft relative to the anchor point is shown below.

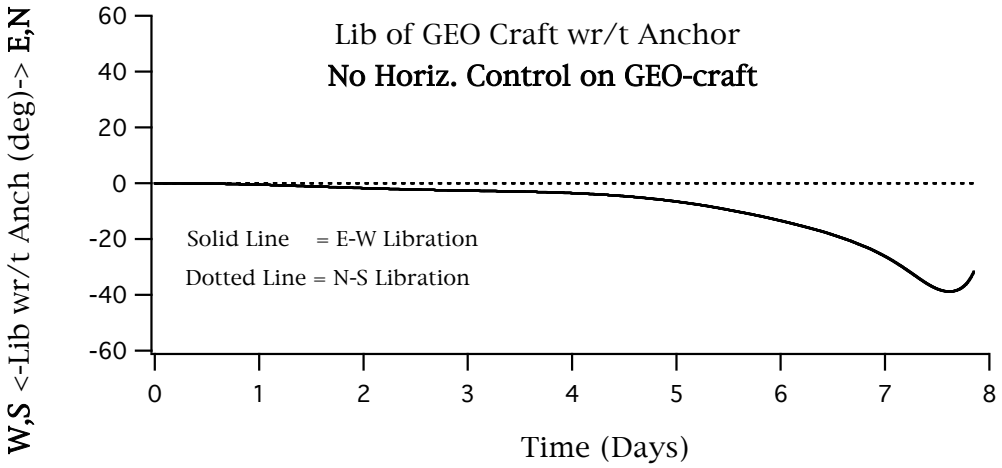

The GEO-craft as it librates, "pulls" the Deploy-craft "in kind" resulting in its being displaced from the anchor point as shown below.

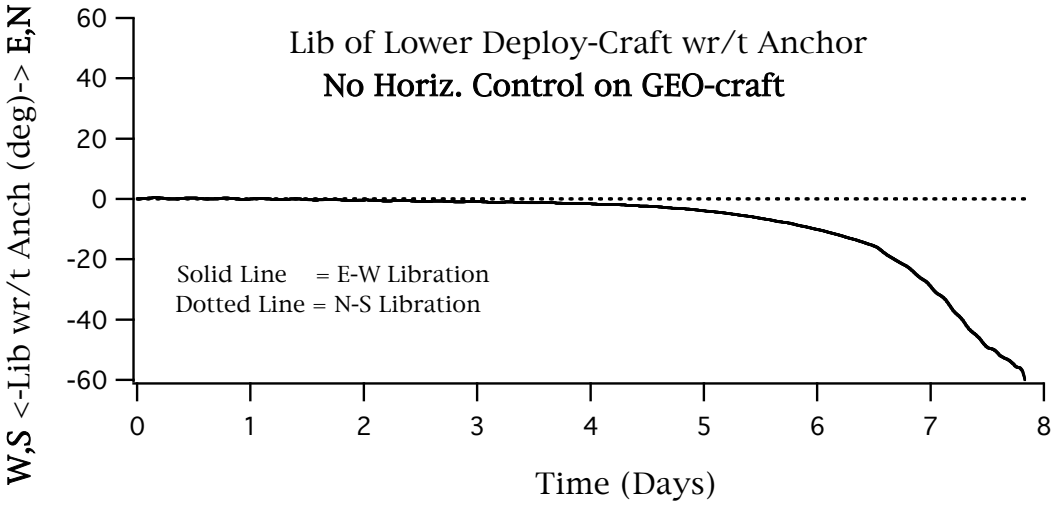

The Deploy-craft (as in previous examples) more or less follows the GEO-craft vertically, as seen below:

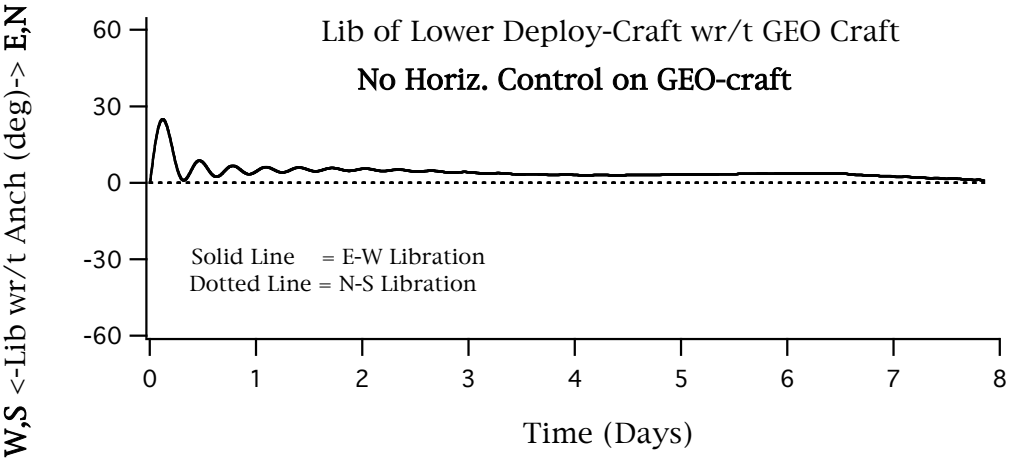

However, since the GEO-craft is strongly displaced, it results in the following "anchor point miss" for the Deploy-craft. The main problem with this final dispersion is its high rate of Horizontal change that must be dealt with to effect a successful grappling at the anchor point.

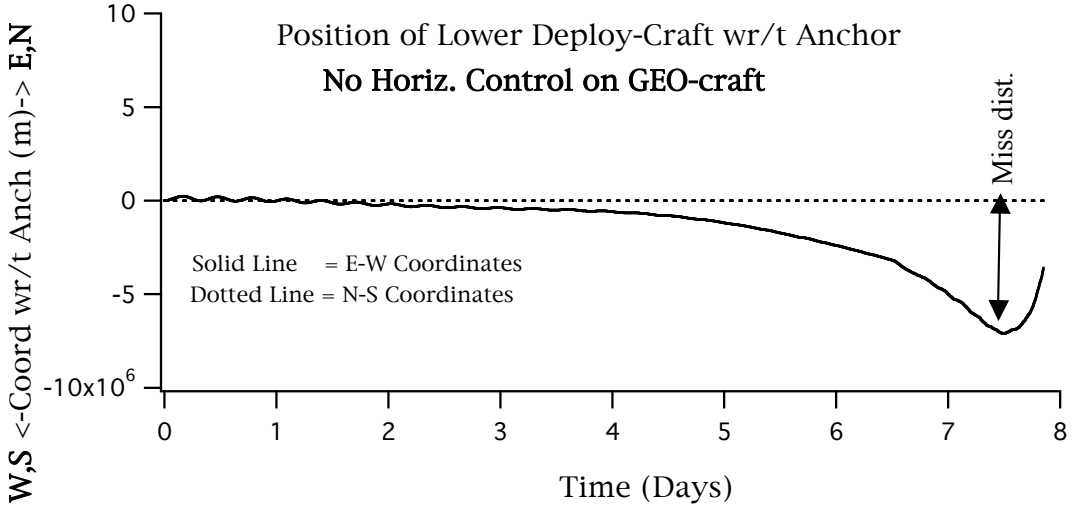

6.9 VERTICAL/HORIZONTAL CONTROL COUPLING

The example below illustrates the phenomenon of coupling between the axes of control on an end-body. In this case it is the GEO-craft controller that is experiencing coupling.

Definition of System Experiencing Coupling

The vertical control mode consists of altitude management to equilibrate the rising tension due to deployment. This results a (more or less) continuously increasing altitude and is achieved by way of a classical, closed-loop, error/error-rate feedback, proportional thrust controller. Gains are chosen to provide a stable/and reasonably tight control.

The horizontal control consists of a simple earth referenced latitude/longitude controller. This control is achieved (as above) via a classical closed-loop error/error-rate feedback proportional thrust controller acting in the horizontal plane. This mode while explicitly managing latitude/longitude is also, in fact, indirectly managing Coriolis effects arising due to altitude-rate along the local vertical.

Origin of the Coupling

As the deployment progresses towards completion, the ribbon and Deploy-craft are encountering ever-intensifying gravity near the earth, with an associated rise in net ribbon tension at the GEO-craft. This in turn, demands that the vertical controller must correspondingly accelerate altitude rate. But this precipitates a greater Coriolis acceleration resulting in libration (the extent of which reflects itself in a net libration oscillation consistent with the gains/effectors in the horizontal plane controller). Now, this libration has a characteristic tension profile associated with it (at the GEO-craft, much like that experienced when one swings on a playground swing). This tension disturbance can be *seen* by the vertical control tension sensors, and will be reacted-to in the fashion for which the vertical controller is designed; thus is seen the mechanism that allows control coupling. In this example, the coupling effect occurs late in the deployment as shown below. The altitude rate divergence starting to appear in the graph below,

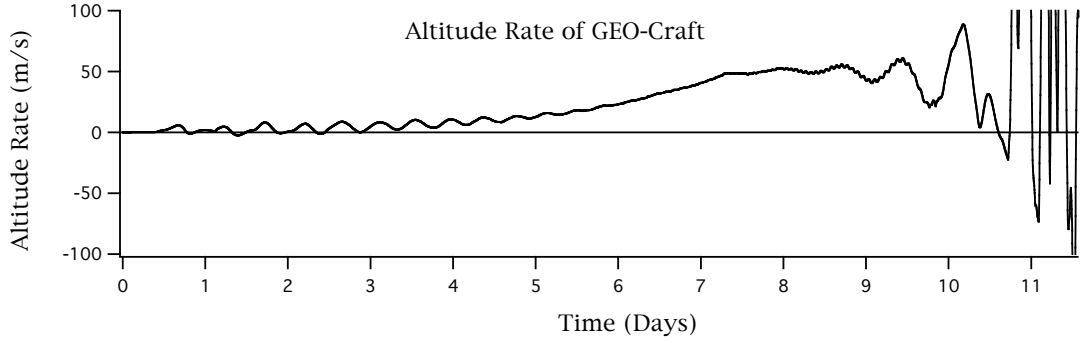

is seen to be in phase with the corresponding libration angle shown below:

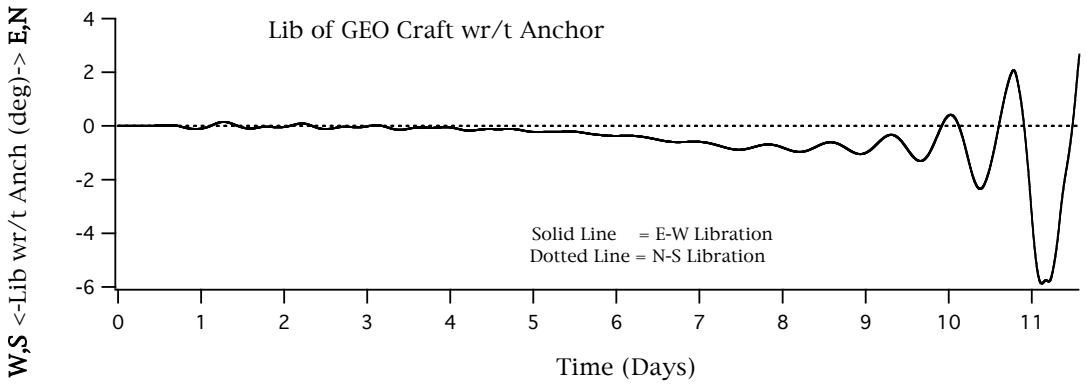

The corresponding tensions in the ribbon are shown below:

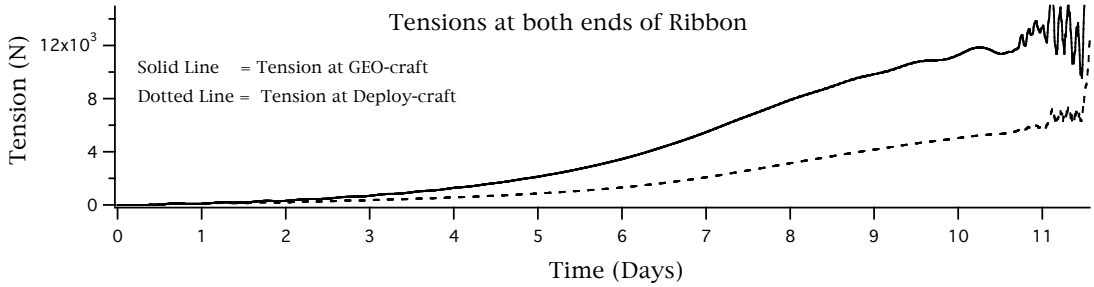

The oscillation in tension is not as evident as the manifestations in libration and altitude rate due to the scale of the tension plot, and the fact that small tensions variations have a large gain with respect to the altitude commanded as a result of incremental tensions.

Resolution of the Problem

The solution to this problem can take many avenues. For example,

1. One classic solution is to filter the sensor signals (tension in this case) to remove frequencies that are coalescing to cause the resonance. But, there is a limited amount of filtering that can be done because the period of the offending oscillations (about 17 hrs) is so great that tension can build up appreciably over this time, and if the GEO-craft altitude controller is denied information of changes in tension over this length of time, the system as a whole can be become out-of-equilibrium, thus defeating the purpose of the equilibration maneuver in the first place. Furthermore, near the end of deployment, tension is changing rapidly, which exacerbates the problem, and forces the GEO-craft to expend propellant to do thrusting equilibration, a likely impractical solution.

2. Lengthen the deployment time (ie slow down the approach into the gravity-well) so that changes in tension are minimal over a period of 17 hours, thus allowing filtering of the tension sensor signal. The problem with this solution is that the total

deployment mission becomes so lengthy that other factors come into play; for instance as total mission time lengthens considerably, so will the propulsion *total impulse* expended just due to, say, the controller's being active to manage GEO-craft attitude increase.

3. Adjust gains on the vertical and horizontal controllers. This is a potentially efficacious solution. For the simulations being conducted in this case, the gains were chosen to produce appropriate control for both the vertical and horizontal axes, and it was those gains which produced the ultimate coupling instability. To decouple the axes gain-wise may well yield controllers with other artifacts the appear during the course of the deployment. Note that frequencies are changing significantly during the course of this deployment. Tension has already been filter for instance to eliminate an undesirable oscillatory phenomenon with a 4000 sec period.

4. The scheme used in this simulation to decouple the axes was a change in the control algorithm. Due to the very specific task that the vertical controller must accomplish, it was not a good candidate for change, but there were many ways that the horizontal controller algorithm could be changed. Basically the solution was to abandon the classical proportional-thrust feedback scheme on latitude/longitude, and replace it with a scheme that provided a Coriolis-countering thrust bias, in conjunction with a classical on-off dead-band controller to maintain latitude /longitude.

The new horizontal control algorithm resulted in the following response for the previous case. Not that the vertical-horizontal coupling is now eliminated.

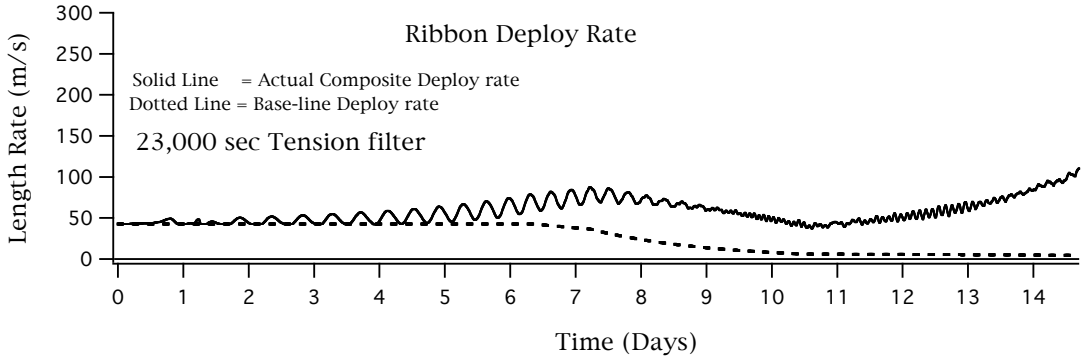

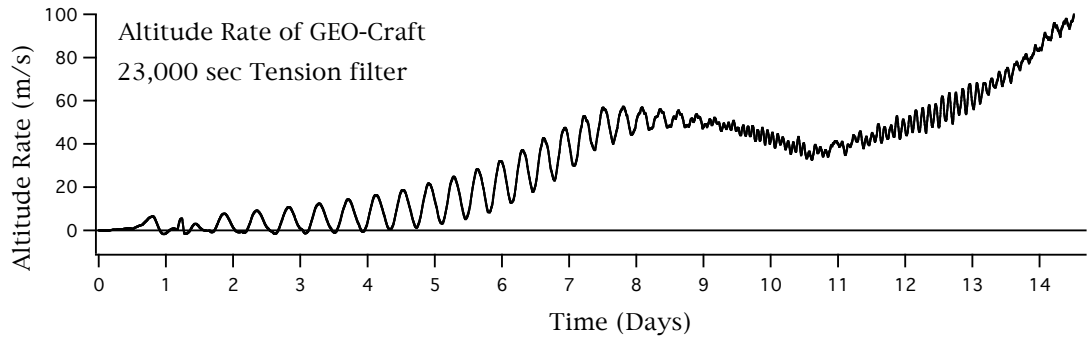

6.10 EFFECTS OF TENSION SENSOR FILTERING

This is an example of using a time-averaging filter to remove an undesirable oscillation from the dynamic response of elevator ribbon deployment. The vertical and horizontal controllers on the GEO-craft are combining with the ribbon deployment algorithm to produce a incessant oscillation that results in "rough deployment". The altitude time history of the deploy craft *before* and *after* insertion of the filter is compared in the two graphs below.

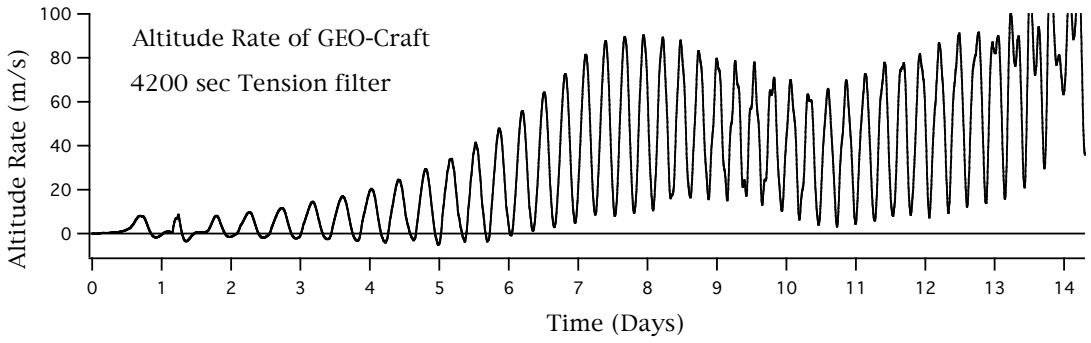

Note that the characteristic oscillation seen above has a period of about 23,000 sec. By applying a 23,000 sec averaging filter to the tension values *seen* by the vertical controller on the GEO-craft, the above response was transformed into that shown below.

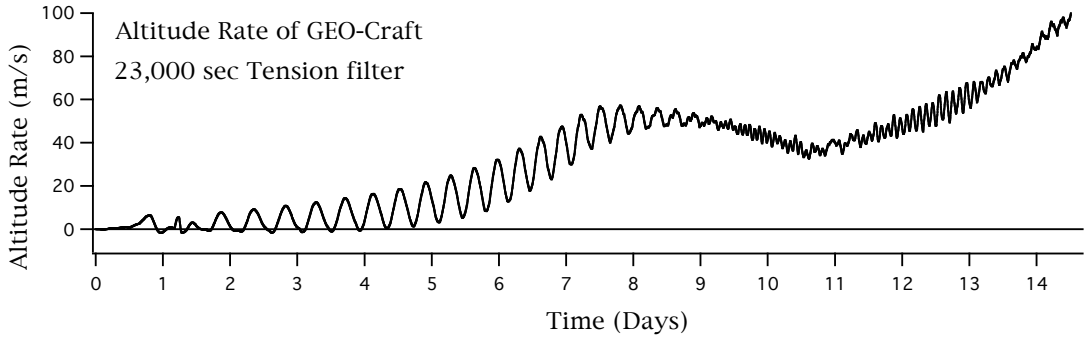

In the definition of the ribbon deployment algorithm, the altitude rate of the GEO-craft plays a direct an critical control, so by eliminating the oscillations, the ribbon deploy rate also becomes much better behaved. The comparison between the ribbon deploy-rate *before* and *after* filtering is shown below:

Deploy rate before filtering:

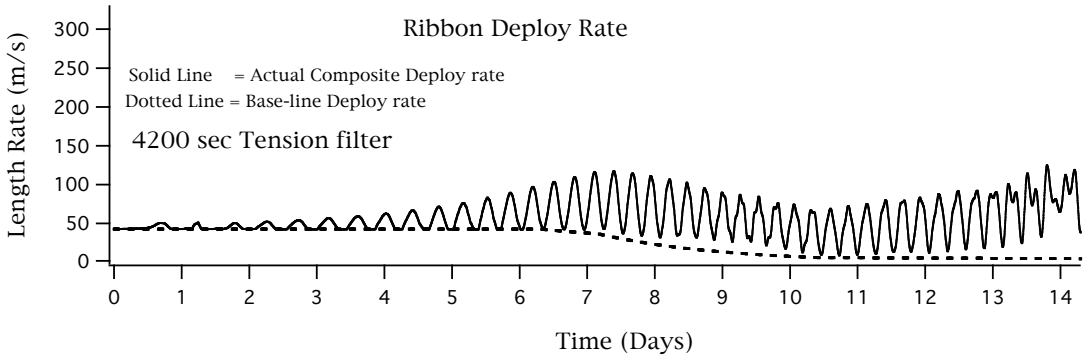

Deploy rate after filtering:

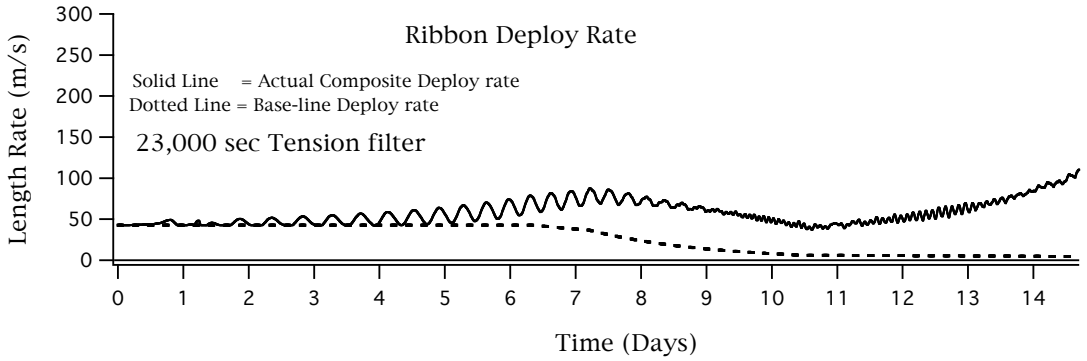

6.11 SUCCESSFUL BALANCED DEPLOYMENT

The example behaviors above have illustrated the natural unruly tendencies and potential difficulties of controlling this system during deployment. The example below now counters the above by showing how system stability might be approached in a controlled fashion to effect a successful deployment of the elevator ribbon.

This particular example demonstrates the possibility of dynamically balancing the vertical ribbon during the course of a deployment, and is the culmination of an investigation that employed multiple combinations of conventional and unsophisticated control in an attempt to render a more or less stable deployment. This study eventuated in a system approaching a level of vertical balance so as to achieve an almost successful deployment in terms of vertical equilibrium and suppressing un-desirable dynamic ribbon responses.

While this run in no way exhibits the fine terminal-behavior required of an actual deployment mission, it does demonstrate the possibility of dynamically balancing such a system by means of control effectors of significantly less force than the steady tensions being managed during the deployment. Given unlimited propulsive control thrust and fuel, this task could of course been accomplished quite nicely, albeit, such a "brute-force" approach would be impractical from many standpoints.

> Point of Interest: While this example in no way exhibits the fine terminal-behavior required of an actual deployment mission, it does demonstrate the possibility of dynamically balancing such a system by means of control effectors of significantly less force than the steady tensions being managed during the deployment. Given unlimited control thrust and propellant, this task could of course been accomplished quite nicely, albeit, such a "brute-force" approach would be impractical from many standpoints.

The crux of this technique revolves around the interplay of a "vertical and horizontal controller" for the GEO-craft *combined with* a "ribbon deployment controller" that recognizes the need to modulate the ribbon deployment rate as a function of the altitude, while paying due regard to ribbon deployment rate required to compensate for the rising altitude of the GEO-craft. The essence of the GEO-craft vertical controller is its algorithm designed to achieve an altitude that will continuously equilibrate the ribbon tension using the centrifugal effect, said equilibration *ideally* occurring with a precision that requires virtually no propulsive-makeup; ideally then, the minimum propulsive force needed would correspond to the "work" that must be done to "lift" the GEO-craft against the gravity field from GEO altitude to Ballast altitude (along with tangential velocity make-up). This vertical controller incorporates logic to minimize modal interaction with the combined elastic ribbon and end-body system, and to respond effectively to tension transients; a particularly insidious problem involves vertical control activity's inducing spurious tensions into the ribbon system in the act of maneuvering, then in turn reacting to these very transients. For this reason the vertical controller uses "filtered tension" to

plan maneuvers, and can also be adjusted to enter into quiescent periods in which it does nothing other than maintain existing commanded altitude. All of these facets are employed to achieve a fairly stable deployment.

In terms of the GTOSS simulation, the above described control effectors were invoked for each of the craft as follows:

GEO-craft as:

- Vertical control option 6 (altitude equilibration based on tension)
  - Error gain = 0.00035
  - Rate gain = 1.0
  - Max Thrust Avail = 1500 lbf
  - Quiescent Time Interval = 500 sec
  - Duration of Tension Filter = 23,000 sec
  - No. of Filter Samples =50

- Horizontal control option 8 (Coriolis thrust-bias w/on-off DB logic)
  - Dead-band = +/- 1.0 deg
  - Max Thrust Avail = 500 lbf

Deploy-craft:

- Vertical control ~ **None Used**
- Horizontal control ~ **None Used**

The Ribbon Deployment:

This was accomplished with a type 12 deployment controller. This controller determines a basic deployment rate profile from a table of "Deploy-rate -vs- Altitude" that represents a simplified ideal rate of descent of the Deploy-craft, then *adds to that* the altitude rate of the GEO-craft (as it rises to equilibrate the ever-building tension). This algorithm is configured for this example (as a user input option) to also inhibit "negative deployment" rate so to limit (to some degree) the deployer's participation in both system longitudinal dynamic modes and GEO-craft controller-induced vertical dynamics.

Under the chosen type 12 deployment, a strain-biased deployment was specified with a reference strain of 0.075 based on a reference tension of 5000 lbf. This allowed for the fact the deployment scenario deploys "un-elongated" tether, which, upon being emitted into the domain of the tether, is destined to undergo strain at the level of tension extant in the tether at the GEO-craft at the moment of deployment. Thus the deployment components associated with both the *Baseline profile* and the *GEO-craft altitude-rate* were reconciled with the real strain conditions extant in the ribbon.

Below is the *base-line* deploy rate that was used for this particular example. This represents a idealization of a possible "altitude-rate -versus- altitude" profile that might be appropriate for a Deploy-craft to experience.

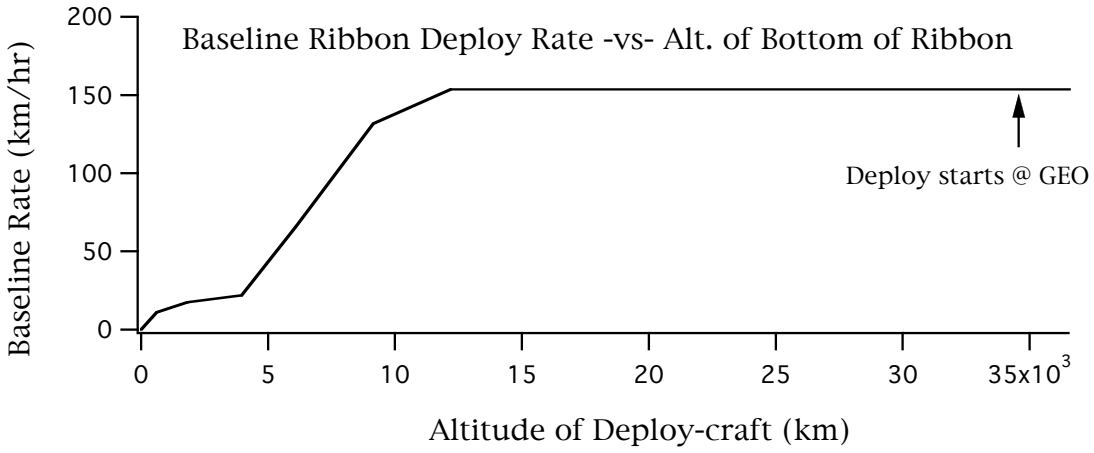

This resulted in the following deploy length and length-rate time history from the deployment scenario algorithm:

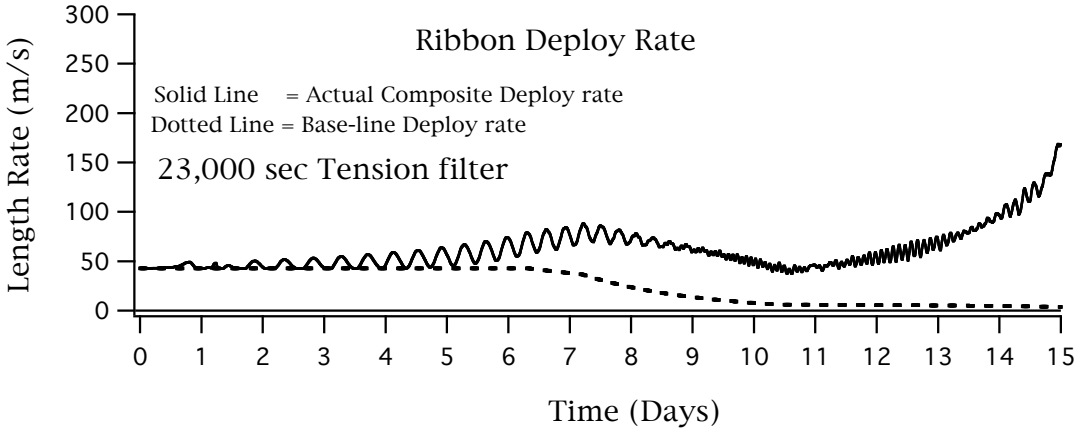

The deviation between the two curves below is representative of the strain within the ribbon as it deploys, and is the quantitative source of the strain-factor definition for the deployment algorithm of this example.

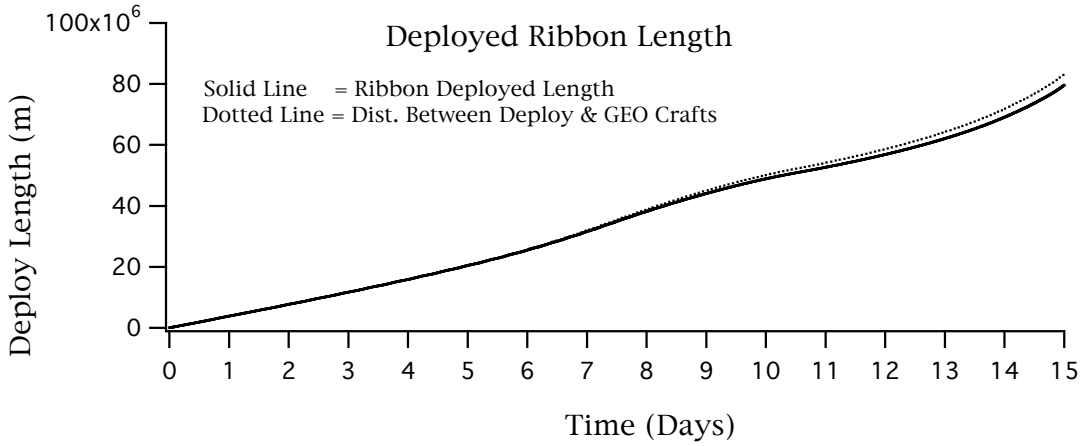

This ribbon deploy profile drove the entire mission in conjunction with the vertical controller on the GEO-craft , resulting in the following altitude histories for the GEO-craft and Deploy-craft:

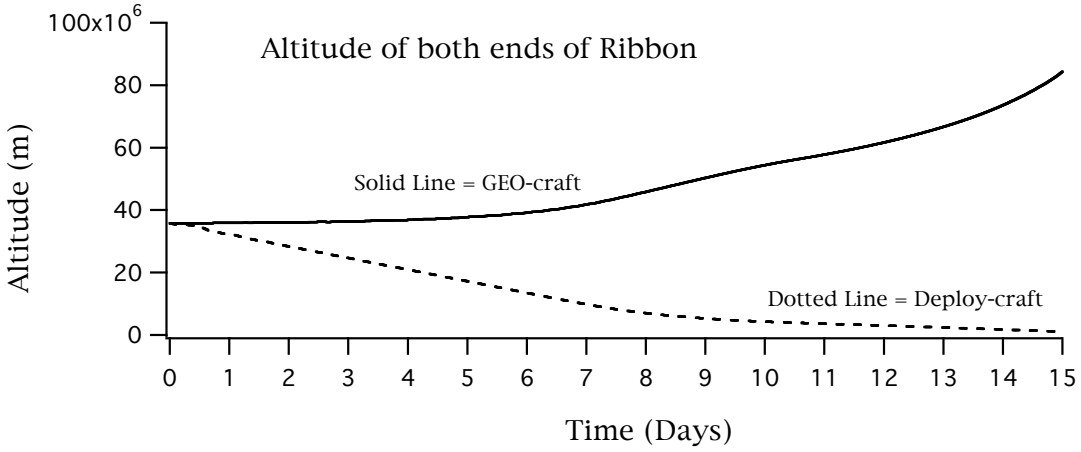

and corresponding to these altitude histories the dynamic response of the deploying system experienced these altitude rates for the ribbon end-objects:

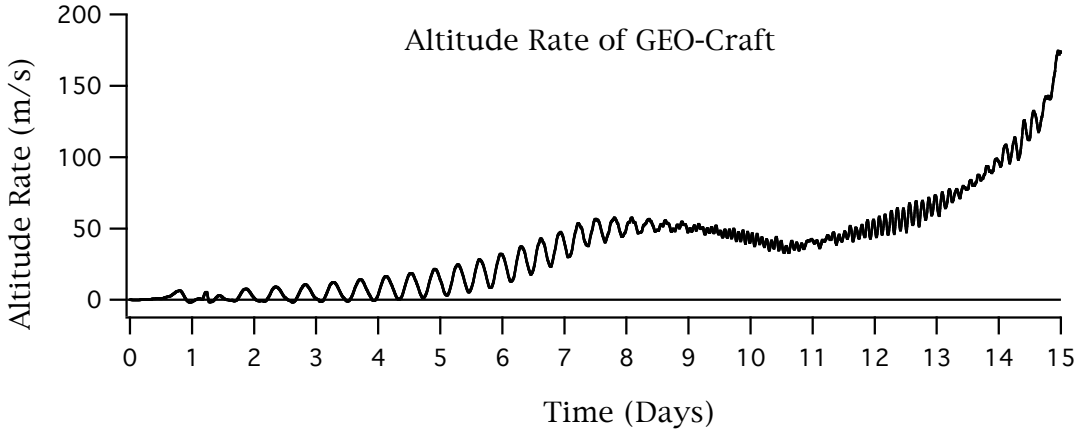

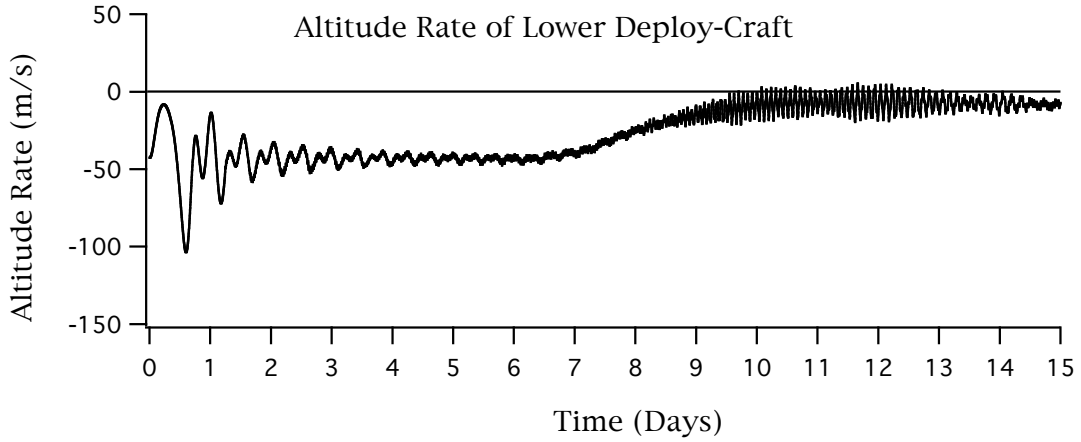

At these altitude profiles, the acceleration of gravity being seen by the end-objects (and ribbon in between), as they traversed the gravity-well is shown below:

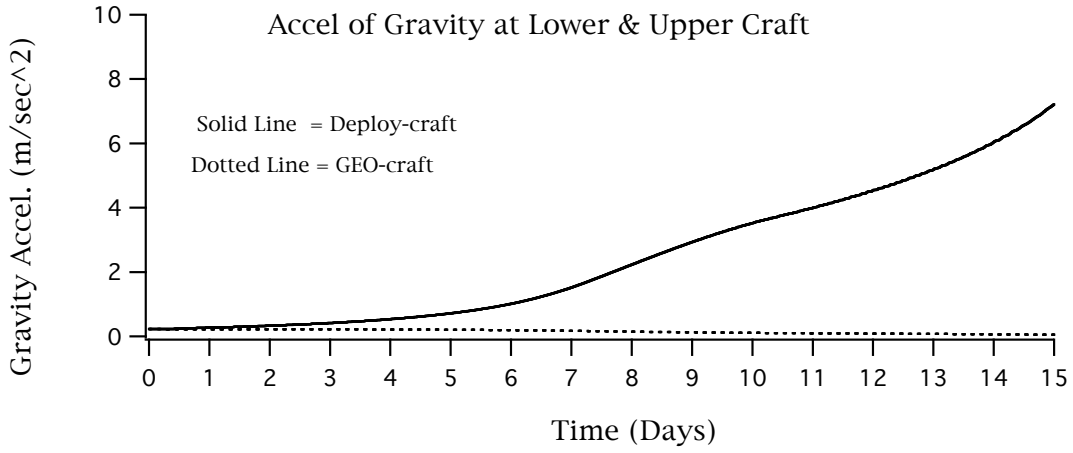

This in turn created the following tension histories at both ends of the ribbon:

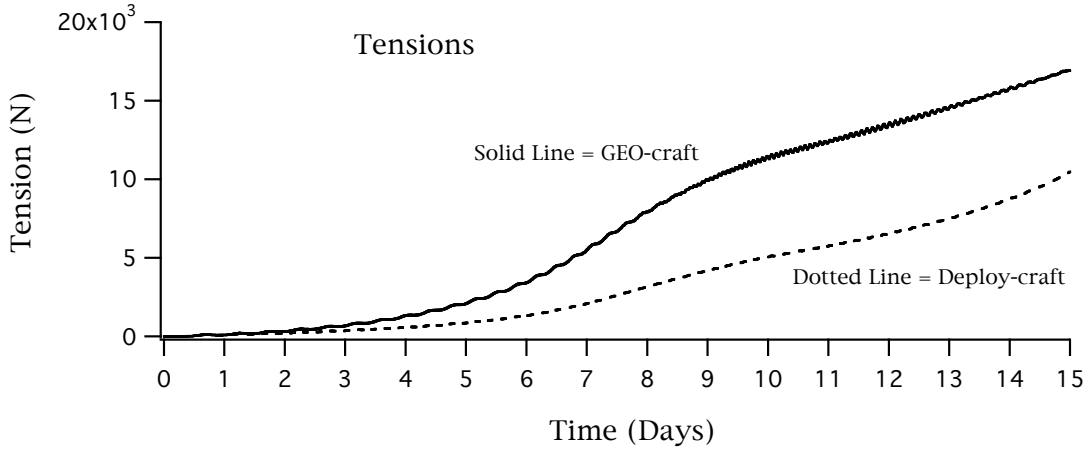

The horizontal state of the Deploy-craft (lower object) reflects NO horizontal control activity and is shown below:

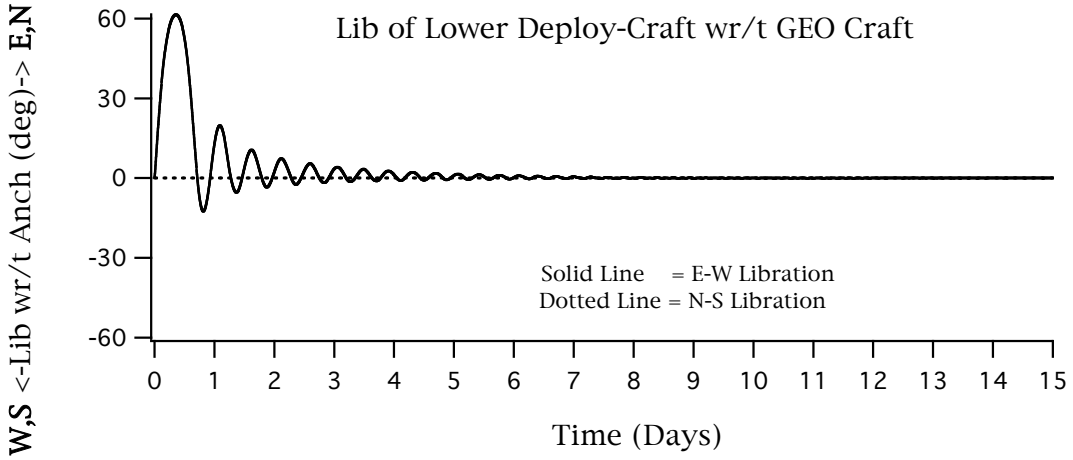

The libration response at the beginning represents the Initial-Phase of the deployment, and quickly damps out (due to natural tendencies of tether deployment dynamics).
The libration of the Deploy-craft as seen by the anchor point is shown below. Note that this is a somewhat different picture than that seen from way above by the GEO-craft. This represents the challenge remaining for Terminal-Phase mission design in effecting a rendezvous with the anchor station. Note also that since libration is defined as a subtended angle, *libration relative to the anchor* will tend to grow as the range between the Deploy-craft and the anchor diminishes (as witnessed below).

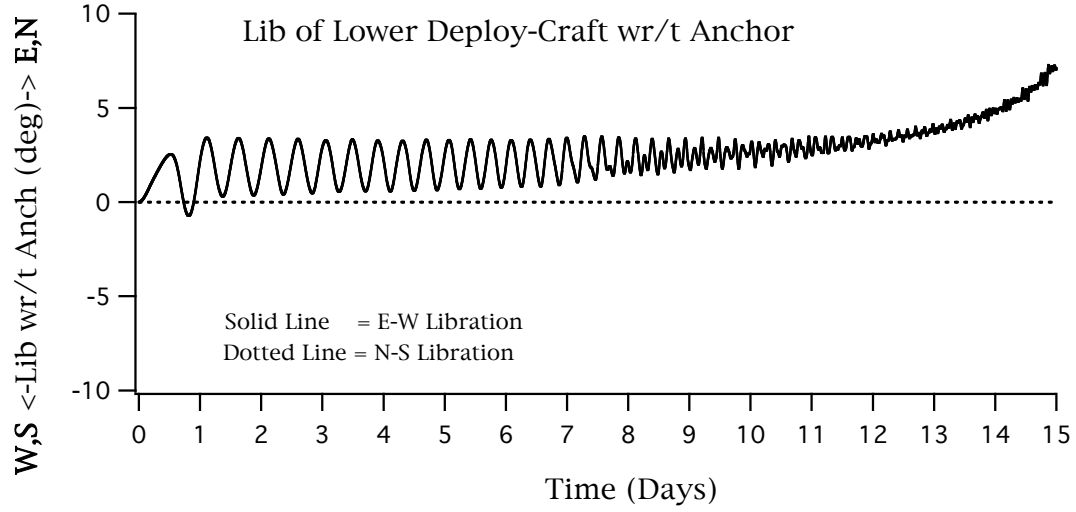

In terms of Terminal-Phase rendezvous with the anchor, a more meaningful expression of the information in the graph above would be the "miss distance" as the ribbon approaches earth. This is shown below:

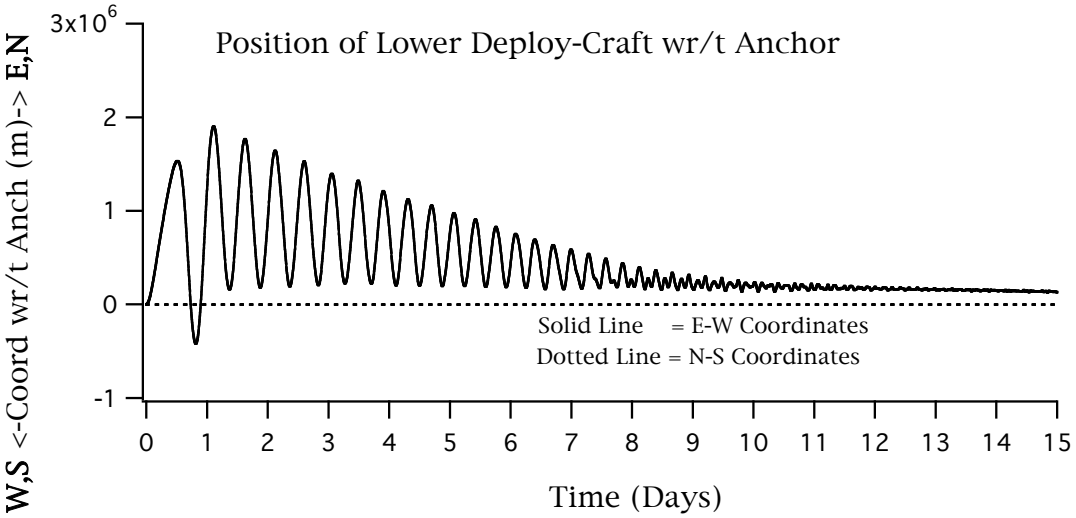

Note that this miss-distance settles out at a steady 14km; this is not an insurmountable distance to manage during terminal phase, and well within designable Deploy-craft control abilities; the management of altitude-rate will likely be a much more challenging task.

As the deployment unfolds, the GEO-craft is itself librating under the action of the dead-band controller. This libration history is shown below:

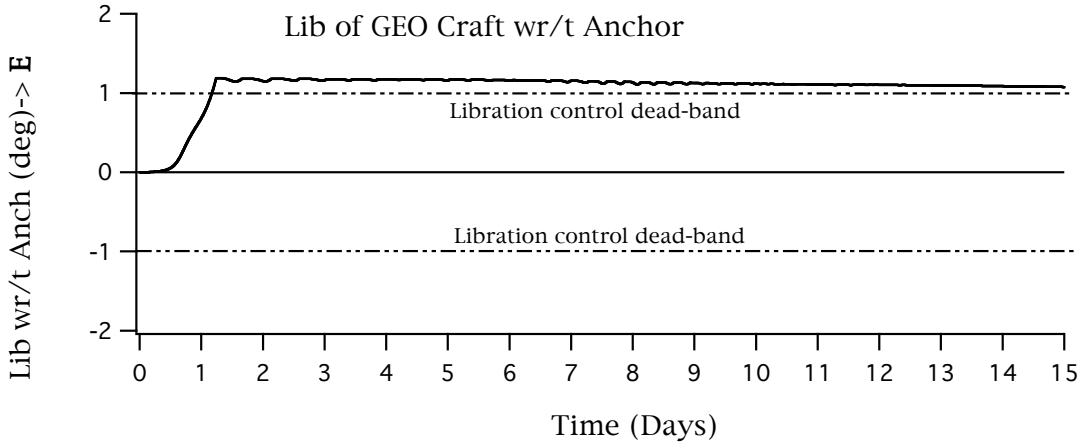

The libration of the GEO-craft relative to the anchor points shows the GEO-craft firmly up against on side of the +/- 1 deg dead-band used in this example; this indicates that the Coriolis management logic is biased, as ideally, this libration angle would be wandering back and forth between its limits (for minimum impulse control).

To understand the propulsion implication of this deploy mission design the, one can examine the total thrusting impulse used by the GEO-craft to accomplish the required control activity. This is shown below:

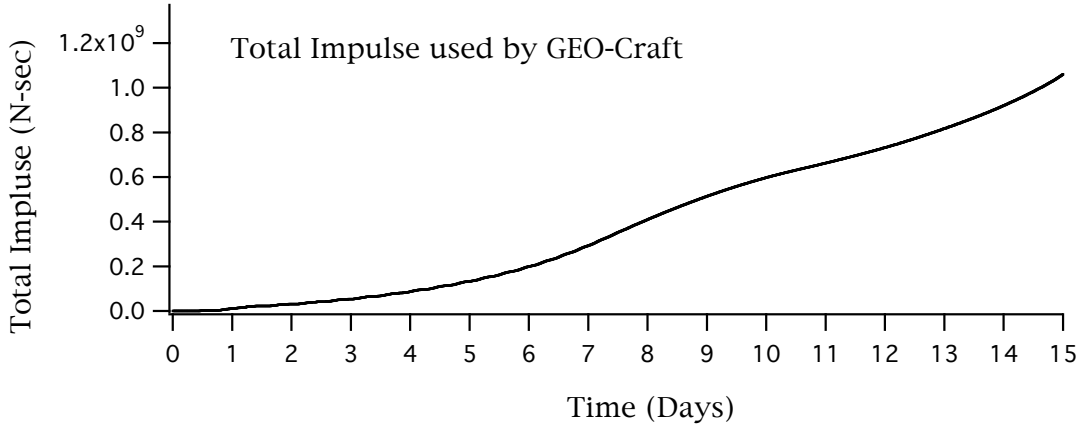

Total Impulse Assessment

The amount of total impulse shown above is a significant value. Converting this to an equivalent propellant budget via a specific impulse of, say, 500 sec (high end of conventional bi-propellant technology) would correspond to a fuel budget of 200,000 kg. However, before jumping to conclusions about this value, one must consider the following:

This total impulse can be thought of as consisting of:

1. Impulse to make-up *tangential* velocity requirement between (the initial) GEO altitude and the Ballast altitude,

2. Impulse expended in overcoming the vertical gravity to raise the GEO-craft from GEO to Ballast altitude, and,

3. Control activity to provide dead-band latitude/longitude control and damp altitude fluctuations, and indirectly provide vertical gravity make-up support that might arise due to imperfect equilibration of the gravity/centrifugal balance against ribbon tension.

Consider now, each of these three contributions:

A total impulse contribution corresponding to **Item 1** is fairly straightforward to assess, since the tangential velocity make-up has associated with it simply a momentum-change. This can be directly equated to an impulse; this corresponds to about 4.8×10^7 Newton-seconds.

A total impulse that might be assigned to **Item 2** is not so straightforward. Here, it becomes evident that the time expended by propulsion against a GEO-craft that, due to imperfection of equilibration maneuver, is tending to "fall" (either up or down), becomes a very significant factor; this is analogous to the classical "gravity-loss" aspect of propulsion performance related to conventional rocket-performance analysis. The amount of work that must be done to lift a GEO-craft from GEO to Ballast-altitude is approximately 4.6×10^{11} Joules. Assuming an average GEO-craft mass of about 43,000 kg, this work equates to an equivalent momentum of about 2×10^8 kg-m/s, thus an equivalent impulse of the same value. This value represents the minimum that must be expended to elevate the GEO-craft to Ballast altitude. It by no means represents what is actually expended, which, is a value that would be very sensitive to the perfection of the vertical equilibration-controller, and mission total lapsed time.

A total impulse that might be assigned to **Item 3** is difficult to assess, but is likely small compared to the first two items.

In summary, the total impulse of 1×10^9 is quite a large value (about 10 times in excess of that identified above as an inescapable minimum requirement), and if it were the last word on propulsion requirements could represent an almost prohibitive obstacle. The caveat below is of paramount importance concerning this investigation:

Important Note: Due to scope limitations, these studies in NO WAY addressed optimizations of the various controllers. Nor did these studies address actual propellant usage and its commensurate impact on mission and vehicle design. ***Any conjecture based on implied fuel usage or propellant budgets derived from this data stands to be in gross error since all of these related factors are closely allied and must he addressed as a whole, rather than in disjoint fashion.***

6.12 DISCUSSION AND CONCLUSIONS

A Possible Methodology for Deployment

This is a summarization of a strategy and control scenario that might be a useful way to envision deployment of the elevator from an initial GEO position.

Initial Phase:

This phase could be accomplished with a simple ejection of an initially minimal Deploy-craft and the ribbon such that the deploy-rate is slightly greater than the Deploy-craft ejection rate. As the Deploy-craft recedes into the gravity field, it will eventually be accelerated to "catch-up" with the ribbon; Prior to this point the Deploy-craft will simply progress below and forward of the GEO-craft in accordance with relative orbital motion (per Clohessy-Wiltshire equations). When the ribbon finally goes taut, then the Deploy-craft will start a harmless libration relative to the GEO-craft. This libration is naturally damped and will eventually become inconsequential to the overall deployment. Of significance here is the fact that this maneuver requires virtually no control intervention by the Deploy-craft (except maybe minimal attitude control to avoid ribbon entanglement) with a corresponding minimal propellant budget.

In general this Initial Phase could be accomplished in any number of ways as it is not a critical phase of the mission from a dynamics standpoint. The design criteria for this phase would be to simply get some ribbon deployed and Deploy-craft removed sufficiently from the GEO-craft to enable a natural gravity gradient driven separation of the two craft culminating in a continuous progression of range between the craft. This would be done so as to preclude any possible entanglement by either craft with ribbon being deployed. Tension would want to be kept to a minimum to facilitate the growing departure between the craft. Ideally this phase would be accomplished with minimal propulsion by either craft.

Mid Phase:

This phase will be a long duration maneuver during which most of the ribbon will be deployed. As the deploy progresses toward the regime in which gravity on the Deploy-craft starts to create consequential tension at the GEO-craft, the GEO-craft must take action to counter this. To avoid being pulled down to earth, the GEO-craft must either provide vertical thrust (with significant, and likely prohibitive fuel budget consequences), or attempt a *dynamic equilibration* of this mounting tension. The best method determined for this relatively crude attempt (described in this handbook) is obtained when:

- a pre-planned altitude-rate -vs- altitude profile for the Deploy-craft is indirectly attempted to be achieved via ribbon deployment alone (ie. using a type 12 *GTOSS Deployment scenario*),

in conjunction with the vertical controller described below,

- an altitude control algorithm for the GEO-craft that attempts to achieve an altitude consistent with *fully equilibrating* the tension being realized at the GEO-craft upper end of ribbon (*GTOSS Object vertical control sub-option 6*).

Horizontal control of the GEO-craft is adopted to provide tangential velocity make-up, and limit libration oscillations that can couple adversely with the vertical control mode; this horizontal control is accomplished via a scheme that will be devoid of resonances or coupling with the vertical axis controller. An example of this is a *Coriolis-makeup* thrust (horizontal thrust proportional to altitude-rate) combined with a classical on-off dead-band latitude/longitude controller. The explicit Coriolis counter-thrust relieves the dead-band controller of the role of indirectly providing this make-up thrust.

Note that for this Mid Phase of deployment, no vertical nor horizontal control was required for the **Deploy-craft**. Mid Phase terminates when the atmosphere is approached. By Mid Phase termination, Deploy-craft altitude rate will have been stabilized and controllable via a combination of ribbon fine-deployment, and propulsive control.

Atmospheric Phase:

Atmospherics can be dealt with via dual actions (1). Delaying atmospheric encounter until that time when minimum wind conditions prevail, (2) Propulsive control *closing the loop* on (say GPS) earth position. Actual simulation of this phase was not within scope of the current effort for the Elevator Dynamics Handbook.

Terminal Phase:

This phase consists of the combined efforts of *fine control* of earth position and altitude/altitude-rate. The altitude control would be accomplished by active propulsion in conjunction with vernier ribbon deployment (as a possibility). Actual simulation of the terminal phase of the rendezvous with the anchor station was not simulated in this study.

The above constituted a reasonably successful Initial-Phase and Mid-Phase deployment in that it showed that it was at least possible, using reasonable thrust levels to keep the system in balance, and effect a potentially successful rendezvous with the anchor station.

Thus, the Deploy-craft experienced essentially "open-loop, passive" control while the GEO-craft used an essentially adaptive control scheme. This becomes evident when it is realized that the actual primary control effector driving the *mission profile* was simply a deploy-rate modulation of the ribbon; this deploy rate was constituted of; the altitude rate that was actually being realized by the GEO-craft (as it attempted to equilibrate ribbon tension), summed with a "canned" deploy-rate that was a function of altitude. These two components of the deploy rate worked together to attempt to achieve a Deploy-craft progression toward earth that followed the "canned rate-vs-altitude profile" by compensating properly for the rising altitude of the GEO-craft, which could only be done by virtue of the total deploy rate directly reflecting the GEO-craft altitude rate.

The GEO-craft used a horizontal control mode that provided a *tangential velocity bias* designed to exactly counteract Coriolis acceleration. This mode was augmented by on-off dead-band thruster logic that tracked earth-referenced latitude/longitude.

Due to the inherent libration-stability of deploying the ribbon downward (with the GEO-craft libration maintained under control) it was possible to perform an uncontrolled Deploy-craft mission right up to the Atmospheric-Phase interface.

Conclusions

This section of the Dynamics Handbook is a work-in-Progress, and **did not address**:

1. Interaction of the ribbon and Deploy-craft with atmospheric disturbances.
2. Final (terminal) rendezvous with the anchor station that would require precision altitude-rate management and latitude/longitude control of the Deploy-craft.
3. Propellant utilization (although total propulsion control impulse was determined for both craft).

As a result of the dynamics behaviors that have been exposed during the course of this attempt to perform a stable space elevator deployment, they following conclusions have been assembled:

1. As deployed ribbon increases in length, the system becomes increasing unstable and problematic to manage; overall system balance (vertical equilibration) becomes an increasing delicate proposition.

2. To achieve a deployment mission with a practical and achievable fuel budget, the GEO craft will be required to raise its altitude consistent with *equilibrating* the building tension in the ribbon during deployment. As the Deploy-craft proceeds deeper into the gravity–well, his entails GEO-craft ever-raising altitude rates eventually mounting to many times greater than the Deploy-craft's descending altitude rate. For this reason, the deploy mission may become a long term affair (weeks) in order to limit deployment mechanism rates to realistic values.

3. Altitude rate control related to terminal rendezvous with the anchor station may be problematic. This is because (the GEO-craft originated) ribbon deployment rate becomes virtually a second-order control effector due to the great distance of the GEO-craft from ground at terminal rendezvous. Furthermore, ribbon deployment originating at the Deploy-craft will likely also be ineffective due to the very low spring-rate of the fully deployed ribbon; this leaves only propulsive control at the Deploy-craft as the alternative, which implies that an appropriate fuel budget must be provided for the Deploy-craft to accomplish this phase of the mission.

4. As ribbon length increases, deliberations driving vertical control inputs for tension and altitude management, by either thrusting or deploy rate modulation, becomes increasingly complex due to the ever greater tension gradient transmission times along the ribbon as well as the attendant excitation of richly varying vertical-modes of oscillation that can serve to obscure intrinsic conditions attempting to be controlled.

5. Failure to maintain system stability will lead to loss of the entire mission (ie the system will crash towards earth or hurtle off into a useless high altitude trajectory).

6. Due to the extreme delicacy of the system, the entire deployment will likely take a significant duration of time (on the order of *weeks*). Smooth, slow deployment is desirable from the standpoint of its minimizing perturbations, but undesirable from the standpoint of propulsive total impulse. Control thrust levels will have to be minimized to limit the total impulse expended for control.

7. The "natural control effectors" that might be used to advantage are ribbon deploy profile, and gravity gradient; both have a limited venue of applicability (compared to the benefits of overt thrusting control), and both become essentially useless to remedy incipient instability, once it has started.

8. The one control effector that commands priority attention is, of course, thrust, but that comes at a big price, namely all propulsion (in the GEO scheme being studied) must be launched to GEO initially. High Isp's (above 500) are obtainable only for electrical-based thrusting, which has notoriously *low thrust*, and high-energy price tags (which implies beamed energy for the deployment). Conversely high thrust will be available with, at best, maximum Isp's of about 500, thus may carry a big penalty in GEO-craft weight (to meet propellant needs).

9. As the ribbon nears the more intense gravity-well gradients (at low altitude, where system response becomes problematic), a GEO-craft ribbon-tension (deployment) control input takes 20 minutes to reach the bottom end of the ribbon (an hour for a fully deployed ribbon), a fact that exacerbates controllability.

10. The LEO-up deployment concept may have benefits over the GEO-down scheme, but likely not for the reason usually touted (ie. ostensibly lower total fuel needs), but rather because the lower end of the ribbon starts *firmly ensconced at a stable, and low altitude in the gravity well*.

11. Both LEO and GEO deployment schemes must deal with the large tangential velocity gradient along the length of the ribbon sooner or later, in their own way. Both schemes must deal with the work required to elevate the Ballast mass to its altitude.

12. Both LEO and GEO deployment schemes must deal with the neutral stability of the system at long ribbon lengths.

14. Likely, Non-Linear optimal control theory will be mandatory to exercise practical control over this deployment, or, possibly artificial Neural Network control theory may be efficacious to exercise practical control over this deployment.

15. Of paramount importance in this system design will be *precise state-recognition* to provide lead-time in heading off any tendencies toward system departure while existing control authority is still sufficient to arrest divergence; error in this regard could easily lead to mission loss.

16. As a corollary to the previous item, a system controller design, robust in the face of *state indeterminacy*, will also be of prime importance.

17. Only insignificant *transverse ribbon oscillation modes* were excited during the process of deployment. While, this was not true during the development of the various control modes and deployment strategies, it was found that as soon as a deployment scenario met even the most elemental of successful mission objectives, then simultaneously, transverse mode deflections became inconsequential. This was probably because *successful* deployment schemes (almost) axiomatically manifested themselves as *smooth* deployment processes.

7.0 ELEVATOR FAILURE MODE DYNAMICS

Work in Progress ……..

7.1 GENERAL FAILURE RESPONSES

- *Categorize response by Break-Altitude*
- *Define possible "worst-case" breaks*

APPENDIX A: GTOSS OVERVIEW

The **G**eneralized **T**ethered **O**bject **S**imulation **S**ystem is a time-domain dynamics simulation code, first developed in 1982 to provide NASA with the capability to simulate the dynamics of combinations of space objects and tethers for flight safety certification of the Shuttle Tethered Satellite System (TSS) missions. Since then, GTOSS has undergone continuous evolution and validation, being applied at some stage in the formulation of virtually every US tethered space experiment flown to date; more than 25 aerospace organizations have employed it. The design criteria for GTOSS featured generality, thus allowing its current use in simulating space elevator behavior. Below is an overview of its features.

• Multiple rigid bodies, with 3 or 6 degree of freedom, connected in arbitrary fashion by multiple tethers, all subject to natural planetary environments, including sophisticated models for earth attributes as well as more rudimentary models for the other planets.

• Tethers represented by either *massless* or *massive* models. The *massive* tether model is a "point synthesis" approach employing a constant number of up to 500 nodes, specifiable by tether (500 is a system configurable limit).

• All tethers can be deployed from, or retrieved into, objects by means of user-definable scenarios. The deployment/retrieval dynamics model includes momentum effects of mass entering or leaving the domain of the tether itself, and produces related forces on objects deploying and retrieving the tether material.

• Tethers can be defined to have length dependent non-uniform material properties. Elastic cross section, aerodynamic cross section, and lineal mass density are independently specified for up to 15 separate regions. Properties at sub-nodal points within each region are determined by interpolation. Each region can have its own modulus of elasticity and material damping attributes.

• Tethers are subject to distributed external forces arising from these environmental effects: aerodynamics in the subsonic and hypersonic; electrodynamics due to the interaction of current-flow with the Earth's magnetic field using current-flow models that incorporate the earth magnetic field and effects of an insulated or bare-wire conductor interacting with the orbital plasma environment model. Note, with an appropriate ribbon-to-plasma electron contact model, this could simulate grounding-current in a conducting elevator ribbon.

• Tethers can experience longitudinal thermal expansion and contraction. A tether gains heat under the influence of direct solar radiation, earth albedo, earth infrared radiation, aerodynamics, and electrical currents; heat loss occurs through radiative dissipation.

• Tethers can be severed at multiple locations during simulation.

• Objects and tethers can be initialized in many ways, including creating a stable configuration for extremely long tether chains, attached to and rotating with a planet (a

space elevator) with due consideration for non-uniform tether properties and the concomitant longitudinally varying strain distribution of elastic tether material.

• GTOSS creates a database containing the response to user-defined configurations, initialization specifications, and environmental options; this permanent data base can then be *post processed* to produce a wide variety of result displays, from tabular data, to graph plots, to animations. In addition to the above, certain handbook section-specific information concerning GTOSS analytical models is provided as appropriate.

Finite Element Resolutions

Dual levels of finite element spatial resolution (nodal spacing) has been used to obtain most of these results due to the impracticality of employing (throughout the entire ribbon length) the same resolution level necessary in the certain regimes of interest. For example, for wind response studies, the spatial resolution in the atmosphere is about 300 times finer than that used for the ribbon above the atmosphere. Either a climber mass was interposed between the two regions of nodal resolution, or, in the absence of a climber, a small mass on the order of a nodal mass. Note: results do not appear to be sensitive to interior mass selections within this nodal mass range.

Climber Configuration

Shown below are nodal resolutions typical of **climber simulation configurations**. These depictions are comprised of dots at each nodal point, thus on the scale of the SE's full length (on the left), the dots are so dense as to appear as a solid line; a subsection, when exploded to a larger scale allows the nodal resolution to become apparent (on the right).

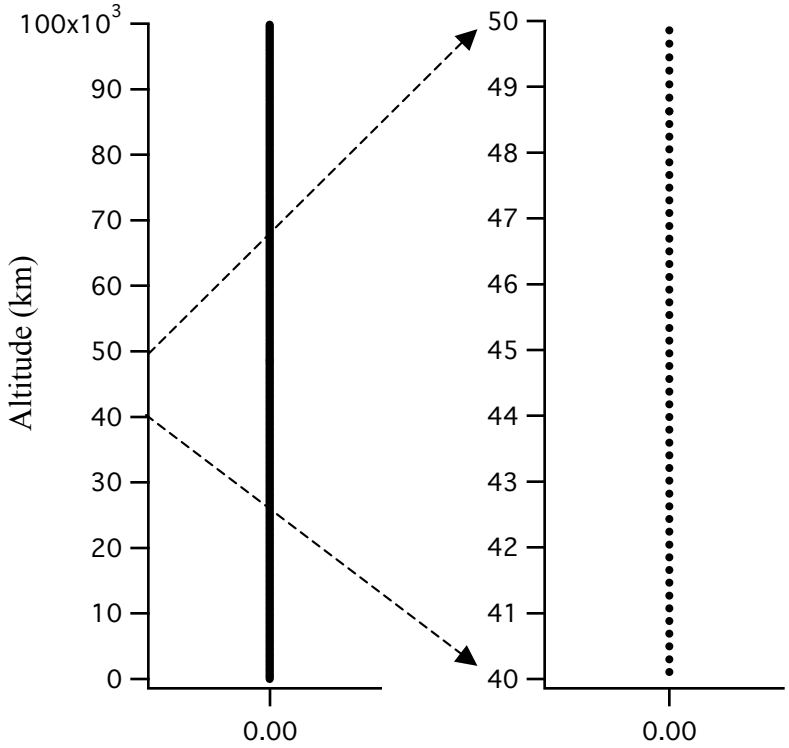

Aerodynamic Response Configuration

Shown below are nodal resolutions typical of **aerodynamic response simulation configurations**. These depictions are comprised of dots at each nodal point, thus on the scale of the SE's full length (graph on the left), the dots are so dense as to appear as a solid line; a subsection of that graph, when exploded to a larger scale, then allows the nodal resolution to become more distinct (graph on the right). Notice that the high nodal resolutions required to resolve atmospheric wind loads within the atmosphere, need 4 levels of graphical down-scaling (starting from full ribbon length) to enable nodal point discreteness to be visually discerned.

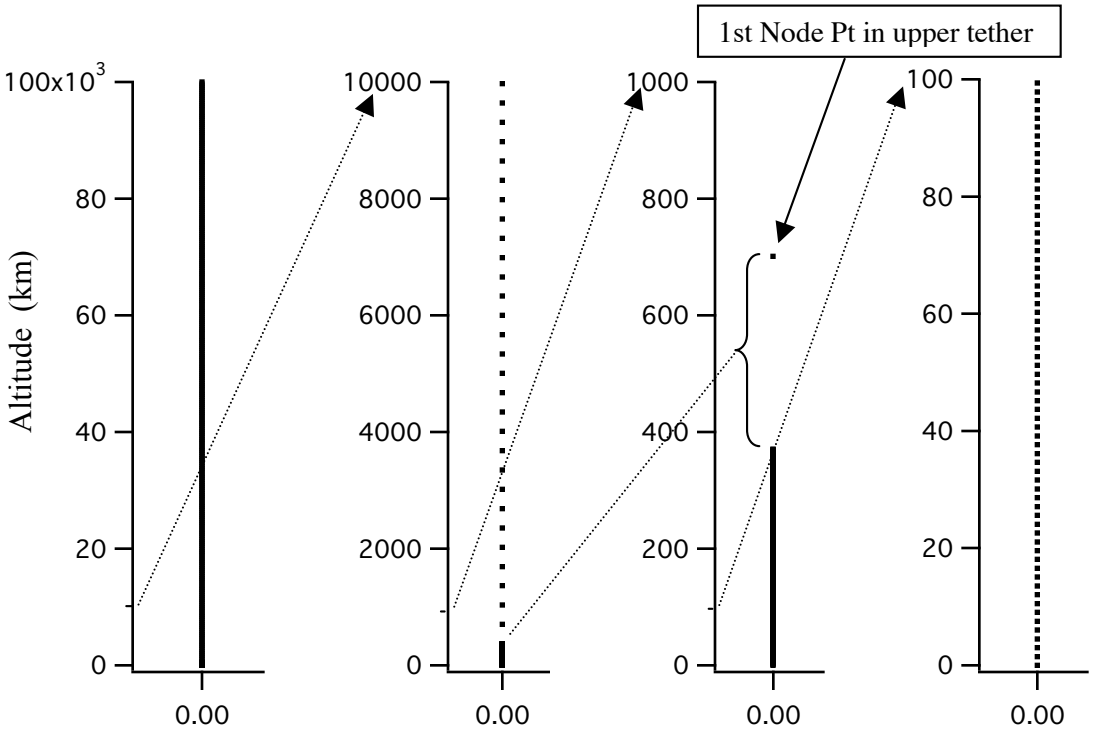

APPENDIX B: GTOSS AERODYNAMICS MODEL

Air loads are calculated separately for each nodal segment, considering for each segment: its relative wind; its effective aerodynamic cross sectional area; and its atmospheric density. The tether's effective aerodynamic cross sectional area is a function of the position along the tether, specified independently of the elastic cross sectional area and mass density variations. The relative wind vector comprises contributions from both the wind disturbance and the tether's motion. Based, on this model, aerodynamic lineal-load-density is determined from which total air load can be calculated on a nodal segment. Note that TOSS does not model a *twisting* degree of freedom (rotation about the *longitudinal* axis of the tether), thus, this model effectively presents the ribbon's full aerodynamic cross section to the relative wind at all times. If the relative wind changes in *azimuth*, then the tether will accordingly accommodate by assuming *a virtual twist* thus producing air loads corresponding to presentation of its maximum area to the wind; hence effects such as rotary flutter, twisting, and *differential windup* are not simulated.

This model is based on calculations often used to simulate kite aerodynamics, derived from a flat plate aerodynamics model. No aerodynamic interaction is assumed to take place between a ribbon segment and its adjacent segments, thus downwash precipitated by one segment does not induce effects on the adjacent segments. A raw *magnitude* of the total air load is found as the product of the dynamic pressure (derived from total relative wind) and the *effective projection* of the segment's surface area *normal* to the *direction* of the relative wind vector; this magnitude is multiplied by a flat-plate drag coefficient (typically between 1 and 1.5) to form the total air load. This resultant air load is assumed to act *normal* to the surface of the segment; segment orientation is derived from a tangent vector to the ribbon and the relative wind. Drag and lift are normal to one another (drag being aligned along the relative wind vector), with both lying in the plane defined by the relative wind vector and a tangent to the ribbon. Thus, the total air load vector is resolved into components *parallel* to and *normal* to the relative wind vector to calculate segment drag and lift densities for use in the GTOSS finite tether code.

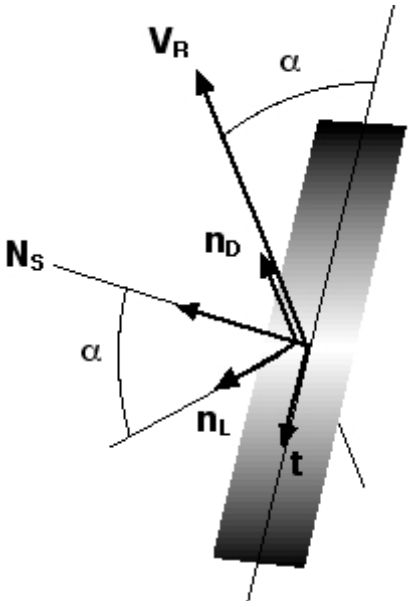

The figure above depicts an element of the ribbon acted upon by the relative wind vector, $\mathbf{V}_R$. Below is an overview of the analytical relationships for this aerodynamic model.

$\mathbf{V}_R$ = relative wind vector acting at the ribbon element
$\mathbf{n}_D$ = unit vector in the direction of $\mathbf{V}_R$
(by definition = unit vector in the direction of Drag)
$\mathbf{n}_L$ = unit vector defining the direction of Lift
(by definition = unit vector normal to Drag)
α = angle between $\mathbf{V}_R$ ribbon tangent vector
$\mathbf{t}$ = unit vector tangent to the ribbon element
Ns = unit vector normal to the ribbon element
A = area of the ribbon element
$\mathbf{A}$ = directed vector area of the ribbon element (= A Ns)
A_n = component of the element's area facing normal to $\mathbf{V}_R$
q = dynamic pressure
C_D = effective drag coefficient
F_A = magnitude of the total air load on the ribbon element
$\mathbf{F}_A$ = total air load vector on the ribbon element (= F_A Ns)
L = Lift on the ribbon element
D = Drag on the ribbon element

From these definitions and the geometry, it follows that,

$$\mathbf{Ns} = \text{unit}[\, \mathbf{t} \times (\mathbf{n}_D \times \mathbf{t}) \,] \qquad (1)$$

The component of area normal to the relative wind is,

$$A_n = \mathbf{A} \cdot \mathbf{n}_D \qquad (2)$$
$$= A \sin\alpha \qquad (3)$$

The total air load vector is,

$$\mathbf{F}_A = C_D A_n q \, \mathbf{Ns} \qquad (4)$$

Lift and Drag is then (in terms of "normal area component"),

$$L = \mathbf{F}_A \cdot \mathbf{n}_L = C_D A_n q \cos\alpha \qquad (5)$$

$$D = \mathbf{F}_A \cdot \mathbf{n}_D = C_D A_n q \sin\alpha \qquad (6)$$

Finally, Lift and Drag is,

$$L = C_D A q \sin\alpha \cos\alpha \qquad (7)$$

$$D = C_D A q \sin^2\alpha \qquad (8)$$

This model, while not sophisticated, should provide a first approximation to the aerodynamic loading on the space elevator. This model presents the tether's maximum aerodynamic area to the relative wind at all times; this can be thought of as differential weather-cocking along the ribbon's length to meet this assumption. This clearly disallows effects such as flutter; besides, such would require unsteady aerodynamics and torsional degrees-of-freedom for the tether, neither of which are included in the present TOSS model.

APPENDIX C: GTOSS CLIMBER SIMULATION

GTOSS possesses the ability to simulate a climber's transit of the ribbon by modeling of *chains* of multiple objects and tethers. The climber would be an object in a *chain* with two adjacent tethers, the earth-side tether undergoing appropriate *deployment*, while the ballast-side tether undergoes complimentary *retrieval* (for upward climbing).

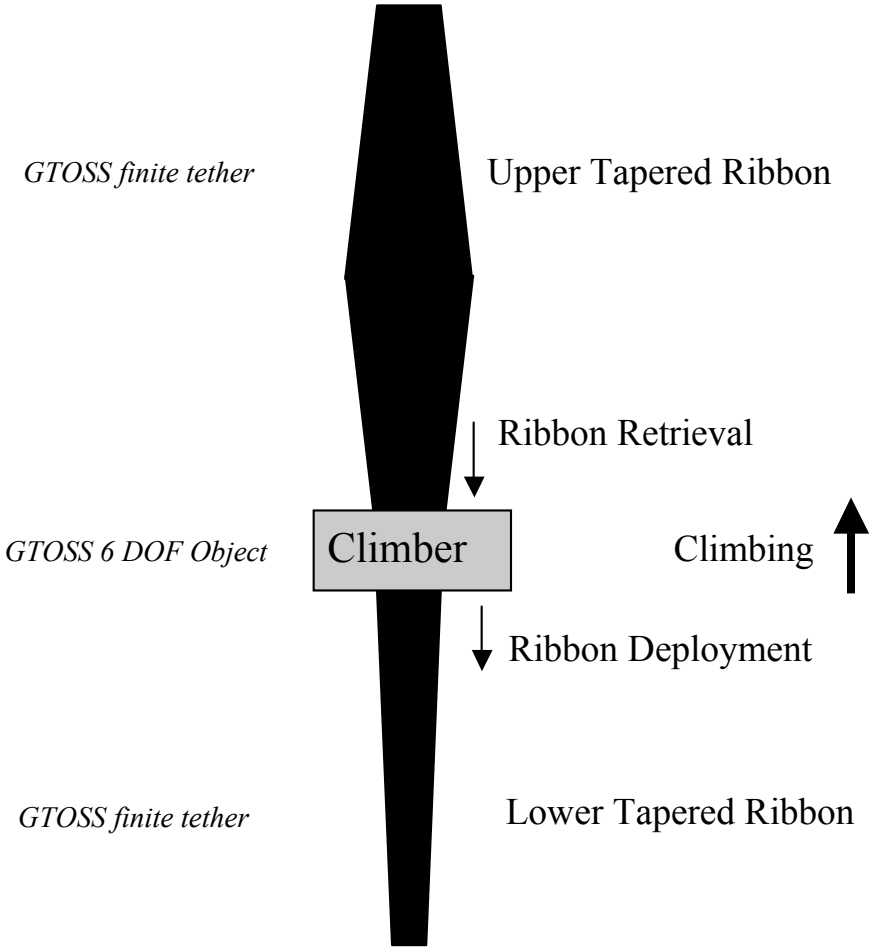

An argument in behalf of this approach starts with the fact that once an element of ribbon enters the "domain of the climber" (ie. gets clenched-in and/or threaded-through rollers, etc.), and until it emerges, that element is within the domain of the climber itself, thus, not a participant in the free dynamic motion of the ribbon lying outside the climber. Such a state of affairs appears to meet all the pertinent criteria for application of a tether deployment/retrieval simulation. So that which is true in nature is extant within GTOSS to simulate climber action. In further affirmation of this viewpoint, note that ribbon strain distribution internal to the climber will, in general, be unlike that of adjacent external ribbon because unique strain states can be imposed upon the ribbon within the climber; indeed, exceeding limit-strain within the climber may be a factor in climber traction designs that engage the ribbon through overlapping roller schemes to take advantage of *capstan effects*. Intuitive reasoning based on a priori knowledge of ribbon continuity must be tempered by the fact that as far as external ribbon dynamics are concerned, there could

just as well be a recycling plant within the climber ingesting ribbon from above, re-synthesizing it to make a new ribbon, and deploying it out the bottom.

For climber studies, the GTOSS configuration consists of a climber containing two reels of ribbon, both of which characterize the ribbon's dual taper design. Earth-side deployment occurs such that the earth-end-taper would emerge first, while for the upward deployed ribbon, the ballast end would emerge first. In this way, no matter where the climber is positioned, the ribbon below and above properly portray the total earth-to-ballast profile.

Conventionally, *deployment* conjures up images of a reel positioned at altitude, with ribbon being dropped down; that is not what is occurring during climber operations. To clarify, consider two points, P1 and P2, between which ribbon is to be dispensed. Two distinct processes can accomplish this, process A and B. In process A, the reel is positioned at P2 remaining stationed there with the ribbon spooled-off and dragged to P1. In process B, the reel starts at P1, and is then transported to point P2, with ribbon being *laid-down* between P1 and P2. These are dynamically distinct processes, in that if observed from a location fixed between P1 and P2, the following would be noted: in process A, there would be a continuous *parade* of different ribbon particles traversing by, while for process B, a single particle of ribbon would appear at the observation point, and remain there throughout the deployment. Process B is realized by GTOSS climber simulation both above and below the climber.

APPENDIX D: GTOSS RIBBON SIMULATION

GTOSS allows a ribbon to have 15 regions of taper definition. These studies employ all 15 regions, and invoke an option to use a quadratic interpolation to define taper attributes interior to a ribbon. The data plots shown for the material attributes of the ribbon reflect this use of 15 regions.

There are two elevator configurations used by GTOSS for these handbook studies; they will be referred to as the ***occupied*** and the ***unoccupied*** configurations. Both share the same *intrinsic* physical property description of the elevator ribbon. Within GTOSS, the unoccupied configuration logically constitutes of a single tether and two objects, the objects being a ballast and a *pseudo object* (fixed to the planet serving as the anchor point). In the case of occupied configurations, an intermediate mass representing a climber is introduced on the ribbon; the occupied configuration is represented by two tethers and three objects, referred to in GTOSS parlance as a *tether chain* manifesting itself as a simple topological chain consisting of Object-*tether*-Object-*tether*-Object. By using appropriate definitions of tether properties above and below the *interior* object, the ribbon properties reflect that of the elevator's tapered design profile along the entire ribbon length.

A variation of the occupied configuration is used within GTOSS for purposes besides representing a climber. Since each finite tether model can have independent properties, assigning a different number of nodes to each tether can achieve dissimilar nodal resolutions at different regions of ribbon. For instance, in the case of aerodynamic studies, the nodal spacing required to provide proper resolution of wind profiles extending over the first 20 km, if used over the entire 100,000 km length of ribbon, would result in an impractical number of nodes. In this use, the *interior* object becomes a transition element within the chain, being assigned a mass commensurate with the nodal masses of the two adjacent tethers. It should be pointed out that tether frequency response characteristics is dependent upon its natural frequencies, and is proportional to its number of degrees of freedom, that in turn depends upon the node count. So the interface between two such tethers has the potential to be a band-pass filter, affecting transmission of disturbances. The power spectrum of response to disturbances can be examined, and if they are within the frequency response of both tethers, this should present no problem.

Unoccupied Elevator Configuration

Data characterizing the elevator configuration varies with length and comprises: mass density, elastic area and modulus, aerodynamic area, and damping properties corresponding to a preliminary baseline ribbon design described in References 1 and 2. A ballast mass of 634,000 kg, at a nominal radius of 100,000 km, produces 200,000 N tension at the ground. The elevator's dual tapered ribbon is nominally initialized by GTOSS to a stable vertical state with a ribbon longitudinal strain distribution that was in equilibrium with gravity and centrifugal loading. The dual tapered ribbon is designed for optimally efficient material usage by achieving a uniform stress distribution over its entire length at a level of approximately half of the ultimate stress capability of 120 giga

Pascal anticipated for an operational ribbon. GTOSS confirms this design objective as shown by the stress profile produced by the simulation (see section 1.2).

Occupied Elevator Configuration

The occupied elevator configuration requires the definition of two ribbon profiles, one ribbon deployed down to the earth, the other up to the ballast mass. GTOSS allows ribbon attributes to be assigned independently, so the *interior* object becomes the source object, from which two ribbons are *deployed* in opposite directions. One tether's deployed profile can be thought of as complementary to the other; thus, the end that would have emerged first downward corresponds to the earth end, while, that first deployed upward corresponds to attributes at the ballast end. Only for occupied elevators in which a climber is in transit would these tethers actually be undergoing time-dependent deployment. For static situations, the deployed ribbon length is automatically determined at initialization to produce a stable configuration. For all cases employing a "nominal reference ribbon", the ribbon is assumed to have an *effective* aerodynamic width of 5 cm; this is referred to as an *effective* width to point out that it can relate to the actual ribbon width to factor-in design attributes such as wind permeability.

Occupied configurations are used (almost) exclusively in studies for this handbook to allow both dissimilar nodal resolutions and enable the study of effects of climber presence on ribbon aerodynamic response. The climber has been assigned a mass corresponding to the nominal 20 ton design; an area of 18 m^2 is assumed in assessing the effects of drag on a climber. Due to its unknown attributes and preliminary design status, the climber has been simulated with 3, rather than a 6, degrees of freedom for this study.

REFERENCES

1. Edwards, Bradley C., Westling, Eric A. "The Space Elevator", published by Spageo Inc, San Francisco, CA, 2002.

2. Edwards, Bradley C., unpublished communications with David Lang, 2002.

3. Lang, David D., "Space Elevator Dynamic Response to In-Transit Climbers", proceedings of the Space Engineering and Space Institute, 2005.

4. Lang, David D., "Approximating Aerodynamic Response of the Space Elevator to Lower Atmospheric Wind", proceedings of the Space Engineering and Space Institute, 2005.

5. Pearson, Jerome, "The Orbital Tower: a Spacecraft Launcher Using the Earth's Rotational Energy", Acta Astronautica. Vol. 2. pp. 785-799

6. Shelef, Ben, "LEO Based Space Elevator Ribbon Deployment", Gizmonics, Inc. Unofficially published (un-dated)